Characterization of a novel cardiac chloride channel and its regulation by cell volume and protein kinase C

By

Dayue Duan

Ph. D.

Department of Pharmacology and Therapeutics
Faculty of Medicine
McGill University
McIntyre Medical Sciences Building
3655 Drummond Street
Montréal, Québec, Canada H3G 1Y6

This thesis is dedicated to

my gorgeous wife, Lingyu (Linda), whose invaluable constant love, encouragement and support were fundamental and essential for pursuing my graduate studies and scientific research. Were it not for her patience, understanding, sacrifice, motivation, and technical assistance during all these years, both at home and in the laboratory, this thesis may have never been completed.

my lovely daughter, Lilu (Marie), whose invaluable constant love, patience, sacrifice, understanding, and encouragement were fundamental and essential for the completion of this thesis.

my brothers, Yiwu and Wenwei, and sister, Fangming, for their persistent love, support, help, motivations, and encouragement.

my parents and parents-in-law, whose persistent love, inspiration, and encouragement granted me the opportunity to come to Canada to pursue and complete my graduate study.

ABSTRACT

The cardiac action potential is generated and regulated by currents through various ion channels. Ion channels are membrane-spanning proteins involved not only in the conduction of electrical impulses but also in the control of cell homeostasis such as cell volume to maintain normal physiological conditions. While chloride (Cl^-) channels have been found to be present in the plasma membrane of most cells, the role of these channels in cardiac physiology is poorly understood. Since the discovery of a cAMP-activated Cl^- current ($I_{Cl.cAMP}$) in heart in 1989, renewed interest in cardiac Cl^- channels has emerged. Evidence has accumulated to show that the heart may express several types of cardiac Cl^- currents activated by stimulators such as protein kinase C ($I_{Cl.PKC}$), purinergic agonists ($I_{Cl.purinergic}$), cell swelling ($I_{Cl.swell}$), and intracellular calcium transients ($I_{Cl.Ca}$). We discovered a novel Cl^- current ($I_{Cl.b}$) which is basally active in rabbit atrial myocytes. The single channel mechanism of $I_{Cl.b}$ and its potential physiological role were then studied. Using the excised inside-out patch clamp technique, a novel single channel of 60-pS conductance which showed strong outward rectification, Cl^--selectivity, and disulphate stilbene Cl^- channel blocker-sensitivity was characterized in rabbit atrial myocytes. The channel resembles outwardly rectifying Cl^- channels in non-cardiac systems, often referred to as ORCC. The ensemble-average current of cardiac ORCC resembles the whole-cell current of $I_{Cl.b}$, making $I_{Cl.b}$ a strong candidate for the macroscopic equivalent of ORCC. The potential physiological role of ORCC was supported by successful recording of ORCC in cell-attached membrane patches. Under basal isotonic conditions, single channel activity typical of ORCC was detected in about 5% (21/367) cell-attached patches. The macroscopic $I_{Cl.b}$ recorded under identical conditions were of the same order as estimated based on ORCC density, current amplitude and open channel probability. Exposure of cells to hypotonic media significantly increased cell volume (cell swelling) and the prevalence of active ORCC in cell-attached patches (to 16%) without affecting the conductance and open probability of the channel. At the whole-cell level, hypotonic cell swelling increased the amplitude of $I_{Cl.b}$ and hypertonic cell shrinking reduced $I_{Cl.b}$. These results indicate that $I_{Cl.b}$ and ORCC are regulated by cell volume, and may therefore play a role in cell volume maintenance of cardiac myocytes. Since it has long been realized that stimulation of α_1-adrenergic receptors causes a prolongation of cardiac action potential duration, the modulation of $I_{Cl.b}$ by α-adrenergic receptors under both isotonic and hypotonic conditions was studied. Application of α-adrenergic receptor agonists (phenylephrine, norepinephrine) caused a concentration-dependent inhibition of the current through a specific stimulation of α_{1A}-adrenergic receptors coupled with a PTX-sensitive G-protein induced activation of protein kinase C. These results suggest that ORCC may be a novel and potentially important membrane channel contributing to the control of cardiac electrical activity, volume status, and neural regulation.

RÉSUMÉ

Le potentiel d'action cardiaque est généré et modulé par les courants passant à travers divers canaux ioniques. Les canaux ioniques sont des protéines transmembranaires impliquées non seulement dans la conduction des impulsions électriques mais aussi dans le contrôle d'homéostasie cellulaire tel que le volume cellulaire de façon à maintenir des conditions physiologiques normales. Malgré le fait que les canaux chlores (Cl^-) ont été retrouvés dans la majorité de cellules, leurs rôles dans la physiologie cardiaque sont encore très mal connus. Depuis la découverte, sur le coeur, d'un courant Cl^- activé par l'AMP cyclique en 1989, l'attention est portée de nouveau aux canaux Cl^- cardiaques. Il a été mis en evidence que plusieurs types de courants Cl^- sont exprimés dans le coeur et activés respectivement par la protéine kinase C ($I_{Cl.PKC}$), des agonistes purinergiques ($I_{Cl.purinergic}$), l'enflement cellulaire ($I_{Cl.swell}$) et le transitoire calcique intracellulaire ($I_{Cl.Ca}$). Sur les myocytes auriculaires du lapin, nous avons découvert un nouveau courant Cl^- qui s'active en condition basale ($I_{Cl.b}$). Le mécanisme du $I_{Cl.b}$ au niveau du canal unitaire et son rôle physiologique ont été étudiés. A l'aide de la technique de 'voltage imposé' en configuration 'inside-out', nous avons detecté un canal ayant une conductance de 60-pS. Il est caractérisé par une forte rectification sortante, une sélectivité au chlore et une sensibilité au stilbène disulfate, un bloqueur des canaux Cl^-. Ce canal ressemble aux canaux Cl^- rectifiants sortants trouvés dans d'autres systèmes autre que le ceour et souvent désignés sous le nom de ORCC. La somme de courants unitaires de l'ORCC cardiaque est similaire au courant $I_{Cl.b}$ global, ce qui fait que le $I_{Cl.b}$ est fort probablement équivalent à l'ORCC macroscopique. Un rôle potentiel de l'ORCC dans la physiologie est suggéré par l'ORCC enregistré sur des morceaux membranaires en configuration 'cell-attached'. En condition isotonique basale, l'activité des canaux unitaires, typique à l'ORCC, a été détectée dans environ 5% (21/367) de cas. Le courant $I_{Cl.b}$ macroscopique enregistré en condition identique est du même ordre que celui de l'ORCC estimé d'après la densité de canaux, l'amplitude de courant unitaire et la probabilité d'ouverture. L'Exposition des cellules à un melieu hypotonique a significativement augmentée le volume cellulaire et la fréquence d'apparition de l'ORCC (de 16%) sur les membranes en configuration 'cell-attached'. Toutefois, cette condition n'a pas modifée la conductance ainsi que la probabilité d'ouverture du canal. Au niveau de la cellule entiere (whole-cell), l'enflement cellulaire hypotonique augmente l'amplitude de $I_{Cl.b}$. À l'inverse, l'enflement cellulaire hypertonique réduit l'amplitude du $I_{Cl.b}$. Ces résultats indiquent que le courant $I_{Cl.b}$ et l'ORCC sont modulés par le volume cellulaire, et pourraient donc jouer un rôle dans le maintien du volume de myocytes cardiaques. Car il a été connu depuis longtemps qu'une stimulation des récepteurs adrénergiques du type α_1 peut entraîner une prolongation du potentiel d'action cardiaque, nous avons étudié la modulation du courant $I_{Cl.b}$ par ces récepteurs en conditions isotonique et hypotonique. La présence des agonistes du récepteur adrénergique du type α (phényléphrine, norépinéphrine) provoque une inhibition du courant de façon dose-dépendante en stimulant spécifiquement les récepteurs adrénergiques du type α_{1A} associés à une activation de la protéine kinase C par la protéine G sensible au PTX. Ces résultats suggèrent que l'ORCC serait un nouveau canal transmembranaire potentiellement important et pourrait contribuer au contrôle de l'activité électrique cardiaque, du volume cellulaire et la régulation neuronale.

ACKNOWLEDGEMENTS

Dr. Stanley Nattel. MD, my supervisor, for his extraordinary supervision, consistent encouragement, close inspiration, and outstanding guidance, and for providing opportunities to study in a novel and exciting area of biomedical sciences. Were it not for his excellent suggestion, constructive discussion, criticism, and his valuable support, his constant availability, and his careful proof reading of the manuscript, this thesis may have never been completed.

Dr. Bernard Fermini. PhD, my teacher and friend, for teaching me patch-clamp techniques and theories, for his excellent supervision, helpful suggestions and discussions, criticisms, and encouragement. Without his initiation of my research on ionic currents in cardiac cells, this thesis may have never been completed.

Dr. A.C. Cuello, MD. Chairman of the Department of Pharmacology and Therapeutics, for allowing me the opportunity to pursue my graduate studies and for his encouragement and helpful advices during these years.

Dr. R. Capek, MD, PhD, my advisor, Vice chairman of the Department of Pharmacology and Therapeutics, for his helpful advice, suggestions, discussions, and encouragement, and for his consistent support in various aspects including the applications for studentships and fellowships.

Dr. Xiu Chen, MD, Professor of Pharmacology, Hunan Medical University, Chairman of Chinese Association of Cardiovascular Pharmacology, for his invaluable friendship, advice, encouragement, motivation, and consistent support. Were it not for his strong recommendation to pursue my PhD study in Dr. Stanley Nattel's laboratory at McGill University, this thesis may have never been completed.

Dr. A. Shrier, PhD. Professor of Physiology, for his encouragement, and consistent support in the applications for studentship.

Dr. N. Leblanc, PhD, my friend, Assistant Professor of Physiology, University of Montreal, for his helpful suggestions, discussion, and encouragement, and for his generous availability of experimental environment and equipment when needed.

Dr. Joseph R. Hume, PhD, Professor of Physiology, University of Nevada, for his invaluable suggestions, encourgement, discussion, and various support.

Ms. Guylain Nicol, for her valuable and excellent technical assistant in experiments and for her friendship and kind help in various aspects.

Dr. Lingyu Ye, MD, my wife, not only for her constant support and motivations and her sharing of weal and woe during all these years, but also for her valuable and excellent technical assistance with experiments.

Dr. Jean-Louis Schwartz, PhD, in the Indtitut de Biotechnologie, Montreal, Canada, for very useful advice regarding single channel data acquisition and analysis techniques.

Dr. Hui Sun, MD, PhD, for generously and carefully translating the "Abstract" into French.

Medical Research Council of Canada, for providing a Studentship Award from 1993 to 1996.

I would also like to express my appreciation to a number of graduate and postdoctoral students from whom I have learnt a lot and got help and encouragement in different aspects during these years, such as Suzanne Ranger, Christine Villemaire, Elias Bou-Abboud, Jinjun Wang, Hui Sun, Keli Hu, Lili Liu, Lixia Yue, Carmelle Remillard, Antonio Guia, Weiya Ma, Dingyou Li, Kai Li, Linsen Hu, Daochao Huang and so on. Special thanks to Dr. B. Esplin, Carol Mathews, Diane Mullins-Plant, Catherine Anley, Emma de-Blasio, Pierre Thai, Josie Buluran, Johanne Doucet, Nancy Turmel and Marie-Andrée Lupien for their friendship and invaluable assistance in different aspects of my study and work.

PREFACE

Note on the format of this thesis:

In accordance with the Faculty of Graduate Studies and Research the candidate has the option of including as part of the thesis the text of original papers already published by learned journals, and original papers submitted or suitable for submission to learned journals. The exact wording relating to this option is as follows:

> **Candidates have the option of including, as part of the thesis, the text of a paper(s) submitted or to be submitted for publication, or the clearly-duplicated text of a published paper(s). This text must be bound as an integral part of the thesis.**
>
> **If this option is chosen, connecting texts that provide logical bridges between the different papers are mandatory. The thesis must be written in such a way that it is more than a mere collection of manuscripts; in other words, results of a series of papers must be integrated.**
>
> **The thesis must still conform to all other requirements of the "Guidelines for Thesis Preparation". The thesis must include: A Table of Contents, an abstract in English and French, an introduction which clearly states the rationale and objectives of the study, a comprehensive review of the literature, a final conclusion and summary, and a thorough bibliography or reference list.**
>
> **Additional material must be provided where appropriate (e.g. in appendices) and in sufficient detail to allow a clear and precise judgment to be made of the importance and originality of the research reported in the thesis.**
>
> **In the case of manuscripts co-authored by the candidate and others, the candidate is required to make an explicit statement in the thesis as to who contributed to such work and to what extent. Supervisors must attest to the accuracy of such statements at the doctoral oral defense. Since the task of the examiners is made more difficult in these cases, it is in the candidate's interest to make perfectly clear the responsibilities of all the authors of the co-authored papers. Under no circumstances can a co-author of any component of such a thesis serve as an examiner for that thesis.**

This thesis is composed of the following published and submitted papers co-authored by myself and others.

Chapter 2

Dayue Duan, Bernard Fermini, Stanley Nattel, Sustained outward current observed after I_{to1} inactivation in rabbit atrial myocytes is a novel Cl^- current. *Am J Physiol* 1992; 263:H1967-H1971.

Chapter 3

Dayue Duan, Stanley Nattel, Properties of single outwardly rectifying Cl^- channels in heart. *Circ Res* 1994; 75:789-795.

Chapter 4

Dayue Duan, Joseph R Hume, Stanley Nattel, Evidence that outwardly-rectifying chloride channels underlie volume-regulated Cl^- currents in rabbit atrial myocytes. *Circ Res* 1996; in revision.

Chapter 5

Dayue Duan, Bernard Fermini, Stanley Nattel, α-adrenergic control of volume-regulated Cl^- current in rabbit atrial myocytes - characterization of a novel ionic regulatory mechanism. *Circ Res* 1995; 77:379-393.

Table of Contents

CHAPTER 6 GENERAL DISCUSSION AND DIRECTIONS FOR FUTURE RESEARCH

LIST OF FIGURES AND TABLES

Chapter 1

Chapter 2

Chapter 3

Chapter 4

Chapter 5

LIST OF ABBREVIATIONS

AC	Adenylyl cyclase
9-AC	Anthracene-9-carboxylate
ACh	Acetylcholine
AP(s)	Action potential(s)
4-AP	4-aminopyridine
APD	Action potential duration
ATP	Adenosine triphophate
AV	Atrioventricular
αAR	α-Adrenergic receptor
βAR	β-adrenergic receptor
cAMP	Adenosine-3',5-cyclic monophosphate
cDNA	Complementary DNA
CEC	Chloroethylclonidine
CF	Cystic fibrosis
CFTR	Cystic fibrosis transmembrane-conductance regulator
cGMP	Guanine-3',5'-cyclic monophosphate
CLC	Cloned voltage-gated chloride channel
CTX	Cholera toxin
DAD	Delayed afterdepolarization
DAG	Diacylglycerol
DIDS	4,4'-Diisothiocyanatostilbene-2,2'-disulfonic acid
DNDS	4,4'-Dinitrostilbene-2,2'-disulfonic acid
DPC	Diphenylamine-2-carboxylic acid
EAD	Early afterdepolarization
ECG	Electrocardiograph
EGTA	Ethylene glycol tetraacetic acid
E_{Cl}	Equilibrium potential for Cl^-
E_{rev}	Reversal potential
E_X	Equilibrium potential for ion X
GABA	γ-aminobutyric acid

GC	Guanylyl cyclase
GHK equation	The Goldman-Hodgkin-Katz constant field equation
G-protein	Guanine triphosphate binding protein
G_{α}	α-subunit of G-protein
$G_{\beta\gamma}$	β- and γ-subunits of G-protein
G_i	Inhibitory G-protein
G_s	Stimulatory G-protein
GTP	Guanine triphosphate
I_A	A-type transient outward current
I_{Ca}	Inward Ca^{2+} current
$I_{Cl.ATP}$	ATP-activated chloride current
$I_{Cl.b}$	Basally active background chloride current
$I_{Cl.Ca}$	Ca^{2+}-activated chloride current
$I_{Cl.cAMP}$	cAMP-activated chloride current
$I_{Cl.LC}$	Large conductance chloride channel
$I_{Cl.PKC}$	Protein kinase C-activated chloride current
$I_{Cl.swell}$	Swelling-induced chloride current
I_f	Hyperpolarization-activated pacemaker current
I_K	Delayed rectifier K^+ current
$I_{K.ACh}$	ACh-activated K^+ current
$I_{K.ATP}$	ATP-sensitive K^+ current
I_{K1}	Inward rectifier K^+ current
$I_{K.pl}$	Plateau-activated K^+ current
I_{Krl}	Rapidly activated delayed rectifier K^+ current
I_{Ks}	Slowly activated delayed rectifier K^+ current
I_m	Membrane current
I_{Na}	Inward Na^+ current
I_{to}	Transient outward current
I_{to1}	4-AP-sensitive, Ca^{2+}-insensitive transient outward current
I_{to2}	Ca^{2+}-sensitive transient outward current

IP_3	Inositol triphosphate
I-V	Current-voltage
5MU	5-methylurapidil
NE	Norepinephrine
NMDG	*N'*-methyl-D-glucamine
NPPB	5-nitro-2-(3-phenylpropylamono)-benzoate
ORCC	Outwardly rectifying chloride channel
PDD	Phorbol 12,13-didecanoate
PDE(s)	Phosphodiesterase(s)
pH_i	Intracellular pH
pH_o	Extracellular pH
PCR	Polymerase chain reaction
P-Gp	P-glycoprotein mediating multidrug resistance
PKA	Protein kinase A, cAMP-dependent
PKC	Protein kinase C
PKI	Protein kinase A inhibitor
pI_{Cln}	A protein giving rise to an outwardly rectifying Cl^- current in *Xenopus* oocytes
PLC	Phospholipase C
PLM	Phospholemman
PMA	4β-phorbol 12-myristate 13-acetate
PTX	Pertussis toxin
RMP	Resting membrane potential
SA	Sino-atrial
SITS	4-acetamido-4'-isothiocyanostilbene-2,2'-disulfonic acid
SR	Sarcoplasmic recticulum
TEA	Tetraethylammonium
V_m	Transmembrane voltage

STATEMENT OF AUTHORSHIP

This thesis is composed of four papers co-authored by myself and others. The following is a statement regarding the contributions of myself and others to this work.

The paper entitled "Sustained outward current observed after I_{to1} inactivation in rabbit atrial myocytes is a novel Cl^- current." (*Dayue Duan, Bernard Fermini, Stanley Nattel, Am J Physiol 1992; 263:H1967-H1971*) describes research in which the initial ideas and hypotheses, design of studies and protocols, performance of experiments, analysis of data, and writing manuscripts were largely my own. Dr. Stanley Nattel served in a close supervisory capacity, helping me clarify ideas and findings, analyzing the data, and improving the writing. Dr. Bernard Fermini actively participated in supervision of voltage-clamp experiments, extensively discussed the data. gave advices and suggestions, and read the manuscript.

The paper entitled "α-adrenergic control of volume-regulated Cl^- current in rabbit atrial myocytes - characterization of a novel ionic regulatory mechanism." (*Dayue Duan. Bernard Fermini, Stanley Nattel, Circ Res 1995; 77:379-393*) describes research in which the initial proposals, ideas and hypotheses, design of studies and experimental protocols, performance of experiments, analysis of data, and writing manuscripts were originally my own. Dr. Stanley Nattel served in a close supervisory capacity, helping me clarify ideas, analyzing the data, and improving the writing of the final version of the manuscript. Dr. Bernard Fermini participated in supervision, discussed the data. gave suggestions. and read the manuscript.

The paper entitled "Properties of single outwardly rectifying Cl^- channels in heart." (*Dayue Duan, Stanley Nattel, Circ Res 1994; 75:789-795*), describe research in which the initial proposals, ideas and hypotheses, design of studies and experimental protocols, performance of experiments, analysis of data, and writing manuscript were originally my own. Dr. Nattel served in a close supervisory capacity, helping me clarify ideas, analyzing the data. and improving the final version of the manuscripts.

The paper entitled "Evidence that outwardly-rectifying chloride channels underlie volume-regulated Cl^- currents in rabbit atrial myocytes." (*Dayue Duan, Joseph R Hume, Stanley Nattel, Circ Res 1996; in revision*) describe research in which the initial proposals, ideas and hypotheses, design of studies and experimental protocols, performance of experiments, analysis of data. and writing manuscript were originally my own. Dr. Joseph R Hume helped me in the analysis of single-channel kinetics. clarifying ideas, and was deeply involved in the rewriting of the final version of the manuscript. Dr. Nattel served in a close supervisory capacity, helping me clarify ideas, analyzing the data, and improving the final version of the manuscripts.

CHAPTER 1

INTRODUCTION

1. Electrophysiology of the heart

The heart has long been recognized as a vital organ whose rhythmic blood-pumping is essential for maintaining human life since the first description of the mammalian circulation by William Harvey in 1621.[1] To date, however, it is still not fully understood how the heart is regulated to meet all the needs for an individual to live in an extremely changeable environment. As technology advanced, first with photographic plates to record the motion of mechanically stimulated tissues and then rudimentary electrical recordings, the idea of the heart as a muscle that contained cellular elements with coordinated electrical activity took hold. With the development of microelectrode techniques over the last five decades came the advancement of cardiac electrophysiology. It is now recognized without doubt that the movement of ions across cardiac cell membrane generates the electrical potentials that activate the heart. The study of the electric activity of cardiac cells has hence become one of the most important approaches to investigating the mechanism of heart function. Today's electrophysiology and molecular biology are providing breathtaking new insights into the regulation of cardiac electrical activity at levels of the single cell, membrane ion channels and molecules.

1.1. Cellular electrophysiology of the heart

Although cardiac electrical activity similar to action potentials was observed in frog heart as early as in the end of 19th century by Burdon-Sanderson and Page[2], it was only after the development of the intracellular microelectrode technique and the successful application of this new technology in nerve and skeletal muscle during the 1940s and the 1950s that the path to the study of cardiac electrophysiology began to open.

Early in 1939, Alan Hodgkin presented strong evidence in favour of the electrical nature of impulse conduction in nerve as against chemically mediated propagation[3], and, about 10 years later, he provided evidence for sodium ion as the carrier for inward-activating current in squid axons[4] and frog skeletal muscle[5] by using the art of pulling and filling glass microelectrodes learned from Gilbert Ling in Chicago[6]. More importantly, Hodgkin and Huxley gave a quantitative description of membrane current and its application to conduction and excitation in nerve[7]. The Hodgkin-Huxley model for action potentials of the squid giant axon was the first model to recognize separate, voltage-dependent permeability changes for different ions. For the first time, in the absence of any knowledge of the membrane molecules involved (the ion channels), the ionic basis of excitation was correctly described and the membrane ionic theory of excitation was finally turned from untested hypothesis into established fact.

The first successful recording of the cardiac action potential was made in 1949 by Silvio Weidmann who was working in Hodgkin's laboratory at Cambridge. About this exciting and important discovery he wrote in a recent review: "On July 19th 1949, Wilhelm Feldberg demonstrated a Starling heart-lung preparation to a class of advanced physiology students. Subsequently, he allowed me to remove the dog's heart. The right ventricular wall was cut open and clamped to microscope stage. A microelectrode was ready to be pushed against the inside of the wall. Before this heart had time to die, I could see a regular sequence of three or four action potentials." [8]. These "three or four action potentials" not only opened the path for him to study cardiac electrical activity, but also ushered the history of cardiac electrophysiology into a new era - that of cellular cardiac electrophysiology. Soon, the theory of electrical transmission of impulse was extended to the heart[9]. In later studies, especially during the past fifteen years, investigators have taken advantage of new techniques like cell isolation and patch-clamp techniques[10] to study the electrophysiological properties of cardiac cells. This allowed a characterization of a number of ionic mechanisms that play a role in resting and action potentials. Cellular cardiac electrophysiology is thus proceeding at a faster pace and considerable knowledge has been gained about the relative contribution of the various ionic mechanisms to electrical activity and impulse propagation in heart. The basic concepts developed in this aspect include:

Cardiac cells, like other excitable cells of the body, are capable of generating a pattern of changes in transmembrane potentials to propagate electrical messages of excitation upon receiving stimuli. They share many bioelectrical properties with other excitable cells but have unique features as well.

Bioelectricity and sarcolemma of cardiac cells. The sarcolemma of cardiac cells is comprised of a phospholipid bilayer with its associated membrane glycoproteins[11]. The phospholipids are arranged so that their polar head groups lie at the inner and outer surfaces of the membrane while their hydrophobic fatty acyl chains are in the membrane core (Figure 1-1)[11]. Proteins can be extrinsic, adsorbed to the membrane surface, or intrinsic, either embedded in one leaflet of the phospholipid bilayer or spanning the entire membrane to make contact with both extra- and intracellular fluid. Intrinsic proteins tend to fold or coil so that their apolar amino acids are on the surface of the protein in the lipid bilayer of the membrane. Despite their relatively small fractional volume, proteins may comprise as much as half the membrane mass. The extrinsic proteins are often glycosylated and provide structural support. The intrinsic proteins serve as receptors, ion channels and pumps. The phospholipid bilayer structure of the sarcolemma poses a barrier to water-soluble molecules. This permeability barrier allows for the maintenance of concentration gradients between the cytoplasm and extracellular fluid. The cytoplasm contains proteins, organic polyphosphates, simple ions (e.g. Na^+, K^+, Cl^-) and other ionized substances that cannot freely permeate the plasma membrane. Typical normal values for ionic concentrations are listed in Table 1-1[12,13].

Bioelectricity is the result of charge movement in tissue.[14] The flow of charged ions across a cell membrane will generate membrane current. Current (I) may be described as the amount of charge (Q) passing a point per unit time, $I = dQ/dt$. One coulomb of charge (a mole of ions contains 96,486 coulombs of charge) per second is one ampere (A). By convention, transmembrane current flow is designated as negative or inward when positively charged ions move into the cell and as positive or outward when positively charged ions move out of the cell. The total transmembrane current (I_m) is the sum of all ionic currents flowing at the instant when measurements are made. The relationship between I_m and the electrical force that causes charges or ions to move , the transmembrane voltage (V_m), is governed by Ohm's law:

$$I_m = V_m/R \qquad (1\text{-}1)$$

where R is resistance. One ohm (Ω) is the amount of resistance that requires 1 V of force to cause 1 A of current flow. When membrane resistance is constant over a range of membrane

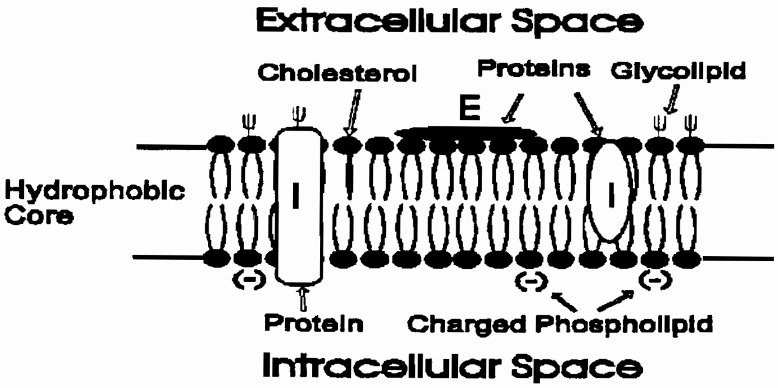

Figure 1-1. Schematic representation of sarcolemma of cardiac cells. The membrane is composed of lipid bilayer in which the polar heads (small circles) of the phospholipid molecules face the extracellular and intracellular surfaces while the fatty acid tails (containing double bonds and represented by the kinked tails) face the core of the bilayer. Proteins can be intrinsic (I) or extrinsic (E). One of the proteins and several of the lipids (glucolipids) are represented as containing a carbohydrate substituent (ψ). The charged phospholipids are shown on the intracellular side. (modified from Stiles GL: Structure and function of cardiovascular membranes, channels, and receptors. In Schlant RC and Alexander RW (eds): The heart, ateries and veins (8th ed.). McGraw-Hill Inc. 1994; 47)[11]

Table 1-1 Free ionic concentrations and equilibrium potentials for cardiac myocytes[12,13]

Ion	Extracellular Concentration $[X]_o$ (mM)	Intracellular concentration $[X]_i$ (mM)	$\frac{[X]_o}{[X]_i}$	Equilibrium Potential E_x (mV)
Na^+	140	25	5.6	+46
K^+	4	150	0.027	-97
Cl^-	120	10 ~ 37	12 ~ 3.2	-65 ~ -30
Ca^{2+}	2	10^{-4}	2×10^4	+120

potential, the current is ohmic or unrectified. Channels are said to rectify when they conductions more efficiently in one direction across the membrane than the other. Membrane behaviour is often described in terms of conductance (g), which is the inverse of resistance and is measured in siemens (S). The conductance for an ion depends on the ion concentration and on membrane permeability to the ion. The hydrophobic bilayer of the sarcolemma is about 50 Å in width and has substantial capacitance to store charge. The amount of charge (q) stored by a capacitor is proportional to the voltage difference across the membrane and its capacitance:

$$q = CV \qquad (1\text{-}2)$$

Total membrane current is equal to the sum of ionic currents and current flowing to charge the capacitance. The capacitance is charged with a time constant proportional to the product of membrane resistance and capacitance - once the capacitance is charged, membrane current is the sum of ionic currents alone.

Resting transmembrane potential and ionic equilibria. In resting cardiac cells, the cytoplasm is usually electrically negative (about -60 to -90 mV) relative to the extracellular fluid.[14] The transmembrane potential at rest is termed resting membrane potential (RMP). The RMP is important in controlling the electrical activity of cardiac cells. A reduction in the degree of electronegativity of RMP (depolarization) may be sufficient for the membrane potential to reach a threshold value and the cell will be excited and a complex sequence of time-dependent changes in transmembrane potentials will occur. In normal cardiac myocytes, RMPs are determined by the concentration gradients of several ions (mainly Na^+, K^+, Ca^{2+}, and Cl^-) on either side of the membrane and the permeability of the membrane to each ion. The resting transmembrane concentration gradients for these ions are established by active ionic pumping and the membrane conductance for these ions. If there is no voltage gradient across the membrane and the membrane were semipermeable to an ion, the movement of the ion will be determined only by the concentration gradient across the membrane and the permeability of the membrane to the ion. The transmembrane voltage at which electrochemical equilibrium occurs is called the equilibrium voltage or equilibrium potential. The Nernst equation can be solved for the equilibrium potential (E_x) for a particular ion (X) that will maintain the existing transmembrane concentration gradient of the ion at a constant value:

$$E_x = \frac{RT}{zF} \ln \frac{[X]_o}{[X]_i} \qquad (1\text{-}3)$$

where R is the gas constant, T is the absolute temperature, z is the valence of the ion, F is the Faraday constant, $[X]_o$ is the concentration of the ion in the extracellular fluid, and $[X]_i$ is the intracellular concentration of the ion. Therefore, the equilibrium potential for an ion can be given by the Nernst equation if the concentrations of the ion in both extra- and intracellular fluids are known. Based on the concentration gradients of some ions measured in cardiac myocytes under physiological conditions as listed in Table 1-1, their equilibrium potentials can be calculated according to equation 1-3 (see Table 1-1).

By assuming that, in the steady state, the sum of the fluxes of Na^+, K^+, and Cl^- is zero, the Goldman-Hodgkin-Katz (GHK) equation provides the membrane potential (V_m):

$$V_m = \frac{RT}{F} \ln \frac{P_{Na}[Na]_o + P_K[K]_o + P_{Cl}[Cl]_i}{P_{Na}[Na]_i + P_K[K]_i + P_{Cl}[Cl]_o} \qquad (1\text{-}4)$$

where P is the permeability coefficient. The GHK equation is known as the constant field equation because the expression for the driving force of the flux of the individual ions are derived by assuming that the electrical field within the membrane is of constant strength. If one of the permeability coefficients in equation 1-4 becomes very large relative to the others, then the predicted membrane potential approaches the equilibrium potential for the highly permeable ion. Since the resting membrane is permeable primarily to K^+, the resting V_m (RMP) of most cardiac cells is close to E_K. However, other ions, such as Na^+, make small contributions to the RMP, as does the Na^+-K^+ pump (it exchanges 3 Na^+ for 2 K^+).[14]

The cardiac action potential. The membrane current due to passive ion flux is a function of driving forces and permeabilities for various ions. Depolarization occurs when positively charged ions enter or negatively charged ions leave the cytosol; the opposite produces repolarization (see Table 1-2). When excited, cardiac cells produce an action potential (AP), i.e., a sudden regenerative depolarization of V_m followed by a complex voltage-time course back to the RMP. For purposes of description and discussion, cardiac APs are divided into five voltage- and time-dependent phases (Figure 1-2B)[15], including a rapid depolarization (upstroke) phase (phase 0), an early-fast repolarization to the plateau level (phase 1), a plateau phase (phase 2), a late repolarization to the resting potential (phase 3) and a diastolic or resting phase (phase 4). The most striking attribute of cardiac APs is a much longer plateau phase and total action potential duration (several hundred milliseconds) compared to the brief APs of nerves and skeletal muscle (typically < 5 ms). The long action potential duration (APD) of cardiac cells has an important physiological significance in preventing cardiac arrhythmia, and several ionic mechanisms are known to contribute to this feature (see details below).

Table 1-2 Ions as charge carriers across cell membrane.

Ion	Charge	Direction of Passive Flux at 0 mV	Current Generated	Effect on Membrane Potential
Na^+	Positive	inward	inward	depolarization
K^+	Positive	outward	outward	repolarization
Cl^-	Negative	inward	outward	repolarization
Ca^{2+}	Positive	inward	inward	depolarization

It is now increasingly recognized that the electrophysiologic behaviour of the heart is highly heterogeneous. This heterogeneity may be physiologic, as occurs during development, or as a function of location within the heart. It has been found that RMPs and APs in heart are different from cell to cell in various anatomical regions (Figure 1-2). While myocytes in atrium and ventricle, and Purkinje fibres have a steady value of RMP during phase 4, automatic cells in the sino-atrial (SA) and atrioventricular (AV) nodes and His-Purkinje system have no well-defined RMP because the membrane depolarizes continuously during phase 4 (pacemaker potential) after reaching a maximal V_m at the end of phase 3.[16] Excitation occurs when the pacemaker potential achieves the critical threshold voltage. The firing rate of a normally automatic cell is determined by a) the value of maximal diastolic voltage, b) the slope of phase 4 depolarization, and c) the value of the threshold voltage. Basal cardiac rhythm originates from the spontaneous depolarization of SA nodal P cells, and the resulting action potential is conducted through muscle cells of crista terminals, atria, AV node, His bundle, and Purkinje fibres in such a sequence as to ensure contraction of the atria followed by contraction of the ventricles [12]. The sequence of the propagation of the cardiac impulse (the depolarization and repolarization waves) can be amplified and recorded on the body surface which is manifest as electrocardiograph (ECG) as shown in Figure 1-2C.

The movement of ions across cardiac cell membrane is regulated by pores formed by members of an extended family of ion channel proteins.[17] These ion channels play crucial roles in generating and regulating cardiac RMP and AP.

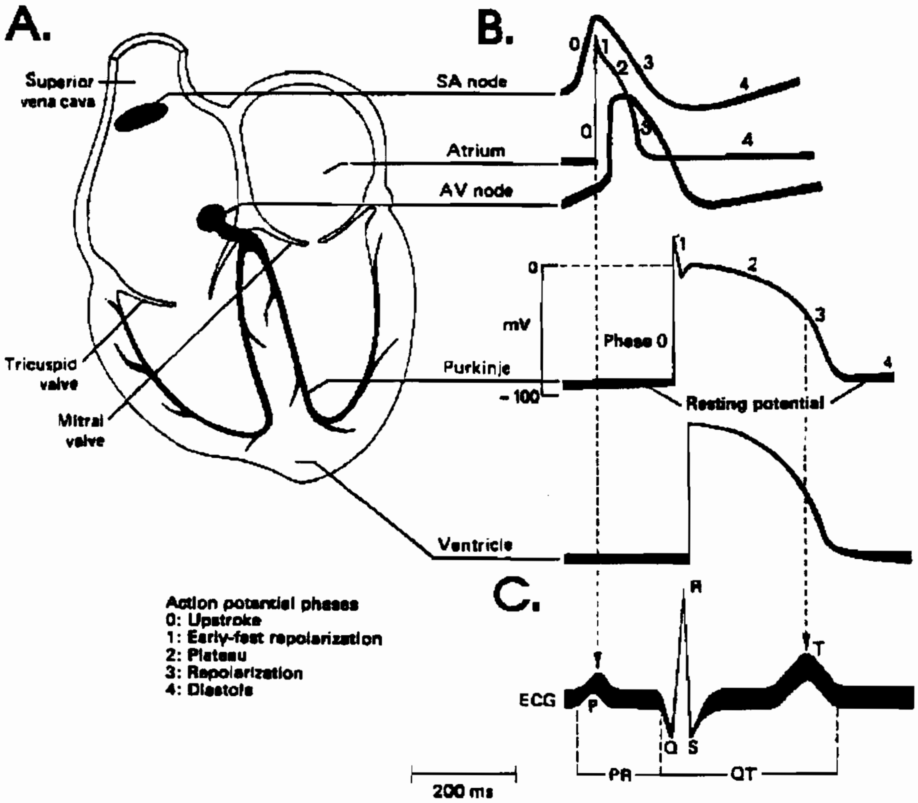

Figure 1-2. Schematic representation of anatomy and characteristic action potentials of the specialized impulse generating and conducting system of the heart. A. Diagram of the conduction system of the heart. B. Typical action potentials from different locations within the heart. The action potentials of atrial and ventricular myocytes and Purkinje fibre have five phases, 0 through 4. They have steady RMP and, when activated, generate a fast-rising, large-amplitude phase 0. The SA and AV nodal cells have no well-defined RMP. When excited, they generate relatively slow rising phase 0 and phase 1, 2, and 3 are not clearly distinguishable from one another. C. Relationship of action potentials to the electrocardiogram (ECG). (Modified from Hondeghem LM and Mason JW: Agent used in cardiac arrhythmias. In: Katzung BG (ed): Basic and clinic Pharmacology (fifth ed). Norwalk, Connecticut/San Mutea, California. 1992; 199)[15]

1.2. Ion channels

Ion channels are membrane-spanning proteins present in most or all eukaryotic cells where they function primarily to regulate the flow of ions across the cell membrane and thereby create ionic currents and control the electrical potential across the cell membrane and many other physiological processes involved in the maintenance of cell homeostasis such as secretion, signal transduction, and regulation of cell volume and intracellular pH.[17, 18] Therefore, ion channels are the fundamental molecular unit in the study of cardiac electrophysiology.

Ion channels can be thought of as a passive conduit through which ions move down a concentration gradient. That is to say, energy in the form of adenosine triphosphate (ATP) is not expended during ion movement. This is in contrast to an energy-dependent ion pump, which can move ions against concentration gradient.[19] Ion channels are often categorized by their ionic selectivity and whether they promote outward or inward currents. The K^+-selective channels allow K^+ to move down its concentration gradient and hence to move out of the cell and generate an outward current. The Cl^--selective channels will allow Cl^- to move into the cell and also generate an outward current. The outward current channels act to hyperpolarize the cell and, therefore, frequently is responsible for repolarization of the action potential. There are two main inward current channels that promote depolarization of the cell: the Na^+ and Ca^{2+} channels (see Table 1-2).

Under the appropriate conditions a single channel can maintain a high degree of specificity toward a single type of ion yet allow more than a million of these ions to pass per second. If the channel were to remain open, an ionic equilibrium would quickly be reached between the outside and inside of the cells and no ionic gradient or electrical potential across the cell membrane would be maintained. This would lead to cellular dysfunction and/or death. To serve their physiological function, ion channels must have the ability to open and close in response to the cell's needs or appropriate stimuli. In fact, the behaviour of ion channels is much more complex, in that channels can exist in three types of functional states: available (closed but ready to open), activated (open), and inactivated (closed and unavailable to open) (Figure 1-3). The process going from the available to the activated state is activation, return to the available from the activated state is deactivation, from the activated to the inactivated state is inactivation, and from the inactivated to the available state is recovery. The kinetic behaviour of channels undergoing these state changes are time- and voltage-dependent and so the channel state can both influence the time course of the AP and be influenced by it. The mechanism of controlling these functional states was first postulated by Hodgkin and Huxley to be a "gating mechanism".[6] In fact, several distinct signalling processes, including voltage changes across the membrane, the binding of hormones or drugs, and mechanical stimulation of the channel, can regulate the function of ion channels. Therefore, ion channels are generally grouped into voltage-gated, ligand-gated, and mechanically-gated channels. Ligand-gated channels such as the nicotinic acetylcholine receptor and γ-aminobutyric acid (GABA) receptor mediate local increases in ion conductance at chemical synapses and thereby depolarize or hyperpolarize the subsynaptic area of the cell. The opening or closing of the channel is dependent on continued occupation of the receptor by the ligand. In contrast, voltage-gated channels mediate rapid, voltage-dependent changes in ion permeability during action potentials in excitable cells and also modulate membrane potentials and ion permeability in many unexcitable cells. The opening and closing of the channel is dependent on the electric field. The fact that external stimuli can regulate channel pore opening and closing immediately begins to give insight into the protein architecture of the channel: 1) a membrane-spanning protein that allows a pore to form; 2) inherent properties of the pore to allow specific ions to enter and traverse the pore; 3) the ability to open and close; 4) regulatory regions through which the appropriate signals

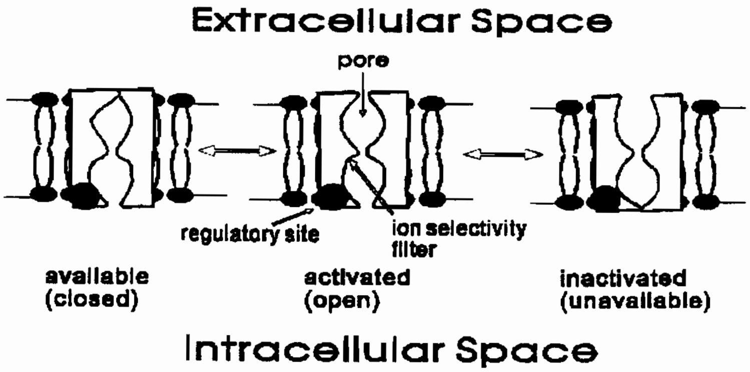

Figure 1-3. Schematic representation of a generic ion channel in lipid bilayers. The major functional features of the channel are depicted. These include a central pore, or "channel", through which ions can pass and a selectivity filter that permits only a specific ion to pass. The regulatory site represents a domain on the protein responsible for regulating the function of the channel. Three discrete functional states of the channel are shown - closed, open, or inactivated. (modified from Stiles GL: Structure and function of cardiovascular membranes, channels, and receptors. In Schlant RC and Alexander RW (eds): The heart, ateries and veins (8th ed.). McGraw-Hill Inc. 1994; 50)[11]

can be imparted to the channel (see Figure 1-3 for a schematic representation). The widespread application of the techniques of protein biochemistry and molecular biology to the elucidation of a tentative structure for various receptors and ion channels of excitable cells including the heart in the past decade has shown that ligand-gated ion channels and voltage-gated ion channels are often encoded by different multigene families.[20] Ligand-gated ion channels belong to the receptor superfamily which contains not only a ligand-binding site but also an ion channel that is activated by ligand-binding (Figure 1-4E). Voltage-gated Na$^+$, Ca^{2+} and many K$^+$ (Kv1, Kv2, Kv3, and Kv4) channels share a distinct six-membrane spanning segment motif and are thought

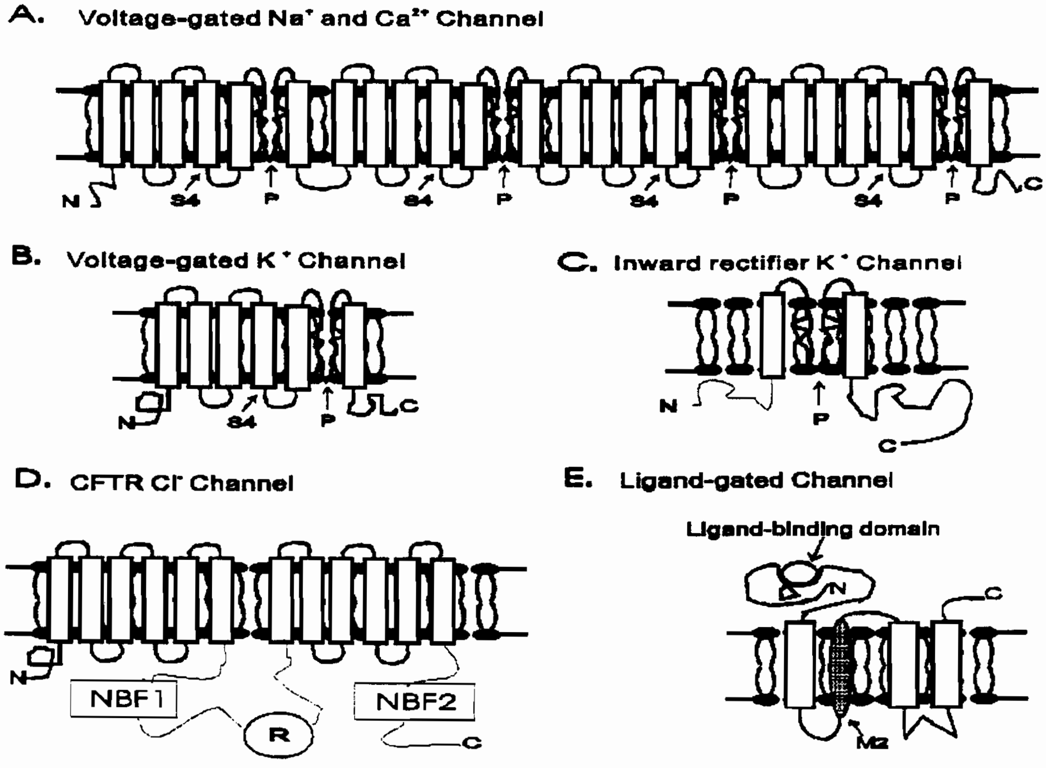

Figure 1-4 Predicted transmembrane topologies of ion channel families. Rectangles are putative transmembrane α-helices. N and C indicate the termini of the amino acid sequence. A. α or α_1 subunit of voltage-gated Na$^+$ or Ca^{2+} channel. The transmembrane regions are grouped into four covalently linked motifs each containing six transmembrane spans. With each motif there is a specific span termed the S4 region that likely contains the voltage sensing region. P indicates the pore region; jugged structure signifies putative β-strand. B. α subunit of voltage-gated K$^+$ channel. A single transmembrane motif comprises the channel pore. Functional channel contains four such motifs which are noncovalently linked. C. Inward rectifier K$^+$ channel. D. CFTR Cl$^-$ channel. NBF1 and NBF2, nucleotide binding folds 1 and 2; R, regulatory domain. E. Ligand-gated channel. Ligand-binding domain is extracellular; M2 pore-lining domain is shown as a dark spindle. (Modified from McDonough S and Lester HA: Overview of the relationship between structure and function in ion channels. Drug Development Research 1994; 33(3):190-202)[20]

to belong to another multigene family which contain a voltage sensor and change their conformational structure upon changes in membrane potential (Figure 1-4A,B). More recently, however, complementary DNA (cDNA) encoding other voltage- or ligand-gated ion channels in the heart which bear no structural similarity to any other ion channels have also been reported, such as a family of inwardly rectifying potassium (Kir) channels (Figure 1-4C), and an alternatively spliced form of the cystic fibrosis transmembrane-conductance regulator (CFTR) which encodes a cardiac chloride channel activated by second messenger intracellular cAMP-protein kinase A (Figure 1-4D) etc [20].

1.3. Relationship between ion channels and cellular electrophysiology

Conformational changes in channel proteins regulate membrane currents and in turn control electrical activities of the heart. With the application of the voltage-clamp and especially the patch-clamp techniques in the past fifteen years, has come the identification of the multiple ion channels whose integrated behaviour makes up the cardiac AP.

The heart is activated by propagated APs whose ***depolarization*** depends on the inward flux of Na^+ or Ca^{2+} through Na^+ or Ca^{2+} channels. The depolarizing currents carried by these two types of channels have different roles in different regions or cells of the heart. Depolarization of fast response cells (atria, ventricles, and His-Purkinje system) is generated by the opening of Na^+ channels. Rapid propagation of the wave of depolarization in atria and ventricles gives rise to the P wave and QRS complex of the ECG, respectively (Figure 1-2C). Depolarization of slow response cells (SA and AV nodal cells) depends on the slower opening of smaller Ca^{2+} channels, so that nodal conduction is much slower than in cardiac tissues that use Na^+ as the depolarizing cation. The slow rate of conduction mediated by Ca^{2+} channels in the AV node is largely responsible for the conduction delay during the PR interval of the ECG (Figure 1-2C).

Na^+ current (I_{Na}): Depolarization to the threshold V_m (about -70 mV) activates the voltage-gated Na^+ channels and results in a very large and brief inward I_{Na} to produce a regenerative depolarization, that underlies the upstroke of the AP and drives impulse propagation in fast response cells. These channels represent a family of large proteins with multiple subunits[21]. The main subunit (α-subunit) contains about 2000 amino acids and includes four major repeated internal sequences that represent four covalently-linked motifs each containing six transmembrane spanning domains (Figure 1-4A). These Na^+ channels are sparse or absent in SA and AV nodal cells.[22] The main modulator of the conductance of the Na^+ channel is the value of V_m at the time of activation.[23] As V_m becomes less negative, the Na^+ channel will inactivate so that the inward current during activation becomes less intense. The weaker the I_{Na}, the smaller the amplitude and rate of rise of phase 0 and the slower impulse conduction will be. The speed of recovery of Na^+ channels from voltage-dependent inactivation determines the rate at which a series of impulses can be generated and conducted. Therefore, the recovery of I_{Na} and the refractory period of the heart are intimately related.[23]

Ca^{2+} current (I_{Ca}): In the heart, I_{Ca} is carried by at least two types of voltage-gated Ca^{2+} channels: the L-type ($I_{Ca.L}$) and T-type ($I_{Ca.T}$) Ca^{2+} channels.[24] **$I_{Ca.L}$** is the Ca^{2+} current that is activated regeneratively from a relatively depolarized threshold potential (-40 mV) to produce depolarization and impulse propagation in SA and AV nodal cells. It is also present in fast response cells, where it contributes to the plateau of the AP and triggers Ca^{2+} release from the sarcoplasmic reticulum (see below). It is inactivated by both depolarization and cytosolic Ca^{2+} ($[Ca^{2+}]_i$), but it lasts long enough to contribute to overall plateau currents. The L-type Ca^{2+} channel also represents a family of proteins with multiple subunits. The structure of the main subunit (α_1-subunit), which determines the voltage- and pharmacological sensitivity of the channel, is quite similar to that of voltage-gated Na^+ channel (Figure 1-4A). $I_{Ca.L}$ is the target for clinically useful Ca^{2+} channel blockers such as the dihydropyridines, verapamil, and diltiazem, and is strongly modulated by neurotransmitters [24](see details in the following section). **$I_{Ca.T}$** activates rapidly at potentials to about -70 mV and decays completely and rapidly. It has been identified in pacemaker tissue and probably contributes inward current to the late stages of phase 4 depolarization in S node and His-Purkinje cells. It may also play a role in abnormal automaticity in atria. It is almost absent from ventricular cells.

Other inward currents contributing to normal action potential under physiological conditions have also been reported.[25,26] I_f has been recorded in SA and AV nodal cells and His-Purkinje cells in various species. It is an inward current carried by Na^+ through a relatively nonspecific cation channel that is activated at hyperpolarizing potentials and generates phase 4 depolarization that contributes to pacemaker function.[25]

Cardiac ***repolarization***, and thus the T wave and the QT interval of the ECG, is caused by outward currents that restore the membrane potential to its initial resting levels after depolarization. It is a much more complicated process than depolarization and is controlled largely by various K^+ and probably Cl^- channels. Some pump (Na-K pump) and exchanger currents (Na-Ca exchanger) have also been demonstrated to play a role in cardiac repolarization. Among these repolarizing currents, K^+ channels are the largest group of ion channels and have long been believed to be the most fundamental and major repolarizing currents in the heart under physiological conditions (and thus are the major targets for many antiarrhythmic agents). More cDNAs have been cloned for K^+ channels than for the other main categories of voltage-gated ion channels such as Na^+, Ca^{2+}, and Cl^- channels. Kv channels are composed of four subunits with each about one quarter the size of the voltage-gated Na^+ channel subunit (Figure 1-4B). Kir channels[39] contain only two transmebrane domains (Figure 1-4C). It has not yet been possible to match definitively the cloned K^+ channels with the naturally functional currents.

Phase 1 repolarization results primarily from the inactivation of I_{Na} and the activation of a short-lived outward current known as the transient outward current (I_{to}).[27,28] A similar current, called I_A, is also found in a variety of other excitable cells. I_{to} in heart has two components, one being voltage-activated (I_{to1}) and the other activated by $[Ca^{2+}]_i$ (I_{to2}).[29-31] Although early studies suggested that I_{to1} was carried by Cl^-,[32-35] extensive evidence from later studies[27,30,36-39] demonstrated it to be carried by K^+ (see Section 3). Until recently it was thought that I_{to2} was also carried by K^+.[29-31] However, recent studies have shown that I_{to2} exhibits a Cl^- dependence, suggesting I_{to2} is carried by a Ca^{2+}-activated Cl^- channel.[40,41] A "notch" (see Figure 1-2B) marks the end of phase 1 repolarization and the onset of the plateau phase in fast response cells. The level of membrane potential achieved during inscription of the notch can profoundly influence both the duration and voltage of the plateau and the remainder of the AP. Therefore, currents flowing in phase 1 and their effects on membrane potential can affect events occurring later in the cardiac cycle.

The plateau of the AP (phase 2) is due to a fine balance between inward and outward currents. The major factors underlying the plateau phase are 1) depolarizing currents through a small number of Na^+ channels that either open with long latencies or remain open because they failed to inactivate; 2) I_{Ca} activated during the upstroke which is an important determinant of both plateau voltage and APD; 3) repolarizing currents carried through three or more distinctive K^+ channels, including the delayed rectifier K^+ current (I_K),[28,39,42] the plateau-activated K^+ current ($I_{K.pl}$),[43] and the Ca^{2+}-activated K^+ current ($I_{K.Ca}$).[39] In addition, at least one other channels can come into play during ischemia, the ATP-sensitive K^+ current ($I_{K.ATP}$).[44] Activation of $I_{K.ATP}$ in response to a decrease in the intracellular ATP level can result in a very powerful, sustained repolarization capable of strongly foreshortening the plateau and APD and accelerating the onset of phase 3.

Phase 3 repolarization starts when I_{Ca} decays as a result of time-, voltage-, and $[Ca^{2+}]_i$-dependent inactivation, and the unopposed repolarizing influence of outward K^+ currents then terminates the plateau. At least two K^+ channels are activated during phase 3; however, their relative importance to the phase 3 repolarization process has been debated.[45] Although opinion is devided, I_K is now thought to play an important and major role in this repolarization process, particularly when the heart rate is high and sustained.[46] The activation and deactivation kinetics of I_K are quite slow (i.e., the time constants for these two processes are in the hundreds of milliseconds),[28,39] and its magnitude varies greatly between different species. Recent studies revealed several biophysically and pharmacologically different I_K channels,[42,46] a subset of which can be modulated by neurotransmitters.[42,47] A rapidly activating I_K (I_{Kr})[42] is recently thought to be encoded by the human ether-a-go-go-related gene (HERG) which is related to chromosome 7-linked long QT syndrome.[48] The inwardly rectifying K^+ current (I_{K1})[39,49] may play a lesser role in determining AP shape because it exhibits strong inward rectification (i.e., it conducts an inward current at potentials negative to E_K with greater conductance than that for the outward current occurring when the membrane is depolarized during the plateau). However, I_{K1} may be the major repolarizing current flowing during late repolariztion when other K^+ channels have undergone either deactivation or inactivation. Enhancement of I_{K1} can shorten APD by accelerating phase 3 and abbreviating the plateau phase.[45] Because I_{to} inactivates very quickly during the plateau phase and recovers very slowly (tens to hundreds of milliseconds),[50] even in the cardiac tissues that are said to exhibit a steady-state I_{to} (i.e., an I_{to} "window current"), there can be little I_{to} available during phase 3 and I_{to} thus may have little significant direct role in the late repolarization. However, as mentioned above, because I_{to} affects the voltage of the plateau and in turn some membrane currents during subsequent repolarization, it can in fact influence late repolarization indirectly. Two electrogenic ion translocation process, the Na^+-K^+ pump (each cycle transports 3 Na^+ out and 2 K^+ into the cell and generates an outward current)[51] and the Na^+-Ca^{2+} exchanger[52] (each cycle exchanges 1 Ca^{2+} for 3 Na^+ and generates a current whose direction depends on the relation between the Na^+ and Ca^{2+} gradients and the membrane potential), also may contribute to repolarization according to their respective voltage dependence and can effect AP shape and duration. Both can also affect the plateau and RMP, although the effect is usually limited to a very few milllivolts. When the cellular membrane resistance is increased, the influence of these currents on RMP and APs can be augmented.

Finally, as the membrane repolarizes to RMP, the Na^+ channels undergo the process of recovery from inactivation and excitability is restored in readiness for generating the next AP. The other currents (I_{Ca}, I_{to}, I_K etc.) return to their steady-state levels with recovery time courses distinctive for each. The membrane conductance again becomes dominated by I_{K1}. I_{K1} is essential for maintaining a stable resting potential near E_K in atrial, AV nodal, His-Purkinje, and ventricular cells.[48] Its absence from SA node cells is important in allowing small currents control the pacemaker rate.

2. Autonomic regulation of cardiac action potential and ion channels

Although the normal cardiac rhythm is determined by the rate of spontaneous depolarization of SA nodal cells, the resultant heart rate is influenced by other various factors, including the activity of autonomic innervation and the levels of circulating hormones, which are superimposed on basal cardiac activity. In fact, the normal mammalian heart responds in a highly coordinated fashion to finely balanced inputs from both sympathetic and parasympathetic limbs of the autonomic nervous system. Stimulation of sympathetic nerve leads to the release of norepinephrine (NE) and epinephrine from adrenal medulla into the blood and NE from its terminals throughout the body. The predominant neurotransmitter released at the parasympathetic nerve terminals is acetylcholine (ACh). These neurotransmitters, hormones, and other paracrine or autocrine factors (e.g., adenosine) may interact directly with the proteins of ionic channels, pumps or exchangers in the heart or influence these proteins through distinct ***receptors*** at the cell surface which, in turn, influence the initiation and propagation of cardiac APs. The receptors in the heart, including muscarinic (mainly M_2), α- (mainly α_1) and β-adrenergic (β_1, β_2), and purinergic (A_1, P_2) receptors, are coupled to their effectors (e.g., enzymes and ion channels) by a family of guanine-triphosphate (GTP)-binding proteins (G-proteins) which lie just inside the membrane.[53] External stimulation of these receptors, such as binding with their agonists, will activate specific G-proteins (Table 1-3). The G-protein can then modulate ion channel activity either *directly* through intramembrane interactions or *indirectly* via a second-messenger intracellular signalling system. Several regulatory cascades have been identified for regulation of ion channels. They include the adenylyl cyclase (AC) system, phosphatidylinositol turnover, the guanylyl cyclase (GC) system, and tyrosine kinases. G-proteins play a critical role in regulation of cardiac electrophysiology.[54-57]

2.1. Signal transduction pathways in the regulation of cardiac ion channels

Ion channels in the heart are regulated in several ways. They are sensitive to changes in transmembrane voltages or directly activated by extracellular hormones and neurotransmitters. They may also be phosphorylated and dephosphorylated by intracellular kinases and phosphatases or directly gated by membranous transduction elements such as G-proteins (Figure 1-5). With

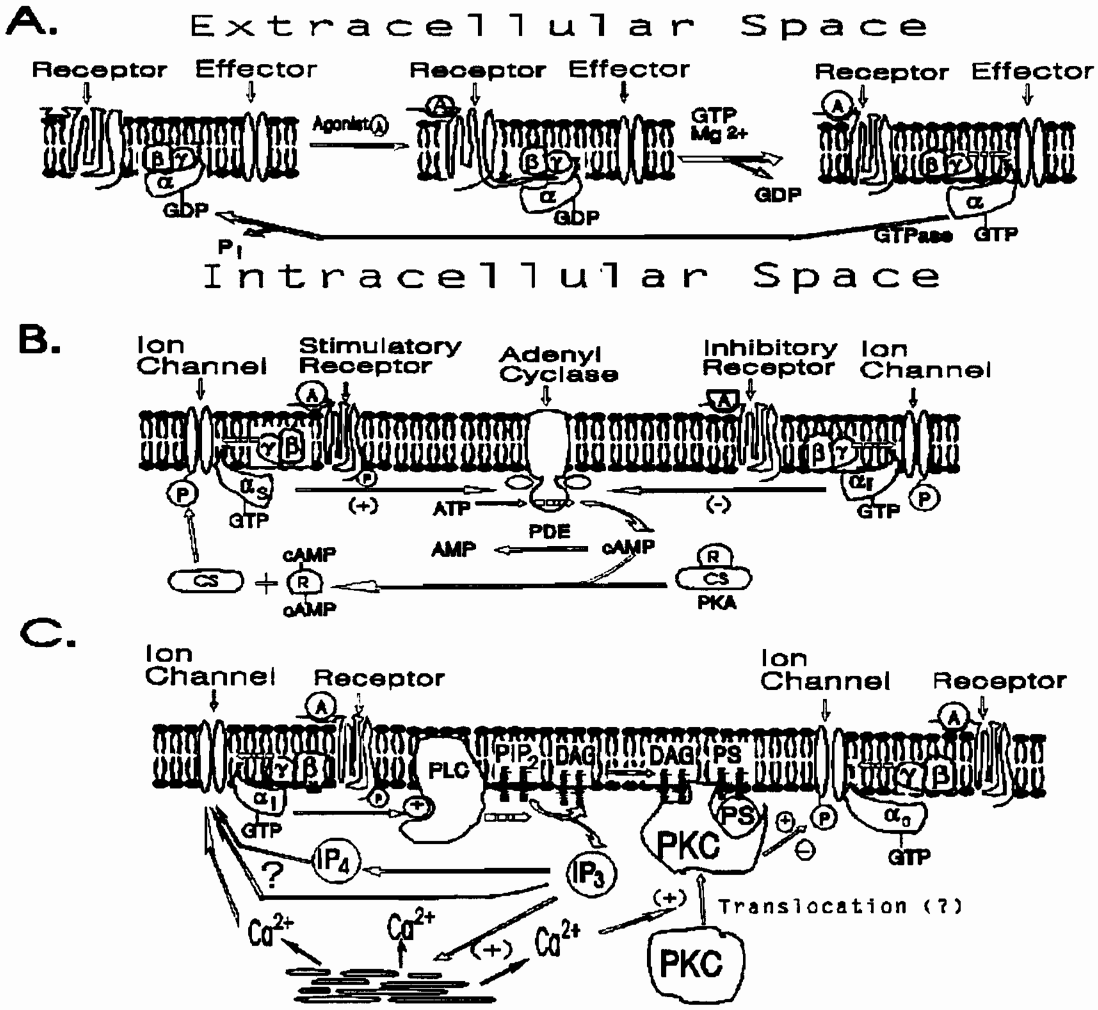

Figure 1-5 Signal transduction pathways in regulation of cardiac ion channels. A. When a heptahelical receptor is bound by agonist (A), G-protein associates with the receptor. The G-protein heterotrimer splits into α- and $\beta\gamma$-subunits as GTP replaces GDP on the α-subunit in the presence of Mg^{2+}. Some α-subunits are attached to the membrane via myristate; most $\beta\gamma$-subunits are hydrophobic. The α-subunit then activates the effector in most cases. $\beta\gamma$-subunits act as activators in the other cases. After hydrolysis of GTP to GDP, α- and $\beta\gamma$-subunits reassociate, ending the cycle. B. Stimulation of β_1-adrenergic and other stimulatory receptors results in G$_s$ activation, activating AC and generating cAMP. cAMP binds to the regulatory subunit of PKA, allowing the catalytic subunit (CS) to catalyze the phosphorylation of a target protein (ion channel). Stimulation of inhibitory receptors (M$_2$-cholinergic and α-adrenergic receptors) activates G$_i$ and inhibits AC activity. C. Activation of G$_i$ or G$_o$ binding of receptor agonists stimulates the enzyme phospholipase C (PLC). PLC catalyzes the division of PIP$_2$ into diacyglycerol (DAG) and inositol triphosphate (IP$_3$). DAG activates PKC in the presence of phosphatidylserine (PS) and Ca^{2+}. PKC can then phosphorylate an ion channel protein. IP$_3$ releases Ca^{2+} from intracellular sources. (Modified from Clapham DE [55]).

the discovery of adenosine 3',5'-cyclic monophosphate (cAMP) in 1957 and AC as the enzy me responsible for its synthesis by Sutherland et al,[54] the second-messenger hypothesis of cell signalling was born. Since then, other membrane-generated messengers have also been identified, including guanosine 3',5'-cyclic monophosphate (cGMP), diacylglycerol (DAG), inositol triphosphate (IP_3), arachidonic acid and its products such as prostaglandins, leaukotrienes, and epoxides. So far, the best understood signal transduction pathways are the AC system and phosphatidylinositol turnover. As shown in Figure 1-5B, stimulation of receptors activates or inhibits AC activity via stimulatory or inhibitory G-proteins (see below). AC generates cAMP from ATP. Two cAMP molecules bind to the regulatory subunit (R) of protein kinase A (PKA) to release the catalytic subunit (C) which then phosphorylates a substrate such as ion channels. Phosphatidylinositol turnover (Figure 1-5C) is more complicated and includes generation of two second messengers, DAG and IP_3. DAG stimulates protein kinase C (PKC), whereas IP_3 releases Ca^{2+} from intracellular stores. PKC may be moved from the cytoplasm to the membrane, at which point it phosphorylates its substrate (e.g, ion channels) in the presence of phosphatidylserine (PS) and Ca^{2+}. PKC has been implicated in the modulation of ion channel function in numerous studies (for review see Shearman et al[58]). Other metabolites of phosphatidylinositol turnover (e.g., IP_4) may also play roles as second messengers in some cell types, but this has not yet been clearly determined in heart. Arachidonic acid can be generated by the sequential action of PKC and DAG lipase, but in most instances it is generated from membrane phospholipids via phospholipase A_2. A less well understood second messenger system is GC which generates cGMP from GTP. Since GC is difficult to reconstitute in solubilized systems, its biochemical characterization has lagged behind that of AC. It is clear cGMP plays a role in channel gating in rods of the eye and in olfactory and taste sensing system, but its function in regulation of cardiac ion channels is not yet defined.[81] A newly discovered group of receptors, after binding with growth hormones or upon activation, can generate tyrosine kinases which phosphorylate various substrate including ion channels. These tyrosine kinase receptors are the products of oncogenes such as *neu* and *erb-b* (epidermal growth factor receptor).[59]

Since the first evidence of a GTP-dependent step in the activation of AC in 1971 by Rodbell et al[60] and the following purification and characterization of a G-protein as a regulator of AC in 1981 by Gilman et al[61], there has been increasing awareness of the role of G-proteins in intracellular signalling reactions. G-protein coupled receptors generally span the membrane seven times and have two interfaces: one with extracellular ligands and the other with intracellular G-proteins. G-proteins are a family of heterotrimeric proteins which are made up of α-, β-, and γ-subunits (G_α, G_β, and G_γ). The β and γ subunits form a dimer that only dissociate when denatured and, are, therefore, a functional monomer ($G_{\beta\gamma}$). G_α interacts reversibly with receptor and effector molecules, and confers specificity to the holoprotein by virtue of its structural heterogeneity relative to the more homogeneous structures of β- and γ-subunits. G_α-subunits contain binding sites for guanine nucleotides and a specific GTP hydrolytic enzyme (GTPase), the activity of which is increased in the presence of $G_{\beta\gamma}$. As shown in Figure 1-5A, in the resting state, the GDP form of the G_α subunit (G_αGDP) forms a high affinity (nM) complex with the $G_{\beta\gamma}$ subunits. Binding of the heterotrimeric complex to an agonist-activated receptor results in the release of GDP. Subsequent GTP binding, in the presence of Mg^{2+}, disrupts the complex with the receptor and leads to the dissociation of G_αGTP from $G_\beta\gamma$. Both activated G_αGTP and the released $G_{\beta\gamma}$ are free to interact with downstream components. As a consequence of an intrinsic GTPase activity in the G_α subunit, GTP is hydrolysed to GDP, thereby returning the system to its heterotrimeric resting state.

The G protein cycle thus gives rise to two potential signalling molecules, G_αGTP and the $G_{\beta\gamma}$. At least 20 G_α, 5 G_β and 12 G_γ subunits provide significant combinatorial signal-transduction options.[62] The bipartite signal of released G_α and $G_{\beta\gamma}$ also doubles the number of classes of potential effectors. Several classes of α subunits have been identified in the heart (Table 1-3). The α_s class stimulates the AC-cAMP-PKA system via a number of membrane receptors including those for β-adrenergic agonists, dopamine, histamine, prostacycline, and peptide hormones. It also directly mediates β-adrenergic modulation of voltage-gated ion channels, such as activation of cardiac Ca^{2+} channel, inhibition of Na^+ channels.[56] The α_i class mediates inhibition of β-adrenergic-stimulated AC activity by muscarinic, α-adrenergic, adenosine A_1-receptor agonists, somatostatin, neuropeptide Y and so on.[63,64] α_i also activates phospholipases and produces PKC, which in turn can phosphorylate ion channel proteins. α_i may directly couple muscarinic receptors to atrial and pacemaker cell K^+ channels.[55,56] Similar to α_i, the α_o class inhibits AC and activates phospholipases. There is ample evidence that α_o regulates Ca^{2+} channel in brain but its role in cardiac function has not been directly demonstrated. Several laboratories have shown that the heart expresses several gene or splice variants for each class of α subunits (four α_s,[11,65] three α_i,[66] and two α_o[67], see Table 1-3). The functional differences in the splice variants are not known. These α subunits posses one or two sites for nicotinamide adenine dinucleotide (NAD)-dependent ADP-ribosylation. This covalent modification is catalyzed by bacterial toxins - by cholera toxin (CTX) in the case of α_s and by pertussis toxin (PTX) in α_i/α_o. ADP-ribosylation of α_s inhibits its GTPase activity, thus irreversibly activating the subunit to stimulate AC and ion channels. ADP-ribosylation of α_i/α_o subunits inhibits the interaction between the subunits and receptors. These functional modifications make ADP-ribosylation a means for detecting, quantifying and localizing G-proteins. Recent studies reported that the heart contains mRNA for another two classes of α subunits whose functions are not modified by either CTX or PTX: the α_z,[68] and the α_q subunit[69]. While the function of α_z is unknown, purified α_q has been shown to activate phospholipase C (PLC) and may be a candidate for the PTX-insensitive G-protein that couples muscarinic and α_1-adrenergic receptors to phosphoinositide hydrolysis in the heart.[70]

Table 1-3 G-protein-coupled receptors in the heart[11,57,70]

G-proteins	Variance (α subunit)	Receptors	Effectors	Response	ADP-ribosylation
G_s	4 (1 gene, 4 splice)	β_1,β_2-adrenergic	Adenylate cyclase	(+)	CTX
			K^+,Ca^{2+} channels	(+)	
G_i	3 (3 genes)	α_1,α_2-adrenergic	Phospholipase C	(+)	PTX
		M_2-muscarinic	Adenylate cyclase	(-)	
			K^+ Channels	(+)	
			Na^+ Channels	(-)	
$G_{k\ (i\text{-}3)}$		M_2-muscarinic	$K^+_{\text{-ACh}}$ channel	(+)	PTX
		A_1-purinergic	$K^+_{\text{-ATP}}$ channel	(+)	
G_o	2 (?)	M_2-muscarinic	Ca^{2+} channel ?	(-)	PTX
		α_2-adrenergic	K^+ channel	(?)	
			Phospholipase C	(?)	
G_q	?	M-muscarinic	Phospholipase A_2	(+)	Neither
		α_1-adrenergic	Phospholipase C	(+)	
G_z	?	?	?		Neither

$G_{\beta\gamma}$ functions to inhibit interactions of G_α with effector proteins by complexing with G_α and facilitate binding of G-proteins to cell membrane.[71] Activated $G_{\beta\gamma}$ can directly regulate ion channels and functions of other effectors such as activation of PLA_2 and PLC.[55-58,72,73] Although some structural and antigenic heterogeneity has also been reported among β-subunits, the similar function of $G_{\beta\gamma}$ from diverse sources and lack of tissue-specific distribution suggests that the various forms of β subunits may be interchangable.[74] Heterogeneity exists to some extent among γ-subunits, allowing the possibility of unique populations of $G_{\beta\gamma}$ that may be specific for distinct receptors.[75]

2.2. Muscarinic regulation of cardiac ion channels

Muscarinic cholinergic receptors mediate parasympathetic control of heart function. The dominant cardiac muscarinic receptor is the M_2 receptor.[76] Its density is 2-5 times higher in the atria than the ventricles.[77] Stimulation of M_2 receptors leads to a decrease in heart rate and contraction force. The M_2 receptor is coupled directly to the ligand-gated K^+ channel ($I_{K.Ach}$) by the G protein G_K (G_{i-3}).[78] In 1987, Yatani et al demonstrated that a purified PTX substrate from human erythrocytes activated K^+ channels in guinea pig atria in a manner similar to that of ACh and GTP.[78] The same group, using purified human erythrocyte G protein subunits, further demonstrated that $G_{i\alpha}$, but not $G_{i\beta\gamma}$, activates K^+ channels in guinea pig atrial membrane patches.[79] However, in the same year, Logothetis et al. found that $G_{i\beta\gamma}$ isolated from brain are the subunits responsible for stimulation of K^+ channels in chick atria[72] The channels opened by $G_{i\beta\gamma}$ displayed the same gating and conductance properties as those opened by ACh and GTP. Now, after a period of debate, it has been shown that $G_{\beta\gamma}$ directly binds and activates numerous effectors.[62] The other major aspect of muscarinic action on the heart is the antagonism of adrenergic effects at the level of AC-cAMP system.[55,78] Whereas β-adrenergic agonists stimulate the AC-cAMP system via G_s, muscarinic agonists such as ACh inhibit the same system via G_i (Figure 1-5B) and in this way affect ion channels that are modulated by the cAMP-dependent protein kinase, including $I_{Ca.L}$, I_f, $I_{Cl.cAMP}$, and presumably I_K.[55,56,78,80] The M_2 (and M_1) receptors are also coupled to phosphoinositide (PI) turnover through a PTX-insensitive G-protein (Figure 1-5C). Stimulation of M_2 receptors through this pathway leads to generation of IP_3 and DAG. The physiologic significance of this pathway is still largely unclear.[70] Recently, Wang and Lipsius reported that ACh activates $I_{K.ATP}$ channels in cat atrial myocytes via M_1 receptor-mediated PI turnover pathway to activate PKC and enhance SR Ca^{2+} release.[158] In addition. ceptor stimulation increases production of cGMP, but the role of cGMP in regulation of cardiac function is not yet defined.[81]

Muscarinic regulation of the atria and ventricles is different. For example, ACh activates $I_{K.ACh}$ in atria but not in ventricles.[82] Muscarinic agonists have strong direct negative chronotropic effects on atrial myocardium and SA and AV nodal tissues. While muscarinic agonists have direct negative inotropic effect on atrial myocardium, they have minimal direct effects on ventricular myocardium, but they indirectly modify ventricular contractility by attenuating the effects of agents that increase cAMP levels. With the recent advances in G-protein biochemistry, efforts have been made to determine whether fundamental differences in G-protein identity, structure, stoichiometry, or function can explain these differences in muscarinic regulation of cardiac function. Martin et al. demonstrated that muscarinic receptor affinity for agonists and regulation of receptor affinity by guanine nucleotides was the same in atrial and ventricular cell membranes.[83] Using PTX catalyzed [^{32}P]-ADP-ribosylation to quantitate $G_{i\alpha}$ and $G_{o\alpha}$ in myocardial membranes from 8-day-old chick embryos, these investigators found these G-proteins to have similar densities and identical peptide maps. Thus $G_{i\alpha}$ and $G_{o\alpha}$ appear to be similar in atria and ventricles. It is possible, therefore, that a unique G-protein is coupled to atrial muscarinic receptors and accounts for certain tissue-specific regulatory mechanisms.

2.3. β-adrenergic regulation of cardiac ion channels

Catecholamines, whether released locally from sympathetic nerve terminals or circulating in the blood, have long been known to make the heart beat faster and stronger through β-adrenoceptors (βARs) which are pharmacologically divided into two subtypes (β_1 and β_2). Both β_1- and β_2-ARs are distributed throughout the mammalian heart. In general, in the atrial myocardium of normal heart, β_1-ARs account for 60-70% of the total βAR population, whereas in ventricular myocardium β_2-ARs comprise 70-80% of all βARs.[84] The relative roles of β_1- and β_2-ARs have not completely been defined and seem to vary among species.[85] It does appear, however, that β_2 stimulation may be more involved in contractile than electrophysiologic events.[85] Although distinct entities, they have a number of properties in common. Stimulation of both β_1- and β_2-ARs generates activated $G_{s\alpha}$ to stimulate the AC-cAMP-PKA system. PKA, in turn, phosphorylates membrane proteins (Figure 1-5B). Some of the proteins phosphorylated by PKA and the associated cellular responses include 1) Na^+ channels to effectively close them when membranes are depolarized;[86] 2) Ca^{2+} channels to increase Ca^{2+} influx across the sacolemma;[87] 3) Cl^- channels to activate them[80] (see details in next section); 4) phospholamban to regulate the activity of Ca^{2+}-ATPase in sarcoplasmic reticulum (SR) membrane;[88] 5) troponin I to decrease the Ca^{2+} affinity of the protein;[89] 6) I_f channels to shift their activation curve to more positive potentials, such that impulse initiation increases.[56] 7) K^+ channels (delayed rectifier[47,90,91], and possibly I_{to1}[91,92]) to activate them. Alternatively, activated $G_{s\alpha}$ may directly gate Ca^{2+}, Na^+, K^+ and I_f channels in the heart without interposition of cAMP.[56,86,87,91] β-adrenergic stimulation of cardiac Ca^{2+} current shows biphasic response.[87] The fast response to isoproterenol occurs within 10 ms and is mediated by direct (non-cAMP dependent) $G_{s\alpha}$ gating of the channel. Diffusion is believed to be rate-limiting in this reaction. The onset of the slow response takes 5-10 sec and is mediated by $G_{s\alpha}$ through an indirect (cAMP dependent) pathway. The accumulation of cAMP appears to be the rate limiting step. Similar regulation has been shown for Na^+ and I_f channels.[56,85] β-adrenergic stimulation also enhances Na-K pump function, which would tend to hyperpolarize cardiac cells, especially those that are partially depolarized as in the setting of acute ischemia.[93]

The net result of β-adrenergic effects on cardiac electrophysiology is to hyperpolarize the membrane and to accelerate repolarization. With the increases in Ca^{2+} current and in intracellular free Ca^{2+}, delayed and early afterdepolarizations (DAD and EAD) can also be induced. The regulation of cardiac ion channels by βARs (sympathetic effect) and muscarinic receptors (parasympathetic effect) is usually a coordinated process. Muscarinic agonists activates $I_{K.ACh}$ channels and inactivate Ca^{2+} and I_f channels, reducing the pacemaker current and automaticity. β-adrenergic agonists activate Ca^{2+} and I_f channels and have a local anesthetic effect on Na^+channels in depolarized membranes. The latter would tend to limit the rate at which the cardiac impulse might propagate during sympathetic stimulation of the ischemic myocardium and could contribute to the proarrhythmic effects of local anesthetics.

2.4. α-adrenergic modulation of cardiac function

Catecholamines modulate heart function by stimulating α-adrenoceptors (αARs) in the heart via mechanisms differing from the βARs.[94-97] In 1948, Alquist reported that the functional responses of a variety of tissues to catecholamines could be separated into 'α' and 'β' types, based on observed relative activities of several catecholamines in mammalian smooth muscle and myocardium,[98] but there was no convincing evidence that the heart expresses functional αARs until Wenzel and Su showed that αAR stimulation increases contractility in rat ventricular muscle in 1966.[99] Based on anatomical location and pharmacological properties, αARs have been divided into two types: α_1- and α_2-ARs. The presence of pre- and post-synaptic α_2-ARs in heart has been suggested, but no evidence for their existence in guinea pig, rat or human cardiac myocytes was obtained with either [^{3}H]-yohimbine[100,101] or [^{3}H]-rauwolscine.[102] In contrast, many studies have shown that α_1-ARs are present in large numbers in the mammalian myocardium.[95,96,100,101] α_1-ARs are structurally and functionally distinct from both α_2- and β-ARs and can be selectively stimulated by agonists such as methoxamine and phenylephrine and blocked competitively by phentolamine and prazosin. α_1-AR activation has a variety of physiological effects, including increased and decreased inotropy and chronotropy,[94-97] control of energy production,[103] preconditioning against ischemic injury,[104] reduction of myocardial stunning,[105] induction of myocyte hypertrophy and gene transcription,[106] and vasoconstriction.[107]

2.4.1. *Electrical and mechanical effects of α_1-adrenoceptor agonists on mammalian heart*

In most mammalian species, the stimulation of cardiac α_1-ARs increases APD and the force of contraction.[94-97] This occurs in rabbit SA node cells,[108] atrial and ventricular muscle.[109-112] rat ventricular myocytes,[113-115] and Purkinje fibers.[116] α-adrenergic prolongation of repolarization has been attributed to the inhibition of a variety of K^+ channels, including I_{to1}, I_{K1}, I_K, and $I_{K.ACh}$.[97,109-115,142-143] The mechanism for the inotropic effects of α_1-AR stimulation is more complicated and may be mediated by 1) an increased calcium sensitivity of the myofibrils;[117] 2) an increase in $I_{Ca.L}$;[118] 3) an activation of the Na-K pump;[119] 4) effects on Na-H and Na-Ca exchangers;[120] 5) an inhibition of K^+ currents and resultant APD prolongation.[97,121] In guinea-pig preparations, however, either no effect on the action potential[122] and contractility[111] or a decrease in APD[123] has been observed. It was suggested that enhancing I_K by α_1-AR stimulation might be the underlying mechanism for the shortening of APD.[124]

2.4.2. *Subtype-selectivity of α_1-adrenoceptors*

There is now general agreement that there are at least two α_1-AR subtypes (α_{1A}, α_{1B}) in the heart,[125-130] linked via G proteins to a series of effectors (Na-K pump,[119] K^+ channels[97,109-115] and phospholipase C[128]) that modulate impulse initiation and repolarization of cardiac AP and the force of contraction in the heart (Figure 1-6).[129] The α_{1A} subtype has a high affinity to the competitive antagonist WB4101 and is not inactivated by the alkylating agent chloroethylclonidine (CEC). The α_{1B} subtype has a 20- to 1500-fold lower affinity for WB4101 and is potently blocked by CEC.[126] It has been reported that other agents like (+)niguldipine[130] and 5-methylurapidil (5MU),[131] can also inhibit α_{1A}-AR, and 5MU may be a superior antagonist for identifying α_{1A}-mediated response.[131] On the basis of molecular cloning, three subtypes (α_{1B}, α_{1C}, and α_{1D}) of α_1-ARs have been identified.[132-134] The cloned α_{1B} corresponds to the native α_{1B} -AR subtype. The cloned α_{1C}, thought originally to be an α_1-AR not recognized in studies of native receptors. now appears to be the molecular equivalent of α_{1A} and because it can be inhibited by 5MU and (+)-niguldipine. although it shows exquisite and equal sensitivity to these two antagonists whereas α_{1A} is >10 times more sensitive to 5MU than to (+)-niguadipine.[133] The α_{1D}-subtype differs from α_{1A} clone by only two amino acids but is sensitive to inhibition by CEC and appears to represent a distinct subtype from α_{1A}.[132] The mRNAs for all three cloned α_1-ARs have been recently demonstrated to be expressed in adult rat cardiac muscle.[134]

Radioligand binding studies in adult rat heart indicate that the relative proportion of α_1-ARs is 80% α_{1B} and 20% α_{1A}.[127] In contrast, the mRNAs for α_{1C} and α_{1B} are present at approximately equal levels in adult rat cardiac myocytes, with α_{1D} somewhat less, by RNase protection assay.[134] Assignment of a physiological effect to a specific α_1-AR has been also very difficult, given the limited selectivity of the available antagonists as well as the possibility that additional subtypes remain to be identified. It has been found that in canine cardiac Purkinje fibers exposed to ischemic conditions the α_{1A}-adrenoceptor is responsible for the induction of abnormal automaticity.[135-136] Different sensitivities of 4-AP-sensitive and -insensitive outward currents in rat ventricular myocytes to α_{1A}- and α_{1B}-adrenoceptors stimulation have also been reported.[114-115] How different α_1-AR subtypes might mediate specific physiological effects is not known. One possibility is that they are coupled to different second messenger pathways. However, it seems that all three subtypes of α_1-AR couple to G-proteins, phosphatidylinositol hydrolysis, cAMP accumulation, and arachidonic acid release when overexpressed in cell lines (see below).[137,138]

2.4.3. *Signal transduction mechanisms for α_1-adrenoceptor-effector coupling*

Various biochemical responses to α_1-AR stimulation have been reported, including PLC and PLA_2 activation, increased intracellular [Ca^{2+}], and changes in intracellular cyclic nucleotide levels.[94,98,126] The most extensively documented signaling pathways involve phosphatidylinositol turnover via activation of PLC, giving rise to various potentially important second messengers such as IP_3 and DAG (Figures 1-5 and 1-6). IP_3 is known to release Ca^{2+} from SR and DAG is thought to be the endogenous activator of PKC. In canine Purkinje fibers PLC produces positive chronotropic response similar to those resulting from α_1-AR stimulation[139]An other pathway implicated in the signal transduction of α_1-AR stimulation is the activation of PLA_2 which can in turn generate arachidonic acid and modulate ion channels.[57,137,138] Accumulating evidence supports that G-proteins (at least two of them are PTX-sensitive and one is PTX-insensitive) are coupled to α_1-AR (Figures 1-5 and 1-6). The effects of α_1-AR on Na-K pump and K^+ conductance[119] and hence the decrease in the rate of impulse initiation in canine Purkinje fibers,[128] the changes in cytosolic Ca^{2+} in hamster cardiac myocytes,[140] and also the positive chronotropic response to α_1-AR agonists in rat hearts[141] are transduced by PTX-sensitive G-proteins, while inhibition of a variety of K^+ currents (I_{K1}, I_K, and I_{to1}) in rabbit atrial myocytes is mediated by a PTX-insensitive G-protein.[97,142,143] The α-subunit of G_q family is responsible for PTX-insensitive activation of a family of PLC-β isozymes.[144] However, it also has been shown that G-protein $\beta\gamma$ subunits activate certain of these PLC-β isozymes, and that this novel activity may account for activation of PLC by G-proteins that are not members of G_q family, including those that account for PTX-sensitive inositol lipid signaling (Figure 1-6C).[144] In Purkinje fibers, it has been suggested that the PTX-sensitive and -insensitive components of the α_1-AR response may be mediated by distinct α_1-AR subtypes (ie, α_{1A} and α_{1B}), as defined by sensitivities of α_1-AR response to WB4101 and CEC.[128] Therefore, cardiac α_1-AR appears to interact with different G-proteins via different subtypes. Han et al[141] have shown that the PTX sensitivity of α_1-AR-mediated chronotropic response increases with developmental age, such that PTX is without effect in neonates, but interferes with α_1-AR function in adults. The distribution of α_1-AR-coupled G-proteins may be also either tissue and/or species-specific.[97]

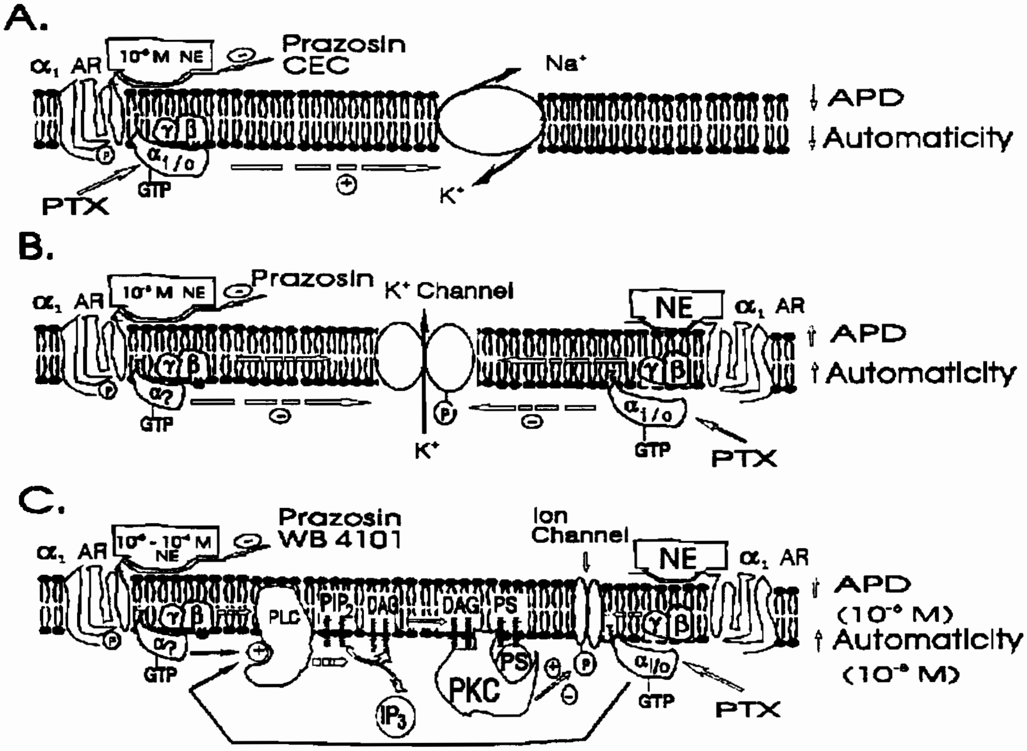

Figure 1-6. The α_1-adrenoceptor-effector coupling pathway. A. A link between α_1-AR and the Na-K pump transduced by a PTX-sensitive G-protein. The result is an increase in pump function and generation of an outward current that would decrease automaticity and accelerate repolarization. This effect can be blocked by CEC, an α_{1B}-AR antagonist. B. A link between the α_1-AR and K^+ channels via a PTX-sensitive or -insensitive G-protein. The result is a decrease in K^+ conductance and increase in automaticity and action potential duration (APD). C. A link between α_1-AR and phospholipase C (PLC) via G-proteins (PTX-sensitive or -insensitive), resulting in increased phosphoinositide metabolism. Increase in automaticity and APD are seen here. For this pathway, higher agonist concentrations are required than for A and B, and can be blocked by WB4101, an α_{1A}-AR antagonist, suggesting a different receptor subtype from A and B. (Modified from Rosen et al [129] and Boyer et al [147])

2.4.4. *Physiological significance of α_1-adrenergic modulation of cardiac function*

In isolated cardiac tissues, α_1-AR stimulation can be arrhythmogenic. α_1-Agonists induce triggered rhythms via DAD or EAD and abnormal automatic rhythms[145,146] in settings where extracellular Ca^{2+} level is elevated, ischemia and reperfusion are simulated, repolarization is prolonged, or infarction is induced. In intact cats after coronary occlusion and reperfusion, there is an increase in α_1-AR number and affinity.[147] This is associated with ventricular tachycardia and fibrillation within 1-3 minutes of reperfusion. Only limited data are available for α_1-AR involvement in human cardiac arrhythmias. The efficacy of α_1-AR blockade by phentolamine against arrhythmias in a small group of patients in the immediate postmyocardial infarction period has been reported.[101] In patients with the congenital LQT syndrome, a subset whose arrhythmias are not blocked by propranolol do respond to left thoracic sympathectomy, leading to the speculation that α_1-AR may be involved.[129] The clinical antiarrhythmic potential of α_1-AR blockade remains largely untested.

2.5. Purinergic modulation of cardiac ion channels

Since the initial observation in 1929 of the effects of adenosine and AMP on the heart and circulation,[148] the physiological significance of purine action on the cardiovascular system has become evident. ATP and adenosine are the two major purinergic agonists. ATP is released from nerve terminals as a cotransmitter with NE and ACh. ATP is also released in response to hypoxia. ATP release precedes adenosine and lactate dehydrogenase release during hypoxia,[149] and is proportional to myocardial workload.[150] ATP in the extracellular space is rapidly degraded into ADP, AMP, and adenosine by ectoenzymes. Purinergic receptors (PRs) are classified as P_1 (recognizing adenosine and selective antagonism by methylxanthines) and P_2 (recognizing ATP and no antagonism by methylxanthines).[151] P_1-PR has been further subdivided into A_1 (or R_i) and A_2 (or R_a),[152,153] and P_2-PR into P_{2T}, P_{2U}, P_{2X}, P_{2Y}, and P_{2Z} subclasses.[154] A_1 is the major P_1-PR in the heart, and is coupled to $I_{K.ATP}$,[155,156] and the facilitated opening of $I_{K.ATP}$ channels by activation of A_1 receptors may be involved in ischemic preconditioning.[157] This effect is thought to use the same effector coupling pathway as muscarinic receptor-mediated activation of $I_{K.ATP}$.[155,158] In frog and guinea-pig atrial cells, extracellular ATP also increases the K^+ conductance via activation of P_2-PR.[159,160] In frog atrium, ATP-induced K^+ conductance is thought to be identical to $I_{K.ACh}$ in the same cells.[159] Later studies reported that ATP modulates almost all voltage-gated ion channels in the heart thus far investigated via various intracellular signal transduction pathways. It increases $I_{Ca.L}$ via a G_s protein, and also increases $I_{Ca.T}$.[161]

However, after full activation of $I_{Ca.L}$ by intracellular GTPγS, ATP inhibits $I_{Ca.L}$ in the rat,[161] and ferret heart.[162] ATP in the presence of P_1-PR antagonist does not affect the basal intracellular cAMP content but decreases βAR-mediated accumulation of cAMP only in isolated fetal, but not in adult, rodent heart cells.[161,163] This effect is PTX-sensitive and is thus likely to be mediated by G_i protein. ATP activates a Cl^- current, $I_{Cl.ATP}$, in guinea pig, rat, and mouse heart cells[164,165,166] ATP accelerates PI turnover and increases PKC activity in cardiomyocytes.[163] ATP triggers redistribution from cytosol to the membrane of two Ca^{2+} insensitive PKC isoforms, ϵ- and δ-PKC, expressed in neonatal and adult cardiac cells.[167] PKC also induces the phosphorylation of myristoylated alanine-rich C kinase substrate, MARCKS, and the expression of *c-fos* in neonatal cells.[167] These observations are of physiologic relevance with regard to the likely specific role of PKC isoforms in cardiac function. Although PKC can activate Cl^- current in heart,[168] there is no direct evidence linking PKC activation to P_2-PR-mediated activation of $I_{Cl.ATP}$. Extracellular ATP, in the presence of a phosphodiesterase inhibitor (IBMX), increases basal cGMP content of isolated cardiac myocytes.[161] A new type of receptor, P_3-PR, has been recently reported to exist in rat heart and to activate Cl^--HCO_3^- exchanger, inducing a large acidification.[169] This effect is prevented by genistein and ST238, two tyrosine kinase inhibitors. Moreover, ATP triggers the phosphorylation of tyrosine residues of a band-3-like protein that mediates anionic exchange in rat cardiac cells.[170] The intracellular acidification is thought to induce an increase in $[Ca^{2+}]_i$[169] and thus to activate a Ca^{2+}-dependent cation conductance.[171] The ATP-induced inward currents (Cl^- and non-selective cation current) and depolarization can reduce cell-to-cell coupling by increasing intracellular $[H^{+}]$ and $[Ca^{2+}]$.[172] Depolarization and an ATP-induced hyperpolarizing shift of I_{Na} availability will reduce Na^+ current and slow conduction. Consequently, ATP released during nerve stimulation, circulatory shock, cardiac overload, or regional ischemia may induce ventricular arrhythmia.

3. Chloride conductance in heart

Chloride (Cl^-) channels are present in plasma membranes of probably every animal cell and most cells express several types of Cl^- channels.[173] Cl^- channels have diverse functions, ranging from control of excitability to regulation of cell volume and transepithelial transport.[18,173]

In the heart, Cl^- channels have been the subject of intensive electrophysiological studies for more than 30 years. In 1961, Hutter and Noble[174] and Carmeliet[175] examined the effects of replacement of $[Cl^-]_o$ by various anions on electrical activity of dog papillary muscle and sheep cardiac Purkinje fibers. Anions less permeable than Cl^- prolonged the AP plateau, had variable effects upon the rate of spontaneous activity and caused small changes in RMP. As shown in Figure 1-7A, replacement of $[Cl^-]_o$ by acetylglycinate prolonged the APD of cardiac Purkinje fibres.[175] The phase 1 was delayed and the notch disappeared. Substitution of $[Cl^-]_o$ by anions more permeable than Cl^- (I^-, Br^-, or NO_3^-) had opposite effects. These studies suggested that Cl^- permeability is low at rest ($<30\%$ of the total resting permeability) and that Cl^- conductance may increase during depolarization and contribute to the repolarization of cardiac AP.

The possible role of a Cl^- conductance in the regulation of the Purkinje fiber AP was later assessed by using two-microelectrode voltage-clamp technique (Figure 1-7B).[32] A $[Cl^-]_o$- but not $[K^+]_o$-sensitive transient outward current, later called "positive dynamic current" by Peper and Trautwein,[176] was identified. In Na^+-free solution, the E_{rev} of the positive dynamic current shifted in response to a reduction of $[Cl^-]_o$ in a manner consistent with Cl^- as the major charge carrier.[32,177]Since the positive dynamic current exhibited both activation and inactivation, McAllister et al used I_{qr} (q for activation and r for inactivation gating variable) for the positive dynamic current to reconstruct the electrical activity of cardiac Purkinje fibers.[178] They had to introduce a time-independent background chloride component, which they denoted as $I_{Cl,b}$, to successfully simulate the effect of chloride removal on the AP.[178] By the 1970's, there was general agreement that phase 1 repolarization of cardiac AP was due to an influx of Cl^- ions through Cl^- channels.

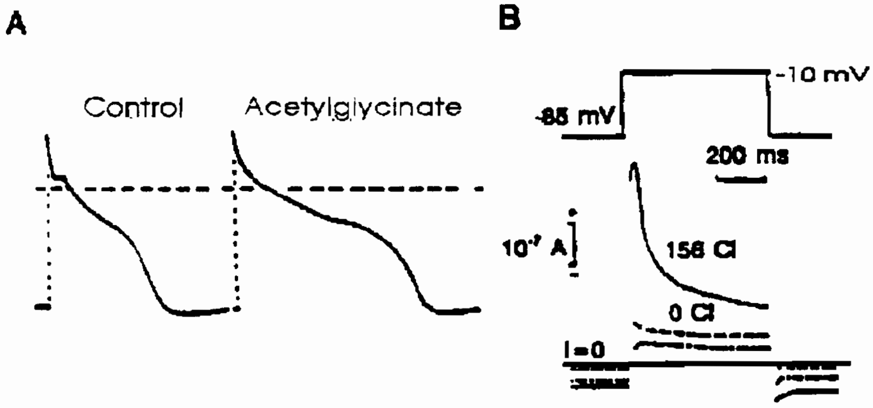

Figure 1-7. Effects of replacement of extracellular Cl^- on action potential and membrane currents of sheep Purkinje fibers. A: replacement of extracellular Cl^- by acetylglycinate caused a prolongation of AP (Adapted from Carmliet EE[175]). B: effects of Cl^--free solution (dashed line) and replacement of extracellular Cl^- by sucrose (dashed and doted line) on transien outward ("positive") membrane current elicited by depolarization to -10 mV from a holding potential of -85 mV. Na^+-free solution was used throughout. (Adapted from Dudel et al[32]).

Later studies raised serious doubts about the original interpretation that the transient outward I_{qr} represents a Cl^- conductance pathway.[36,37,179] Kenyon and Gibbons[179] showed that phase 1 repolarization and the notch were usually not affected by removal of extracellular Cl^- ions if extracellular Ca^{2+} activity was constant; and the transient outward current could be blocked by the K^+ channel blockers TEA[36] and 4AP.[37] With the application of the patch-clamp technique to enzymatically dispersed cardiac cells, a lot of evidence suggest that I_{qr} is largely a K^+ current, named I_{to} or I_{to1},[27-31,38,39,50,109-110,180-182] and there was little or no experimental evidence supporting the existence of Cl^- channels in the heart. Cl^- channels in the heart were ignored for ten years until 1989, when two independent groups discovered a new cardiac Cl^- current which is regulated by βARs through the AC-cAMP-PKA pathway.[80,183] Over the last 5 to 6 years, voltage-clamp experiments on isolated cardiac myocytes have dramatically changed the landscape of cardiac Cl^- channel studies, with evidence suggesting that there may be nearly as many various Cl^- channels in heart as there are K^+ channels, and that these Cl^- channels possess a much larger repertoire of functions than expected.[184]

3.1. Basic physiology of cardiac chloride conductance pathways

Measurements using ion-selective microelectrodes have shown that intracellular Cl^- activity (a^i_{Cl}) in mammalian cardiac tissue is in the range of 10 - 20 mM,[185] higher than expected if Cl^- were passively distributed. This has been interpreted to mean that Cl^- must be actively transported into cardiac cells.[185,186] The most extensively studied anion-exchange mechanism in cardiac tissue is the Cl^-/HCO_3^- exchanger in sheep cardiac Purkinje fibers.[186-188] The activity of this exchanger was studied by examining with Cl^-- and pH-sensitive microelectrodes the fall of $[Cl^-]_i$ in Cl^--free solution and the reaccumulation of $[Cl^-]_i$ during re-exposure to $[Cl^-]_o$. The reaccumulation of $[Cl^-]_i$ required external HCO_3^-/CO_2 and was inhibited by 4-acetamido-4'-isothiocyanostilbene-2,2'-disulfonic acid (SITS). Reaccumulation of $[Cl^-]_i$ was accompanied by an intracellular acidification, suggesting that Cl^- influx is accompanied by extrusion of HCO_3^-. Another mechanism for Cl^- influx was suggested by the finding that elevation of $[K^+]_o$, which depolarizes the membrane, also produced a SITS-insensitive elevation of $[Cl^-]_i$. These observations led to the proposal of a model for the regulation of $[Cl^-]_i$ in cardiac Purkinje fibers. As shown in Figure 1-8, Cl^-/HCO_3^- exchange is electroneutral, but not at equilibrium due to constant Cl^- efflux through a leakage pathway possibly involving sarcolemma Cl^- channels. Intracellular acidification due to HCO_3^- extrusion by the exchanger is believed to be balanced by acid efflux by the Na^+-H^+ exchanger. In cultured embryonic chick heart, Cl^-/HCO_3^-

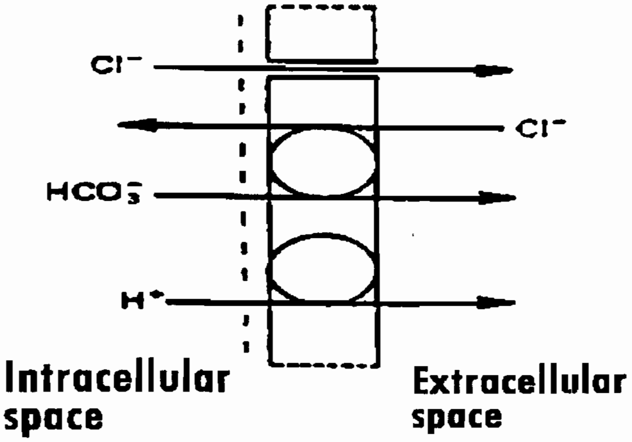

Figure 1-8. A model proposed for $[Cl^-]_i$ regulation, which was the most compatible with experimantal observations. In this model, Cl^-/HCO_3^- does not reach equilibium because of a net outward efflux of Cl^- by an other membrane pathway, possibly involving Cl^- channel.(Adapted from Vaughan-Jones RD[188]).

exchange may play a direct role in the regulation of intracellular pH.[189] Other mechanisms for the control of $[Cl^-]_i$ have been suggested, including Na^+-Cl^- and Na^+-K^+-$2Cl^-$ cotransport.[190,191] The two transport systems can be separated by the use of inhibitors, the former inhibited by SITS and the latter by chlorothiazide. An electroneutral K^+-Cl^- cotransport may contribute to the SITS-insensitive $[Cl^-]_i$ increase observed in response to elevation of $[K^+]_o$ in cultured chick heart cells. Under physiologic conditions this system may function to lower $[Cl^-]_i$ and oppose Cl^- uptake mediated by Cl^-/HCO_3^- exchange and Na^+-K^+-$2Cl^-$ cotransport.[192]

The nonpassive distribution of Cl^- may be the reason that in many areas of the heart the E_{Cl} is more positive than the RMP. Under normal physiologic conditions, the E_{Cl}, thus the reversal potential (E_{rev}), for Cl^- in heart ranges from -65 to -40 mV.[13,32,33,175,186] This places Cl^- channels in a unique position to play potentially important roles in the regulation of the cardiac AP. At membrane potential negative to E_{Cl}, Cl^- channels would pass inward current (Cl^- efflux), causing a diastolic depolarization of RMP, whereas at membrane potential positive to E_{Cl}, Cl^- channel opening would conduct an outward current (Cl^- influx) and facilitate repolarization, causing a shortened APD.

3.2. Cardiac chloride currents identified to date

At least five distinct Cl^- conductances have been identified in the sarcolemma of mammalian cardiac myocytes (Figure 1-9).[184,193] These include Cl^- conductances activated by stimulation of cAMP-PKA ($I_{Cl.cAMP}$),[80,183] PKC ($I_{Cl.PKC}$),[168] intracellular Ca^{2+} ($I_{Cl.Ca}$),[40,41] extracellular ATP ($I_{Cl.ATP}$),[164-166] and cell-swelling or membrane stretch ($I_{Cl.swell}$).[194-196]

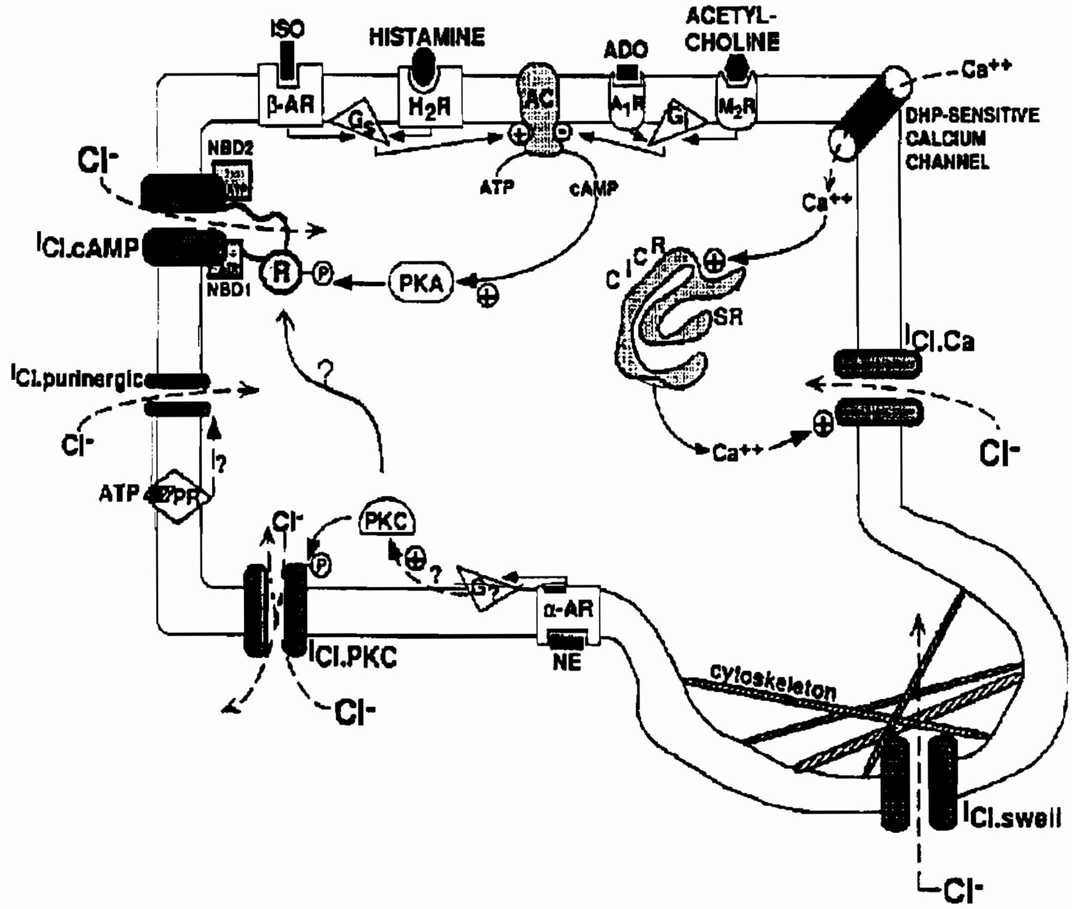

Figure 1-9. Signal transduction pathways of cardiac chloride channels. Schematic representation of signaling pathways leading to the activation of five distinct macroscopic chloride currents ($I_{Cl.cAMP}$, $I_{Cl.PKC}$, $I_{Cl.Ca}$, $I_{Cl.swell}$, and $I_{Cl.purinergic}$) in the cardiac cell. (Iso, isoproterenol; H_2R, histamine (type II) receptor; ADO, adenosine; A_1R, adenosine (type I) receptor; CICR, calcium-induced calcium release; NBD, nucleotide-binding domain). (Modified from Ackerman and Clapham[193])

3.2.1. $I_{Cl.cAMP}$

$I_{Cl.cAMP}$ is the most thoroughly characterized cardiac Cl^- conductance. $I_{Cl.cAMP}$ was first identified in the heart by Harvey and Hume[80] and Bahinski et al[183] in 1989, and the single channel identity of this current was identified in 1990 as a 13pS anion channel.[197] Substantial information is now available about the physiologic role of these channels, their regulation by intracellular pathways, and their biophysical and molecular properties.

Biophysical properties of $I_{Cl.cAMP}$. With a physiological Cl^- gradient ($[Cl]_o/[Cl]_i$ = 151.4/40 mM), the I-V relationship of isoproterenol-induced Cl^- current exhibits outward rectification with an E_{rev} close to the predicted E_{Cl} (-33 mV). When the Cl^- gradient is made symmetrical ($[Cl]_o/[Cl]_i$ = 151.4/150 mM), however, the I-V relationship becomes nearly linear, and the E_{rev} shifts to 0 mV, a value close to E_{Cl}.[198] Overholt et al[199,200] determined the anion permeability sequence of the isoproterenol-activated Cl^- channels to be $NO_3^- > Br^- \geq Cl^- \geq I^- >$ isethionate$^-$ $\geq$ glutamate$^-$, based on shifts of the reversal potential of whole-cell current in guinea-pig ventricular myocytes. Although it is suggested that nonlinearity of the I-V relationship observed with physiological Cl^- gradients may be due to the asymmetrical Cl^- gradient and is reasonably well described by the GHK equation,[200-203] Overholt et al found no comparable inward rectification after reversing the $[Cl^-]$ gradient and an outward rectifying, rather than linear, I-V with symmetrical low $[Cl^-]$.[200,201] They suggested that the outward rectification is not strictly a function of the Cl^- gradient but a property of ion channel permeation that would occur under physiological conditions. The outward rectification reflects channel block by the less permeant anions (such as glutamate, aspartate) used to replace Cl^- in the intracellular solution. They were able to account for I-V relationship obtained over a range of $[Cl^-]$ with a one-site, two-barrier model based on Eyring rate theory.[200] Single channel I-V relationships of $I_{Cl.cAMP}$ published so far (see below) show outward rectification with roughly physiological $[Cl^-]$[197,204] and are approximately linear,[204] or slightly outwardly rectifying,[205] with nearly symmetrical high $[Cl^-]$.

Pharmacological characteristics of $I_{Cl.cAMP}$. Inhibitors of the electroneutral anion exchanger, such as the stilbene derivatives SITS, 4,4'-diisothiocyanatostilbene-2,2'-disulfonic acid (DIDS), and 4,4'-dinitrostilbene-2,2'-disulfonic acid (DNDS), also block certain Cl^- channels including those from *Torpedo* electroplax,[206] and epithelial outwardly rectifying chloride channel (ORCC).[207] In cardiac myocytes, $I_{Cl.cAMP}$ is insensitive to DIDS and SITS.[183,198202] DNDS has no direct effect on cardiac $I_{Cl.cAMP}$ channels but, at a high concentration, it may interfere with their regulation via some indirect pathway.[202] Harvey[208] found an enhancement of the current by SITS and DIDS that was not seen when forskolin or 8-Br-cAMP activated the conductance, which suggests an effect on βARs. Anthracene-9-carboxylate (9AC), an effective inhibitor of Cl^- channels in skeletal muscle,[209] reduces isoproterenol-activated cardiac $I_{Cl.cAMP}$ in a voltage-independent manner[198] by 90% at 200 μM.[210-211] Reports of effects of arylaminobenzoates such as 5-nitro-2-(3-phenylpropylamino)-benzoate (NPPB) and DPC on $I_{Cl.cAMP}$ are varied. Walsh[211] reported that 50 μM NPPB and 1 mM DPC strongly inhibited $I_{Cl.cAMP}$, whereas Hwang et al[202] found no noticeable effects on forskolin-induced $I_{Cl.cAMP}$ of a brief exposure to 200 μM DPC. The $I_{K.ATP}$ channel blocker glibenclamide has also been reported to block cardiac $I_{Cl.cAMP}$ in a voltage-independent manner.[212] An ideal and specific blockers of $I_{Cl.cAMP}$ is presently missing.

Signal transduction pathways for regulation of $I_{Cl.cAMP}$ (Figure 1-9). $I_{Cl.cAMP}$ is elicited by β-AR activation,[80,198,213-214] by exposure to forskolin,[183,201-202] or histamine,[215] or more directly by intracellular application of cAMP[183,201,216-217] or of the catalytic subunit of PKA.[183,218] A synthetic inhibitor peptide (PKI) specific for PKA can completely abolish $I_{Cl.cAMP}$ induced by isoproterenol,[201] forskolin,[203] or cAMP.[183] These results have established the cAMP-PKA signaling system as the major regulatory pathway for cardiac $I_{Cl.cAMP}$ channels. Unlike other PKA-regulated channels like $I_{Ca.L}$,[36] and I_K[90], $I_{Cl.cAMP}$ is absent in the absence of PKA-mediated phosphorylation. The basis for this apparent difference remains unclear, however, because recent evidence[219-221] supports the idea[222] that $I_{Ca.L}$ channels require phosphorylation by PKA before they can be opened. Deactivation of $I_{Cl.cAMP}$ in myocytes following sudden withdrawal of agonists or introduction of pipette PKI is rapid and complete, which indicates the presence of endogenous protein phosphatase.[203] Pipette application of specific inhibitors of phosphatases 1 and 2A (PP1, PP2A) such as okadaic acid or microcystin causes an increase in the steady-state level of phosphoprotein and of the activated $I_{Cl.cAMP}$, and slows its subsequent deactivation.[203] But even after complete inhibition of PP1 and PP2A, some deactivation of $I_{Cl.cAMP}$ accompanies withdrawal of forskolin, implying that some other phosphatase can also dephosphorylate the $I_{Cl.cAMP}$ channel.

Several experimental observations support the involvement of a G-protein (likely G_s) in the acitivation of $I_{Cl.cAMP}$ through βARs or histaminergic receptors: a) Withdrawal of GTP from pipette solutions reversibly abolishes activation of $I_{Cl.cAMP}$ by maximally effective concentrations of isoproterenol or histamine, but not its activation by forskolin or pipette cAMP.[223] b) Introducing a high concentration of GDPβS prevents activation of $I_{Cl.cAMP}$ by isoproterenol, but not by forskolin.[201] c) With the nonhydrolyzable GTP analogue GTPγS or GppNHp in the pipette, a brief exposure to isoproterenol or histamine, but not to forskolin, causes persistent activation of $I_{Cl.cAMP}$.[201] Unlike cardiac $I_{K.ACh}$, $I_{Ca.L}$ and I_{Na},[55,56] direct membrane-delimited activation of $I_{Cl.cAMP}$, is unlikely because:[201] a) Pipette application of PKI abolishes $I_{Cl.cAMP}$ induced by isoproterenol. b) Isoproterenol does not activate $I_{Cl.cAMP}$ in the presence of PKI. c) Isoproterenol causes no further increase in $I_{Cl.cAMP}$ after maximal stimulation of the PKA pathway with forskolin or intracellular cAMP.

Stimulation of muscarinic receptors by ACh or carbachol (CCh) decreases $I_{Cl.cAMP}$ induced by isoproterenol or forskolin,[80,198,201,216] but not that activated by pipette cAMP,[201,216] which indicates that inhibition is at the level of the AC and not the βAR, kinase, or phosphatases. The muscarinic inhibition of $I_{Cl.cAMP}$ is presumably mediated by G_i because it reguires GTP,[223] and is abolished by PTX or a high concentration of GDPβS.[201] It appears, then, that β-adrenergic and muscarinic pathways converge on AC, via G_s and G_i proteins, respectively, to regulate $I_{Cl.cAMP}$ channels, as previously suggested for regulation of $I_{Ca.L}$ in guinea-pig[224] and frog[225] cardiac myocytes. Because phosphodiesterases (PDEs) hydrolyze cAMP, the PKA signal pathway can also be modulated by controlling the activity of the PDEs. Ono et al[226] found in guinea-pig myocytes that pipette application of cGMP enhanced $I_{Cl.cAMP}$ induced by submaximal, but not by supermaximal, concentration of isoproterenol, foskolin, or intracellular cAMP, consistent with cGMP-mediated inhibition of PDEs. Abolition of the cGMP effect by milrinone, a specific inhibitor of cGMP-sensitive PDE, confirmed that conclusion.[226]

Activation of $I_{Cl.cAMP}$ in guinea-pig ventricular myocytes shows $[Na^+]_o$-dependence.[183,198,214] Some authors have suggested that the $[Na^+]_o$-dependence may be intracellular and downstream of PKA regulation.[198,214] Tareen et al[217] claim that it is mainly due to direct antagonism between Na^+ and isoproterenol at the level of βARs but not due to secondary changes in $[Na^+]_i$ because they found that replacement of $[Na^+]_o$ by TEA caused the same diminution of isoproterenol-induced $I_{Cl.cAMP}$ regardless of pipette $[Na^+]$.[217] Another study from Zakharov et al[227] suggested that the observed $[Na^+]_o$-dependence may be related to muscarinic agonist activity of Na^+ substitutes ($Tris^+$ or TMA^+) which inhibit AC activity via G_i activation. It is concurred by all authors at present that cardiac $I_{Cl.cAMP}$ channels are not directly influenced by $[Na^+]_o$, a conclusion corroborated by the finding that unitary $I_{Cl.cAMP}$ current amplitudes in excised membrane patches are unaffected by replacement of $[Na^+]_o$ by $NMDG^+$.[204]

Molecular biological characterization of cardiac $I_{Cl.cAMP}$. The biophysical, biochemical, and pharmacological properties of cardiac $I_{Cl.cAMP}$ are identical to those of CFTR-expressed Cl^- conductance observed in epithelial cells[227,228] or *Xenopus* oocytes[229,230] (see below). A 550 bp PCR product from rabbit ventricular mRNA shared about 93% sequence homology (98% amino acid identity) with NBF1 from human epithelial CFTR.[231,232] This PCR product hybridized to a 6.5 kb transcript, consistent with the size of CFTR. Nagel et al[204] showed that total RNA purified from guinea-pig heart or lung, but not from brain, hybridized with a full-length antisence riboprobe derived from human CFTR cDNA. In a more recent study, Horowitz et al[233] further sequenced and amplified cDNA from rabbit ventricle and cloned fragments corresponding to each of the two predicted membrane-spaning domains, M1-M6 and M7-M12, of the epithelial CFTR transcript. This work revealed a deletion of 30 amino acids (corresponding to exon 5) at the C-terminal end of the predicted first cytoplasmic loop (Figure 1-4D), suggesting the cardiac isoform is an alternatively spliced product of CFTR. Outside this region, the cardiac CFTR transcript shows >95% identity to that from human epithelia.[233] In rabbit and guinea-pig, expression of the isoforms seems mutually exclusive because only the cardiac isoform was found in heart, and only the epithelial transcript appeared in epithelia.[233] On the other hand, spliced and unspliced forms are expressed in atria and ventricles of both simian and human hearts.[234] The functional significance of this alternative splicing of CFTR remains unclear. Southern analysis of heart reverse transcription PCR products only showed hybridization to cardiac tissues which electrophysiologically exhibit $I_{Cl.cAMP}$ in native cells.[233] For a variety of species and tissues, the distribution of $I_{Cl.cAMP}$ is highly variable.[164,195,196,235] In general, functional measurements of $I_{Cl.cAMP}$ correlate with the regional distribution of the alternatively spliced CFTR transcript.[184,233] A very recent report of Hart et al[235] provided the complete sequence of a cDNA encoding cardiac $I_{Cl.cAMP}$. An exon 5 splice variant (exon 5-) of CFTR (>90% identity to human epithelial CFTR cDNA) is expressed in rabbit heart. Expression of this cDNA in *Xenopus* oocytes gave rise to robust $I_{Cl.cAMP}$. Antisense oligodeoxynucleotides directed against CFTR significantly reduced the density of $I_{Cl.cAMP}$ in cultured cells, establishing a direct link between cardiac expression of CFTR and the endogenous cardiac chloride channel.[235]

3.2.2. $I_{Cl.PKC}$

Guinea-pig ventricular cells contain a Cl^- current sensitive to PKC ($I_{Cl.PKC}$).[168,236] After eliminating cationic currents, phorbol ester stimulation in the presence of PKC dialyzed via the pipette activated a time-independent, Cl^--sensitive linear current in asymmetric [Cl^-] which was inhibited by aromatic monocarboxylic acid.[238] In the absence of pipette PKC, Zhang et al[237] found that phorbol esters activated an 9-AC-sensitive Cl^- current in feline ventricular myocytes. Effects of PKA and PKC on Cl^- were not additive in guinea-pig ventricular cells. In contrast to $I_{Cl.cAMP}$ channels, in which I^- permeability is less than or equal to that of Cl^-,[160,199] a large outward current in I^- was observed. Therefore ,Walsh et al concluded that $I_{Cl.PKC}$ may be due to Cl^- channel similar but not identical to $I_{Cl.cAMP}$ channel.[160] However, in feline ventricle it was concluded that both $I_{Cl.PKC}$ and $I_{Cl.cAMP}$ are due to the same Cl^- channel, because once the channels were maximally activated by PKA, PKC did not activate additional current.[237] Collier and Hume[238] found that in cell-attached patches from guinea-pig ventricular myocytes phorbol ester activates a 10 pS linear single chloride channel and subsequent application of IBMX increases its open probability (P_o) but does not alter channel conductance, supporting the identity of $I_{Cl.cAMP}$ and $I_{Cl.PKC}$. In epithelial CFTR Cl^- channels, serines 686 and 790 in the R domain are phosphorylated by PKC (see below),[239] and pre-exposure to PKC greatly potentiates the rate and extent of channel activation by PKA.[240,241] Although less effective than PKA, PKC itself can also activate epithelial CFTR Cl^- channels.[242] In cell-attached patches on HT-29cl.19A (human colon carcinoma) cells, PKC failed to activate Cl^- channels but increased the number of channels activated by forskolin without altering P_o.[243] Thus, the issue of whether PKC and PKA activate the same Cl^- channel protein is still unresolved.

3.2.3. $I_{Cl.Ca}$

Inhibition of Ca^{2+} release from the sarcoplasmic reticulum (SR) by caffeine and ryanodine delays phase 1 repolarization, a finding attributed to inhibition of a contraction-related transient outward current that was first identified by Siegelbaum and Tsien in 1980.[244] A similar 4-AP-resistant $[Ca^{2+}]_i$-activated current was subsequently found in cardiac tissues from elephant seal atrial fibers,[245] human atrial cells,[29] rabbit[30] and canine[31] ventricular myocytes, and sheep Purkinje fibers.[246] Zygmunt and Gibbons demonstrated that the charge carrier for Ca^{2+}-dependent I_{to} (I_{to2}) in rabbit ventricular[40] and atrial[41] myocytes is Cl^- ($I_{Cl.Ca}$). $I_{Cl.Ca}$ was reduced by reduction of external chloride, anion transport blockers DIDS and SITS, and agents that reduce the cytosolic Ca^{2+} transient. Activation of $I_{Cl.Ca}$ requires SR Ca^{2+} release since $I_{Cl.Ca}$ is abolished by caffeine and ryanodine, without affecting Ca^{2+} current activation. Sipido et al[247] showed that the amplitude of $I_{Cl.Ca}$ in rabbit cardiac Purkinje fibers is directly related to that of the $[Ca^{2+}]_i$ transient. Zygmunt later demonstrated that $I_{Cl.Ca}$ exists in canine ventricular epicardial and midmyocardial cells.[248] $I_{Cl.Ca}$ has a bell-shaped I-V relationship with a peak at +40 mV. $I_{Cl.Ca}$ activates and then decays rapidly during a depolarizing voltage step. Two possible mechanisms were proposed for this relaxation of $I_{Cl.Ca}$. First, whole cell $I_{Cl.Ca}$ relaxation reflects the decay of the underlying subsarcolemmal Ca^{2+} transient. The Ca^{2+} transient near the membrane is difficult to measure. Studies in which cell shortening or calcium-sensitive fluorescence have been used as a measure of bulk cytosolic Ca^{2+} concentration would suggest a poor correlation between the relatively long-lasting Ca^{2+} transient and a much briefer $I_{Cl.Ca}$.[247] However, relaxation of $I_{Cl.Ca}$ might still mirror the decay of the Ca^{2+} transient near the membrane because Ca^{2+} may be not uniform throughout the cell.[249,250] Second, $I_{Cl.Ca}$ channels may contain two Ca^{2+} binding sites: a high-affinity activation site and a low-affinity inactivation site. Channels would become inactivated at high concentration of $[Ca^{2+}]_i$ or during slow changes in the Ca^{2+} transient. This is supported by findings from Sipido et al that $I_{Cl.Ca}$ was present when $[Ca^{2+}]_i$ transient were fast but not during a slow transient.[247] However, Zygmunt[248] found that when constant changes in $[Ca^{2+}]_i$ were produced, $I_{Cl.Ca}$ became time-independent over a wide range of potentials, indicating $I_{Cl.Ca}$ behaves as a purely ligand-gated current. $I_{Cl.Ca}$ in Ca^{2+}-overloaded cells contains two components:[248] an oscillating and a steady inward current at diastolic potentials. The steady component is not what one would have expected if elevation of $[Ca^{2+}]_i$ caused inactivation of $I_{Cl.Ca}$. Modulation and regulation of $I_{Cl.Ca}$ may be even more complicated. Two components of $I_{Cl.Ca}$ have recently been identified in rabbit Purkinje fiber cells.[251] The first component quickly activated and relaxed before intracellular Ca^{2+} reached a peak, whereas the second component showed slower activation and lower Ca^{2+} sensitivities. The second component may arise from the same channel as the first and be related to spatial and teporal inhomogeneities of $[Ca^{2+}]_i$. or from a different Cl^- channel.[251] $I_{Cl.Ca}$ is believed to contribute to rate- and rhythm-dependent repolarization[245-248] and may play a role in triggered arrhythmias associated with delayed afterdepolarizations.[248]

3.2.4. $I_{Cl.swell}$

Cell swelling or membrane stretch induces a distinct type of Cl^- current ($I_{Cl.swell}$) in mammalian hearts, including dog ventricle[194] and atrium,[195,254] rabbit SA node and atrium,[196] human atrium,[255] and guinea-pig atrium[164] and ventricle,[256,257] and in cultured embryonic chick heart myocytes.[258,259] Pathologic states such as ischemia initiate myocardial swelling and may unmask this Cl^- conductance. However, little is now known about the single channel identity, molecular properties, activation and regulation mechanisms, and physiologic roles of these channels in heart.

Biophysical properties of $I_{Cl.swell}$. Cell swelling caused by exposure of cardiac cells to hypotonic media[164,194,195,254-259] or membrane stretch by inflating the cells via the patch pipette[196] activates a Cl^--sensitive membrane conductance with similar biophysical properties. They are aparently time-independent and have an outwardly rectifying I-V relationship under either asymmetrical[194-196] or symmetrical Cl^- gradients,[256] and a linear relation between E_{rev} and E_{Cl}.[198] The anion permeability sequence of swelling- or stretch-activated Cl^- currents in guinea-pig cardiac myocytes[256] or rabbit supraventricular cells[196], is $SCN^- > I^- \geq NO_3^- > Br^- > Cl^- > F^- > Asp^-$, based on shifts of the reversal potential of whole-cell currents.

While most authors[194,195,254-259] who investigated cardiac $I_{Cl.swell}$ in osmotically stressed cardiomyocytes did not detect or report time- and voltage-dependence of the current, Shuba et al recently reported that hyposmotic cell swelling-induced $I_{Cl.swell}$ inactivated remarkedly during 100 ms pulses to positive potentials.[257] Incrementing the holding potential in the positive direction depressed the $I_{Cl.swell}$ elicited at a constant positive test potential; the Boltzmann distribution describing this response has a half-potential near -25 mV and a slope factor near 20 mV. Although the voltage dependence of $I_{Cl.swell}$ reported by Shuba et al[257] is at odds with previous studies in cardiac cells,[194-196,254-256,258] it appears to have a close counterpart in a number of epithelial cells,[260-264] and *Xenopus* oocytes[265,266] (see below).

Pharmacological characteristics of $I_{Cl.cAMP}$. A detailed analysis of the pharmacological properties of $I_{Cl.swell}$ in dog atrial cells[254] showed that niflumic acid (100 μM), NPPB (10 to 40μM), IAA-94 (100 μM) fully inhibited $I_{Cl.swell}$ without a decrease in cell size. DIDS (100 μM) and DNDS (5 mM) fully inhibited outward currents but only partially inhibited inward current. while 9-AC (1 mM) only inhibited 50 % of the current. The effects of 9-AC on $I_{Cl.swell}$ observed in dog atrium are somewhat different from those in dog ventricular myocytes,[194] and guinea-pig atrial and ventricular cells,[256] or stretch-activated Cl^- current in rabbit SA nodal and atrial cells,[196] in which 1 mM 9-AC caused a 70-80% or complete inhibition of $I_{Cl.swell}$. An anti-oestrogen, tamoxifen, was found to be a strong blocker of $I_{Cl.swell}$ in guinea-pig atrial and ventricular cells.[256] While activation of $I_{Cl.swell}$ in rabbit supraventricular cells[196] and dog ventricular cells[194] was unaffected by protein kinase inhibitors (H-7[196] and H-8[194]), $I_{Cl.swell}$ in dog and human atrial myocytes could be augmented by isoproterenol[195] and forskolin.[254] On the other hand, $I_{Cl.swell}$ in chick heart is inhibited by isoproterenol.[258] The reason for these discrepancies is unknown.

Activation mechanism of $I_{Cl.swell}$. $I_{Cl.swell}$ developed over time during whole-cell patch clamp experiments in dog atrial myocytes with osmotically matched pipette and bath solutions.[195] $I_{Cl.swell}$ can be activated by hypotonic media and inhibited by hypertonic extracellular solution.[195] It can also be activated by cell membrane stretch.[196] At present, the mechanism for activation of $I_{Cl.swell}$ is not known. In order to determine whether activation of $I_{Cl.swell}$ is due to changes in cell volume or alteration in the membrane shape, Tseng studied the effects of anionic and cationic amphipaths (shape-altering agents)[252] on membrane currents in dog ventricular myocytes.[194] While no descernible change in cell width during or after applications of the anionic amphipath DPM (dipyridamole) or TNP (2,4,6-Trinitrophenol), which is preferentially inserted into the outer leaflet of the membrane to create a membrane shape change ("crenation") that is similar to the change occuring during cell swelling, induced an 9-AC-sensitive Cl^- current.

excluding the possibility of cell volune increase as a necessary mechanism for activation of the current. On the other hand, a cationic amphipath, CPZ (chlorpromazine HCl) which is preferentially inserted into the inner leaflet of the cell membrane to cause a morphological change ("cup') in the membrane that resembles the change induced by cell shrinkage, decreased the membrane conductance both under basal conditions and after cell swelling.[194] One possible explanation of these effects is that these agents caused membrane shape changes which created a tension in the lipid bilayer and resulted in opening or closing of the membrane channels. Cell swelling may activate membrane channels by exerting an outward tension in the lipid bilayer (mimicked by anionic amphipaths); and cell shrinkage may inhibit the channels by an increse in tension in the inward direction (mimicked by cationic amphipaths). These suggestions are in agreement with observations on the Cl^- channels in frog skeletal muscles: activation by cell swelling and inhibition by shrinkage;[253] but is different from that of the stretch-activated channel in the cell membrane of *E. coli* which can be activated by tension in the lipid bilayer in either directions, as revealed by channel activation by both pressure and suction or by both anionic and cationic amphipaths.[252] To test the hypothesis that an interaction between the cytoskeleton and channel proteins in the membrane activates $I_{Cl.swell}$, Taeng also examined the effect of dihydrocytochalasin B, an agent that can interrupt the polymerization of a component of the cytoskeleton (actin filaments), on the membrane conductance of dog ventricular cells.[194] In three of five cells studied, there was an increase in membrane conductance, accompanied by morphological changes. However, in the remaining two cells, no changes in either membrane conductance or cell morphology were observed.[194] A third possible mechanism is the dilution of intracellular regulatory factors. This hypothesis has not been tested in heart.

Distinctness of cardiac $I_{Cl.swell}$. The molecular identity of $I_{Cl.swell}$ in heart is not known. Since $I_{Cl.swell}$ does not require cAMP-PKA phosphorylation to be activated,[194.196] has different anion selectivity[196.199.200.204] and electrophysiological and pharmacological properties[196.208.254] from $I_{Cl.cAMP}$, $I_{Cl.swell}$ may be mediated by a distinct channel from $I_{Cl.cAMP}$. Recently, Vandenberg et al[256] and Shuba et al[257] found that both swelling-induced and protein kinase-activated chloride currents are functionally expressed in guinea-pig atrial and ventricualr myocytes. While $I_{Cl.swell}$ was inhibited by SITS,[257] DIDS and tamoxifen,[256] $I_{Cl.cAMP}$ induced by isoproterenol and forskolin and $I_{Cl.PKC}$ induced by PMA in guinea-pig ventricular cells were not sensitive to these agents.[208.255-257] Moreover, kinase-induced $I_{Cl.cAMP}$ and $I_{Cl.PKC}$ were relatively time- and voltage-independent, whereas hyposmotic swelling-induced currents inactivated during 100 ms pulses to positive potentials,[257] further that suggesting distinct channels are responsible for $I_{Cl.swell}$, $I_{Cl.cAMP}$, and

$I_{Cl.PKC}$. In mammalian cardiac cells, $I_{Cl.swell}$ could be activated under nominally calcium-free conditions in the presence of ryanodine, indicating that this current has a distinct activation mechanism from that of $I_{Cl.Ca}$.[40,41,250] The activation mechanism of mammalian cardiac $I_{Cl.swell}$ may also differ from avian cardiac $I_{Cl.swell}$ in that chick heart $I_{Cl.swell}$ is dependent on the elevation of $[Ca^{2+}]_i$ and inhibited by isoproterenol,[258,259] suggesting that $I_{Cl.swell}$ in avian and mammalian heart cells may be carried by distinct channels.

3.2.5. Other cardiac chloride currents

ATP binding of purinergic receptors activates a Ca^{2+}- and cAMP-independent chloride current ($I_{Cl.ATP}$ or $I_{Cl.purinergic}$) from guinea-pig atrial[164] and rat[165] and mouse[166] ventricular myocytes. The type of purinoceptor involved was not consistent in these studies. In guinea-pig atria, there was no clear order of P_1 or P_2 agonist potency since ATP, AMP, and adenosine were equally effective.[164] In rat and mouse ventricular cells, activation likely involes a P_2-PR because ATP, but not AMP and adenosine, was effective.[165,166] ATPγS activated $I_{Cl.ATP}$ in mouse but not in rat ventricular myocytes. Initial activation of $I_{Cl.ATP}$ by ATP in mouse ventricular myocytes occurred after a latency of about 30 to 40 seconds, suggesting the involement of a second messenger.[56] Activation of $I_{Cl.ATP}$ may not occur via a cAMP dependent pathway since pharmacological manipulations which raised cAMP stimulated Ca^{2+} currents failed to activate chloride currents in the same cells of mouse ventricle.

A small SITS-sensitive, 4-AP- and Cd^{2+}-insensitive transient outward Cl^- current has also been reported in about 30% of ferret ventricular myocytes.[267] The Ca^{2+}-dependence of this current was not specifically studied. Although 3 mM Cd^{2+} was used to block Ca^{2+} influx, the possibility of a free Ca^{2+} transient elicited by Na^+-Ca^{2+} exchanger could not be excluded.

3.3 Single cardiac chloride channels and relation to identified whole-cell chloride currents

Identification of the single-channel mechanisms responsible for macroscopic currents allows a direct determination of single-channel conductance, direct examination of gating properties, estimates of channel density and distribution and facilitates study of regulatory mechanisms.[268,269] Cardiac chloride channels were first recorded in 1982 when Coronado and Latorre[270] identified a 55-pS outwardly rectifying anion-selective channel from calf myocardial sarcolemma incorporated into planar lipid bilayers. However, this channel has not been related to any specific membrane channel or physiological function. The first identified and the only well-characterized cardiac unitary Cl^- channel resposible for a well-established macroscopic current is the $I_{Cl.cAMP}$ channel.[197,204,205]

3.3.1. *Cardiac $I_{Cl.cAMP}$ single channels*

In 1990, Ehara and Ishihara[197] found that epinephrine and dibutyryl cAMP activated a 13-pS channel with a reversal potential near estimated E_{Cl} and outward rectification under physiological asymmetrical [Cl^-] in guinea-pig ventricular myocytes. Based on previous estimates[198,214] of membrane Cl^- conductance, a channel density of ~0.02 - 0.1 μm^{-2}, or ~300 - 1400 channels/cell was estimated. Single $I_{Cl.cAMP}$ channels had a high open probability (mean P_o = 0.69) and their kinetics did not change over time even though the macroscopic current increased further while exposure to stimulators;.[205] however, an increase in the number of active channels was observed in some patches with progressive cell dialysis, and the newly activated channels also showed a high P_o. These results suggest that the cAMP-PKA system makes latent Cl^- channels available without influencing their kinetic behavior and the available channels may intrinsically exhibit a high P_o. The channel seemed to have at least one open state (time constant ~1 s) and two closed states (time constants around 0.2 and 1 s). In outside-out patches, a conductance varying between ~9 and ~15 pS was found at extreme negative and positive potentials, respectively, indicating a slight outward rectification with symmetric high [Cl^-].

Nagel et al[204] analyzed the mechanism of PKA-phosphorylation of cardiac $I_{Cl.cAMP}$ in inside-out giant patches from guinea-pig ventricular myocytes. They found that phosphorylation by the PKA catalytic subunit plus Mg-ATP elicits discrete Cl^- channel currents. In symmetrical [Cl^-] (150 mM), single-channel currents show a linear I-V relationship with a conductance of 12 pS. Activation of these cardiac Cl^- channel requires PKA-mediated phosphorylation. However, the phosphorylated channels close rapidly when ATP is withdrawn and reopen promptly after reapplication of ATP. Neither ADP, which has no γ-phosphate, nor AMP-PNP, which cannot donate γ-phosphate, are able to reopen phosphorylated channels that have been closed by withdrawal of ATP. Opening of the phosphorylated channels requires hydrolysable ATP, indicating that phosphorylation by PKA is necessary but not sufficient for channel activation.

3.3.2. **Other cardiac chloride single-channel conductances**

In 1989, Hill, Coronado, and Strauss[271] reported a 45-pS Cl^- channel, which is similar to a dimeric Cl^- channel from *Torpedo* electroplax. and an 18-pS Cl^- channel reconstituted from human ventricular tisue. No particular macroscopic Cl^- conductance equivalent has been specified.

Coulombe et al have reported two large-conductance (200 - 250 pS and 400 - 450 pS) Cl^- channels ($I_{Cl.LC}$) in cultured[273] and freshly dissociated[274] newborn rat cardiac myocytes and activated by strong membrane distension such as membrane blebs or cell swelling.[274] Channels were activated after a long period (mean 95 s) of superfusion with the hypotonic solution. Once the channel was activated, $I_{Cl.LC}$ exhibited multiple substates and underwent inactivation when submitted to large voltage steps. Inactivation increased more and more with increasing hyperpolarizations, whereas long-lasting currents corresponding to a conductance of about 50 pS occur during the remainder of the voltage pulse. The number of channels observable in a patch of membrane at the beginning of large voltage steps and undergoing subsequent inactivation was generally larger in cells submitted to hypotonic media than in membrane blebs. Channel activity was more frequently observed in the inside-out than in the cell-attached configuration. However, the application of tension to the membrane patch via a negative pressure imposed on the patch pipette failed to activate the channel. Neither colchicine, a substance preventing microtubule assembly, nor cytochalasin D, which disturbs the microflament system, could activate the channel, suggesting that disorganization of the cytoskeleton may not be involved in the activation of $I_{Cl.LC}$ and that $I_{Cl.LC}$ may not be a stretch-induced channel. Activation of $I_{Cl.LC}$ is $[cAMP]_i$- and $[Ca^{2+}]_i$-independent, distinguishing it from $I_{Cl.cAMP}$ and $I_{Cl.Ca}$. Since $I_{Cl.LC}$ has never been observed in adult heart cells and the corresponding macroscopic current has not been identified, the physiological role of $I_{Cl.LC}$ is not known.

Collier et al investigated the possible single-channel equivalents for $I_{Cl.PKC}$[240] and $I_{Cl.Ca}$[275]. In guinea-pig ventricular myocytes, bath application of PMA resulted in the appearance of unitary Cl^- channel current in cell-attached patches with properties nearly identical to those of PKA-activated Cl^- channels in terms of I-V relationship and voltage-dependence, slope conductance, Cl^--dependence, mean open probability and kinetics, and insensitivity to DIDS.[240] Ca^{2+} applied to the cytoplasmic surface of inside-out membrane patches from canine ventricular myocytes activated small conductance (1.0 - 1.3 pS) channels.[275] These channels were Cl^--selective with rectification properties which could be described by the GHK equation (1-4). Channel activity exhibited time-independence when cytoplasmic Ca^{2+} was held constant and sensitivity to Cl^- channel blockers DIDS and niflumic acid as seen for macroscopic whole-cell $I_{Cl.Ca}$ in the same preparation.[248] The number of channels opened and their open probability (P_o) increased upon increase in $[Ca^{2+}]_i$ in a concentration-dependent manner. These properties of the small conductance Cl^-channel in heart compare well with those recorded in *Xenopus* oocytes,[277] endocrine cells[278] and smooth muscle cells.[279]

3.4. Non-cardiac chloride conductances and their molecular physiology

There is probably no cell without some types of Cl^- channel.[280-283] Extensive studies on non-cardiac Cl^- channels have provided important insights not only into the basic biophysical, electrophysiological, and molecular properties, signal transduction pathways, and regulatory mechanisms of Cl^- channels in non-cardiac tissues, but also into the gating mechanism and functions of Cl^- channels in the heart. In this section, I will focus on the basic and molecular physiology of the sarcolemmma membrane anion channels, such as the Cl^- channels activated by cAMP, cell swelling- or membrane stretch, and Ca^{2+}, the voltage-gated Cl^- channel and ORCC, which have a close relation to my present study of cardiac sarcolemma chloride channels. I will not deal with the large area of ligand-gated chloride channels such as GABA- and glycine-receptor channels, even though a large number of exciting developments have taken place in this area. Intracellular Cl^- channels will also not be included in this section.

3.4.1. Cyclic AMP-activated chloride channel and CFTR

Cystic fibrosis (CF), the most common fatal genetic disease among Caucasians, is characterized by abnormal electrolyte transport in several organs, including lung, sweat gland, intestine and pancreas.[283,284] Defective regulation of the apical membrane cAMP-PKA-regulated Cl^- channel ($I_{Cl.cAMP}$) that control the rate of transepithelial Cl^- transport is now well documented in CF epithelia.[234,280,283-287] At the whole-cell level, $I_{Cl.cAMP}$ exhibits time- and voltage-independence and a linear I-V curve under conditions of symmetric $[Cl^-]$, and is blocked by DPC and glibenclamide but not by DIDS and SITS.[287-290] $I_{Cl.cAMP}$ has a distinct halide permeability sequence of $Br^- > Cl^- > I^- > F^-$ (Cl^- to $I^- \approx 2:1$).[288] At single channel level, a low conductance (7-15 pS) cAMP-activated Cl^- channel with similar biophysical and pharmacological properties as whole-cell $I_{Cl.cAMP}$ was characterized first in pancreatic duct cells[291] and then in other epithelial cells.[292] It has now been established that the molecular basis of $I_{Cl.cAMP}$ is CFTR.

CFTR is a CF gene product with 1480 amino-acid containing two motifs, each having six transmembrane-spaning domains and a cytoplasmic nucleotide-binding fold (NBF). Between these two motifs lies a 240-amino-acid regulatory (R) domain containing several sites for PKA and PKC dependent phosphorylation (Figure 1-4D), placed it in the large family of ATP-binding cassette (ABC) transport proteins that includes the multidrug-resistant gene product, P-glucoprotein (P-Gp), and yeast and bacterial transporters.[293] All members of the ABC superfamily contain NBFs which bind ATP and/or couple ATP hydrolysis to the transport process, but the R domain is apparently unique to CFTR. The evident homology of CFTR structure to the members of the ABC family has fueled the persistent notion that CFTR might also function as a transporter that somehow modulate epithelial Cl^- channels.[294] Regardless of the eventual resolution of this proposal,[289] several lines of evidence have removed any lingering doubt that CFTR does indeed function as a small-conductance, ohmic Cl^- channel whose gating is regulated by PKA and hydrolyzable ATP. Although CFTR was originally identified primarily in cells of epithelial origin, a 6.5 kB transcript has been identified in rabbit and guinea-pig ventricle and human atrium, demonstrating expression of a transcript homologous to CFTR in heart .[233,235]

Interestingly, Reisin et al[298] have recently demonstrated that the expression of CFTR was associated not only with a cAMP-inducible Cl^- channel but also with the appearance of a cAMP - dependent ATP channel that is inhibited by DPC but not by DIDS. Single-channel analysis of the ATP and Cl^- currents indicate that the same conductive pathway is responsible for both ionic movements, supporting the hypothesis that CFTR is a multifunctional protein with more than one anion transport capability and the transport of ATP by CFTR may serve several regulatory functions: the facilitation of CFTR Cl^- conductance, the activation of ORCC through P_{2U}-PR,[289] and the regulation of other ion channels such as the Na^+ channel.[299].

3.4.2. Voltage-gated Cl^- channels from Torpedo and the CLC family

In the plasma membrane of the electric organ of *Torpedo Californica* resides a Cl^- channel whose function is to establish the electroplax cell as a source of electric current in stunning its prey.[300] At the single-channel level, this channel exhibits an unusual gating behavior: a bursting process in which the open channel displays three distinguishable equaly-spaced conductance substates. Miller et al[300,301] proposed that the three active substates result from the independent opening and closing of two identical Cl^- diffusion pathways, or "protochannel". In this scheme, the dimeric channel complex may exist with both protochannels simultaneously open, with one open and one closed, or with both closed. This "double barreled shotgun" model for the channel is well supported by several lines of evidence: the equal spacing in conductance of the three substates, the binomially distributed probability of the appearance of the substates, and pharmacologically, the ability of short exposure (5 - 30 s) of the channel to DIDS to convert this three-level active channel into a "conventional" two-level channel, but longer exposure to eliminate all channel function.[300,301] A cDNA encoding a voltage-gated Cl^- channel (named CLC-0) from *Torpedo marmorata* electric organ was cloned by expressing hybrid-depleted mRNA in *Xenopus* oocytes in 1990 by Jentsch et al.[302] The protein has up to 13 putative membrane-spaning domains, which are considered to be a hallmark of ion channels and other transport proteins. Database searches showed it to be a novel protein, while matrix comparisons revealed no significant similarity to glycine and GABA receptors, the ligand-gated Cl^- channels, or band 3, the electroneutral anion exchanger of erythrocytes. Expression of a single *Torpedo* cDNA in *Xenopus* oocytes forms a double-barreled Cl^- channel,[303] consistent with the original description by Miller et al.[300,301] Sequence homology-based strategies, including low stringency screening of cDNA libraries and PCR using degenerate primers, permitted the identification of four additional genes in the rat (CLC-1, CLC-2, CLC-K1, and CLC-K2), all sharing significant homology with CLC-0.[304-307] CLC-1 is the major mammalian skeletal muscle Cl^- channel. Its importance is underscored by the observation that mutations in this gene lead to myotonia (a defect in muscle relaxation) in both mice[308] and people.[309] CLC-2 is ubiquitously expressed in epithelial and non-epithelial cells.[305] It can be activated both by strong hypopolarization and by cell swelling. It is probably involved in cell-volume regulation (see below). Position-independent structures important for its activation have been localized to the amino terminus.[310] The CLC-K1 gene is specifically expressed in kidney and its transcription is induced by dehydration of the animal, suggesting that it may contribute to Cl^- reabsorption. Homology screening in the kidney has also resulted in the cloning of CLC-3.[311] It is less than 30% identical to previously known CLC proteins, but in contrast to the CLC-K proteins shows a broad expression pattern (e.g. in brain, lung and kidney). In the course of mapping human X chromosomes another member of this gene family, dubbed CLC-4,[312] has been identified and found to be expressed predominantly in human skeletal muscle, brain and heart. It belongs to the same branch of the CLC gene family as CLC-3, as it is 77% identical to CLC-3 at the amino acid level. No functional expression studies of CLC-4 was reported. Common features of the CLC family include a $Cl^- > Br^- > I^-$ selectivity (with apparent exceptions reported for CLC-K1[306] and CLC-3[311]) and a low single-channel conductance (CLlC-0 having a conductance of 10 pS and CLC-1 being still lower, less than 1 pS). Functional expression of CLC-3 in somatic cell line revealed a large-conductance outwarly rectifying Cl^- channel current with four conductance levels (0, 40, 100, 140 pS) which were dependent on $[Ca^{2+}]_i$.[313] CLC-3 single channel activity could only be recorded in cell-free excised patches but not in cell-attached patches, suggesting the existence of a intracellular inhibition mechanism.[313]

3.4.3. Ca^{2+}-activated chloride channels

Ca^{2+}-activated chloride channels are widely distributed and involved in important physiological processes.[314] $I_{Cl.Ca}$ was originally identified in rod segments from the salamander retina[315] and in *Xenopus* oocytes.[276] Subsequently, this current has been observed in many types of tissue including exncrine[316,317] and edocrine cells,[277] neurons,[318] epithelial cells,[288] smooth muscle cells,[278,279] and cardiac myocytes.[40,41,247,248,276] In rat lacrimal glands, $I_{Cl.Ca}$ was predicted to have a very small conductance and found to be more permeable to I^- and Br^- than to Cl^-.[316,317] Young et al[319] studied $I_{Cl.Ca}$ from Xenopus oocyte membranes reconstituted into planar lipid bilayers. The channel was poorly selective, activated by micromolar concentrations of Ca^{2+}, and had a conductance of 380 pS in symmetric 1 M Cl^-. This is comparable to single-channel $I_{Cl.Ca}$ in rabbit colonic smooth muscle cells,[320] but is much larger than the conductance (2-5 pS) estimated by single-channel analysis for $I_{Cl.Ca}$ in frog oocytes,[276] lacrimal gland,[317]and cultured endocrine cells from mammalian pars intermedia.[277] In vascular smooth muscle, $I_{Cl.Ca}$ has been described in cells isolated from rabbit and rat portal vein, rabbit ear artery, rabbit and pig coronary and human mesenteric arteries and cultured pig aorta cells.[278,279,321-324] $I_{Cl.Ca}$ can be activated by calcium release from intracellular stores or by calcium entry through voltage-gated Ca^{2+} channels. It is blocked by DIDS, SITS, NPPB, 9-AC, and niflumic acid. Single $I_{CL.Ca}$ channel has conductance of 2.8 pS in human mesenteric artery smooth muscle,[278] and 1.8 pS in A7r5 cultured aortic smooth muscle cells.[279]

3.4.4. Cell swelling- and stretch- induced chloride channels, pI_{CLn} and P-Gp

$I_{CL.swell}$ has been observed in virtually all mammalian cells studied to date (reviewed by Strange and Jackson[325]). A similar outwardly rectifying swelling-activated conductance has been observed in *Xenopus* oocyte[266] and hepatocytes isolated from the little skate *Raja erinacea*[326]. The characteristics of these conductances at the whole-cell level are nearly identical and can be summorized as follows:

Ion selectivity. $I_{CL.swell}$ exhibits a high selectivity for anions over cations with relative cation permeabilities (P_{cation}/P_{Cl}) of < 0.03 - 0.05.[262,263,327,328] Anion selectivity is broadly consistent across cell types, and is $I^- \approx NO_3^- > Br^- \geq Cl^- > F^-$. [262,263,266,325,326]

Pharmacology. $I_{Cl.swell}$ is inhibited by polyunsaturated fatty acids,[263,328] ketoconazole,[328] NPPB,[262,263,328] 1,9-dideoxyforskolin (DDF),[328,329] lanthanum,[266] tamoxifen,[256,330] and various stilbene compounds (DIDS, SITS, DNDS etc.).[194,196,263,327] Drug sensitivity varies among cell types. For example, the anion conductance in C_6 glioma cells is redily inhibited by 100 μM ketokonazole.[328] In contrast, this drug has no effect on $I_{Cl.swell}$ in skate hepatocytes.[326] DDF inhibits the current in C_6 glioma cells,[328] P-Gp-transfected NIH/3T3 cells,[329] and Hela cells[331] but has no effects on $I_{Cl.swell}$ or I^- efflux in colchicine-selective NIH/3T3 cells,[332] T84 cells,[333] and lung carcinoma epithelial cells.[334]

Inhibition by extracellular nucleotides. Millimolar concentrations of extracellular nucleotides such as cAMP and ATP also inhibit $I_{Cl.swell}$.[266,326,335] The physiological relavance of this inhibition is unclear. Inhibition by ATP increases open channel noise, is voltage dependent, is sensitive to the direction of net Cl^- flux through the channel, and shows depolarization-induced inactivation,[325] suggesting that ATP blocks $I_{Cl.swell}$ by interacting with the channel pore.

Voltage-dependent gating. In T84 cells,[261,262] intestinal cells,[263] fibroblasts,[331,332,336] airway epithelial cells,[260,337,338] sweat duct cells,[261] Hela cells,[331] C_6 glioma cells,[335] *Xenopus* oocytes,[266] and guinea-pig ventricular myocytes,[257] membrane depolarization to > +60 mV inactivates $I_{Cl.swell}$ in a time- and voltage-dependent manner. The time constant for inactivation is pH-sensitive and is decreased by extracellular acidification.[266,335] Membrane hyperpolarization reactivates the conductance in C_6 glioma cells[335] and intestinal epithelial cells.[263] Voltage sensitivity is highly variable, ranging from little or no effect of depolarization[326] to nearly complete inactivation in response to 1- to 2-s voltage steps above +90 mV.[263,335]

Single channel properties. The unitary properties of the channel responsible for $I_{Cl.swell}$ were uncertain until recently. Stationary noise analysis studies in chromaffin cells,[339] neutrophils,[340] T lymphocytes,[327] and human endothelial cells[341] suggested a very low single-channel conductance ($\leq$ 1-2 pS at 0 mV). Based on these findings, Lewis et al[327] termed the channel the "mini" volume-sensitive Cl^- channel. In contrast, single-channel measurements in various epithelial cells demonstrated the existance of a swelling-induced outwardly rectifying anion channel with a unitary conductance of 40-90 pS at strongly depolarizing voltages.[261,262,342] Solc and Wine[261] reported a cell-swelling induced single Cl^- channel with properties somewhat different from ORCC in that cell-attached ORCC were often closed at resting voltages, started to inactivate at more positive voltages, rectified more and had lower conductance, shorter mean open durations and more open-channel noise than cell-swelling-induced channels. They could not, however, differentiate whether two types of single Cl^- channel currents caused by cell-swelling are due to separate channel proteins or from the same channel in different states . Very recently, Strange and Jackson utilized stationary and nonstationary noise analyses and single-channel current measurements to determine the unitary properties of $I_{Cl.swell}$ in C_6 glioma cells[343] and rat inner medullary collecting duct cells.[344] It was assumed[17] that 1) there are N independent and identical channels in the membrane, 2) the channels have two conductance states (open and closed) that obey binomial statistics, and 3) graded changes in macroscopic current (I) are due to graded changes in channel open probability (P_o). Then current variance, σ^2, is defined as

$$\sigma^2 = iI - I^2/N \qquad (1\text{-}5)$$

where i is single-channel current. Measurements of whole-cell current variance therefore allow the estimation of single-channel conductance and channel density. Using this model, analysis of stationary current noise yielded a unitary conductance of ~0.5 pS at -50 mV and ~1 pS at 0 mV and a channel density of ~60,000 - 70,000 channels/cell.[343,344] These results are the same as those reported previously for chromaffin cells, neutrophilis, T lymphocytes, and endothelial cells.[327,340-341] In contrast, analysis of nonstationary current noise during depolarization-induced inactivation predicted that the channel has a conductance of ~40-50 pS at +120 mV (~15 pS at 0 mV) and that there are ~1,000-3,000 channels/cell.[343,344] In inside-out patches, they observed unitary anion currents with characteristics identical to the whole-cell conductance. At negative holding potentials, single-channel transitions were rarely detected in the membrane patches. When the patches were depolarized, however, single-channel closures were readily observed.[262,343] Measurements of these channel closure events confirmed the nonstationary noise analysis results.[343,344] The channel has a conductance of 40-50 pS at +120 mV and the P_o is near unitary once a channel is activated by cell swelling.[261,342-344]

Molecular identity of $I_{Cl.swell}$. At molecular level, the protein identity and the molecular mechanisms involved in activation and regulation of $I_{Cl.swell}$ remain largely unknown. To date, at least three proteins (ClC-2, pI_{Cln} and P-Gp) have been proposed to be candidates for the volume-regulated Cl^- channel or regulator.

CLC-2 is a member of CLC family and can be activated by hyperpolarization or hypotonicity-induced cell swelling when expressed in amphibian oocytes. However, CLC-2 differs from typical volume-regulated Cl^- channels investigated to date in its ion selectivity, pharmacology, and voltage-dependence.[305,310] In contrast to $I_{Cl.swell}$, CLC-2 is activated at voltages more negotive than -90 mV. Hyperpolarization-induced activation does not saturate with voltages up to -180 mV. The channel rapidly inactivates when the membrane is depolarized to -30 mV.[305] The instaneous I-V relationship assessed by tail current analysis shows slight inward rectification. CLC-2 is selective for Cl^- over other anions, has an anion permeability sequence of $Cl^- \geq Br^- > I^-$, and a unitary conductance of 3-5 pS.[310] The channel is partially blocked by 1 mM 9-AC and 1 mM DPC, but is largely unaffected by 1 mM DIDS.

pI_{Cln} is a protein encoded by a cDNA cloned from a kidney cell line by expression in *Xenopus* oocytes.[265] Injection of pI_{Cln} mRNA into oocytes generates a Cl^- current with characteristics very close to those of $I_{Cl.swell}$ seen in many different cell types including cardiac myocytes. However, about 4% of uninjected oocytes had been found to possess similar currents[265] and such current can be evoked in native, uninjected oocytes by exposure to hypotonicity.[266] It was the postulated that pI_{Cln} is either identical to the cell-swelling activated channel (which may be partially open without cell swelling after overexpression,) or that it activates the channel. Since hydropathy analysis did not predict any transmembrane span for pI_{Cln}, a β-barrel structure similar to that of voltage-dependent anion channels (mitonchodrial porin, VDAC) was postulated.[265] Okada et al[345] have cloned a cDNA encoding a swelling-induced Cl^- current related protein from the rabbit heart of which the primary structure is highly homologous to that of pI_{Cln}, the role of this protein is still unclear. pI_{Cln} has recently been further characterized as an abundent, soluble, highly acidic protein located primarily in the cytoplasm of MDCK and heart muscle cells.[346] pI_{Cln} forms tight oligomeric complexes with other cytoplasmic proteins including actin. The cytoplasmic location and biochemical characteristics of the protein are unexpected for a membrane ion channel. An endogenous pI_{Cln} also exists in *Xenopus* oocytes. It has therefore been proposed that pI_{Cln} is an indirect regulator instead of a plasma membrane Cl^- channel or part thereof,[346] and consequently, that overexpression of pI_{Cln} in oocytes activated the endogenous volume-regulated Cl^- channel, whose molecular identity is so far unknown but may be different from pI_{Cln} .[347]

P-Gp is a member of the ABC family mediating multidrug resistance (MDR) in tumor cells. Expression of P-Gp in fibroblasts or lung cells results in a cell swelling-induced outwardly rectifying, DIDS-sensitive Cl^- current resembling those found in many native cells.[329,336] Because the ABC family also includes CFTR which has been proved to be a Cl^- channel, it was consequently proposed that P-Gp may be a protein with channel and transporter activity. However, whether P-Gp is itself a channel protein responsible for $I_{Cl.swell}$ or a regulator of endogenous channel proteins remain unclear, since volume-sensitive Cl^- current has not been associated with P-Gp in all cell lines.[348] It has been reported that activation of PKC inhibits P-Gp-conferred Cl^- current, and recent studies suggest that P-Gp, instead of being a channel itself, may act as a PKC-mediated regulator of an endogenous volume-sensitive Cl^- channel whose molecular identity remains to be determined.[349]

In summary, none of these proteins expressed from cloned genes initially hypothesized to be Cl^- channels underlying $I_{Cl.swell}$ have been conclusively confirmed, and it now seems that they may rather be activators of native Cl^- channels in cells used for expression studies.

3.4.5 ORCC - Outwardly rectifying chloride channels

ORCCs are widely distributed in nature and are thought to mediate volume regulation, signal transduction, and transepithelial transport.[261,283,350-353] ORCCs have a 20-30 pS single-channel conductance at hyperpolarizing voltages and a 40-70 pS conductance at depolarizing voltages, consistent with their outwardly rectifying I-V relationship.[261,288,350-353] ORCC single-channel currents can be activated by prolonged depolarizing voltages (to+60 mV) and inactivated, in some instances, by strong hyperpolarizing voltages (>-90 mV).[352] Several signal transduction pathways involved in the regulation of ORCC have been reported. cAMP-dependent protein kinase phosphorylation can activate ORCC.[357,358] Phosphorylation by PKC has dual effects that depend on $[Ca^{2+}]_i$. At low $[Ca^{2+}]_i$ PKC activates ORCC whereas at high $[Ca^{2+}]_i$ (1 μM) PKC inactivates ORCC[352,354]. Increases in $[Ca^{2+}]_i$ activate ORCC through Ca^{2+}-calmodulin-dependent kinase (CaMK).[287] Activation of ORCC by temperature, trypsin, and depolariztion has also been reported.[355] ORCCs are blocked by DPC, stilbene derivatives (DIDS, SITS, DNDS), or calixarenes.[356] ORCCs have a halide permeability sequence of $I^- > Br^- > Cl^- > F^-$ (I^- to Cl^- = 2:1).[288,350-353]

Before the CF gene was cloned and CFTR was characterized, it was believed that defective regulation of ORCC in epithelia might be the primary defect in CF.[356] However, ORCC could not be detected readily in cell-attached and whole-cell configurations. Expression of CFTR in heterologous cells produced not the expected 40-60 pS ORCC but a smaller channel (10 pS) with a linear I-V curve. cAMP-stimulated whole cell Cl^- currents had properties most consistent with activation of CFTR Cl^- currents, while ORCC currents were not observed on stimulation with agonists that increase intracellular cAMP. As a consequence, it was suggested that ORCC did not contribute to $I_{Cl.cAMP}$ in epithelial cells, leading to a debate about whether ORCC plays any significant functional role in cell physiology and in CF.[351]

Guggino et al[357] resolved this apparent inconsistency when they found that, indeed, ORCC was present in CF epithelia and that this channel could not be opened by PKA. Transfection with CFTR restored the stimulatory effect of the kinase.[357] So CFTR was, after all, not only a transmembrane conductance protein but also a regulator of other effectors such as ion channels (see General Discussion). Because ORCC is present in the CFTR knockout mice, they must be separate gene products.[358] While many workers are trying to clone epithelial ORCC,[20] the molecular identity of ORCC is presently unknown.

3.4.6 Phospholemman - a hyperpolarization activated chloride channel?

Phospholemman (PLM) is a small protein with a single transmembrane span which is a major target for phosphorylation in the cardiac plasma membrane.[359] Its function is presently unclear, and its homology to the γ-subunit of the Na-K-ATPase[360] does not provide a clue. When expressed in *Xenopus* oocytes, it produces a Cl^- current that is slowly activated upon strong hyperpolarization.[361] The simplest explanation is that PLM is a Cl^- channel; however, some batches of *Xenopus* oocytes display endogenous current with many similar characteristics, including similar voltage-dependence, kinetics, halide selectivity ($I^- > Cl^-$) and pharmacology (e.g., blocked by Ba^{2+}).[361-363] Thus, it seems possible that PLM activates this endogenous oocyte current. Overexpression of I_{sK}, a small K^+ channel protein having just one transmembrane span,[364] also leads to 'PLM-like' Cl^- currents in oocytes.[363] Certain mutations in I_{sK} led to a loss of K^+ channel induction, while others destroyed its potential to activate Cl^- channels. Some mutations in PLM alter the kinetics of currents,[361] but not the ion selectivity. In contrast, mutations in I_{sK} changed the ion selectivity of the cation current.[365] This suggests that I_{sK}, in addition to somehow activating Cl^- channels, is indeed a K^+ channel. Expression of an otherwise non-functional mutant of the muscle CLC-1 also induces similar Cl^- currents when overexpressed in oocytes.[366] Thus, overexpression of at least three unrelated proteins elicits similar Cl^- currents, sugesting (but not proving) that they may result from activation of endogenous oocyte channels.

4. Functions of chloride channels

Chloride is the most abundant anion in most biological systems. Cl^- channels have been shown to have important functions in a wide variety of animal cells. In transporting epithelia. Cl^- channels can regulate fluid secretion or electrolyte absorption by controlling the amount of Cl^- that is co-transported with its counter-ion.[283] Voltage-gated Cl^- channels in nerve cells can control the frequency of repetitive action potentials.[367] In myotonia, skeletal muscle is hyperexcitable due to decreased resting conductance caused by the absence of functional Cl^- channels in the membrane.[308,309] The protein kinase-mediated regulation of Cl^- channels is very important in the normal function of epithelia[283,352-354] and cardiac myocytes.[80,183,193]

4.1. Regulation of cell membrane potential

As mentioned above, activation of Cl^- channels can contribute both inward and outward currents to regulation of membrane potential. The degree to which activation of Cl^- channel to depolarizes the resting potential (by inward currents due to Cl^- efflux) or accelerates repolarization (by outward currents due to Cl^- influx) depends on the E_{Cl} and the magnitude of the Cl^- conductance relative to the total membrane conductance.

4.2. Regulation of cell volume

Maintenance of a constant cell volume in the face of osmotic stress is an evolutionarily ancient homeostatic process. Under physiologic conditions, most mammalian cells are not exposed to anisotonicity. The osmolality of body fluids is normally ~285 mOsm/kg H_2O and is regulated within extremely narrow limits (±3%) by body fluid homeostasis. Under pathophysiological conditions, disturbances of body fluid homestasis can be encountered, with plasma fluid osmolalities ranging from 220 to 350 mOsm/kg H_2O.[368.369] Under these extreme conditions the cells of the body would, in the absence of volume-regulating mechanisms, swell and shrink by ~50 and 20 % respectively.[368-369] Besides maintaining a constant volume under resting isotonic conditions, most cells are also capable of counteracting volume perturbations by volume recovery mechanisms. Swollen cells tend to reduce their volume toward initial values by loss of KCl and concomitant loss of water (regulatory volume decrease, RVD), and shrunken cells often show the capacity to increase their volume toward initial values by net uptake of KCl and concomitant uptake of water (regulatory volume increase, RVI). In animal cells, after swelling in hypotonic media, the simultaneous activation of K^+ and Cl^- channels is believed to be the initial, time-determining step in cell volume regulation.[370-371] The activation of both pathways is functionally linked and enables cells to lose ions and water, leading to cell shrinkage and readjustment of the initial volume.[258]

4.3. Regulation of intracellular pH

In view of the marked pH sensitivity that is expected for virtually all cellular processes, the importance of intracellular pH (pH_i) regulation is unquestionable. Most animal cells appear to have pH_i levels more alkaline than predicted if H^+ and HCO_3^- were passively distributed across the plasma membrane. The pH_i values of nerve and muscle cells with membrane potential of -50 to -90 mV would be 0.8 - 1.5 pH units lower than the extracellular pH (pH_o) if H^+ was at electrochemical equilibrium across the cell membrane. The transmembrane pH differences are, however, much lower, in the range of 0.2 to 0.5 pH values.[372] The tendency of cells to become acidified by the passive fluxes of H^+ and HCO_3^- must therefore be counteracted by regulatory acid-extruding mechanisms. Cl^--HCO_3^- exchanger is one of the major mechanisms of HCO_3^- extrusion.[189] Control of $[Cl^-]_i$, therefore, becomes very important in regulation of pH_i, while the

Cl^--HCO_3^- exchanger itself does not regulate $[Cl^-]_i$.[18] In addition to Cl^--Na^+, $2Cl^-$-Na^+-K^+, and Cl^--K^+ cotransporters, Cl^- channels play an important role in regulation of $[Cl^-]_i$ and pH_i.[18,188]

4.4. Evidence for a functional role of chloride channels in heart

The functional roles of most Cl^- channels in the heart are still largely unclear, but given the known biophysical and electrophysiological characteristics of these channels and their possible regulatory mechanisms, some reasonable predictions can be made (Figure 1-10).[193]

Early voltage-clamp experiments suggested that Cl^- conductances contributed to the normal frequency of spontaneously beating Purkinje fibers and papillary muscles by supplying a part of the depolarizing current from rest as well as contributing to the shape and duration of cardiac AP via a time- and voltage-dependent outward current.[174,175] The Cl^- channel responsible for this outward current has now been demonstrated to be $I_{Cl.Ca}$.[40,41,247,248] $I_{Cl.Ca}$ may contribute to the arrhythmogenic transient inward current in canine ventricular myocytes.[248]

Activation of $I_{Cl.cAMP}$ causes a slight but consistent depolarization of RMP and a 50% decrease in the APD in ventricular cells, suggesting that under normal conditions (E_{Cl} in the range of -65 to -40 mV) the major physiological function of activating $I_{Cl.cAMP}$ is to minimize (counteract) the significant AP prolongation associated with βAR stimulation of I_{Ca}.[198,214] However, a significantly larger diastolic depolarization occurs when $[Cl^-]_i$ is increased substantially,[198] mediated presumably by an increased driving force for efflux, changes in the Cl^- equilibrium, and removal of the outward rectification seen under normal physiological conditions.[200] Thus, upon increase of $[Cl^-]_i$, activation of $I_{Cl.cAMP}$ would enhance automaticity. The effects on cardiac electrical activity of activation of $I_{Cl.PKC}$, $I_{Cl.ATP}$ and $I_{Cl.swell}$, although not yet tested, may be similar to those of $I_{Cl.cAMP}$ (Figure 1-10), because the macroscopic conductances are indistinguishable.

Recent work suggests that Cl^- currents may underlie some of the electrophysiologic abnormalities associated with acute myocardial ischemia. Ischemia could potentially elicit Cl^- currents by releasing NE (through $I_{Cl.cAMP}$), and by causing Ca^{2+} overload (via $I_{Cl.Ca}$), cell swelling (via $I_{Cl.swell}$), and accumulation of adenosine and related metabolites (via $I_{Cl.purinergic}$). In isolated whole heart, disulfonic stilbene-Cl^- channel blockers DIDS and SITS lengthened APD in normoxia and attenuated the early APD abbreviation in hypoxia.[373] In isolated cells, DIDS did not affect the glibenclamide-sensitive outward current but DPC blocked Cl^- currents induced by isoproterenol.[373] The replacement of $[Cl^-]_o$ by nitrate ions protects rat hearts against ventricular arrhythmia during acute myocardial ischemia and reperfusion,[374] and this has been interpreted as suggesting a role for Cl^- currents in ischemic cardiac arrhythmias.

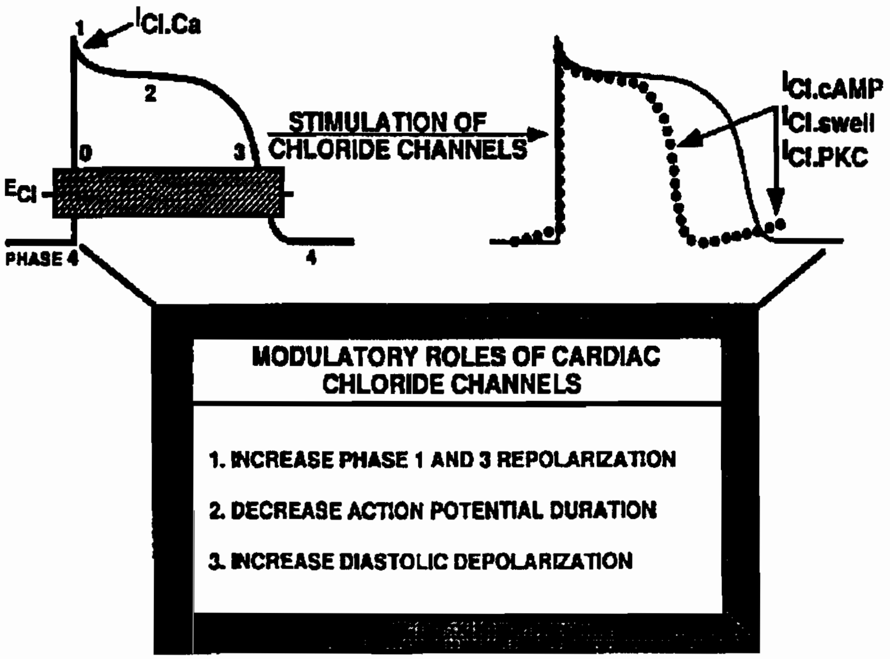

Figure 1-10. Modulation of the cardiac action potential by chloride channels. Model representation of a cardiac action potential elicited from ventricular myocytes. The ability to modulate the action potential by chloride channel activation via sympathetic catecholamine stimulation or cell swelling is shown in the setting when other currents (i.e., I_{Ca} and I_K) are blocked. $I_{Cl.Ca}$ contributes a portion of the rapid phase 1 repolarization. The precise modulatory role of chloride currents will depend on E_{Cl}, which may vary substantially. (Modified from Ackerman and Clapham[193]).

5. Statement of the problem

The contributions of cation (Na^+, K^+, and Ca^{2+}) channels to cardiac electrical activity have been studied extensively and intensively by many investigators over the last 30 years. Consequently, substantial knownledge has been acquired regarding the role of Na^+, K^+, and Ca^{2+} channels in cardiac electrophysiology. Anion channels have received much less attention and much is still unknown about the following questions:

1) All described Cl^- currents need to be activated and do not show basal activity. What is the exact functional role of these channels under normal physiological conditions? Is there any Cl^- current other than the five showed in Figure 1-9 which is basally active and contributes

relevant current to the total membrane conductance under normal resting conditions as proposed by McAllister et al[178] in 1975? Only when an $I_{Cl.b}$ was introduced into their simulation model, could McAllister et al successfully reconstruct the electric activity of cardiac tissue and simulated the effect of Cl^- removal on the AP.[178] In many animal cells, including cardiac cells[186], resting background Cl^- conductance is significant.[173] Yet, classical electrophysiological investigation has not been able to demonstrate a macroscopic cardiac Cl^- current under basal conditions, as was done for Na^+, K^+, and Ca^{2+} currents. One of the reasons is that Cl^- currents often has a time- and voltage-dependence similar to leakage current, thus the two components are lumped together and difficult to separate.[173]

2) Knowledge regarding the single channel properties underlying macroscopic cardiac Cl^- currents is very limited.[193] The only cardiac Cl^- current whose single-channel equivalent is well-established is $I_{Cl.cAMP}$.[197,204,205]

3) Catecholamines released from sympathetic terminals stimulate both αAR and βAR in the heart. Although many investigators have studied the modulation of caridac Cl^- current by βAR stimulation, the effects of αAR stimulation on cardiac Cl^- currents has not been extensively investigated. While preliminary data has shown that α-adrenergic agonist phenylephrine activates $I_{Cl.PKC}$ in cat ventricular myocytes,[375] the ability of α-adrenergic stimulation to modify other cardiac Cl^- channels is unknown.

4) In rabbit atrial myocytes, as in many other cardiac tissues of various species, a sustained residual outward current (I_{sus}) is present after the inactivation of I_{to1}.[27,28] The ionic nature of I_{sus} is unclear. In rat ventricular myocytes, it has been shown that the residual component is insensitive to 4-AP and responds differently to α-adrenergic stimulation, suggesting that I_{sus} may be a current component independent from the transient outward current I_{to1}. I_{sus} in rabbit atrial myocytes may not be a component of I_K, because it is present before I_K activation in the same cell.[28] Can a Cl^- current contribute to I_{sus} in rabbit atrium? If so, what is hte nature of this Cl^- current?

With the use of patch-clamp technique in isolated rabbit atrial myocytes at both whole-cell and single-channel (inside-out and cell-attached) levels, this thesis addressed the questions asked above by focusing on further characterization of the single-channel identity, the modulation mechanisms, and the potential physiological role of this novel Cl^- current in rabbit atrial myocytes, and provided potentially important information about functions and regulation mechanisms of cardiac Cl^- channels.

6. REFERENCES

1. Harvey W: Exercitatio Anatomica de Moto Cordis et Sanquinis in Animalibus. 1628
2. Burdon-Sanderson J and Page FMJ: On the time relations of the excitatory process in the ventricle of the frog. *J Physiol (Lond)* 1880; 2:384-435
3. Hodgkin AL:Evidence for electrical transmission in nerve. Parts 1 and 2. *J Physiol(Lond)* 1939; 90:183-210,
4. Hodgkin AL and Katz, B.: The effects of sodium ions on the electrical activity of the giant axon of squid. *J Physiol (Lond)* 1949;108:37-77
5. Nastuk WL and Hodgkin AL: The electrical activity of single muscle fibres. *J Cell Comp Physiol* 1950; 35:39-73
6. Ling G and Gerard RW: The normal membrane potential of frog sartorius fibres. *J Cell Comp Physiol* 1949; 34:383-396.
7. Hodgkin A and Huxley AF: A quantitative description of membrane current and its application to conduction and excitation in nerve. *J Physiol (Lond)* 1952;117:500-544
8. Weidmann S: Cardiac action potentials, membrane currents, and some personal reminiscences. *Annu Rev Physiol* 1993; 55:1-14.
9. Weidmann S: Effect of current flow on the membrane potential of cardiac muscle. *J Physiol. (Lond)* 1951; 115:227-236.
10. Hamill OP, Marty A, Neher E, Sakmann B and Sigworth FJ: Improved patch-clamp techniques for high resolution current recording from cells and cell-free membrane patches. *Pflügers Arch* 1981; 391:85-100
11. Stiles GL: Structure and function of cardiovascular membranes, channels, and receptors. In Schlant RC and Alexander RW (eds): *The heart, ateries and veins (8th ed.)*. McGraw-Hill Inc. 1994; 47-58
12. Bigger Jr. JT: The electrical activity of the heart. In: In Schlant RC and Alexander RW (eds): *The heart, ateries and veins (8th ed.)*. McGraw-Hill Inc. 1994; 645-658
13. Baumgarten CM and Fozzard HA: Intracellular chloride activity in mammalian ventricular muscle. *Am J physiol* 1981; 241 (Cell Physiol 10):C121-129
14. Fozzard HA and Arnsdorf MF: Cardiac electrophysiology. In:Fozzard HA, Haber E, Jennings RB, et al. (eds): *The heart and cardiovascular system: Scientific foundations*. 2nd ed. New York, Raven, 1991:63-98
15. Hondeghem LM and Mason JW: Agent used in cardiac arrhythmias. In: Katzung BG (ed): *Basic and clinic Pharmacology (fifth ed)*. Norwalk, Connecticut/San Mutea,

California. 1992; 199

16. Irisawa H and Giles W: Sinus and Atrioventricular node cells: Cellular electrophysiology. In: Zipes D.P. and Jalife J. (eds): *Cardiac electrophysiology: From cell to bedside.* Philadelphia: WB Saunders Company, 1990:95-102
17. Hille B: Ion channels of excitable membranes. 1992; Sunderland, Massachusetts: Sinauer Associate
18. Hoffmann EK and Simonsen LO: Membrane mechanisms in volume and pH regulation in cells. *Physiol Rev* 1989; 69:315-382.
19. Alberts B, Bray D, Lewis J, Raff M, Roberts K, and Watson JD (eds): *Molecular biology of the cell (2nd ed).* New York, Garland, 1989
20. McDonough S and Lester HA: Overview of the relationship between structure and function in ion channels. *Drug Development Research* 1994; 33(3):190-202
21. Catterall, WA: Structure and function of voltage-sensitive ion channels. *Science* 1988; 242:50-61
22. Brown HF: Electrophysiology of the sinoatrial node. *Physiol Rev* 1982; 62:505-530
23. Weidman, S: The effect of the cardiac membrane potential on the rapid availability of the sodium-carrying system. *J Physiol (Lond)* 1955; 127:213-224
24. Pelzer D, Pelzer S and MacDonald TF: Properties and regulation of calcium channels in muscle cells. *Rev Physiol Biochem Pharmacol* 1990; 114:107-207
25. DiFrancesco D, Ferroni A, Mazzanti M and Tromba C: Properties of the hyperpolarizing-activated current (I_f) in cells isolated from the rabbit sinoatrial node. *J physiol (Lond)* 1986; 377:61-88
26. Ehara T, Noma A and Ono K: Calcium activated non-selective cation channel in ventricular cells isolated from adult guinea pig heart. *J Physiol (Lond)* 1988; 403:117-133
27. Giles WR and van Ginneken ACG: A transient outward current in isolated cells from the crista terminals of rabbit heart. *J Physiol (Lond)* 1985;368:243-264
28. Duan D, Fermini B and Nattel S: Potassium channel bloking properties of propafenone in rabbit atrial myocytes. *J Pharmacol Exp Ther* 1993; 264:1113-1123
29. Escande D, Coulombe A, Faivre JF, Deroubaix E and Coraboeuf E: Two types of transient outward currents in adult human atrial cells. *Am J Physiol* 1987; 252 (Heart Circ Physiol 21):H142-148
30. Hiraoka M and Kawano S: Calcium-sensitive and insensitive transient outward current in rabbit ventricular myocytes. *J Physiol (Lond)* 1989; 410:187-212

31. Tseng GN and Hoffman BF: Two components of transient outward current in canine ventricular myocytes. *Circ Res* 1989;64:633-647

32. Dudel J, Peper K, Rudel R and Trautwein W: The dynamic chloride component of membrane current in Purkinje fibers. *Pfluegers Arch* 1967; 295:197-212

33. Fozzard A and Hiraoka M: The positive dynamic current and its inactivation properties in cardiac Purkinje fibers. *J Physiol (Lond)* 1973; 234:569-586

34. Coraboeuf E: Ionic basis of electrical activity in cardiac tissue. *Am J Physiol* 1978; 234 (Heart Circ Physiol 3): H101-H116

35. Carmeliet EE and Vereecke J: Electrogenesis of the action potential and automaticity. In: *Handbook of Physiology. The Cardiaovascular System. The Heart.* Bethesda, MD, Am Physiol Soc 1979; Sect 2, Vol I, Chapt 7:269-334

36. Kenyon JL and Gibbons WR: Influence of chloride, potassium, and tetraethylammonium on the early outward current of sheep cardiac Purkinje fibers. *J Gen Physiol* 1979; 73:117-138

37. Kenyon JL and Gibbons WR: 4-Aminopyridine and the early outward current of sheep cardiac Purkinje fibers. *J Gen Physiol* 1979;73:139-157

38. Kukushkin NI, Gainullin RZ and Sosumov EA: Transient outward current and rate dependence of action potential duration in rabbit cardiac ventricular muscle. *Pfluegers Arch* 1983;399:87-92

39. Giles WR and Imaizumi Y: Comparison of potassium currents in rabbit atrial and ventricular cells. *J Physiol (Lond)* 1988; 405:123-145

40. Zygmunt AC and Gibbons WR: Calcium-activated chloride current in rabbit ventricular myocytes. *Circ Res* 1991; 68:424-437

41. Zygmunt AC and Gibbons WR: Properties of the calcium-activated chloride current in heart. *J Gen Physiol* 1992;99:391-414

42. Sanguinetti Mc and Jukiewicz NK: Two components of cardiac delayed rectifier K current: Differential sensitivity to block by class III antiarrhythmic agents. *J Gen Physiol* 1990; 96:195-215

43. Yue DT and Marban E: A novel cardiac potassium channel that is active and conductive at depolarized potentials. *Pfluger Arch* 1988; 413:127-133

44. Carmeliet E, Storms L and Vereecke J: The ATP-dependent K channel and metabolic inhibition. In: Zipes D.P. and Jalife J. (eds): *Cardiac electrophysiology: From cell to bedside.* Philadelphia: WB Saunders Company, 1990:103-108

45. Wasserstrom JA and Ten Eick RE: The electrophysiology of mammalian ventricular muscle. In Dangman KH and Miura DS (eds): *Electrophysiology and pharmacology of the heart*. Marcel Dekker, New York, 1991; 199-233

46. Wible BA and Brown AM: Function and structure of voltage-dependent potassium channels. *Drug Development Res* 1994;33:225-234

47. Walsh KB and Kass RB: Regulation of a heart potassium channel by protein kinase A and C. *Science* 1988; 242:67-69

48. Sanguinetti MC, Jiang C, Curran ME and Keating MT: A mechanistic link between an inherited and an acquired cardiac arrhythmia: HERG encodes the I_{Kr} potassium channel. *Cell* 1995; 81:299-307

49. Nichols CG, Makhina EN, Pearson WL, Sha O and Lopatin AN: Inward rectification and implications for cardiac excitability. *Circ Res* 1996; 78:1-7

50. Fermini B, Wang Z, Duan D and Nattel S: Differences in the rate dependence of the transient outward current in rabbit and human atrium. *Am J Physiol* 1992; 263 (Heart Circ Physiol 32): H1747-H1754

51. Gadsby DC: The Na/K pump of cardiac cells. *Ann Rev Biophys Bioeng* 1984; 13:373-378

52. Sheu S-S, Blaustein MP: Sodium/calcium exchange and regulation of cell calcium and contractility in cardiac muscle, with a note about vascular smooth muscle. In Forzzard HA, Haber E, Jennings RB, Katz AM and Morgan HE (eds): *The heart and cardiovascular system*. New York, Raven Press Publishers 1986; 509-535

53. Gilman AG: G proteins: Transducers of receptor-generated signals. *Ann Rev Biochem* 1987;56:615-649

54. Murad F, Chi Y-M, Rall TW and Sutherland EW: Adenyl cyclase: III. The effect of catercholamines and choline esters on the formation of adenosine 3',5'-phosphate by preparations from cardiac muscle and liver. *J Biol Chem* 1962;237:1233-1238

55. Clapham DE: Direct G protein activition of ion channels? *Annu Rev Neurosci* 1994; 17:441-464

56. Brown AM: Membrane-delimited cell signalling complex: Direct Ion channel regulation by G proteins. *J Membrane Biol* 1993; 131:93-104

57. Neer EJ and Clapham DE: Signal transduction through G proteins in the cardiac myocytes. *Trends Cardiovasc Med* 1992; 2:6-11

58. Shearman MS, Sekiguchi K and Nishizuka Y: Modulation of ion channel activity: a key

function of the protein kinase C enzyme family. *Pharmacol Rev* 1989;41:211-237

59. Daub H, Weiss FU, Wallasch C and Ullrich A: Role of transactivation of the EGF receptor in signalling G-protein-coupled receptors. *Nature* 1996;379:557-560
60. Rodbell M, Krau HMJ, Pohl SL and Birnbaumer L: The glucagon-sensitive adenylyl cyclase system in plasma membrnaes: IV. Binding of glucagon: Effects of guanyl nucleotides. *J Biol Chem* 1971;246:1872-1876
61. Hanski E, Sternweis PC, Northup JK, Dromerick AW and Gilman AG: The regulatory component of adenylyl cyclase: Purification and characterization of the turkey erythrocyte protein. *J Biol Chem* 1981;256:12911-12919
62. Clapham DE: The G-protein nanomachine. *Nature* 1996; 379:297-299
63. Bohm M, Bruckner R, Neumann J, Schmitz W, Scholz H, Starbatty J: Role of guanine nucleotide-binding protein in the regulation by adenosine of cardiac potassium conductance and force of contraction: Evaluation with pertussis toxin. *Naunyn Schmiedebergs Arch Pharmacol* 1986;332:403-405
64. Neumann J, Schmitz W, Scholz H, Stein B: Effects of adenosine analogous on contractile response and cAMP content in isolated guinea-pig ventricular myocytes.in. *Naunyn Schmiedebergs Arch Pharmacol* 1989;340:689-695
65. Foster KA, McDermott PJ and Robishaw JD: Expression of G proteins in rat cardiac myocytes: effect of KCl depolarization. *Am J Physiol* 1990; 259 (Heart and Circ Physiol ??):H432-
66. Kim S, Ang S-L, Block DB, et al: Identification of cDNA encoding an additional α subunit of a human GTP-binding protein: expression of three α_i subtypes in human tissue and cell lines. *Proc Natl Acad Sci USA* 1988;85:4153-
67. Strathmann M, Wilkie TM and Simon MI: Alternative splicing produces transcripts encoding two forms of the α subunit of GTP-binding protein G_o. *Proc Natl Acad Sci USA* 1990; 87:6477-
68. Fong HKW, Yoshimoto KK, Eversole-Cire P and Simon MI: Identification of a GTP-binding protein α subunit that lacks an apparent ADP-ribosylation site for pertussis toxin. *Proc Natl Acad Sci USA* 1988; 85:3066
69. Strathmann M and Simon MI: G protein diversity: a distinct class of α subunits is present in vertabrates and invertabrates. *Proc Natl Acad Sci USA* 1990; 87:9113-
70. Fleming JW, Wisler DL Watanabe AM: Signal transduction by G proteins in cardiac tissue. *Circulation* 1992;85:420-433

71. Gilman AG: G-proteins and regulation of adenylyl cyclase. *JAMA* 1989; 292:1819-1825

72. Logothetis DE, Kurachi Y, Galper J, Clapham DE and Neer EJ: The $\beta\gamma$ subunits of GTP-binding protein activate the muscarinic K channel in heart. *Nature* 1987;325:321-326

73. Huang C-L, Slesinger PA, Casey PJ, Jan YN and Jan LY: Evidence that direct binding of $G_{\beta\gamma}$ to the GIRK1 G protein-gated inwardly rectifying K^+ channel is important for channel activation. *Neuron* 1995;15:1133-1143

74. Hinsch K-D, Tychowiecka E, Gausephohl H, Frank R, Rosenthal W, Schultz G: Tissue distribution of β-subunits of regulatory guanine nucleotide-binding protein. *Biochim Biophys Acta* 1989;1013:60-67

75. Casey PJ and Gilman AG: G-protein involvement in receptor-effector coupling. *J Biol Chem* 1988;262:2577-2580

76. Peralta EG, Ashkenazi A, Winslow JW, Smith DH, Ramachandran J and Capon DJ: Distinct primary strucutres, ligand-binding properties and tissue-specific expression of four human muscarinic acetylcholine receptors. *EMBO J* 1987; 6:3923-3929

77. Fields JZ, Roeske WR, Morkin E and Yamamura HI: Cardiac muscarinic cholinergic receptors: Biochemical identification and characterization. *J Biol Chem* 1978;253:3251-3258

78. Yatani A, Codina J, Brown AM and Birnbaumer L: Direct activation of mammalian atrial muscarinic potassium channels by GTP regulatory protein G_K. *Science* 1987;235:207-211

79. Codina J, Yatani A, Grenet D, Brown AM and Birnbaumer L: The α subunit of the GTP regulatory protein G_K opens atrial muscarinic potassium channels. *Science* 1987; 236:442-451

80. Harvey RD and Hume JR: Autonomic regulation of chloride current in heart. *Science* 1989;244:983-985

81. Schimerlik MI: Structure and regulation of muscarinic receptors. *Ann Rec Physiol* 1989;51:217

82. Josephson I and Sperelakis N: On the ionic mechanism underlying adrenergic -cholinergic antagonism in ventricular muscle. *J Gen Physiol* 1982; 79:69-86

83. Martin JM, Subers EM, Halvorsen SW and Nathason NM: Functional and physical properties of chick atrial and ventricular GTP-binding proteins: Relationship to muscarinic acetylcholine receptor-mediated responses. *J Pharmacol Exp Ther* 1987; 240:683-688

84. Brodde O-E: The functional importance of $beta_1$ and $beta_2$ adrenoceptors in the human heart. *Am J Cardiol* 1988;62:24C-29C

85. Cerbai E, Masini I and Muggeli A: Electrophysiological characterization of cardaic β_2-adrenoceptors in sheep Purkinje fibers. *J Mol Cell Cardiol* 1990;22:859-870

86. Yatani A and Brown AM: Rapid beta-adrenergic modulation of calcium channel current by a fast G protein pathway. *Science* 1989;245:71-74

87 Schubert B, VanDongen AMJ, Kirsch GE and Brown AM: β-adrenergic inhibition of cardiac sodium channels by dual G protein pathways. *Science* 1989;245:516-519

88. Lindemann JP, Jones LR, Hathway DR, HEnry BG and Watanabe AM: Beta-adrenergic stimulation of phospholamban phosphorylation and Ca^{2+}-ATPase activity in guinea pig ventricles. *J Biol Chem* 1983;258:464-471

89. Adelstein RS and Eisenberg E: Regulation and kinetics of the actin-myosin-ATP interaction. *Annu Rev Biochem* 1980;49:921-956

90. Yazawa K and Kameyama M: Mechanism of receptor-mediated modulation of the delayed outward potassium current in guinea pig ventricular myocytes. *J Physiol (Lond)* 1990; 421:135-150

91. Freeman LC, Kwok W-M and Kass RS: Phosphorylation-independent regulation of cardiac I_K by guanine nucleotides and isoproterenol. *Am J Physiol* 1992; 262 (Heart Circ Physiol 31):H1298-H1302

92. Nakayama T and Fozzard HA: Adrenergic modulation of the transient outward current in isolated canine Purkinje cells. *Circ Res* 1988; 62:162-172

93. Gadsby DC: Effects of β adrenergic catecholamines on membrane currents in cardiac cells. In Rosen MR, Janse MJ and Wit AL (eds.): *Cardiac electrophysiology: A textbool.* Mount Kisco, NU, Futura Publishing Company, Inc 1990; p857-p576

94. Exton JH: The roles of calcium and phosphoinositides in the mechanism of α_1-adrenergic and other agonists. *Rev Physiol Biochem Pharmacol* 1988; 111:117-224

95. Benfey BG: Function of myocardial α_1-adrenoceptors. *Life Sci* 1990;46:743-757

96. Rosen MR: Membrane effects of α adrenergic catecholamines. In: Rosen MR, Janse MJ and Wit AL (eds): *Cardiac Electrophysiology: A text book.* Mt Kisco, NY: Futura Publishing Co. 1990;847-856

97. Fedida D, Braun AP and Giles WR: α_1-adrenoceptors in myocardium: functional aspects and transmembrane signalling mechanisms. *Physiol Rev* 1993;73:469-487

98. Ahlquist RP: A study of adrenotropic receptors. *Am J Physiol* 1948;153:586-600

99. Wenzel DG and Su JL: Interactions between sympathetic amines and blocking agents on the rat ventricle strip. *Arch int Pharmacodym Ther* 1966;160:379-389

100. Karliner JS, Barnes P, Hamilton CA and Dollery CT: Alpha$_1$-adrenergic receptors in guinea-pig myocardium: identification by binding of a new radioligand (^{3}H)-prazosin. *Biochem Biophys Res Commun* 1979; 90:142-149

101. Davey MJ: Alpha adrenoceptors - an overview. *J Mol Cell Cardiol* 1986;18 (suppl 5):1-15

102. Kaumann AJ: The function of α- and β-adrenoceptors in isolated heart muscle of man.. *J Mol Cell Cardiol* 1986;18 (suppl 1):1-12

103. Clark MG, Patten GS and Filsell OH: Evidence for an α_1-adrenergic receptor-mediated control of energy production in heart. *J Mol Cell Cardiol* 1982;14:313-321

104 Banerjee A, Locke-Winter C, Rogers KB, Mitchell MB, Brew EC, Cairns CB, Bensard DD and Harken AH: Preconditioning against myocardial dysfunction after ischemia and reperfusion by an α_1-adrenergic mechanism. *Circ Res* 1993;73:656-670

105. Kitakaze M, Hori M, Sato H, Iwakura K. Gotoh K, Inoue M, Kitabatake A and Kamada: Beneficial effects of α_1-adrenoceptor activity on myocardial stunning in dogs. *Circ Res* 1991;68:1322-1339

106. Kariya K, Farrance IKG and Simpson PC: Transcriptional enhancer factor-1 in cardiac myocytes interacts with an α_1-adrenergic and protein kinase C-induced element in the rat β-myosin heavy chain promotor. *J Biol Chem* 1993;268:26658-26662

107. Miyamoto MI, Rockman HA, Guth BD, Heusch G and Ross J Jr: Effect of α-adrenergic stimulation on regional contractile function and myocardial blood flow with and without ischemia. *Circulation* 1991;84:1715-1724

108. Satoh H and Hashimoto K: Effect of α-adrenoceptor stimulation with methoxamine and phenylephrine on spontaneously beating rabbit sino-atrial cells. *Naun Schmied Arch Pharmacol* 1984; 325:47-53

109. Fedida D, Shimoni S and Giles WR: A novel effect of norepinephrine on cardiac cells is mediated by α_1-adrenoceptors. *Am J Physiol* 1989; 256:H1500-H1504

110. Fedida D. Shimoni S and Giles WR: α-adrenergic modulation of the transient outward current in rabbit atrial myocytes. *J Physiol* (Lond) 1990;423:257-277

111. Hescheler J, Nawrath H, Tang M and Trautwein: Adrenoceptor-mediated changes of excitation and contraction in ventricular heart muscle from guinea-pigs and rabbits. *J Physiol* (Lond) 1990;423:257-277

112. Miura Y and Inui J: Multiple effects of α-adrenoceptor stimulation on the action potential of the rabbit atrium. *Naun Schmied Arch Pharmacol* 1984; 325:47-53

113. Apkon M and Nerbonne JM: Alpha$_1$-adrenergic agonists selectively suppress voltage dependent K^+ current in rat ventricular myocytes. *Proc Natl Acad Sci USA* 1988; 85:8756-8760

114. Ravens U, Wang X-L and Wetterwer E: Alpha adrenoceptor stimulation reduces outward currents in rat ventricular myocytes. *J Pharmacol Exp Ther* 1989;250:364-370

115. Wang X-L, Wettwer E, Gross G and Ravens U: Reduction of cardiac outward currents by alpha-1 adrenoceptor stimulation: a subtype-specific effect? *J Pharmacol Exp Ther* 1991;259:783-788

116. Giotti A, Ledda F and Mannaioni PF: Effects of noradrenaline and isoprenaline, in combination with α- and β-receptor blocking substances, on the action potential of cardiac Purkinje fibers. *J Physiol* (Lond) 1973;229:99-113

117. Endoh M and Blinks JR: Actions of sympathetic amines on the Ca^{2+} transients and contractions of rabbit myocardium: reciprocal changes in myofibrillar responsiveness to Ca^{2+} mediated through α- and β-adrenoceptors. *Circ Res* 68:1179-1190

118. Alvarez JL, Mongo KG and Vassort G: Effects of α_1-adrenergic stimulation on the Ca current in single ventricular frog cells. *J Physiol* (Lond) 1987;390:66P

119. Shah A, Cohen IS and Rosen MR: Stimulation of cardiac alpha receptors increases Na/K pump current and decreases gK via a pertussis toxin sensitive pathway. *Biophys J* 1988;54:219-225

120. Iwakura K, Hori M, Watanabe Y, Kitabatake A, Cragoe EJ Jr., Yoshida H and Kamada T: α_1-adrenoceptor stimulation increases intracellular pH and Ca^{2+} in cardiomyocytes through Na^+/H^+ and Na^+/Ca^{2+} exchange. *Eur J Pharmacol* 1990;186:29-40

121. Fedida D and Bouchard RA: Mechanisms for the positive inotropic effect of α_1-adrenoceptor stimulation in rat cardiac myocytes. *Circ Res* 1992;71:673-688

122. Sanchez-Chapula J: Multiple effects of putative of α-adrenoceptor agonists on the elaectrical and mechanical activity of guinea pig papillary muscle. *Naun Schmied Arch Pharmacol* 1981; 316:108-111

123. Dirksen RT and Sheu SS: Modulation of ventricular action potential by α_1-adrenoceptors and protein kinase C. *Am J Physiol* 1990; 258:H907-H911

124. Tohse N, Nakaya H and Kanno M: α_1-adrenoceptor stimulation enhances the delayed rectifier K^+ current of guinea pig ventricular cells through the activation of protein kinase

C. *Circ Res* 1992;71:1441-1446

125. Han C, Abel PW and Minneman KP: α_1-adrenoceptor subtypes linked to different mechanisms for increasing intracellular Ca^{2+} in smooth muscle. *Nature* 1987;329:333-335

126. Minneman KP: α-adrenergic receptor subtypes, inositol phosphates, and sources of cell Ca^{2+}. *Pharmacol Rev* 1988; 40:87-119

127. Michel MC, Hanft G and Grob G: Radioligand binding studies of α adrenoceptor subtypes in rat heart. *Br J Pharmacol* 1994;111:533-538

128. del Balzo U, Rosen MR, Malfatto G, Kaplan LM and Steinberg SF: Specific α_1 adrenergic receptor subtypes modulate catecholamine induced increases and decreases in ventricular automaticity. *Circ Res* 1990;67:1535-1551

129 Rosen MR, Jeck CD and Steinberg SF: Autonomic modulation of cellular repolarization and of the electrocardiographic QT interval. *J Cardiovasc Electrophysiol* 1992;3:487-499

130. Boer R, Grassgger A, Schudt CH and Glossman H: (+)-niguldipine binds with very high affinity to Ca^{2+} channels and to subtype of α_1-adrenoceptors. *Eur J Pharmacol* 1989;172:131-145

131. Han C and Minneman KP: Interaction of subtype-selective antagonists with α_1-adrenergic receptor binding sites in rat tissue. *Mol Pharmacol* 1991;40:531-538

132. Perez D, Piascik MT and Graham RM: Solution-phase library screening for the identification of rare clones: isolation of an α_{1D}-adrenergic receptor cDNA. *Mol Pharmacol* 1991;40:8776-883

133. Forray C, Bard JA, Wetzel JM, Chiu G, Shapiro E, Tang R, Lepor H, Hartig PR, Weinshank RL, Brancheek TA and Gluchowski C: The α_1-adrenergic receptor that mediates smooth muscle contraction in human prostate has the pharmacological properties of the cloned human α_{1C} subtype. *J Pharmacol Exp Ther* 1994;45:703-708

134. Stewart AFR, Rokosh DG, Bailey BA, Karns LR, Chang KC, Long CS, Kariya K-I and Simpson PC: Cloning of the rat α_{1C}-adrenergic receptor from cardiac myocytes: α_{1C}, α_{1B}, and α_{1D} mRNAs are present in cardiac myocytes but not in cardiac fibroblasts. *Circ Res* 1994;75:796-802 .

135. Anyukhovsky EP, Rybin VO, Nikashin AV, Budanova OP and Rosen MR: Positive chronotropic responses induced by α_1-adrenergic stimulation of normal and "ischemic" Purkinje fibers have different receptor-effector coupling mechanisms. *Circ Res* 1992; 71:526-534.

136. Anyukhovsky EPSteinberg SF, Cohen IS and Rosen MR: Recptor-effector coupling

pathway for α_1-adrenergic modulation of abnormal automaticity in "ischemic" canine Purkinje fibers. *Circ Res* 1994;74:937-944

137. Perez D, De Young MB and Graham RM: Coupling of expressed α_{1B}- and α_{1D}-adrenergic receptor to multiple signalling pathways is both G protein and cell type specific. *Mol Pharmacol* 1993;44:784-795
138. Schwinn DA, Page SO, Middleton JP, Lorenz W, Liggett SB, Yamamoto K, Lapetina EG, Caron MG, Lefkowitz RJ and Cotecchia SL: The α_{1C}- adrenergic receptor: characterization of signalling transduction pathways and mammalian tissue heterogeneity. *Mol Pharmacol* 1991;40:619-626
139. Molina Viamonte V, Steinberg SF, Chow Y-K, Legato MJ, Robinson RB and Rosen MR: Phospholipase C modulates automaticity of canine cardiac Purkinje fibers. *J Pharmacol Exp Ther* 1990;252:886-893
140. Sen L, Liang BT, Colucci WS and Smith TW: Enhanced α_1-adrenergic responsiveness in cardiomyopathic hamster cardiac myocytes: Relation to the expression of pertussis toxin-sensitive G protein and α_1-adrenergic receptors. *Circ Res* 1990;67:1182-1192
141. Han H-M, Robinson RB, Bilezikian JP and Steinberg SF: Developmental changes in guanine nucleotide regulatory proteins in the rat myocardial α_1-adrenergic receptor complex. *Circ Res* 1989;65:1763-1773
142. Braun AP, Fedida D, Clark RB and Giles WR: Intracellular mechanisms for α_1 adrenergic regulation of the transient outward current in rabbit atrial myocytes. *J physiol* (Lond) 1990;431:689-712
143. Braun AP, Fedida D and Giles WR: Activation of α_1-adrenoceptors modulates the inwardly rectifying current of mammalian atrial myocytes. *Pflugers Arch* 1992;421:431-439
144. Boyer JL, Paterson A and Harden TK: G-protein-mediated regulation of phospholipase C: Involvement of $\beta\gamma$ subunits. *Trends Cardiovas Med* 1994;4:88-95
145. Hamra M and Rosen MR: Alpha-adrenergic receptor stimulation during simulated ischemia and reperfusion in canine cardiac Purkinje fibers. *Circulation* 1988;78:1495-1502
146. Kimura S, Cameron JS, Kozlovskis PL, Bassett AL and Myerburg RJ: Delayed afterdepolarization and triggered activity induced in filine Purkinje fibers by alpha-adrenergic stimulation in the presence of elevated calcium level. *Circulation* 1984; 70: 1074-1082

147. Sheridan PJ, Penkoske PA, Sobel BE and Corr PB: Alpha adrenergic contribution to dysrhythmia during myocardial ischemia and reperfusion in cats. *J Clin Invest* 1980; 65:161-171

148. Drury AM and Szent-Györgyi A The physiological activity of adenine compounds with specifial reference to their action upon the mammalian heart . *J Physiol (Lond)* 68:213-237

149. Vial C, Owen P, Opie LH and Posel D: Significance of release of adenosine triphosphate and adenosine induced by hypoxia or adrenaline in perfused rat heart. *J Mol Cell Cardiol* 1987;19:187-197

150. Doyle TB and Forrester T: Appearance of adenosine triphosphate in the perfusate from working frog heart. *Pflugers Arch* 1985; 405:80-82

151. Burnstock G: A basis for distinguishing two types of purinergic receptor. In: Straub RW, Bolis L (eds): *Cell Mebrane Receptors for Drugs and Hormones: A Multidisciplinary Approach.* New York, Raven Press, Publishers, 1978; p107-118

152. Van Calker D, Miller M and Hamprecht B: Adenosine regulates via two different types of receptors: The accumulation of cyclic AMP in culatured brain cells. *J Neurochem* 1979;33:999-1005

153. Londos C, Cooper DM and Wolff J: Subclasses of external adenosine receptors. *Proc Natl Acad Sci USA* 1980;77:2551-2554

154. Gordon JL: Extracellular ATP: effects, sources and fate. *Biochem J* 1986; 233:309-319

155. Kirsch GE, Codina J, Birnbaumer Land Brown AM: Coupling of ATP-sensitive K^+ channels to A_1 receptors by G proteins in rat ventricular myocytes. *Am J Physiol* 1990: 259:H820-H826

156. Ito H, Verreecke J and Carmeliet E: Mode of regulation by G protein of the ATP-sensitive K^+ channel in guenia-pig ventricular cell membrane. *J Physiol* (Lond) 1994;478:101-107

157. Van Winkle DM, Chien GL, Wolff RA, Soifer BE, Kuzume K and Davis RF: Cardioprotection provided by adenosine receptor activation is abolished by blockade of the K_{ATP} channel. *Am J Physiol* 1994; 266:H829-H839

158. Wang Y-G and Lipsius SL: Acetylcholine activates a glibenclamide-sensitive K^+ current in cat atrial myocytes. *Am J Physiol* 268 (Heart Circ Physiol 37):H1322-H1334

159. Friel DD and Bean BP: Teo ATP-activated conductances in bullfrog atrial cells. *J Gen Physiol* 1988; 91:1-27

160. Hirano Y, Abe S, Sawanobori T and Hiraoka M: External ATP-induced changes in $[Ca^{2+}]_i$ and membrane currents in mammalian atrial myocytes. *Am J Physiol* 1991; 260:C673-C680

161. Scamps F, Nilius B, Alvarez Jand Vassort G: A G_s protein couples P_2-purinergic stimulation to cardiac Ca channels without cyclic AMP production. *J Gen Physiol* 1992;100:675-701

162. Qu Y, Himmel HM, Campbell DL and Strauss HC: Effects of extracellular ATP on I_{Ca}, $[Ca^{2+}]_i$, and contraction in isolated ferret ventricular myocytes. *Am J Physiol* 1993;264:C702-C708

163. Yamada M, Hamamori Y, Akita H and Yokoyama M: P_2-purinoceptor activation stimulates phosphoinositide hydrolysis and inhibits accumulation of cAMP in cultured ventricular myocytes. *Circ Res* 1992;70:477-485

164. Matsuura H and Ehara T: Activation of chloride current by purinergic stimulation in guinea-pig heart cells. *Circ Res* 1992;70:851-855

165. Kaneda M, Fukui K and Doi K: Activation of chloride current by P_2-purinoceptors in rat ventricular myocytes. *Br J Pharmacol* 1994;111:1355-1360

166. Levesque PC and Hume JR: ATP_o but not $cAMP_i$ activates a chloride conductance in mouse ventricular myocytes. Cardiovas Res 1995;29:336-343

167. Pucéat M and Brown JH: Protein kinase C in the heart. In Kuo JF (ed): *Protein Kinase C.* Oxford, Oxford University Press, 1994; pp249-268

168. Walsh KB and Long KJ: Properties of a protein kinase C-activated chloride current in guinea-pig ventricular myocytes. *Circ Res* 1994;74:121-129

169. Pucéat M, Clément O and Vassort G: Extracellular MgATP activstes the Cl^-/HCO_3 exchanger in single rat cardiac cells. *J Phisol* (Lond) 1991;444:241-256

170. Pucéat M, Cassoly R and Vassort G: Purinergic stimulation induces a tyrosine phosphorylation of a band-3-like protein in isolated rat cardiac cells. *J Phisol* (Lond) 1993;459:226p

171. Colquhoun D, Neher E, Reuter H and Stevens CF: Inward current channels activated by intracellular Ca in cultured cardiac cells. *Nature* 1981;294:752-754

172. Mazet F, Dunia I, Vassort G and Mazet JL: Ultrastructural changes in gap junctions associated with CO_2 uncoupling in frog atrial fibres. *J Cell Sci* 1985;74:51-63

173. Franciolini F and Petris A: Chloride channels of biological membranes.. *Biochim Biophys Acta* 1990;1031:247-259

174. Hutter OF and Noble D: Anion conductance of cardiac muscle. *J Physiol (Lond)* 1961; 157:335-350

175. Carmeliet EE: Chloride ions and the membrane potential of Purkinje fibres. *J Physiol (Lond)* 1961;156:375-388

176. Peper K and Trautwein W: A membrane current related to the plateau of the action potential of Purkinje fibers. *Pflugers Arch* 1968;303:108-123

177. Hiraoka M and Hiraoka M: The role of positive dynamic current on the action potential of cardiac Purkinje fibers. Jpn J Physiol 1975;25:705-717

178. McAllister RE, Noble D and Tsien RW: Reconstruction of the electrical activity of cardiac Purkinje fibers. *J Physiol* (Lond) 1975; 251:1-59

179. Kenyon JL and Gibbons WR: Effects of low-chloride solutions on action potentials of sheep cardiac Purkinje fibers. *J Gen Physiol* 1977;70:635-660

180. Boyett MR: Effect of rate-dependent changes in the transient outward current on the action potential in sheep Purkinje fibers. *J Physiol* (Lond) 1981;319:23-41

181. Nakayama T and Irisawa H: Transient outward current carried by potassium and sodium in quiescent atrioventricular nodal cells of rabbit. *Circ Res* 1985;57:65-73

182. Castle NA: Selective inhibition of potassium currents in rat ventricle by clofilium, and its tertiary homolog. *J Pharmacol Exp Ther* 1990;257:342-350

183. Bahinski A, Nairn AC, Greengard P and Gadsby DC: Chloride conductance regulated by cyclic AMP-dependent protein kinase in cardiac myocytes. *Nature (Lond)* 1989; 340:718-721

184. Hume JR and Horowitz B: A plethora of cardiac chloride conductances: Molecular diversity or a related gene family. *J Cardiovas Electrophysiol* 1995; 6:325-331

185. Walker JL: Intracellular inorganic ions in cardiac tissue. In Fozzard HA (ed): *The Heart and Cardiovascular System. New York: Raven.* 1986; pp561-572

186. Vaughan-Jones RD: Chloride activity and its control in skeletal and cardiac muscle. *Phil Trans R Soc Lond [Biol]* 1982;299:537-548

187. Vaughan-Jones RD: Regulation of chloride in quiescent sheep heart Purkinje fibers studied using intracellular chloride and pH-sensitive microelectrodes. *J Physiol* (Lond) 1979;295:111-137

188. Vaughan-Jones RD: An investigation of chloride-bicarbonate exchange in the sheep cardiac Purkinje fibre. *J Physiol* (Lond) 1986;379:377-406

189. Liu S, Piwnica-Worms D and Lieberman: Intracellular pH regulation in cultured

embryonic chick heart cells. *J Gen Physiol* 1990;96:1247-1270

190. Baumgarten CM and Duncan SWN: Regulation of Cl^- activity in ventricular muscle: Cl^-/HCO_3^- exchange and Na^+-dependent Cl^- cotransport. In Dhalla NS (ed): *Heart Function and Metabolism.* Boston, MA 1987; p117-131
191. Cailie JP, Ruiz-Ceretti E and Schanne OF: Intracellular chloride activity in rabbit papillary muscle: effect of ouabain. *Am J Physiol* 1981;240 (Cell Physiol 9): C183-C188
192. Piwnica-worms D, Jacob R, Horres CR and Lieberman M: transmembrane chloride cotransport in cultured chick heart cells. *Am J Physiol* 1985;249 (Cell Physiol 18):C337-C344
193. Ackerman MJ and Clapham DE.: Cardiac chloride channels. *Trends Cardiovas Med* 1993; 3:23-28
194. Tseng G-N: Cell-swelling increases membrane conductance of canine cardiac cells: Evidence for a volume sensitive Cl^- channel. *Am J Physiol* 1992;262:C1056-C1068
195. Sorota S: Swelling-induced chloride-sensitive current in canine atrial cells revealed by whole-cell patch-clamp method. *Circ Res* 1992;70:679-687
196. Hagiwara N, Masuda H, Shoda M, Irisawa HJ: Stretch-activated anion currents of rabbit atrial myocytes. *J Physiol* (Lond) 1992;456:285-302
197. Ehara T and Ishihara K: Anion channels activated by adrenaline in cardiac myocytes. *Nature. (Lond)* 1990; 347:284-286.
198. Harvey RD, Clarck CD and Hume JR: Chloride currents in mammalian cardiac myocytes - novel mechanism for autonomic regulation of action potential duration and resting membrane potential. *J Gen Physiol* 1990; 95:1077-1102
199. Overholt JL, Hobert ME and Harvey RD: On the mechanism of rectification of isoproterenol-activated chloride current in guinea-pig ventricular myocytes. *J Gen Physiol* 1993; 102:871-895
200. Overholt JL, Saulino A, Drumm ML and Harvey RD: Rectification of whole cell cystic fibrosis transmembrane conductance regulator chloride current. *Am J physiol* 1995;2687 (Cell Physiol 37):C636-C646
201. Hwang TC, Horie M, Nairn AC and Gadsby DC: Role of GTP-binding proteins in the regulation of mammalian cardiac chloride conductance. *J Gen Physiol* 1992; 99:465-489
202. Hwang TC, Horie M, Dousmanis AG and Gadsby DC: Regulation of PKA-activated Cl conductance in guinea pig ventricular myocytes: whole-cell studies. *J Gen Physiol* 1992; 100:69a

203. Hwang TC, Horie M and Gadsby DC: Functionally distinct phosphoforms underlie incremental activation of PKA-regulated Cl^- conductance in mammalian heart. *J Gen Physiol* 1993; 101:629-650

204. Nagel GA, Hwang TC, Nastiuk KI, Nairn AC and Gadsby DC: The protein kinase A-regulated Cl^- channel resembles CFTR (Cystic Fibrosis Transmembrane Conductance Regulator). *Nature* 1992; 360:81-84

205. Ehara T and Matsuura H: Single channel study of the cyclic AMP-regulated chloride current in guinea-pig ventricular myocytes. *J Physiol* (Lond) 1993;464:307-320

206. White MM and Miller C: A voltage-gates anion channel from the electric organ of Torpedo california. *J Biol Chem* 1979;254:10161-10166

207. Tilmann M, Kunzeimann K, Frobe U, Cabantchik I, Lang HJ, Englert HC and Greger R: Different types of blockers of the intermediate-conductance outwardly rectifying chloride channel in epithelia. *Pflugers Arch* 1991;418:556-563

208. Harvey RD: Effects of stilbenedisulfonic acid derivatives on the cAMP-regulated chloride current in cardiac myocytes. *Pflugers Arch* 1993;422:436-442

209. Palade PT and Barchi RL: On the inhibition of muscle membrane chloride conductance by aromatic carboxylic acids. *J Gen Physiol* 1977;69:879-896

210. Levesque PC, Clark CD, Zakarov SI, Rosenshtraukh LV and Hume JR: Anion and cation modulation of the guinea pig ventricular action potential during β-adrenoceptor stimulation. *Pflugers Arch* 1993; 424:54-62

211. Walsh KB: Agents which block heart Cl^- channels also inhibit Ca^{2+} current regulation. *Biophys J* 1994;66:A239

212. Tominaga M, Horie M, Sasayama S and Okada Y: Glibenclamide, an ATP-sensitive K^+ channel blocker, inhibits cardiac cAMP-activated Cl^- conductance. *Circ Res* 1995;77:417-423

213. Harvey RD and Hume JR: Isoproterenol activates a chloride current, not the transient outward current, in rabbit ventricular myocytes. *Am J physiol* 1989; 257 (Cell Physiol 26):C1177-1181

214. Matsuura H, Ehara T and Noma A: Chloride-sensitive nature of the adrenaline-induced current in guinea pig cardiac myocytes. *J Physiol (Lond)* 1990; 425:579-598

215. Harvey RD and Hume JR: Histamine activates the chloride current in cardiac ventricular myocytes. *J Cardiovasc Electrophysiol* 1990;1:309-317

216. Tareen FM, Ono K, Noma A and Ehara T: β-adrenergic and muscarinic regulation of

the chloride current in guinea-pig ventricular cells. *J Physiol* (Lond) 1991; 440:225-241

217. Tareen FM, Yoshida A and Ono K: Modulation of β-adrenergic responses of chloride and calcium currents by external cations in guinea-pig ventricular cells. *J Physiol* (Lond) 1992; 457:211-228

218. Harvey RD, Jurevicius JA and Hume JR: Intracellular Na^+ modulates the cAMP-dependent regulation of ion channels in the heart. *Proc Natl Acad Sci USA* 1991;88:6946-6950

219. Ono K and Fozzard HA: Phosphorylation restores activity of L-type Ca^{2+} channels after rundown in inside-out patches from rabbit cardiac cells. *J Physiol (Lond)* 1992; 454:673-688

220. Ono K and Fozzard HA: Two Phosphatase sides on the Ca^{2+} channel affecting different kinetic functions. *J Physiol (Lond)* 1993; 470:73-84

221. Herzig S, Patil P, Neumann J, Staschen C-M and Yue DT: Mechanisms of β-adrenergic stimulation of cardiac Ca^{2+} channels revealed by discrete-time Markov analysis of slow gating. *Biophys J* 1993;65:1599-1612

222. Armstrong D and Eckert R: Voltage-activated calcium channels that must be phosphorylated to respond to membrane depolarization. *Proc Natl acad sci USA* 1987;84:2518-2522

223. Horie M, Hwang TC and Gadsby DC: Pipette GTP is essential for receptor-mediated regulation of Cl^- current in dialyzed myocytes from guinea-pig ventricle. *J Physiol* (Lond) 1992;455:235-246

224. Hescheler J, Kameyama M and Trautwein W: On the mechanism of muscarinic inhibition of the casrdiac Ca current. *Pflugers Arch* 1986;407:182-189

225. Parsons TD, Lagrutta A, White RE and Hartzell HC: Regulation of Ca^{2+}current in frog ventricular casrdiomyocytes by5'-guanylylimidodiphosphate and acetylcholine. *J Physiol* (Lond) 1991;432:593-620

226. Ono K, Tareen FM, Yoshida A and Noma A: Synergistic action of cyclic GMP on catecholamine-induced chloride current in guinea-pig ventricular cells. *J Physiol* (Lond) 1992;453:647-653

227. Anderson MP, Berger HA, Rich DP, Gregory RJ, Smith AE and Welsh MJ: Nucleoside triphosphates are required to open CFTR chloride channel. *Cell* 1991;67:775-784

228. Berger HA, Anderson MP, Gregory RJ, Thompson S, Hward PW, Maurer RA, Mulligan R, Smith AE and Welsh MJ: Generation of cAMP-activated chloride currents

by expression of CFTR. *J Clin Invest* 1991;88:1422-1431

229. Bear CE, Duguay F, Naismith Al, Kartner N, Hanrahan HW and Riordan JR: Cl⁻ channel activity in *Xenopus* oocytes expressing the cystic fibroses gene. *J Biol Chem* 1991; 266:19142-19145

230. Drumm ML, Wilkerson DJ, Smit LS, Worrell RT, Strong TV, Frizzell RA, Dawson DC and Collins FS: Chloride conductance expressed by delta F508 and other mutant CFTRd in *Xenopus* oocytes. *Science* 1991;254:1797-1799

231. Levesque PC, Hart PJ, Hume JR, Kenyon JL and Horowitz B: Exression of cystic fibrosis transmembrane regulator Cl⁻ channels in heart. *Circ Res* 1992;71:1002-1007

232. Riordan JR: The cystic fibrosis transmembrane conductance regualtor. *Ann Rev Physiol* 1993;55:609-630

233. Horowitz B, Tsung SS, Hart PJ, Levesque PC and Hume JR: Alternative splicing of CFTR Cl⁻ channels in heart. *Am J Physiol* 1993;264:H2214-H2220

234. Hume JR, Hart P, Levesque PC, Collier ML, Geary Y, Warth JD, Chapman T and Horowitz B: Molecular physiology of CFTR Cl channels in heart. *Jpn J Physiol* 1994;44 (suppl 1):S177-S182

235. Hart P, Warth JD, Levesque PC, Collier ML, Geary Y, Horowitz B and Hume JR: Cystic fibrosis gene encodes a cAMP-dependent chloride channel in heart. *Proc Natl Acad Sci USA* 1996; in press

236. Walsh KB: Activation of a cardiac chloride current during stimulation of protein kinase C. *Mol Pharmacol* 1991;40:342-346

237. Zhang K, Barrington PL, Martin RL and Ten Eick RE: Protein kinase-dependent Cl⁻ currents in feline ventricular myocytes. *Circ Res* 1994;75:133-143

238. Collier ML and Hume JR: Unitary chloride channels activated by protein kinase C in guinea pig ventricular myocytes. *Circ Res* 1995; 76:317-324

239. Picciotto M, Cohn J, Bertuzzi G, Greengard P and Nairn AC: Phosphorylation of the cystic fibrosis transmembrane conductance regulator. *J Biol Chem* 1992;267:12742-12752

240. Chang X-B, Tabcharani JA, Hou YX, Jensen TJ, Kartner N, Riordan JR and Hanrahan JW: Protein kinase A (PKA) still activates CFTR chloride channel after mutagenesis of all 10 PKAconsensus phosphorylation sites. *J Biol Chem* 1993;268:11304-111311

241. Tabcharani JA, Chang X-B, Riordan JR and Hanrahan JW: Phosphorylation-regulated Cl⁻ channel in CHO cells stably expressing the cystic fibrosis gene. *Nature* 1991;352:628-631

242. Berger HA, Travis SM and Welsh MJ: Regulation of the cystic fibrosis transmembrane conductance regulator Cl^- channels by specific kinase and protein phosphatases. *J Biol Chem* 1993;268:2037-2047

243. Bajnath RB, Groot JA, De Jonge HR, KansenM and Bijman J: Synergistic activation of non-rectifying small-conductance chloride channels by forskolin and phorbol esters in cell-attached patches of the human colon carcinoma cell line HT-29cl.19A. *Pflugers Arch* 1993;425:100-108

244. Seigelbaum SA and Tsien RW: Calcium-activated transient outward current in calf cardiac Purkinje fibers. *J Physiol* (Lond) 1980;299:485-506

245. Maylie J and Morad M: A transient outward current related to calcium release and development of tension in elephant seal atrial fibers. *J Physiol* (Lond) 1984;357:267-292

246. Coraboeuf E and Carmeliet E: Existence of two transiet outward current in calf vardiac purkinje fibers. *Pflugers Arch* 1982;392:352-359

247. Sipido KR, Callewaert G and Carmeliet E: $[Ca^{2+}]_i$ transient and $[Ca^{2+}]_i$-dependent chloride current in single Purkinje cells from rabbit heart. *J Physiol* (Lond) 1993;468:641-667

248. Zygmunt AC: Intracellular calcium activates a chloride current in canine ventricular myocytes. *Am J Physiol* 1994;267:H1984-1995

249. Callewaert G: Excitation-contraction coupling in mammalian cardiac cells. *Cardiovasc Res* 1992;26:923-932

250. Petrozzino JJ, Pozzo Miller LD and Connor JA: Micromolar Ca^{2+} transients in dendritic spines of hippocampal pyramidal neurons in brain slice. *Neuron* 1995;14:1223-1231

251. Papp Z, Sipido KR, Callewaert G and Carmeliet E: Two components of $[Ca^{2+}]_i$-activated Cl^- current during large $[Ca^{2+}]_i$ transients in single rabbit heart Purkinje cells. *J Physiol* (Lond) 1995;483:319-330

252. Martinac B, Adler J and Kung C: Mechanosensitive ion channels of *E. coli* activated by amphipaths. *Nature* 1990;348:262-263

253. Sperelakis N and Schneider MF: Membrane ion conductances of frog sartorious fibers as a function of tonicity. *Am J Physiol* 1968;215:723-729

254. Sorota S: Pharmacologic properties of the swelling-induced chloride current of dog atrial myocytes. *J Cardiovasc Electrophysiol* 1994;5:1006-1016

255. Oz MC and Sorota S: Forskolin stimulates swelling-induced chloride current, not cardiac cystic fibrosis transmembrane-conductance regulator current, in human cardiac myocytes.

Circ Res 1995;76:1063-1079

256. Vandenberg JI, Yoshida A, Kirk K and Powell T: Swelling-activated and isoproterenol-activated chloride currents in guinea-pig cardiac myocytes have distinct electrophysiology and pharmacology. *J Gen Physiol* 1994; 104:977-1017
257. Shuba LM, Ogura T and McDonald TF: Kinetic evidence distinguishing volume-sensitive chloride current from other types of guinea-pig ventricular myocytes. *J Physiol* (Lond) 1996;491:69-80
258. Zhang J, Rasmusson RL, Hall SK and Liberman M: A chloride current associated with swelling of cultured chick heart cells. *J Physiol* (Lond) 1993;472:801-820
259. Zhang J, Hall SK and Liberman M: An early transient current activates the swelling-induced chloride conductance in cardiac myocytes. *Biophys J* 1994;66:A422 (abstract)
260. McCann JD, Li M and Welsh MJ: Identification and regulation of whole cell chlordie currents in airway epithelium. *J Gen Physiol* 1989;94:1015-1036
261. Solc CK and Wine JJ: Swelling induced and depolarization-induced Cl$^-$ channels in normal and cystic fibrosis epithelial cells. *Am J Physiol* 1991;261:C658-C674
262. Worrel RT, Butt AG, Cliff WH and Frizzell RA: A volume-sensitive chloride conductance in human colonic cell line T84. Am J Physiol 1989;256:1111-1119
263. Kubo M and Okada Y: Volume-regulatory Cl$^-$ channel currents in cltured human epithelial cells. *J Physiol* (Lond) 1992;456:351-371
264. Anderson JW, Jirsch JD and Fedida D: Cation regulation of anion current activated by cell swelling in two types of human epithelial cancer cells. *J Physiol* (Lond) 1995;483:549-557
265. Paulmichl M, Li Y, Wickman K, Ackerman M, Paralta E and Clapham D: New mammalian chloride channel identified by expression cloning. *Nature* 1992;356:238-241
266. Ackerman MJ, Wickman KD and Clapham D: Hypotonicity activates a native chloride currents in *Xenopus* oocytes. *J Gen Physiol* 1994;103:153-179
267. Bouron A, Potreau D and Raymond G: Possible involvement of a chloride conductance in the transient outward current of whole-cell voltage-clamped ferret ventricular myocytes. *Pflugers Arch* 1991;419:534-536
268. Sigworth FJ: The patch clamp is more useful than anyone had expected. *Federation Proc* 1986;45:2673-2677
269. Earm YE, Noble D, Noble SJ and Spindler AJ: Taurine activates a sodium-dependent inward current in isolated guinea-pig ventricular myocytes. *J Physiol* (Lond)

1989;417:56P (abstract)

270. Coronado R and Latorre R: Detection of K^+ and Cl^- channels from calf cardiac sarcolemma in planar lipid bilayer membranes. *Nature* 1982;298:849-852

271. Hill JA, Coronado R and Strauss HC: Reconstitution of ionic channels from human heart. *J Mol Cell Cardiol* 1989;21:31?-322

272. Rousseau E: Single chloride-sensitive channel from cardiac sarcoplasmic reticulum studied in planar lipid bilayers. *J Membr Biol* 1989;110:39-47

273. Coulombe A, Duclohier H, Coraboeuf E and Touzet N: Single chloride-permeable channels of large conductance in cultured cardiac cells of new-born rats. *Eur Biophys J* 1987;14:155-162

274. Coulombe A and Coraboeuf E: Large-conductance chloride channels of new-born rat cardiac myocytes are activated by hypotonic media. *Pflugers Arch* 1992;422:143-150

275. Collier ML, Levesque PC, Kenyon JL and Hume JR: Unitary Cl^- channels activated by cytoplasmic Ca^{2+} in canine ventricular myocytes. *Circ Res* 1996; 78:936-944

276. Takahashi T, Neher E and Sakmann B: Rat brain serotonin receptors in Xenopus oocytes are coupled by intracellular calcium to endogenous channels. *Proc Natl Acad Sci USA* 1987;84:5063-5067

277. Taleb O, Feltz P, Bossu JL and Feltz A: Small-conductance chloride channels activated by calcium on cultured endocrine cells from mammalian pars intermedia. *Pflugers Arch* 1988;412:641-646

278. Klöckner U: Intracellular calcium ions activate a low-conductance chloride channel in smooth-muscle cells isolated from human mesentric artery. *Pflugers Arch* 1993;424:231-237

279. Van Renterghem C and Lazdunski M: Endothelin and vasopressin activate low conductance chloride channels in aortic smooth muscle cells.*Pflugers Arch* 1993; 425:156-163

280. Frizzell RA, Halm DR, Rochkemmer G and Shoemaker RL: Chloride regulation in secretory epithelia. *Fed Proc* 1986;45:2727-2731

281. Bretag AH: Muscle chloride channels. *Physiol Rev* 1987;65:310-356

282. Greger R: Chloride channel blockers. *Meth Enzymol* 1990;191;:793-810

283. Welsh MJ: Electrolyte transport by airway epithelia. *Physiol Rev* 1987;67:1143-1184

284. Quinton PM: Cystic fibrosis: a disease in electrolyte transport. *FASEB J* 1990;4:2709-2717

285. Welsh MJ: Abnormal regulation of ion channels in cystic fibrosis epithelia. *FASEB J* 1990;4:2718-2725

286. Schoumacher RA, Shoemaker RL, Halm DR, Tallant RW, Wallace RW and Frizzell RA: Phosphorylation fails to activate chloride channels from cystic fibrosis airway cells. *Nature* 1987;330:752-754

287. Wagner JA, Cozens AL, Schulman H, Gruenert DC, Stryer L and Gardner P: Activation of chloride channels in normal and cystic fibrosis airway epithelial cells by multifunctional calcium.calmodulin-dependent protein kinase. *Nature* 1991;349:793-796

288. Cliff WH and Frizzell RA: Separate Cl^- conductances activated by cAMP and Ca^{2+} in Cl^--secreting epithelial cells. *Proc Natl Acad Sci USA* 1990;87:4956-4960

289. Schwiebert EM, Flotte T, cuting GR and Guggino WB: Both CFTR and outwardly rectifying chloride channels contribute to cAMP-stimulated whole cell chloride currents. *Am J Physiol* 1994;266:C1464-C1477

290. Devor DC, Forrest Jr JN, Suggs WK and Frizzell RA: cAMP-activated Cl^- channels in primary cultures of spiny dogfish (Squalus acanthias) rectal gland. *Am J Physiol* 1995;268:C70-C79

291. Gray MA, Harris A, Colman L, Greenwell JR and Argent BE: Two types of chloride channelin on duct cells cultured from human fetal pancreas. *Am J Physiol* 1989;257:C240-C251

292. Tabcharani JA, Low D, Elie D and Hanrahan JW: Low-conductance chloride channel activated by cAMP in the epithelial cell line T84. *FEBS Lett* 1991;270:157-164

293. Higgins CF: ABC transporters: From microorganisms to man. Annu Rev Cell Biol 1992;8:67-113

294. Hyde SC, Emsley P, Hartshorn MJ, Mimmack MM, Gileadi U, Pearce SR, Gallagher MP, Gill DR, Harbbard RE and Haggins CF: Structural model of ATP-binding proteins associated with cystic fibrosis, multidrug resistance and bacterial transport. *Nature* 1990; 346:362-365

295. Kartner N, Hanrahan JW, Jensen TJ, Naismith AL, Sun S, Ackerly CA, Reyes EF, Tsui L-C, Rommens JM, Bear CE and Riordan JR: Expression of the cystic fibrosis gene in non-epithelial invertebrate cells produces a regulated anion conductance. *Cell* 1991;64:681-691

296. Anderson MP, Gregory RJ, Thompson S, Souza DW, Paul S, Mulligan RC, Smith AE and Welsh MJ: Demonstration that CFTR is a chlordie channel by alteration of its anion

selectivity. *Science* 1991;253:202-204

297. Bear CE, Li C, Kartner N, Bridges RJ, Jensen TJ, Ramjeesingh M and Riordan JR: Purification and functional reconstitution of the cystic fibrosis transmembrane conductance regualtor (CFTR). *Cell* 1992;68:809-818

298. Reisin IL, Prat AG, Abraham EH, Amara JF, Gregory RJ, Ausiello DA and Cantiello HF: The cystic fibrosis transmembrane conductance regulator is a dual ATP and chloride channel. J Biol Chem 1994;269:20584-20591

299. Stutts MJ, Canessa CM, Olsen JC, Hamrick M, Cohn JA, Rossier BC and Boucher RC: CFTR as a cAMP-dependent regulator of sodium channel. *Science* 1995;269:847-850

300. Miller C: Open-state substructure of single chloride channels from *Torpedo* electroplex. *Philos Trans R Soc Lond B Biol Sci* 1982;299:401-411

301. Miller C and White MM: Dimeric structure of single chloride channels from *Torpedo* electroplex. *Proc Natl Acad Sci USA* 1984;81:2772-2775

302. Jentsch TJ, Steinmeyer K and Schwarz G: Primary structure of *Torpedo marmorata* chloride channel isolated by expression cloning in *Xenopus* oocytes. *Natture* 1990;348:510-514

303. Bauer CK, Steinmeyer K, Schwartz JR and Jentsch TJ: Completely functional double-barreled chloride channel expressed from a single *Torpedo* cDNA. *Proc Natl Acad Sci USA* 1991;88:11052-11056

304. Steinmeyer K, Ortland C and Jentsch TJ: Primary structure and functional expression of a developmentally regulated skeletal muscle chloride channel. *Natture* 1991;354:301-304

305. Thiemann A, Gründer S, Pusch M and Jentsch TJ: A chloride channel widely expressed in epithelial and non-epithelial cells. *Natture* 1992;356:57-60

306. Uchida S, Sasaki S, Furukawa T, Hiraoka M, Imai T, Hirata Y and Marumo F: Molecular cloning of a chloride channel that is regulated by dehydration and expressed predominantly in kedney medulla. *J Biol Chem* 1993;268:3821-3824

307. Kieferle S, Fong P, Bens M, Vandewalle A and Jenstch TJ: Two highly homolougous members of the CLC chloride channel family in both rat rat and human kidney. *Proc Natl Acad Sci USA* 1994; 91:6943-4947

308. Gronemeier M, Codie A, Prosser J, Steinmeyer K and Jentsch TJ: Nonsense and missense mutations in the muscular chloride channel CLC-1 of myotonic mice. *J Biol Chem* 1994;269:5963-5967

309. Koch MC, Steinmeyer K, Lorenz C, Richer K, Wolf E, Otto M, Zoll B, Lehmann-Horn

F, Grzeschik KH and Jentsch TJ: The skeletal muscle chloride channel in dominant and recessive human myotonial. *Science* 1992;257:797-800

310. Gründer S, Thiemann A, Pusch M and Jentsch TJ: Regions involved in the opening of CLC-2 chloride channel by voltage and cell volume. *Natture* 1992;360:759-762

311. Kawasaki M, Uchida S, Monkava T, Miyawaki A, Mikoshiba K, Marumo F and Sasaki S: Cloning and expression of a protein kinase C -regulated chloride channel abundantly expressed in rat brain neuronal cells. *Neuron* 1994;12:597-604

312. Van Slegtenhorst MA, Bassi MT, Borsani G, Wapenaar MC, Ferrero GB, De Conciliis L, Rugarli E, Grillo A, Franco B, Zoghbi HY and Ballabio A: A gene from the human Xp22.3 region shares homology with voltage-gated chloride chsnnels. *Hum Mol Genet* 1994;3:547-552

313. Kawasaki M, Suzuki M, Uchida S, Sasaki S, and Marumo F: Stable and functional expression of the CLC-3 chloride channel in somatic cell lines. *Neuron* 1995;14:1285-1291

314. Marty A: The physiological role of calcium-dependent channels. *Trends Neurosci* 1989;12:420-424

315. Bader CR, Bertrand D and Schwartz EA: Voltage-activated and calcium-activated currents studied in solitary rod inner segments from the salamander retina. *J Physiol* (Lond) 1982;331:253-284

316. Marty A, Tan YP and Trautmann A: three types of calcium-activated channels in rat lacrymal glands. *J Physiol* (Lond) 1984;357:293-325

317. Evans MG and Marty A: Calcium-activated chloride currents in isolated cells from rat lacrymal glands. *J Physiol* (Lond) 1986;378:437-460

318. Owen DG, Segal M and Barker JL: A Ca-dependent Cl-conductance in cultured mouse spinal neurons. *Nature* 1984;311:567-570

319. Young GPH, Young JD, Deshpande AK, Goldstein M, Kiode SS and Cohn ZA: A Ca^{2+}-activated channel from *Xenopus laevis* oocyte membrane reconstituted into planar bilayers. *Proc Natl Acad Sci USA* 1984;81:5155-5159

320. Sun XP, Supplisson S, Torres R, Sachs G and Mayer E: Characterization of large conductance chloride channels in rabbit colonic smooth muscle. *J Physiol* (Lond) 1992;448:355-382

321. Amébée T, Large WA and Wang Q: Characteristics of chloride currents activated by noradrenaline in rabbit ear artery cells. *J Physiol* (Lond) 1990;428:501-516

322. Byme NG and Large WA: Membrane ionic mechanisms activated by noradrenaline in cells isolated from rabbit portal vein. *J Physiol* (Lond) 1988;404:557-573

323. Droogmanns G, Callewaert G, Declerck I and Casteels R: ATP induced Ca^{2+}-release and Cl^- current in cultured smooth muscle cells from pig aorta. *J Physiol* (Lond) 1991;440:623-634

324. Pacaud P, Loirand G, Baron A, Mironneau C and Mironneau J: Ca^{2+} channel activation and membrane depolarization mediated by Cl^- channels in response to noradrenaline in vascular myocytes. *Br J Pharmacol* 1991;104:1000-1006

325. Strange K and Jackson PS: Swelling-activated organic osmolyte efflux: a new role for anion channels. *Kidney Inv* 1995;48:994-1003

326. Jackson PS, Churchwell K, Ballatorl N, Boyer JL and Strange K: Swelling-activated anion conductance in skate hepatocytes: regulation by cell Cl and ATP. *Am J Physiol* 1996;270:C57-C66

327. Lewis RS, Ross PE and Cahalan MD: Chloride channels activated by osmotic stress in T lymphocytes. *J Gen Physiol* 1993;101:801-826

328. Jackson PS and Strange K: Volume-sensitive anion channels mediate swelling-activated inosital and taurin efflux: *Am J Physiol* 1993;265:C1489-C1500

329. Valverde MA, Diaz M and Sepulveda FV: Volume-regulated chlorride channels associated with the human muktidrug-resistance P-glycoprotein. *Nature* 1992;355:830-833

330. Ehring GR, Osipchuk YV and Cahalan MD: Swelling activated chloride channels in multdrug-sensitive and -resistant cells. *J Gen Physiol* 1994;104:1129-1161

331. Diaz M, Valverd MA, Higgins CF, Rucareanu C and Sepulveda FV: Volume-activated chloride channels in Hela cells are blocked by verapamil and dideoxyforskolin. *Pflugers Arch* 1993;422:347-353

332. Luckie DB, Krouse ME, Harper KL, Law TC and Wine JJ: Selection for MDR1/P-glycoprotein enhances swelling-actrivated K and Cl current in NIH/3T3 cells. *Am J Physiol* 1994;267:C650-C658

333. McEwan GTA, Hunter J, Hirst BH and Simmons NL: Volume-activated Cl secretion and transepithelial vinblastine secretion mefiated by P-glycoprotein are not correlated in cultured human T84 intestinal epithelial layers. *FEBS Lett* 1992;304:233-236

334. Munkonge FM, Osborne LR, Geddes DM and alton EWFW: Lack of inhibition by dideoxy-forskolin and verapamil of DIDS-sensitive volume-ativated Cl secretion in human squamous lung carcinoma epithelial cells. *Biochim Biophys Acta* 1994;1224:342-348

335. Jackson PS and Strange K: Characterization of the voltage-dependent properties of a volume-sensitive anion conductance. *J Gen Physiol* 1995;105:661-676

336. Gill DR, Hyde SC, Higgins CF, Valverde MA, Mintenig GM and Sepulveda FV: Separation of drug transport and chloride channel functions of the human multidrug resistance P-glycoprotein. *Cell* 1992; 71:23-32

337. Rasola AL, Galietta JV, Gruenert DC and Romeo G: Ionic selectivity of volume-sensitive currents in human epithelial cells. *Biochim Biophys Acta* 1992;1139:319-323

338. Chan H-C, Goldstein J and Nelson DJ: Alternative pathways for chloride conductance activation in normal and cystic fibrosis airway epithelial cells. *Am J Physiol* 1992;262:C1273-C1283

339. Doroshenko P and Neher E: Volume-sensitive chloride conductance in bovin chromaffin cell membrane. *J Physiol* (Lond) 1992;449:197-218

340. Stoddard JS, Steinbach JH and Simchowitz L: Whole cell Cl current in human neutrophilis induced by cell swelling. Am J Physiol 1993;C156-C165

341. Nilius B, Oike M, Zahradnik I and Droogmans G: Activation of a Cl^- current by hypotonic volume increase in human endothelial cells. *J Gen Physiol* 1994;103:787-805

342. Okada Y, Peterson CCH, Kubo M, Morishima S and Tominaga M: Osmotic swelling activates intermediate-conductance Cl^- channels in human intestinal epithelial cells. *Jpn J Physiol* 1994;44:403-409

343. Jackson PS and Strange K: Single channel propertoes of a swelling-activated anion conductance: current activation occurs by abrupt switching of closed channels to an open states. *J Gen Physiol* 1995;105:643-660

344. Boese S, Wehner F, Jackson PS, Strange K and Kinne RHK: Volume-sensitive anion channels in rat inner medullary collecting duct (IMCD) cells: single channel properties. *FASEB J* 1995;9:A$ (abstract)

345. Okada H, Ishii K, Nunoki K and Taira N: Cloning of a swelling-induced chloride current related protein from rabbit heart. *Biochim Biophys Acta* 1995; 145-148

346. Krapivinsky GB, Ackerman, MJ, Gordon EA, Krapivinsky LD and Clapham DE: Molecular characterization of a swelling-induced chloride conductance regulatory protein, pI_{Cln}. *Cell* 76:439-448, 1994

347. Ackerman MJ, Krapivinsky GB, Gordon E, Krapivinsky L and Clapham DC: Characterization of a native swelling-induced chloride current, ICl.swell, and its regulatory protein, pICln, in Xenopus Oocytes. *Jap J Physiol* 1994; 44:S17-S24

348. Altenberg GA, Vanoye CG, Han ES, Deitmer JW and Reuss L: Relationships between rhodamine 123 transport, cell volume, and ion-channel function of P-glycoprotein. *J Biol Chem* 1994; 269:7145-7149

349. Hardy SP, Goodfellow HR, Valverde MA, Gill DR, Sepulveda FV and Higgins: Protein Kinase C -mediated phosphorylation of the human multidrug resistence P-glycoprotein regulates cell volume-activated chloride channels *EMBO J* 1995; 14:68-75

350. Lukacs GL and Moczydlowski E: A chloride channel from lobster walking leg nerves: characterization of single-channel properties in planar bilayers. *J Gen Physiol* 1990;96:707-733

351. Guggino WB: Outwardly rectifying chloride channels and CF: A devorce and remarriage. *J Bioenerg Biomemb* 1991;25:27-35

352. Hwang T-C, Lu L, Zeitlin PL, Gruenert DC, Huganir R and Guggino WR: Chloride channels in CF: lack of activation by protein kinase C and cAMP-dependent protein kinase. *Science* 1989; 244:1351-1353

353. Li M, McCann JD, Liedtke CM, Nairn AC, Greengard P and Welsh MJ: Cyclic AMP-dependent protein kinase opens chloride channels in normal but not in cystic fibrosis airway epithelium. *Nature* 1988;331:358-360

354. Li M, McCann JD, Anderson MP, Clancy JP, Liedtke CM, Nairn AC, Greengard P and Welsh MJ: Regulation of chloride channels by protein kinase C in normal and cystic fibrosis airway cells. *Science* 1989;244:1353-1356

355. Welsh MJ, Li M and McCann JD: Activation of normal and cystic fibrosis chloride channels by voltage, temperature and trypsin. *J Clin Invest* 1989:84:2002-2007

356. Tilmann M, Kunzelmann K, Fröbe U, Cabantchik L, Lang HJ, Englert HC and Greger R: Different types of blockers of the intermediate-conductance outwardly rectifying chloride channel in epithelia. *Pflugers Arch* 1991; 418:556-561

357. Egan M, Flotte T, Afione S, Solow R, Zeitlin PL, Carter BJ and Guggino WB: Defective regulation of outwardly rectifying Cl^- channels by protein kinase A corrested by insertion of CFTR. *Nature* 1992; 358:581-584

358. Gabriel SE, Clarke LL, Boucher RC and Stutts M: CFTR and outward rectifying chloride channels are distinct proteins with a regulatory relationship. *Nature* 1993;363:263-266

359. Palmer CJ, Scitt BT and Jones LR: Purification and completesequence determination of the major palsma membrane substrate for cAMP-dependent protein kinase and protein kinase C in myocardium. *J Biol Chem* 1991;266:11126-11130

360. Mercer RW, Biemesdorfer D, Bliss DP, Collins JH and Forbush B: Molecular cloning and immunological characterization of the γ polypeptide, a small protein associated with the Na,K-ATPase. *J Cell Biol* 1993;121:579-586

361. Moorman JR, Palmer CJ, John JE, Durieux ME and Jones LR: Phospholemman expression induces a hyperpolarization-activated chloride-current in *Xenopus* oocytes. *J Biol Chem* 1992;267:14551-14554

362. Kowdley CC, Ackerman SJ, John JE, Jones LR and Moorman JR: Hyperpolarization-activated chloride currents in *Xenopus* oocytes. *J Gen Physiol* 1994;103:217-230

363. Attali B, Guillemare E, Lesage F, Honore E, Romey G, Lazdunski M and Barhanini J: The protein I_{sK} is a dual activator of K^+ and Cl^- channels. Nature 1993;365:850-852

364. Takumi T, Ohkubo H and Nakanishi S: Cloning of a membrane protein that induces a slow voltage-gated potassium current. *Science* 1988;242:1042-1045

365. Goldstein SAN and Miller C: Site-specific mutations in a minimal voltage-dependent K^+ channel alter ion selectivity and open-channel block. *Neuron* 1991; 7:403-408

366. Steinmeyer K, Lorenz C, Pusch M, Koch MC and Jentsch TJ: Multimeric structure of CLC-1 chloride channel revealed by mutations in dominant myotonia congenita (Thomsen). *EMBO J* 1994;13:737-743

367. Eccles JC: *The physiology of synapses*. Berlin:Springer 1964

368. Macknight ADC: Volume regulation of in mammalian kidney cells. Mol Physiol 1983;4:17-31

369. Macknight ADC and Leaf A: Cellular response to extracellular osmolality. In: Seldin DW and Giebisch G (eds): *The kidney: Physiology and pathophysiology*. New Yor:Raven 1985;P117-132

370. Paulmichl M, Friedrich F, Maly K and Lang F: The effect of hypoosmolarity on the electrical properties of Madin Darby canine kidney cells. *Pflugers Arch* 1989;413:456-462

371. Lang F, ´Völkl H and Häussinger D: General principles in cell volume regulation. *Comp Physiol* 1990;4:1-25

372. Ross A and Boron WF: Intracellular pH. *Physiol Rev* 1981;61:296-434

373. Petrich ER, Zumino AP and Schanne OF: Early action potential shortening in hypoxic heart: role of chloride current(s) mediated by catechlamine release. *J Mol Cell Cardiol* 1996;28:279-290

374. Ridley PD and Curtis MJ: Anion manipulation: a new antiarrhythmic approach: action

of substitution of chloride with nittrate on ischemia- and reperfusion-induced ventricular fibrillation and contractile function. *Circ Res* 1992;70:617-632

375. Zhang K, Barrington P and Ten Eick RE: A Cl^--dependent current induced by PHE and PMA mimics isoproterenol-induced DIDS-sensitive I_{Cl}. *Biophys J* 1992;61:A146 Abstract

CHAPTER 2

CHARACTERIZATION OF A NOVEL CHLORIDE CURRENT - A BASALLY ACTIVE CHLORIDE CURRENT ($I_{Cl.b}$) IN RABBIT ATRIAL MYOCYTES

This work originated from question number (4) in Chapter 1, section 6. I was curious about the nature of a sustained outward current observed after I_{to1} inactivation in rabbit atrial myocytes. When I_K, I_{K1} and I_{Ca} are blocked by TEA, Ba^{2+} and Cd^{2+}, respectively, the outward currents elicited by a series of 5-second depolarizing pulses applied to the cell from a holding potential of -80 mV have two components. One is the transient component, which is the I_{to1}. The other is the sustained component which exists after inactivation of I_{to1}. While it is well-established that the transient component is a K^+ current, the property of the sustained current is not clear. There are at least two possible explanations of this sustained current. One is that the sustained current is a noninactivating component of I_{to1} , in an other word, is carried by the same channel as I_{to1}. The other is that the sustained current is a new current different from I_{to1}.

To test these possibilities, I first applied the I_{to1} channel blocker 4-AP to the cell. I then studied the effects of changes in extracellular K^+ concentrations and Cl^- transmembrane gradients and Cl^--transporter blockers on the outward currents.

rapid communication

Sustained outward current observed after I_{to1} inactivation in rabbit atrial myocytes is a novel Cl^- current

DA-YUE DUAN, BERNARD FERMINI, AND STANLEY NATTEL
Department of Medicine, University of Montreal, Montreal H3C 3G7; Montreal Heart Institute, Montreal H1T 1C8; and Department of Pharmacology and Therapeutics, McGill University, Montreal, Quebec H3G 1Y6, Canada

Duan, Da-Yue, Bernard Fermini, and Stanley Nattel. Sustained outward current observed after I_{to1} inactivation in rabbit atrial myocytes is a novel Cl^- current. *Am. J. Physiol.* 263 (*Heart Circ. Physiol.* 32): H1967–H1971, 1992.—In rabbit atrial myocytes, depolarization of the membrane results in a rapidly activating transient outward current (I_{to}) that then decays to a sustained level. The sustained current (I_{sus}) remains constant for at least 5 s during continued depolarization. The present study was designed to identify the ionic mechanism underlying I_{sus} with the use of whole cell voltage-clamp techniques. After exposure to 2 mM 4-aminopyridine (4-AP), the 4-AP-sensitive transient outward current (I_{to1}) was abolished, but I_{sus} was unaffected. I_{sus} was not blocked by the K^+ channel blockers tetraethylammonium chloride and Ba^{2+}, was not changed by increasing superfusate K^+ concentration, and was still present when K^+ was replaced by Cs^+ in both the superfusate and the pipette. I_{sus} was significantly reduced by the Cl^- transport blockers 4-acetamido-4′-isothiocyanatostilbene-2,2′-disulfonic acid and 4,4′-diisothiocyanatostilbene-2,2′-disulfonic acid. The current-voltage relations of I_{sus} showed outward rectification, and the reversal potential of I_{sus} shifted with changes in the transmembrane Cl^- gradient in the fashion expected for a Cl^- current. We conclude that I_{sus} in rabbit atrium is due to a noninactivating Cl^- current which, unlike previously described cardiac Cl^- currents, is manifest in the absence of exogenous stimulators of adenosine 3′,5′-cyclic monophosphate formation, cytosolic Ca^{2+} transients, or cell swelling.

chloride current; action potential; cardiac outward currents; transient outward current; cardiac repolarization; atrial arrhythmias; antiarrhythmic drugs

IN MANY TISSUES manifesting a prominent transient outward current (I_{to}) on depolarization, a residual outward current is present at the end of a depolarizing clamp step (3–5, 8, 15, 19). The ionic nature of this residual current is unclear. During relatively short pulses, a proportion of this current may be due to incomplete inactivation of I_{to}. On the other hand, the residual current in rat ventricular myocytes is insensitive to 4-aminopyridine (4-AP), suggesting that it is independent of the 4-AP-sensitive transient outward current (I_{to1}; 14, 17). Furthermore, the transient and sustained components of depolarization-induced outward current in rat myocytes respond differently to α-adrenergic receptor stimulation (17, 20).

We have previously shown that the delayed rectifier K^+ current (I_K) can frequently be recorded from rabbit atrial myocytes and can contribute to the sustained current at the end of a depolarizing pulse (6). However, a substantial outward current is present before I_K activation. The inward rectifier channel can also conduct a constant outward K^+ current (I_{K1}), but its strong inward rectifying properties limit its role at positive potentials. The present study was designed to identify the ionic nature of the sustained outward current elicited by depolarization of rabbit atrial myocytes.

MATERIALS AND METHODS

Single atrial cells were obtained from rabbit hearts using an enzymatic dissociation technique as previously described (7). Rabbits (1.5–2.0 kg) were killed by cervical dislocation, and then the hearts were perfused in the Langendorff mode. Hearts were first perfused with an *N*-2-hydroxyethylpiperazine-*N*′-2-ethanesulfonic acid (HEPES)-buffered Tyrode solution at 37°C, then with a nominally Ca^{2+}-free solution until cardiac contraction ceased, and finally with the same solution containing 0.2% collagenase type II and 1.0% bovine serum albumin (Sigma) for 15 min. The left atrium was removed and dissected into small pieces, and cell dissociation was achieved by gentle mechanical agitation. All cells studied were rod shaped, exhibited clear cross striations, and lacked any visible blebs.

The solution for cell isolation contained (in mM) 126 NaCl, 5.4 KCl, 2.0 $CaCl_2$, 1.0 $MgCl_2$, 0.33 NaH_2PO_4, 10 glucose, and 10 HEPES; pH was adjusted to 7.4 with NaOH. Nominally Ca^{2+}-free solution differed only in the omission of $CaCl_2$. The standard superfusate was identical to the solution for cell isolation, except for lower concentrations of $CaCl_2$ (1.0 mM), $MgCl_2$ (0.8 mM), and glucose (5.5 mM). The standard internal (pipette) solution contained (in mM) 65 KCl, 65 K aspartate, 1.0 $MgCl_2$, 10 HEPES, 5.0 ethylene glycol-bis(β-aminoethyl ether)-*N*,*N*,*N*′,*N*′-tetraacetic acid (EGTA), and 5.0 Mg-ATP; pH of the internal solution was adjusted to 7.4 with KOH. The pure powdered forms of 4-acetamido-4′-isothiocyanatostilbene-2,2′-disulfonic acid (SITS; Sigma) and 4,4′-diisothiocyanatostilbene-2,2′-disulfonic acid (DIDS; Sigma) were dissolved directly in the superfusate to achieve the desired concentrations. All solutions containing SITS or DIDS were prepared and used in a darkened room. Solution osmolarity was measured by freezing point depression (model 3MO osmometer, Advanced Instruments, Needham Heights, MA).

The whole cell, voltage-clamp configuration of the patch-clamp technique was employed as previously described (7). After adhesion to the bottom of a 1-ml chamber, the cells were superfused at 3 ml/min and 30 ± 1°C. Borosilicate glass electrodes (1.0 mm OD) with resistances of 2–5 MΩ when filled were connected to a patch-clamp amplifier (either Axopatch 200 or Axopatch 1D, Axon Instruments, Burlingame, CA). Junction potentials were zeroed before formation of the membrane-pipette seal (mean seal resistance 16.5 ± 1.6 GΩ, range 5–40 GΩ).

0363-6135/92 $2.00 Copyright © 1992 The American Physiological Society

After seal formation, the membrane patch was ruptured with brief additional suction.

Capacitance and pipette series resistance were compensated to minimize the duration of the capacitive surge. The time constant of the capacitive transient averaged 292 ± 11 μs, and series resistance averaged 4.8 ± 0.2 MΩ after compensation. Mean cell capacitance was 65 ± 2 pF. Cells likely to have a significant leak (seal resistance <5 GΩ) were rejected. In a small number of cells, residual leak current was minimized by determining the current response to 5-mV hyperpolarizations and subtracting a linearly scaled, inverted current from the records obtained on depolarization. All data presented are from cells studied without leakage compensation. Voltage-clamp pulses were generated and data were acquired by digital routines under the control of pCLAMP software (Axon Instruments). All pulses were applied at a frequency of 0.033 Hz to ensure full recovery of I_{to} and to avoid use-dependent unblocking of 4-AP. The amplitude of peak and sustained currents was measured relative to the 0 current level.

All results are expressed as means ± SE. Statistical analyses were performed either by analysis of variance (ANOVA) with Scheffé contrasts for multiple comparisons or by Student's *t* test. A two-tailed $P < 0.05$ was taken to indicate statistical significance.

RESULTS

Relationship between the sustained outward current (I_{sus}) and I_{to1}. The most prominent outward current elicited by depolarization of rabbit atrial cells is the 4-AP-sensitive I_{to1}. To establish the relationship between I_{to1} and I_{sus}, after seal formation, the standard superfusate was modified to inhibit other ionic currents. Cl^- salts of Ba^{2+} (0.5 mM, to block I_{K1}), tetraethylammonium chloride (TEA chloride; 10 mM, to block I_K), and Cd^{2+} [100 μM, to block Ca^{2+} current and the Ca^{2+}-sensitive component of I_{to} (I_{to2})] were added and choline chloride was used to replace NaCl (and eliminate Na current). Muscarinic effects were excluded by showing that 1 μM atropine did not alter I_{sus} in the presence of 126 mM choline.

Figure 1*A* shows the family of currents elicited by a series of 5-s depolarizing pulses. A transient component is observed, which inactivates to a steady-state level that remains constant during continued depolarization. Figure 1*B* shows the effect of 4-AP on the current elicited by a depolarization to +40 mV. In 11 cells, 4-AP (2 mM) reduced the transient current (I_{to1}, measured from the peak outward current to the steady-state level at the end of the pulse) by a mean of 99 ± 1% ($n = 11$, $P < 0.001$ vs. control), without altering I_{sus} [measured from the 0 current level to the value at the end of the pulse; mean change −4 ± 11%; P = not significant (NS)].

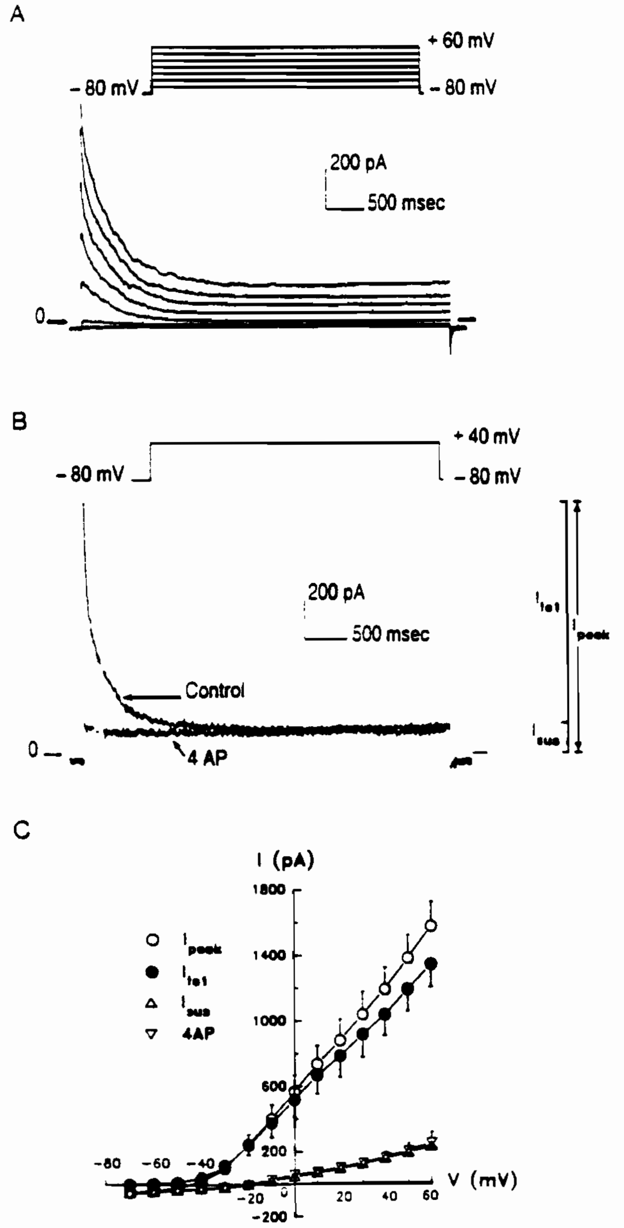

Fig. 1. Effect of 4-aminopyridine (4-AP) on the 4-AP-sensitive transient outward current (I_{to1}) and the sustained outward current (I_{sus}). *A*: family of outward currents elicited by 5-s, 20-mV incrementally depolarizing voltage-clamp increments shown in *inset*. *B*: 4-AP (2 mM) completely inhibited I_{to1}, revealing a time-independent residual I_{sus}. *C*: current-to-voltage (*I-V*) relations for peak outward current relative to 0 current level (I_{peak}), I_{to1} (peak to end-pulse value), and I_{sus} (current at end of the pulse relative to 0), along with current recorded in presence of 4-AP. *I-V* curves of I_{sus} and 4-AP-resistant current are identical and reverse at ∼−20 mV. *I-V* curves are means ± SE from 6 cells at each point. Superfusion solution included (in mM) 10 tetraethylammonium chloride (TEA chloride), 0.5 $BaCl_2$, 0.1 $CdCl_2$, and 126 choline chloride substituted for NaCl.

Figure 1*C* shows the current-voltage relation for peak current (measured from the 0 current level), I_{to1}, and I_{sus} before and after 4-AP in six cells. I_{sus} reverses at ∼−20 mV, shows outward rectification, and is not affected by 4-AP. I_{sus} is thus distinct electrophysiologically and pharmacologically from I_{to1}.

Relationship among I_{sus} and K^+ currents other than I_{to1}. Barium and TEA chloride were used to prevent expression of other K^+ currents in analyzing the relationship between I_{sus} and I_{to1}. Separate experiments were performed to determine whether these agents suppress currents that contribute to I_{sus}. On depolarization to +40 mV, Ba^{2+} (12 cells) and TEA chloride (8 cells) had no significant effect on I_{sus}, reducing it by 7.3 ± 7.4 and 4.6 ± 8.8%, respectively. Ba^{2+} substantially reduced the inward current on hyperpolarization to −140 mV (by 76 ± 6%, $P < 0.001$), indicating that I_{K1} was effectively inhibited.

The role of K^+ as a possible charge carrier for I_{sus} was further evaluated as illustrated in Fig. 2. Whereas increasing superfusate K^+ concentration ($[K^+]$) to 130 mM (by

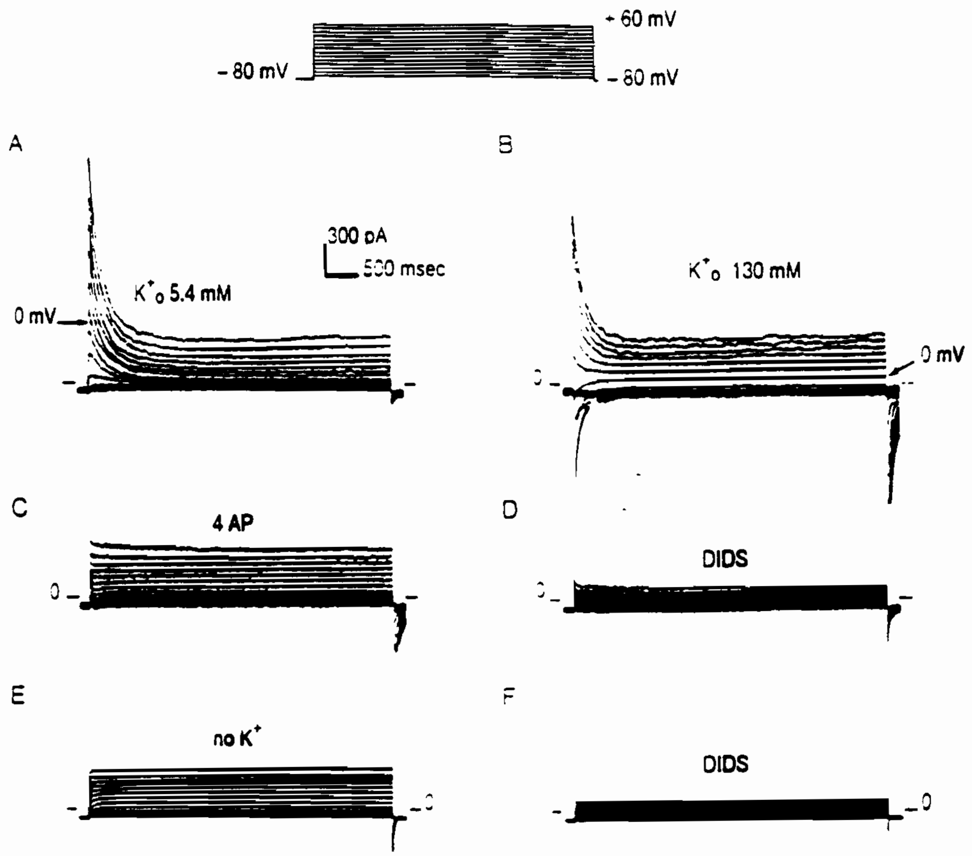

Fig. 2. Response of I_{sus} and I_{to1} to various manipulations of extracellular milieu. Current tracings in *A-F* were elicited by 5-s, 10-mV depolarizing voltage-clamp increments from a holding potential of −80 mV, as shown schematically at *top*. *A*: control tracings, in standard superfusate with (in mM) 10 TEA chloride, 0.5 Ba^{2+}, and 0.1 Cd^{2+} added, and 126 choline chloride substituted for NaCl, in the presence of 5.4 mM superfusate K^+ (K_o^+) concentration. Arrow, current recorded on depolarization to 0 mV. *B*: currents from same cell shown in *A*, in the presence of increased K_o^+ concentration (130 mM). Voltage dependence of I_{to1} is substantially altered, with reversal between 0 and +10 mV. I_{sus}, however, is not significantly changed. *C*: results from same cell as in *A* and *B*, after addition of 2 mM 4-AP to 130 mM KCl-containing superfusate. I_{to1} is blocked but I_{sus} remains largely unaffected. When 150 μM 4,4′-diisothiocyanatostilbene-2,2′-disulfonic acid (DIDS) is subsequently added to the superfusate (*D*), I_{sus} is reduced by over 60% (same cell as in *A-C*). *E*: recording from a different cell, with pipette and superfusate K^+ replaced by Cs^+. I_{to1} is absent, but I_{sus} is clearly present. *F*: suppression of I_{sus} in same cell as in *E* by exposure to 150 μM DIDS.

substituting KCl for choline chloride) substantially altered the reversal potential of I_{to1} (to +4.0 ± 0.8 mV in 6 cells), it produced only minor changes in I_{sus} (Fig. 2, *A* and *B*). Figure 2*E* shows typical recordings obtained when K^+ was replaced by equimolar Cs^+, in both the pipette solution and the superfusate. Whereas the transient outward current is absent, large sustained outward currents were recorded from this and eight other similarly studied cells.

Role of Cl^- current in I_{sus}. Because I_{sus} did not appear to be carried by K^+, we evaluated the possible contribution of Cl^- to I_{sus}. Figure 2*F* shows the effect of 150 μM DIDS in the absence of K^+ in the pipette and the superfusate on I_{sus} recorded from the cell illustrated in Fig. 2*E*. Under these conditions, DIDS reduced I_{sus} at all potentials tested by an average of 62 ± 9% at +40 mV ($P < 0.01$, $n = 5$). Figure 2*C* shows currents from the same cell as in Fig. 2, *A* and *B*, after the addition of 2 mM 4-AP. In the presence of 2 mM 4-AP, the addition of DIDS (Fig. 2*D*) substantially reduced I_{sus}, measured at +40 mV, by an average of 65 ± 7% ($P = 0.001$, $n = 6$). Similar experiments were performed with another Cl^- transport blocker, SITS (2 mM), and a similar reduction in I_{sus} was observed (66 ± 7%, $P < 0.05$, $n = 4$).

In the presence of (in mM) 10 TEA chloride, 0.1 $CdCl_2$, and 0.5 $BaCl_2$, the superfusate Cl^- concentration ($[Cl^-]$) was 146.2 mM. With the assumption of full equilibration of $[Cl^-]$ between the standard pipette solution ($[Cl^-] = 67$ mM) and the intracellular milieu, the estimated equilibrium potential for Cl^- (E_{Cl}; −20.4 mV) is close to the observed reversal potential of I_{sus} as shown in Fig. 1 (−21.8 ± 0.8 mV). Changes in pipette $[Cl^-]$ achieved by reciprocally altering pipette $[Cl^-]$ and aspartate concentration substantially altered the *I-V* relation of I_{sus} (Fig. 3*A*). As intracellular $[Cl^-]$ ($[Cl^-]_i$) was reduced, the reversal potential became more negative and the current showed stronger outward rectification (Fig. 3*A*). The reversal potential of I_{sus} was linearly related to the logarithm of pipette $[Cl^-]$, with a slope of 45.3 mV per decade (Fig. 3*B*). When the reversal potential was measured with K^+ in the superfusate and pipette solutions replaced by Cs^+, the reversal potential was −19.9 ± 2.8 mV ($n = 9$ cells) and −39.8 ± 1.8 mV ($n = 5$) at pipette $[Cl^-]$ of 67 and 22 mM, respectively, values very similar to those recorded in the presence of K^+, as illustrated in Fig. 3. In six additional cells, I_{sus} was recorded before and after replacement of Cl^- in the superfusate by methanesulfonate. Cl^- replacement reduced I_{sus} as measured at +40 mV by 91 ± 4% ($P < 0.05$, $n = 6$).

Osmotic cell stretch produces a Cl^- current in canine atrial (16) and ventricular (18) myocytes. In those studies, the current increased progressively over the course of an experiment. In our work, I_{sus} showed no important change for periods as long as 2 h. To exclude cell swelling before patch formation, we studied the effect of superfusion solutions made hypertonic (measured osmolarity 329 mosM, compared with 260 mosM for the standard superfusate and 258 mosM for the pipette solution) by the addition of 75 mM mannitol, which Sorota (16) showed to suppress the stretch-dependent Cl^- current. After 30 min of exposure to mannitol, I_{sus} was reduced by an average of 12 ± 6% (P = NS, $n = 6$ cells).

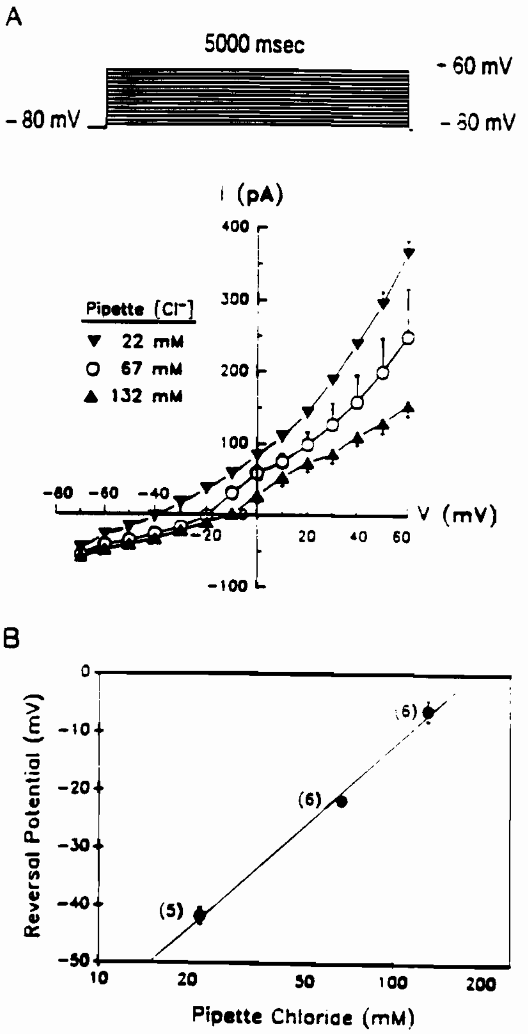

Fig. 3. *A*: *I-V* relation for I_{sus}, with 3 different pipette Cl^- concentrations ($[Cl^-]$; means ± SE). *B*: relationship between reversal potential of I_{sus} and logarithm of pipette $[Cl^-]$ from experiments shown in *A* (number of cells studied at each pipette $[Cl^-]$ is shown in parentheses). Relation was linear with a correlation coefficient of 0.996 and a slope of 45.3 mV/decade change in $[Cl^-]$.

DISCUSSION

In these experiments, we have shown that depolarization of rabbit atrial myocytes to potentials positive to E_{Cl} elicits a sustained outward current that is distinct from I_{to1} in ionic permeability, voltage dependence, and pharmacological response. The sensitivity of this current to the Cl^- transport blockers SITS and DIDS, along with its response to changes in pipette $[Cl^-]$, indicates that it consists largely of a Cl^- current.

A role for Cl^- current in cardiac electrophysiology was first suggested by Carmeliet (1) and Hutter and Noble (13), but, beginning in the late 1970s, Cl^- currents were thought to play a minor role, if any, in the heart. There has been a resurgence of interest in Cl^- currents since Harvey and Hume (10, 12) reported the existence of isoproterenol-activated Cl^- currents in guinea pig and rabbit ventricular myocytes. Subsequent work has indicated that other interventions that increase intracellular adenosine 3′,5′-cyclic monophosphate (cAMP) levels, such as histamine and colforsin, also produce Cl^- currents in cardiac myocytes (9, 11) and that Ca^{2+} transients induce a Cl^- current responsible for I_{to2} (21, 22). More recent work has shown that cell swelling can induce Cl^- currents in canine atrial (16) and ventricular (18) myocytes.

The Cl^- current that we studied differs from these previous observations in that it is evident in the absence of cell swelling, interventions that increase intracellular cAMP, and Ca^{2+} transients. A role for cell swelling was excluded by the fact that the current was unaltered by exposure to a hypertonic superfusate, and the potential contribution of Ca^{2+} transients was minimized by the use of Cd^{2+} in the superfusate and by EGTA (5 mM) in the pipette. It remains to be determined whether the cAMP-, Ca^{2+}-, and swelling-induced Cl^- currents are carried by ion channels distinct from I_{sus} or whether the modulation of a common Cl^- channel is responsible for the various cardiac Cl^- currents that have been reported.

The slope of the relation between the I_{sus} reversal potential and pipette $[Cl^-]$ (45.3 mV/decade) is less than that expected for a pure Cl^- current, assuming complete dialysis of cellular contents (60 mV/decade). This discrepancy may be due to incomplete dialysis through the pipette or to finite permeability to other ions. Our observations resemble those of Harvey and Hume (11), who found a slope of 49 mV/decade for histamine-induced Cl^- current in guinea pig ventricle, although the same group reported a somewhat steeper Cl^- dependency in other studies (9, 12).

The current we have studied in these experiments may play a significant role in cellular electrophysiology. Because of its lack of inactivation, it can contribute to cellular repolarization, as suggested by the early observations of Carmeliet (1). I_{sus} could be a target for selective autonomic- (20) or antiarrhythmic drug- (2) induced changes in action potential duration. If Ca^{2+} transients can increase the amplitude of I_{sus}, the latter could contribute to the production of arrhythmogenic delayed afterdepolarizations.

The authors thank Guylaine Nicol for expert technical assistance and Christiane Lussier for secretarial help.

This research was supported by grants from the Medical Research Council of Canada, the Quebec Heart Foundation, and the Fonds de Recherche de l'Institut de Cardiologie de Montréal.

B. Fermini is a Knoll-Fonds de la Recherche en Santé du Québec (Knoll-FRSQ) Research Scholar, and S. Nattel is a Nordic-FRSQ Senior Research Scholar.

Address for reprint requests: S. Nattel, Montreal Heart Institute, 5000 Belanger St. E., Montreal, Quebec H1T 1C8, Canada.

Received 17 July 1992; accepted in final form 17 September 1992.

REFERENCES

1. **Carmeliet, E. E.** Chloride ions, and the membrane potential of Purkinje fibers. *J. Physiol. Lond.* 156: 375–388, 1961.
2. **Castle, N. A.** Selective inhibition of potassium currents in rat ventricle by clofilium, and its tertiary homolog. *J. Pharmacol. Exp. Ther.* 257: 342–350, 1990.
3. **Clark, R. B., W. R. Giles, and Y. Imaizumi.** Properties of the transient outward current in rabbit atrial cells. *J. Physiol. Lond.* 405: 147–168, 1988.
4. **Dukes, I. D., and M. Morad.** The transient K^+ current in rat ventricular myocytes: evaluation of its Ca^{2+} and Na^+ dependence. *J. Physiol. Lond.* 435: 395–420, 1991.
5. **Escande, D., A. Coulombe, J. F. Faivre, E. Deroubaix, and E. Coraboeuf.** Two types of transient outward currents in adult

human atrial cells. *Am. J. Physiol.* 252 (*Heart Circ. Physiol.* 21): H142-H148, 1987.

6. **Fermini, B., and S. Nattel.** Evidence for a delayed rectifier potassium current, I_k, in rabbit atrial myocytes (Abstract). *Biophys. J.* 59: 266A, 1991.
7. **Fermini, B., Z. Wang, D.-Y. Duan, and S. Nattel.** Differences in the rate dependence of the transient outward current in rabbit and human atrium. *Am. J. Physiol.* 263 (*Heart Circ. Physiol.* 32):H1747-H1754, 1992.
8. **Giles, W. R., and Y. Imaizumi.** Comparison of potassium currents in rabbit atrial and ventricular cells. *J. Physiol. Lond.* 405: 123-145, 1988.
9. **Harvey, R. D., C. D. Clark, and J. R. Hume.** Chloride current in mammalian cardiac myocytes: novel mechanism for autonomic regulation of action potential duration and resting membrane potential. *J. Gen. Physiol.* 95: 1077-1102, 1990.
10. **Harvey, R. D., and J. R. Hume.** Autonomic regulation of a chloride current in heart. *Science Wash. DC* 244: 983-985, 1989.
11. **Harvey, R. D., and J. R. Hume.** Histamine activates the chloride current in cardiac ventricular myocytes. *J. Cardiovasc. Electrophysiol.* 1: 309-317, 1990.
12. **Harvey, R. D., and J. R. Hume.** Isoproterenol activates a chloride current, not the transient outward current, in rabbit ventricular myocytes. *Am. J. Physiol.* 257 (*Cell Physiol.* 26): C1177-C1181, 1989.
13. **Hutter, O. F., and D. Noble.** Anion conductance of cardiac muscle. *J. Physiol. Lond.* 157: 335-350, 1961.
14. **Kilborn, M. J., and D. Fedida.** A study of the developmental changes in outward currents of rat ventricular myocytes. *J. Physiol. Lond.* 430: 37-60, 1990.
15. **Nakayama, T., and H. A. Fozzard.** Adrenergic modulation of the transient outward current in isolated canine Purkinje cells. *Circ. Res.* 62: 162-172, 1988.
16. **Sorota, S.** Swelling-induced chloride-sensitive current in canine atrial cells revealed by whole cell patch-clamp method. *Circ. Res.* 70: 679-687, 1992.
17. **Tohse, N., H. Nakaya, Y. Hattori, M. Endou, and M. Kanno.** Inhibitory effect mediated by α_1-adrenoceptors on transient outward current in isolated rat ventricular cells. *Pfluegers Arch.* 415: 575-581, 1990.
18. **Tseng, G.-N.** Cell swelling increases membrane conductance of canine cardiac cells: evidence for a volume-sensitive Cl channel. *Am. J. Physiol.* 262 (*Cell Physiol.* 31): C1056-C1068, 1992.
19. **Tseng, G.-N., and B. F. Hoffman.** Two components of transient outward current in canine ventricular myocytes. *Circ. Res.* 64: 633-647, 1989.
20. **Wang, X.-L., E. Wettwer, G. Gross, and U. Ravens.** Reduction of cardiac outward currents by alpha-1 adrenoceptor stimulation: a subtype-specific effect? *J. Pharmacol. Exp. Ther.* 259: 783-788, 1991.
21. **Zygmunt, A. C., and W. R. Gibbons.** Calcium-activated chloride current in rabbit ventricular myocytes. *Circ. Res.* 68: 424-437, 1991.
22. **Zygmunt, A. C., and W. R. Gibbons.** Properties of the calcium-activated chloride current in heart. *J. Gen. Physiol.* 99: 391-414, 1992.

In summary, we found that the sustained current after I_{to1} inactivation was

1) Not $[K]_o$- and $[K]_i$-dependent
2) Not blocked by 4-AP, TEA, Ba^{2+}
3) Reverses at potentials close to E_{Cl}
4) Reduced by $[Cl]_o$ substitution
5) Inhibited by DIDS and SITS
6) Outwardly rectifying

These features indicate that the sustained current observed after I_{to1} inactivation in rabbit atrial myocytes is not a K^+ current but a novel Cl^- current which is active under basal conditions. One of the major differences of this Cl^- current from previously reported cardiac chloride currents is that it shows basal activity, so we called it $I_{Cl.b}$. Our next question was to ask whether single channel associated with $I_{Cl.b}$ could be identified and whether it is the same channel as the only reported cardiac single chloride channel CFTR.

CHAPTER 3

CHARACTERIZATION OF A NOVEL CHLORIDE CHANNEL - AN OUTWARDLY RECTIFYING Cl^- CHANNEL (ORCC) IN RABBIT ATRIAL MYOCYTES

An important step in characterizing an ionic current is the elaboration of its single-channel properties. These permit detailed analyses of channel kinetics, studies of mechanisms of regulation and drug-induced inhibition, and comparisons with other native and cloned channels. If the biophysical and physiological significance of Cl^- channels in heart is to be established it is important to characterize in detail the single channels responsible for each of the different types of macroscopic Cl^- currents. Since the properties of macroscopic Cl^- currents as mentioned in chapter 1 are often very similar, it is not known whether these currents are mediated by similar or distinctly different channel proteins. The identification of the single channel responsible for $I_{Cl.b}$ will certainly help resolve this question and will be very valuable for future studies which aim to clone these channels and functionally express them in heterologous expression systems.

This work was performed to identify the possible single-channel mechanism underlying $I_{Cl.b}$ by using the inside-out configuration of patch clamp[26] because this allows controlling the intracellular components.

Brief Definitive Communication

Properties of Single Outwardly Rectifying Cl⁻ Channels in Heart

Dayue Duan, Stanley Nattel

Abstract A variety of potentially important macroscopic Cl⁻ currents have been described in the heart. Although the single-channel properties of the cAMP-dependent current ($I_{Cl,cAMP}$) have been well described, the single-channel equivalents of the other forms of cardiac Cl⁻ current remain unknown. Unlike $I_{Cl,cAMP}$, many of these currents show prominent outward rectification in the presence of symmetrical transmembrane Cl⁻ gradients and sensitivity to disulfonic stilbene Cl⁻ transport blockers. We used the patch-clamp technique to search for single Cl⁻ channels in inside-out patches from rabbit atrial cell membranes, under conditions minimizing the chances of observing channels carrying Na^+, Ca^{2+}, or K^+. Under symmetrical Cl⁻ conditions, single-channel activity was seen in 14 (9%) of 155 patches. Channels showed strong outward rectification and a unitary conductance of 60±3 picosiemens (mean±SEM) at positive voltages. The current-voltage relation was not altered by replacement of cations by the impermeant cation N-methyl-D-glucamine (NMDG) and shifted as expected for a Cl⁻-selective channel when methanesulfonate was substituted for Cl⁻. The Cl⁻ transport blockers DIDS (diisothiocyanatostilbene-2,2′-disulfonic acid, 100 μmol/L) and SITS (4-acetamido-4′-isothiocyanatostilbene-2,2′-disulfonic acid, 1 mmol/L) strongly and reversibly inhibited channel activity when added to the bath and caused channel flickering suggesting open-channel block. Ensemble-average currents showed no time dependence, and the form of the ensemble-average current-voltage relation was similar to that of macroscopic background Cl⁻ current. We conclude that single Cl⁻ channels showing outward rectification and sensitivity to disulfonic stilbenes are present in rabbit atrial cell membranes and may play a role in the regulation of cardiac electrical activity. (***Circ Res*. 1994;75:789-795.**)

Key Words • ion currents • Cl⁻ channels • cardiac arrhythmias • cell swelling • action potential

Early studies of cardiac electrophysiology suggested the participation of Cl⁻ currents in the cardiac action potential,[1-3] but subsequent work led to doubt about the importance of cardiac Cl⁻ currents. The discovery of a cAMP-regulated Cl⁻ current ($I_{Cl,cAMP}$) in the heart in 1989[4-6] caused renewed interest in the potential role of Cl⁻ channels in regulating cardiac electrical activity. Since then, several other types of cardiac Cl⁻ currents have been reported, including a Ca^{2+}-activated current,[7-9] a current induced by cell swelling or stretch,[10-12] a background current,[13] a current elicited by stimulation of purinergic receptors,[14] and a Cl⁻ current resulting from phosphorylation by protein kinase C (PKC).[15,16] Cardiac $I_{Cl,cAMP}$ is carried by a small-conductance (12- to 15-picosiemen [pS]) channel with a nearly linear current-voltage (I-V) relation under symmetrical Cl⁻ conditions[17-19] and with properties that strongly resemble those of channels encoded by the cystic fibrosis transmembrane conductance regulator (CFTR) gene.[20-23] In contrast to $I_{Cl,cAMP}$, most of the other cardiac Cl⁻ currents studied to date display greater outward rectification under symmetrical Cl⁻ gradients, and their single-channel equivalent has not yet been identified.[24] The purpose of the present experiments was to determine whether single Cl⁻ channels can be identified in inside-out membrane patches from rabbit atrial myocytes and, if so, to establish the biophysical properties of these channels and their response to disulfonic stilbene Cl⁻ transport blockers.

Materials and Methods

Single myocardial cells were obtained from rabbit left atrium by using a previously described enzymatic cell dissociation technique.[13,25] All cells studied were rod-shaped, exhibited clear cross striations, and lacked any visible blebs. The inside-out patch configuration was used to record single-channel currents.[26] Borosilicate glass electrodes (outer diameter, 1.5 mm) with resistances of 2 to 5 MΩ when filled were connected to a patch-clamp amplifier (Axopatch 200, Axon Instruments). A bridge (3 mol/L KCl in agar salt) between the bath and a Ag/AgCl reference electrode immersed in pipette solution was used to minimize changes in liquid junction potential, and junction potentials were zeroed before formation of the membrane-pipette seal. After a gigaohm seal had been established, the membrane patch was excised and superfused at 3 mL/min and 30±1°C (temperature regulated by a temperature control device purchased from N.B. Datyner, Stony Brook, NY). Commercial software from Axon Instruments (pCLAMP, FETCHEX, and FETCHAN) was used for voltage-clamp protocols, data acquisition, and data analysis. Voltage-clamp pulses were generated by a 12-bit digital-to-analog converter, and membrane current data filtered with a 5-kHz low-pass filter (eight-pole Bessel filter) were acquired by an analog-to-digital converter at 100 kHz (Medical Systems, Corp) and stored on videotape (at 5 kHz) or on the hard disk of an IBM PC/AT-compatible computer (at 1 kHz). All command voltages and membrane currents are displayed as they would be measured at the intracellular side of the membrane; ie, the values given are the negative of the values measured by the pipette at the extracellular surface.

The pipette (extracellular side of membrane) and bath (intracellular side) solutions were designed to prevent currents through K^+ and Ca^{2+} channels. Na^+ currents were minimized by holding the membrane at 0 mV, to inactivate Na^+ channels,

---

Received February 7, 1994; accepted June 6, 1994.

From the Department of Medicine, Montreal Heart Institute and University of Montreal, and the Department of Pharmacology and Therapeutics, McGill University, Montreal, Quebec, Canada.

Correspondence to Dr Stanley Nattel, Montreal Heart Institute, 5000 Belanger Street East, Montreal, Quebec, Canada H1T 1C8.

between test pulses. No ATP or kinases were included in the solutions. To minimize the ionized [Ca^{2+}] on the intracellular side of the membrane, we omitted Ca^{2+} in the bath and included 5 mmol/L EGTA. The standard pipette solution contained (mmol/L) NaCl 130, CsCl 5.4, CaCl$_2$ 1.0, MgCl$_2$ 0.8, CdCl$_2$ 0.1, NaH$_2$PO$_4$ 0.33, HEPES 10, and glucose 5.5, pH 7.4 (NaOH). The bath solution contained (mmol/L) NaCl 116, CsCl 20, MgCl$_2$ 1.0, EGTA 5.0, and HEPES 10, pH 7.4 (NaOH). To evaluate the ionic selectivity of channels studied, we used equimolar replacement of NaCl in the bath or pipette solution by sodium methanesulfonate (Sigma Chemical Co). In some experiments, the large, impermeant cation *N*'-methyl-D-glucamine (NMDG, obtained from Sigma) was used to replace Na$^+$ and Cs$^+$ ions on both sides of the membrane. The specific compositions of altered pipette and bath solutions are indicated in the appropriate figure legends. The disulfonic stilbene Cl$^-$ transport blockers DIDS (4,4'-diisothiocyanatostilbene-2,2'-disulfonic acid) and SITS (4-acetamido-4'-isothiocyanatostilbene-2,2'-disulfonic acid) were purchased from Sigma and made up as fresh solutions on the day of each experiment.

To compare I-V properties of the single Cl$^-$ channel current with those of the macroscopic background Cl$^-$ current[13] under similar conditions, the whole-cell configuration of the patch-clamp technique was used. Pipettes had a tip resistance of 2 to 5 MΩ when filled with a solution containing (mmol/L) NaCl 118, CsCl 20, MgCl$_2$ 1.0, EGTA 5.0, and HEPES 10, pH adjusted to 7.4 with NaOH. The bath solution contained (mmol/L) either NaCl 130, CsCl 5.4, MgCl$_2$ 0.8, CaCl$_2$ 1.0, NaH$_2$PO$_4$ 0.33, CdCl$_2$ 0.1, dextrose 5.5, and HEPES 10, pH 7.4 (NaOH), to study symmetrical Cl$^-$ conditions or sodium methanesulfonate 116, CsCl 20, MgCl$_2$ 0.8, CaCl$_2$ 1.0, NaH$_2$PO$_4$ 0.33, CdCl$_2$ 0.1, dextrose 5.5, and HEPES 10, pH 7.4 (NaOH) to study the effect of reducing [Cl]$_o$ on macroscopic currents. Ensemble averages of single-channel current were obtained by analyzing data from patches with a single channel and by averaging the recordings of 15 two-second pulses to each of a variety of voltages from a holding potential of 0 mV.

The open probability (P$_o$) of single channels was obtained from the ratio of the area under the curve representing open events (fitted with a gaussian equation by a curve-fitting program in FETCHAN, Axon Instruments) divided by the sum of the areas under the open- and closed-event histograms. The kinetics of open and closed events were analyzed for patches containing only one channel with a half-amplitude algorithm incorporated in FETCHAN, and all events were manually reviewed. Statistical comparisons were performed by Student's *t* test for paired data. All group data are expressed as mean±SEM.

Results

Under symmetrical Cl$^-$ conditions, 11 (9%) of 117 patches exhibited single-channel currents, which reversed at 0 mV and showed outward rectification (Fig 1). The majority of patches containing channels showed activity immediately after excision from the cell (6 of 11 patches studied in symmetrical Cl$^-$), but some patches (5 of 11) required strong depolarization (to +80 mV or greater) for 1 to 10 minutes before consistent channel activity was seen. Once a channel was activated by depolarization, channel opening was observed at membrane potentials from −80 to +80 mV and was stable for 20 to 100 minutes. Under symmetrical Cl$^-$ conditions, the ratio of the absolute value of mean current at +70 mV (3.6±0.2 pA, mean±SEM, n=7) to that at −70 mV (−1.3±0.1 pA) averaged 2.9±0.2, indicating substantial outward rectification. The average slope conductance of the channel under symmetrical Cl$^-$ conditions was 60±3 pS over the range of 0 to +80 mV.

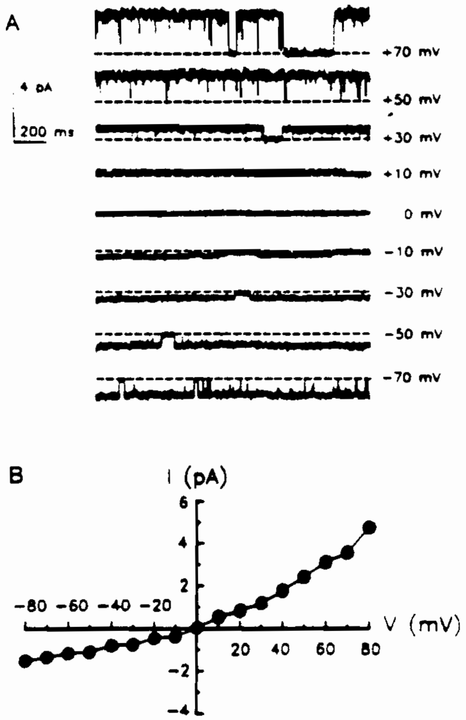

FIG 1. Voltage dependence of single-channel currents recorded in an inside-out patch. A, Tracings of channel currents obtained at various transmembrane potentials in the presence of a symmetrical Cl$^-$ gradient ([Cl$^-$]$_i$/[Cl$^-$]$_o$=138/139.2 mmol/L. The patch was held at 0 mV to inactivate Na$^+$ channels, and 2-second voltage steps to various potentials were applied at 0.1 Hz. Signals were acquired with low-pass filtering by an eight-pole Bessel filter at 5 kHz, and recordings were displayed after digital filtering at 1 kHz. B, Graph showing average current-voltage (I-V) relation obtained from seven patches under the same conditions as in panel A. Standard error bars fall within symbols for means.

Channel activity showed long-duration openings, which were interrupted, at all voltages, by either brief or longer-lasting closing events (Fig 2A). In 7 of 11 patches, amplitude histograms of the type shown in Fig 2B were consistent with the presence of only one channel with single, dominant closed and open states (indicated by the letters C and O in the figure). Mean P$_o$ (Fig 2B) was 0.84±0.04 at +70 mV (n=11) and was not voltage dependent, averaging 0.82±0.07 at +50 mV, 0.84±0.04 at +30 mV, 0.79±0.03 at −50 mV, and 0.81±0.09 at −70 mV. No obvious changes in channel kinetics were observed over time after voltage steps from the holding potential of 0 mV. Open- and closed-time histograms of current at +70 mV are shown in Fig 2C and 2D. In four experiments, patches containing only one channel were held for sufficiently long periods to permit detailed kinetic analysis. Open and closed events were both fitted by biexponential functions, with time constants averaging 43±6 and 988±107 milliseconds, respectively, for open events and 10±3 and 697±116 milliseconds, respectively, for closed events.

Ionic selectivity was assessed by the ion-substitution experiments illustrated in Fig 3. When a patch was exposed to 139 mmol/L Cl$^-$ in the pipette (extracellular side) and 22 mmol/L Cl$^-$ in the bath (intracellular) solution, outward currents remained large, but inward currents were strongly reduced (Fig 3A) compared with results with symmetrical [Cl$^-$] (Fig 1). The reversal

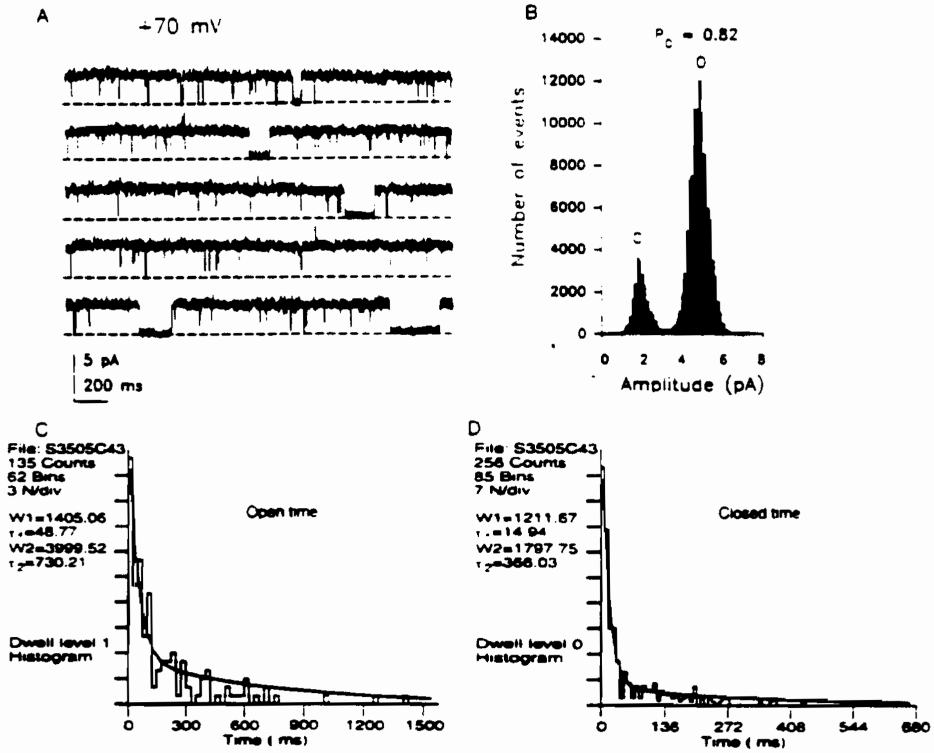

FIG 2. Kinetics of a single channel at +70 mV. A. Tracings of single-channel currents (low-pass–filtered at 1 kHz) from a patch held at +70 mV for 60 seconds in the presence of a symmetrical Cl⁻ gradient. B. Histogram of current amplitude from the patch illustrated in panel A. The open probability (P_o) of the channel was obtained from the ratio of the area under the curve representing open events (fitted with a gaussian equation by a curve-fitting program in FETCHAN, Axon Instruments) divided by the sum of the areas under the open- and closed-event histograms, which are indicated by the O and C, respectively, on the figure (because of an offset current, the closed state corresponds to the peak at ≈2.0 pA). P_o was 0.82 in this patch. C. Open-time histogram of channels from the same patch at the same voltage. Time bins are 25 milliseconds. The histogram was well-fitted to a biexponential function with time constants τ_1 and τ_2 of 49 and 730 milliseconds, respectively. D. Closed-time histogram. Time bins are 8 milliseconds. Closed times were also well-fitted by a biexponential function with time constants τ_1 and τ_2 of 15 and 366 milliseconds, respectively. Open and closed events were analyzed with a half-amplitude algorithm incorporated in FETCHAN, and all events were manually reviewed. N/div indicates number of events per division on vertical scale; W1 and W2, area under each exponential component.

potential (V_r) was between −30 and −50 mV. When a patch was exposed to the opposite [Cl⁻] gradient (24 mmol/L pipette [Cl⁻], 138 mmol/L bath [Cl⁻]), inward currents increased, outward currents became smaller, and V_r shifted in the positive direction (to between +30 and +50 mV, Fig 3B). The average I-V curves recorded for different [Cl⁻] gradients are shown in Fig 3C. Changes in the transmembrane [Cl⁻] gradient shifted V_r in a fashion indicating Cl⁻ selectivity of the channel. When mean V_r is plotted as a function of log ($[Cl^-]_i/[Cl^-]_o$), the points fall on a line (r=.999), with a slope of 41 mV per decade (Fig 3D). The predicted slope of a Cl⁻-specific channel would be somewhat higher (60 mV per decade, dashed line in Fig 3D), suggesting that the channel may have some permeability to the anion (methanesulfonate) substituted for Cl⁻. When cations (Na^+ and Cs^+) were replaced by NMDG under symmetric Cl⁻ conditions, single-channel currents (Fig 3E) were recorded with approximately the same frequency (3 [8%] of 38 patches) as with the standard solutions described above. I-V curves recorded in NMDG-containing solutions (Fig 3C, △) are shown to be superimposed on those recorded in solutions containing Cs^+ and Na^+ (Fig 3C, ○), suggesting no significant cation permeability of the channel.

Disulfonic stilbene compounds are effective blockers of a variety of cardiac[7-9,13,24,27] and noncardiac[28-30] Cl⁻ currents. Therefore, we assessed the effects of two members of this class, DIDS and SITS, on single-channel activity. The addition of 100 μmol/L DIDS (Fig 4A) or 1 mmol/L SITS (Fig 4B) to the bath (intracellular side of the patch) rapidly inhibited channel opening by increasing closed times and causing increased flickering during the open state. At +70 mV, P_o was reduced from 0.83±0.05 to 0.33±0.07 (P=.002, n=6) by DIDS and from 0.86±0.05 to 0.28±0.10 (P<.001, n=5) by SITS. Channel inhibition by DIDS and SITS was reversible on washout, as shown in Fig 4.

The final series of experiments was performed to relate single-channel currents to a possible macroscopic equivalent, background Cl⁻ current.[13] Whole-cell currents were recorded under ionic conditions similar to those used in single-channel experiments. In the presence of a symmetrical Cl⁻ gradient, an outwardly rectifying current was recorded (Fig 5A, tracings at a), with a mean V_r in seven experiments of −0.4±1.3 mV (calculated Cl⁻ equilibrium potential, −0.2 mV). When $[Cl]_o$ was reduced, macroscopic outward currents became much smaller (Fig 5A, tracings at b), and V_r shifted to +37±2 mV (n=7; estimated Cl⁻ equilibrium potential, +46 mV). Macroscopic currents returned to

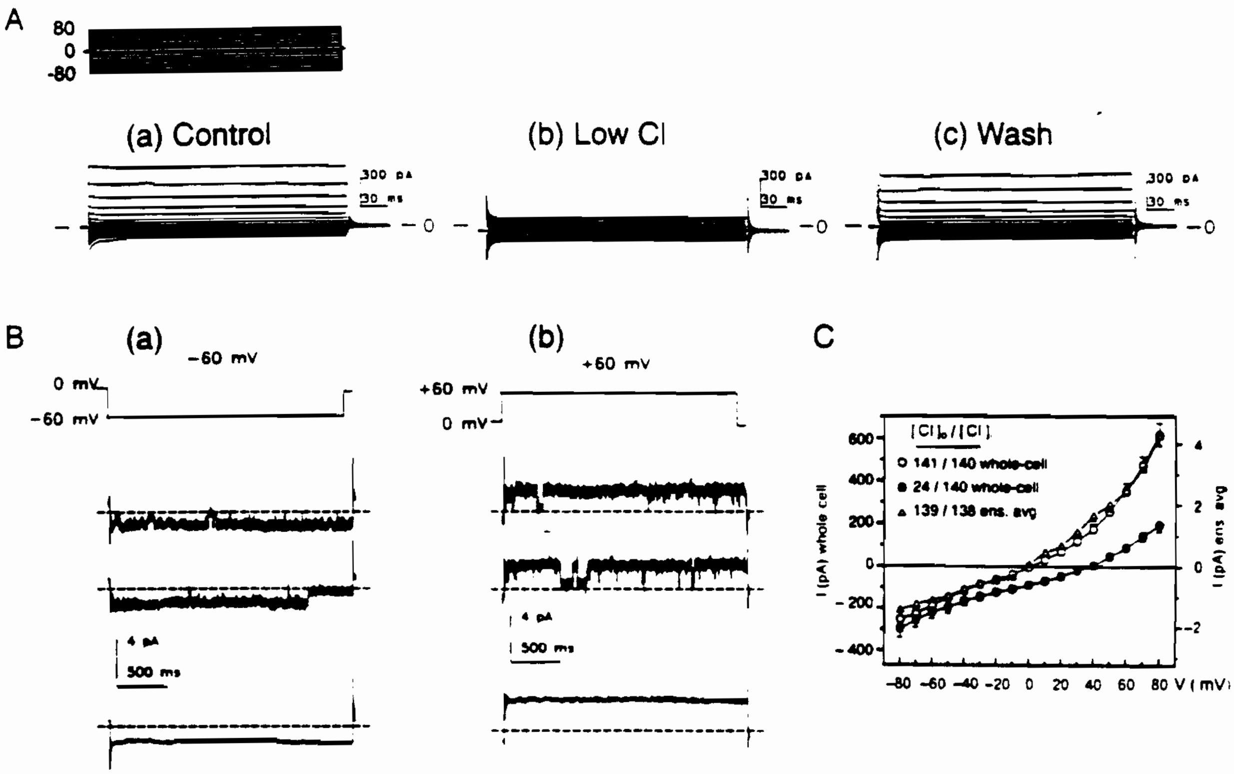

Fig 5. Macroscopic Cl⁻ current and ensemble-average current carried by single channels. Voltage protocol is shown in inset. A, Macroscopic currents elicited by 300-millisecond pulses from a holding potential of 0 mV. Tracings at a show currents under symmetric Cl⁻ conditions ($[Cl^-]_o$=141 mmol/L, $[Cl^-]_i$=140 mmol/L). Tracings at b show macroscopic currents after reduction of $[Cl^-]_o$ by replacement of sodium chloride by sodium methanesulfonate ($[Cl^-]_o$=24 mmol/L, $[Cl^-]_i$=140 mmol/L). Tracings at c show return to symmetrical [Cl⁻] gradient. Results shown in a, b, and c are from the same cell. B, Ensemble-average currents (bottom) obtained by averaging 15 single-channel current recordings (two examples shown at each voltage) obtained with voltage steps shown at the top of each panel. The preparation was held at 0 mV and pulsed to −60 mV (a) or +60 mV (b) for 2 seconds at a frequency of 0.1 Hz under symmetrical Cl⁻ conditions. Dashed line indicates closed-state level. C, Graph showing whole-cell current voltage (I-V) relation (scale at left) under symmetrical Cl⁻ conditions as in panel A (a) (○, n=7) and with reduced $[Cl^-]_o$ as in panel A (b) (●, n=7). Ensemble-average I-V relation (△, scale at right) is plotted for symmetrical Cl⁻ conditions. Results shown for ensemble averages are from four patches studied with the protocol and analysis procedure shown in panel B.

currents, ensemble-average currents showed outward rectification and a lack of time dependence.

Fig 5C shows the mean I-V relation for whole-cell currents under symmetrical Cl⁻ conditions (○, n=7) and after Cl⁻ replacement in the bath (●, n=7). Mean ensemble-average currents are also shown (△, n=4, scale at right). The form of the I-V relation for ensemble-average currents is similar to that of whole-cell currents obtained with similar (symmetrical Cl⁻) conditions.

Discussion

Relation to Previously Described Cl⁻ Channels

We have shown that single Cl⁻ channels displaying strong outward rectification and sensitivity to disulfonic stilbene Cl⁻ transport blockers are present in a significant number of membrane patches from rabbit atrial myocytes. To our knowledge, this is the first such report in the literature. Previous published reports of single Cl⁻ channel activity in cardiac cells have been limited to a low-conductance channel activated by cAMP[17-19] and resembling single Cl⁻ channels encoded by CFTR[20-23] and a very large-conductance (400-pS) channel seen only in neonatal rat hearts.[31] The conductance, pharmacologic, and rectification properties of the channel we studied resemble those of outwardly rectifying Cl⁻ channels (ORCCs) previously described in secretory epithelia,[32] neuroglia,[33] fibroblasts,[34] and lymphocytes.[30,35] Like ORCCs in other systems, the cardiac channel has a conductance in the range of 60 pS at positive voltages, rectifies strongly in the outward direction, may require strong depolarization to enter an active mode, and is sensitive to inhibition by disulfonic stilbenes. A Cl⁻ channel with similar conductance properties was observed in 1982 in calf cardiac sarcolemmal preparations incorporated in artificial lipid bilayers,[36] but its properties and potential significance were unknown at the time.

Possible Functional Role

The properties of a variety of macroscopic Cl⁻ currents in the heart, including Ca²⁺-dependent,[7-9] swelling-induced,[10-12] and purinergic currents,[14] have recently been reviewed by Ackerman and Clapham.[24] These currents may show outward rectification and are sensitive to disulfonic stilbenes.[24] Low-conductance channels and macroscopic cAMP-dependent currents corresponding to CFTR show little rectification under symmetrical Cl⁻ conditions,[17,18] as do macroscopic currents resulting from activation of Cl⁻ conductances by cAMP[6,37] and by PKC.[15,16] Recent detailed studies also indicate that cAMP-dependent[38] and PKC-activated[16] Cl⁻ currents are not inhibited by disulfonic stilbenes.

Interventions that enhance or elicit macroscopic cardiac Cl^- currents and have also been found to increase ORCC activity in noncardiac cells include cell swelling or stretch[39-41] and purinergic stimulation with extracellular ATP.[42]

Our finding of channels with the properties of ORCCs in the heart raises the possibility that ORCCs may underlie macroscopic cardiac Cl^- currents. The most obvious candidate macroscopic current to correspond to ORCC is the background Cl^- current.[13] Fig 5C shows that the form of the I-V relation of background macroscopic Cl^- current is similar to that of ensemble-average ORCC current, consistent with this possibility. The potential relation between ORCC and outwardly rectifying macroscopic cardiac Cl^- currents requires further investigation.

We observed ORCCs in the absence of Ca^{2+} and in the presence of 5 mmol/L EGTA in the bath, indicating that cardiac ORCCs in cell-free membrane patches may be active and have a high probability of opening in the absence of free intracellular Ca^{2+} and weighing against ORCC as the channel underlying Ca^{2+}-dependent Cl^- current. There is evidence that endogenous cytoplasmic inhibitors prevent ORCC from opening in intact cells.[43,44] Therefore, it is possible that an increase in free intracellular Ca^{2+} could liberate ORCCs from endogenous inhibitors, permitting them to enter an active mode and increasing Cl^- conductance. Arguments to support this type of regulation of ORCCs by intracellular Ca^{2+} have been put forward on the basis of data obtained in epithelial cells.[45]

Preliminary data have been presented that suggest a potentially important role for disulfonic stilbene–sensitive Cl^- currents in mediating action potential abbreviation caused by hypoxia in rabbit hearts.[46] Since ORCCs are, in contrast to cAMP-dependent Cl^- channels, sensitive to disulfonic stilbenes, they may underlie such Cl^- currents. The replacement of extracellular Cl^- by nitrate ions protects against ventricular fibrillation induced by myocardial ischemia and reperfusion in isolated rat hearts,[47] and this has been interpreted as suggesting a role for Cl^- current in ischemic cardiac arrhythmias.

Limitations

We studied single Cl^- channels only in cell-free patches. Potential functional roles of the channels that we identified need to be assessed critically with the use of cell-attached patches. Even with cell-attached patches, potential modification of the membrane under the patch by suction, pipette solutions, and seal formation could lead to the introduction of artifacts. We used HEPES to buffer pH in the bath and pipette solutions. Buffers like HEPES have the potential to modify the properties of ORCCs,[48] and our results must be interpreted in this light. On the other hand, most previous studies of ORCCs in noncardiac tissues were performed with HEPES as a buffer.

We found that the addition of DIDS and SITS to the bath effectively inhibited single-channel activity from the cytoplasmic side of the membrane. In previous studies of the inhibition of macroscopic cardiac Cl^- currents by disulfonic stilbenes, the latter were added to the superfusate and would have achieved access from the extracellular side. Because the anionic groups of disulfonic stilbenes limit their ability to traverse the membrane,[49] caution must be exercised in relating our findings regarding DIDS and SITS sensitivity of single-channel currents to the response of macroscopic Cl^- currents to superfusion with the same compounds. There is evidence that disulfonic stilbenes can permeate across the cell membrane, albeit to a limited extent,[49] and that such compounds can effectively block ORCCs at a single blocking site from either side of epithelial membranes.[28,29]

Conclusions

We have found that single Cl^- channels, which demonstrate properties different from those of cAMP-dependent Cl^- channels, are present in a significant number of inside-out rabbit atrial membrane patches. The properties of these channels identify them with an outwardly rectifying Cl^- channel previously described in many noncardiac tissues. Like a variety of macroscopic cardiac currents, these channels show outward rectification in the presence of symmetrical $[Cl^-]$ and sensitivity to inhibition by disulfonic stilbene compounds. The channels that we identified are a candidate to underlie macroscopic Cl^- currents of potential importance in the regulation of cardiac electrical activity.

Acknowledgments

This study was supported by grants from the Medical Research Council of Canada, the Quebec Heart Foundation, and the Fonds de Recherche de l'Institut de Cardiologie de Montreal. Dr Duan is supported by a graduate studentship award from the Medical Research Council of Canada. We thank Mary Morello and Martine Dufort for secretarial assistance, Guylaine Nicol for technical support, and Dr Jean-Louis Schwartz of the Institut de Biotechnologie, Montreal, Canada, and Dr Bernard Fermini of the Montreal Heart Institute for advice regarding data acquisition and analysis techniques.

References

1. Hodgkin AL, Horowicz P. The influence of potassium and chloride ions on the membrane potential of single muscle fibers. *J Physiol (Lond)*. 1959;148:127-160.
2. Carmeliet EE. Chloride ions and the membrane potential of Purkinje fibers. *J Physiol (Lond)*. 1961;156:375-388.
3. Hutter OF, Noble D. Anion conductance of cardiac muscle. *J Physiol (Lond)*. 1961;157:335-350.
4. Harvey RD, Hume JR. Autonomic regulation of a chloride current in heart. *Science*. 1989;244:983-985.
5. Harvey RD, Hume JR. Isoproterenol activates a chloride current, not the transient outward current, in rabbit ventricular myocytes. *Am J Physiol*. 1989;257:C1177-C1181.
6. Bahinski A, Nairn AC, Greengard P, Gadsby DC. Chloride conductance regulated by cyclic AMP-dependent protein kinase in cardiac myocytes. *Nature*. 1989;340:718-721.
7. Zygmunt AC, Gibbons WR. Calcium-activated chloride current in rabbit ventricular myocytes. *Circ Res*. 1991;68:424-437.
8. Zygmunt AC, Gibbons WR. Properties of the calcium-activated chloride current in the heart. *J Gen Physiol*. 1992;99:391-414.
9. Sipido KR, Callewaert G, Carmeliet E. $[Ca^{2+}]_i$ transients and $[Ca^{2+}]_i$-dependent chloride current in single Purkinje cells from rabbit heart. *J Physiol (Lond)*. 1993;468:641-667.
10. Sorota S. Swelling-induced chloride-sensitive current in canine atrial cells revealed by whole-cell patch-clamp method. *Circ Res*. 1992;70:679-687.
11. Tseng GN. Cell swelling increases membrane conductance of canine cardiac cells: evidence for a volume-sensitive Cl channel. *Am J Physiol*. 1992;262:C1056-C1068.
12. Hagiwara N, Masuda H, Shoda M, Irisawa HJ. Stretch-activated anion currents of rabbit cardiac myocytes. *J Physiol (Lond)*. 1992;456:285-302.

13. Duan D. Fermini B. Nattel S. Sustained outward current observed after I_{to1} inactivation in rabbit atrial myocytes is a novel Cl^- current. *Am J Physiol.* 1992:263:H1967-H1971.
14. Matsuura H. Ehara T. Activation of chloride current by purinergic stimulation in guinea pig heart cells. *Circ Res.* 1992:70:851-855.
15. Walsh KB. Activation of a heart chloride current during stimulation of protein kinase C. *Mol Pharmacol* 1991:40:342-346.
16. Walsh KB. Long KJ. Properties of a protein kinase C–activated chloride current in guinea pig ventricular myocytes. *Circ Res.* 1994:74:121-129.
17. Ehara T. Ishihara K. Anion channels activated by adrenaline in cardiac myocytes. *Nature.* 1990:347:284-286.
18. Nagel G. Hwang TC. Nastiuk KL. Nairn AC. Gadsby DC. The protein kinase A-regulated cardiac Cl^- channel resembles the cystic fibrosis transmembrane conductance regulator. *Nature.* 1992:360:81-84.
19. Ehara T. Matsuura H. Single-channel study of the cyclic AMP-regulated chloride current in guinea-pig ventricular myocytes. *J Physiol (Lond).* 1993:464:307-320.
20. Berger HA. Anderson MP. Gregory RJ. Thompson S. Howard PW, Maurer RA, Mulligan R, Smith AE. Welsh MJ. Identification and regulation of the cystic fibrosis transmembrane conductance regulator-generated chloride channel. *J Clin Invest.* 1991:88:1422-1431.
21. Kartner N. Hanrahan JW. Jensen TJ. Naismith AL. Sun S. Ackerley CA. Reyes EF. Tsui LC. Rommens JM. Bear CE. Riordan JR. Expression of the cystic fibrosis gene in nonepithelial invertebrate cells produces a regulated anion conductance. *Cell.* 1991:64:681-691.
22. Bear CE. Duguay F. Naismith AL. Kartner N. Hanrahan JW. Riordan JR. Cl^- channel activity in *Xenopus* oocytes expressing the cystic fibrosis gene. *J Biol Chem.* 1991:266:19142-19145.
23. Cliff WH. Schoumacher RA. Frizzell RA. cAMP-activated Cl channels in CFTR-transfected cystic fibrosis pancreatic epithelial cells. *Am J Physiol.* 1992:262:C1154-C1160.
24. Ackerman MJ. Clapham DE. Cardiac chloride channels. *Trends Cardiovasc Med.* 1993:3:23-28.
25. Duan D. Fermini B. Nattel S. Potassium channel blocking properties of propafenone in rabbit atrial myocytes. *J Pharmacol Exp Ther.* 1993:264:1113-1123.
26. Hamill OP. Marty A. Neher E. Sakmann S. Sigworth FJ. Improved patch-clamp techniques for high-resolution current recording from cells and cell-free membrane patches. *Pflugers Arch.* 1981:391:85-100.
27. Bouron A. Potreau D. Raymond G. Possible involvement of a chloride conductance in the transient outward current of whole-cell voltage-clamped ferret ventricular myocytes. *Pflugers Arch.* 1991:419:534-536.
28. Singh AK. Afink GB. Venglarik CJ. Wang R. Bridges RJ. Colonic Cl channel blockade by three classes of compounds. *Am J Physiol.* 1991:260:C51-C63.
29. Tilmann M. Kunzelmann K. Fröbe U. Cabantchik I. Lang HJ. Englert HC. Greger R. Different types of blockers of the intermediate-conductance outwardly rectifying chloride channel in epithelia. *Pflugers Arch.* 1991:418:556-563.
30. Garber SS. Outwardly rectifying chloride channels in lymphocytes. *J Membr Biol.* 1992:127:49-56.
31. Coulombe A. Coraboeuf E. Large-conductance chloride channels of new-born rat cardiac myocytes are activated by hypotonic media. *Pflugers Arch.* 1992:422:143-150.
32. Frizzell RA. Cystic fibrosis: a disease of ion channels? *Trends Neurosci.* 1987:10:190-193.
33. Barres BA. Chun LL. Corey DP. Ion channel expression by white matter. *Glia.* 1988:21:10-30.
34. Bear CE. Phosphorylation-activated chloride channels in human skin fibroblasts. *FEBS Lett.* 1988:237:145-149.
35. Chen JH. Schulman H. Gardner P. A cAMP-regulated chloride channel in lymphocytes that is affected in cystic fibrosis. *Science.* 1989:243:657-660.
36. Coronado R. Latorre R. Detection of K^+ and Cl^- channels from calf cardiac sarcolemma in planar lipid bilayer membranes. *Nature.* 1982:298:849-852.
37. Harvey RD. Hume JR. Histamine activates the chloride current in cardiac ventricular myocytes. *J Cardiovasc Electrophysiol.* 1990:1:309-317.
38. Harvey RD. Effects of stilbenedisulfonic acid derivatives on the cAMP-regulated chloride current in cardiac myocytes. *Pflugers Arch.* 1993:422:436-442.
39. McCann JD. Li M. Welsh MJ. Identification and regulation of whole-cell chloride currents in airway epithelium. *J Gen Physiol.* 1989:94:1015-1036.
40. Worrell RT. Butt AG. Cliff WH. Frizzell RA. A volume-sensitive chloride conductance in human colonic cell line T84. *Am J Physiol.* 1989:256:C1111-C1119.
41. Solc CK. Wine JJ. Swelling-induced and depolarization-induced Cl^- channels in normal and cystic fibrosis epithelial cells. *Am J Physiol.* 1991:261:C658-C674.
42. Stutts MJ. Chinet TC. Mason SJ. Fullton JM. Clarke LL. Boucher RC. Regulation of Cl^- channels in normal and cystic fibrosis airway epithelial cells by extracellular ATP. *Proc Natl Acad Sci U S A.* 1992:89:1621-1625.
43. Kunzelmann K. Tilmann M. Hansen CP. Greger R. Inhibition of epithelial chloride channels by cytosol. *Pflugers Arch.* 1991:418:479-490.
44. Krick W. Disser J. Hazama A. Burckhardt G. Frömter E. Evidence for a cytosolic inhibitor of epithelial chloride channels. *Pflugers Arch.* 1991:418:491-499.
45. Frizzell RA. Rechkemmer G. Shoemaker RL. Altered regulation of airway epithelial cell chloride channels in cystic fibrosis. *Science.* 1986:233:558-560.
46. Petrich ER. Zumino AP. Yergeau P. Chartier D. A chloride current contributes to action potential shortening in hypoxic rabbit hearts. *J Mol Cell Cardiol.* 1992:24(suppl I):S106. Abstract.
47. Ridley PD. Curtis MJ. Anion manipulation: a new antiarrhythmic approach: action of substitution of chloride with nitrate on ischemia- and reperfusion-induced ventricular fibrillation and contractile function. *Circ Res.* 1992:70:617-632.
48. Hanrahan JW. Tabcharani JA. Inhibition of an outwardly rectifying anion channel by HEPES and related buffers. *J Membr Biol.* 1990:116:65-77.
49. Cabantchik ZI. Greger R. Chemical probes for anion transporters of mammalian cell membranes. *Am J Physiol.* 1992:262:C803-C827.

So far, we have shown that single channels displaying strong outward rectification, Cl-dependence, and sensitivity to disulfonic stilbene chloride channel blockers are present in a significant number of membrane patches from rabbit atrial myocytes. This is the first such report in the literature. The slope conductance, the outward rectification property and the pharmacological properties of this channel are quite different from those of $I_{Cl.cAMP}$, which was the only identified cardiac Cl^- channel at the time. However, the properties of this novel cardiac chloride channel are very similar to those of the outwardly rectifying Cl^- channel (ORCC) described in non-cardiac tissues such as epithelial cells. Now, while there is agreement that CFTR plays an important role in epithelial ion transport, many people doubt the physiological role of ORCC in cell function. Two major reasons caused this debate. One is the lack of clear macroscopic Cl^- current corresponding to ORCC. The other is that single ORCC activity has not been clearly demonstrated in cell-attached patches. To test the potential physiologic role of cardiac ORCC, we performed experiments to relate single ORCC currents to a possible macroscopic equivalent, the $I_{Cl.b}$. The form of the I-V relation of $I_{Cl.b}$ is similar to that of ensemble-average ORCC current, supporting the notion that ORCC may underlie $I_{Cl.b}$.

CHAPTER 4

REGULATION OF $I_{Cl.b}$ AND ORCC BY CELL-VOLUME

The cell-attached mode of patch-clamp provides a method to record single-channel activity under a more physiological condition. This work was designed to answer the following questions:

1) Can unitary ORCC current be detected in cell-attched membrane patches under basal condition?

2) What is the single-channel mechanism for $I_{Cl.swell}$? Is it due to a different channel from ORCC or the same as ORCC but with a regulatory relationship?

Evidence that Outwardly-Rectifying Chloride Channels Underlie Volume-Regulated Chloride Currents In Heart

Dayue Duan,[†‡] Joseph R Hume,[‡] Stanley Nattel[†]

Short title: Volume-Regulated Cardiac Cl^- Channels

From[†] the Department of Pharmacology and Therapeutics, McGill University; the Department of Medicine, University of Montreal; and the Department of Medicine and Research Centre, Montreal Heart Institute, Montreal, Quebec, Canada; and [‡] the Department of Physiology and Cell Biology, University of Nevada, School of Medicine, Reno, NV 89557-0046, USA

Correspondence to Stanley Nattel, MD, Montreal Heart Institute, 5000 Belanger Street, Montreal, Quebec H1T 1C8, Canada.

Tel: (514) 376-3330; Fax: (514) 376-1355.

Abstract Swelling-induced Cl^- current ($I_{Cl.swell}$) is present in most cardiac tissues, but the unitary channel mechanism underlying $I_{Cl.swell}$ is unknown. We used the cell-attached patch-clamp technique to assess the single-channel mechanism of $I_{Cl.swell}$ and the basally-active Cl^- current ($I_{Cl.b}$) in rabbit atrial myocytes. Under isotonic conditions, single outwardly-rectifying Cl^- channels (ORCC) with a chord conductance of 28 ± 1 pS were observed in 21/367 (5.7%) patches. Unconditional kinetic analysis revealed at least three open and four closed channel states. Hypotonic superfusion-induced swelling resulted in the appearance of active channels in 41/265 (15.5%) patches without channel activity under isotonic conditions, and caused a second active channel to appear in 3/14 patches showing a single channel under isotonic conditions. Overall, channels were seen in 54/336 patches under hypotonic conditions (16.1%, $p<0.001$ versus isotonic conditions). The current-voltage relations, reversal potential-$[Cl^-]_o$ relations, open probability, and kinetics of swelling-induced channels were indistinguishable from those of ORCC under isotonic conditions. Unitary ORCC, $I_{Cl.b}$ and $I_{Cl.swell}$ were strongly and similarly inhibited by tamoxifen. Swelling-induced increases in macroscopic Cl^- current were attributable to an increase in the number of active ORCC with no significant effects on single-channel amplitude or open probability. Estimated macroscopic currents based on cell surface area, patch dimensions, single-channel ORCC current amplitude, open probability, and density were consistent with measured values of $I_{Cl.b}$ and $I_{Cl.swell}$. We conclude that ORCC underlie volume-regulated basal and swelling-induced Cl^- currents in rabbit atrial myocytes.

Key Words ● **heart** ● **cell swelling** ● **cardiac electrophysiology** ● **chloride channel** ● **action potential**

Introduction

Chloride channels have been found to be present in the plasma membranes of most cells and play potentially important roles in the control of cell volume, intracellular pH and membrane potential.[1,2] Over the past few years, evidence has accumulated to show that the heart may express several types of Cl^- channels.[3] A cell-swelling-induced Cl^- current ($I_{Cl.swell}$) has been reported to exist in various cardiac cell types, such as canine atrial and ventricular cells,[4,5] rabbit atrial cells,[6] guinea pig atrial and ventricular cells,[7] human atrial cells,[8-10] and cultured chick heart cells.[11,12] Although a 400-pS Cl^- channel has been reported to be activated by hypotonic solution in neonatal rat cardiac cells,[13] this channel has not been observed in adult cardiac cells. The nature of the unitary channel(s) underlying cardiac $I_{Cl.swell}$ is thus unclear.

In rabbit atrial myocytes, we have previously observed a basal macroscopic Cl^- current ($I_{Cl.b}$),[14,15] and more recently, have found that $I_{Cl.b}$ may be regulated by cell volume and α_1-adrenoceptor-coupled pertussis toxin-sensitive G-protein-mediated activation of protein kinase C, a mechanism similar for the regulation of $I_{Cl.swell}$ in the same preparation.[6] While outwardly-rectifying chloride channels (ORCC) of approximately 60-pS were identified in inside-out patches excised from rabbit atrial myocytes which resemble macroscopic $I_{Cl.b}$,[15] a definitive identification between ORCC and $I_{Cl.b}$ is still lacking. Furthermore, the single channel underlying $I_{Cl.swell}$ remains unknown. In the present study, we used the patch-clamp technique to identify unitary Cl^- channels in cell-attached mode in rabbit atrial myocytes during superfusion with isotonic and hypotonic solutions and study their properties. Macroscopic $I_{Cl.b}$ and $I_{Cl.swell}$ were also studied with the use of whole-cell voltage-clamp technique to compare their properties with those of single-channel currents under similar conditions. Preliminary data from these studies have been presented in abstract form.[16,17]

Materials and Methods

Preparation of single cells.

Single atrial cells were obtained from rabbit hearts using a previously described dissociation technique.[6,14,15] Briefly, rabbits (1.5 to 2.0 kg) were killed by a blow on the neck and the hearts were quickly removed and perfused in the Langendorff mode, first with a modified HEPES-buffered Tyrode solution at 37°C, then with a nominally Ca^{2+}-free Tyrode solution until the heart ceased to beat, and finally with the same solution containing 0.04% collagenase (CLSII, Worthington Biochemical) and 1.0% bovine serum albumin (Sigma Chemicals) for 10 min. The left atrium was removed and further dissected into small pieces, and cell dissociation achieved by gentle mechanical agitation. All cells studied were rod-shaped, exhibited clear cross-striations, and lacked any visible blebs under isotonic conditions. Cell dimensions were determined with a calibrated graticule in the microscope, and cell volumes were estimated with assumed right cylindrical geometry according to the following equation: $V=\pi L(W/2)^2$, where V, L and W are cell volume, length and width respectively.

Electrophysiological recording.

The cell-attached configuration of the patch-clamp technique[18] was employed to record single chloride channel currents. The tight-seal whole-cell voltage clamp configuration of the patch-clamp technique was used to record the macroscopic $I_{Cl.b}$ and $I_{Cl.swell}$ and compare their current-voltage (I-V) and other properties with those of the single channel currents under similar conditions. Recording pipettes were prepared from borosilicate glass electrodes (1.5 mm O.D.) with tip resistances of 2-5 MΩ when filled with pipette solution. A 3 M KCl in agar salt bridge between the bath and a Ag-Ag-Cl reference electrode immersed in pipette solution was used to minimize changes in liquid junction potential, and junction potentials were zeroed prior to establishing a membrane seal. A tight seal between the cell membrane and the pipette tip (seal resistance > 10GΩ) was achieved by applying light suction. Recordings were made using an Axopatch 200A amplifier (Axon Instruments). Commercial software from Axon Instruments (pCLAMP 6; Clampex. Clampfit, Fetchex, Fetchan and Pstat routines) was used for control of voltage-clamp protocols, data acquisition and data analysis. Voltage-clamp pulses were generated by a 12-bit digital-to-analog (D/A) convertor. Single-channel currents were recorded at a gain of 500 mV/pA and low-pass filtered with an eight-pole Bessel filter at 5 kHz and stored on video tape, or at 1-2 kHz and simultaneously digitized (Digidata 1200, Axon Instruments Inc.) at a sampling rate of 2-5 kHz and stored on the hard disk of an IBM PC/AT compatible computer.

To obtain single-channel I-V relations, the membrane was clamped from a holding potential of 0 mV relative to the resting potential (RP) to a series of test potentials for 4 seconds at a time. The voltage of all cell-attached single-channel voltage clamps in this manuscript will be expressed as RP+V, where RP is the cell membrane resting potential and V is the transpatch voltage step applied by the amplifier as would be measured at the intracellular side of the patch membrane. Hyperpolarizing and depolarizing pulses were imposed at 0.1 Hz in +10 mV increments between RP-40 and RP+140 mV. Ensemble averages of single-channel current were obtained by analyzing data from patches with a single channel, and averaging the records of 60 two-second pulses. All command voltages and single channel currents are displayed as they would be measured at the intracellular side of the membrane, ie, the values given are the negative of the values measured by the pipette at the extracellular surface.

The cell-attached patch configuration was checked at the end of each experiment by rupturing the patch to confirm a passage from the cell-attached to the whole-cell configuration. The average intracellular potential measured immediately after membrane rupture was 63.6±1.6 mV (n=53). All experiments were performed at 30±1 °C. Inward cation currents such as I_{Na}, I_{Ca} and non-selective cation currents were prevented by using the large impermeant cation N'-methyl-D-glucamine (NMDG) to replace the cations in the pipette solution. $CdCl_2$ (200 μM), $BaCl_2$ (2 mM), 4-aminopyridine (4-AP) (2 mM) and TEA-Cl (10 mM) were present continuously in the bath solution to block I_{Ca} and potassium currents (I_{K1}, I_{to} and I_K), respectively.

Solutions and drugs

The modified Tyrode solution for cell isolation contained (mM): NaCl 126, KCl 5.4, $CaCl_2$ 2.0, $MgCl_2$ 1.0, NaH_2PO_4 0.33, glucose 10, 4-(2-hydroxyethyl)-1-piperazineethanesulfonic acid (HEPES) 10; pH adjusted to 7.4 with NaOH. The high-potassium cell storage solution contained (mM): KCl 20, KH_2PO_4 10, glucose 10, L-glutamic acid 70, ß-hydroxibutyric acid 10, taurine 10, EGTA 10 and Albumin 1%, pH 7.4 (KOH). Osmolarity was adjusted to 290-300 mOsm/kg H_2O by adding mannitol.

The standard pipette (external) solution for cell-attached patch-clamp recording contained (mmol/L): N'-methyl-D-glucamine chloride (NMDGCl) 108, HEPES 5, Glucose 5.5 (total pipette Cl^- concentration ($[Cl^-]_p$) = 108 mmol/L). The pH was adjusted to 7.40 with NMDGOH and osmolarity was adjusted to 285-295 mOsm/kgH_2O by adding mannitol. To evaluate the ionic selectivity of the channels studied, the concentration of the ion of interest was reduced by equimolar replacement of NMDG with Tris or of Cl^- with aspartate in the pipette solution. When high $[Cl]_p$ was needed, the concentration of NMDGCl in the pipette solution was increased. The pipette (internal) solution for whole-cell patch-clamp recordings contained (mmol/L): NMDG aspartate 100, NMDGCl 24, Mg-ATP 5, HEPES 10 (total $[Cl]_i$ = 24 mmol/L).

The standard hypotonic bath (external) solutions for both cell-attached and whole-cell recordings contained (mmol/L): NaCl 85, KCl 5.0, $BaCl_2$ 2, TEA-Cl 10, $CdCl_2$ 0.2, 4-aminopyridine 5, $MgCl_2$ 0.8, $CaCl_2$ 1.0, NaH_2PO_4 0.33, HEPES 10, glucose 5.5; pH adjusted to 7.4 with NaOH (220 mOsm/kgH_2O); total $[Cl]_o$ = 108 mmol/L. When experiments were performed with decreased $[Cl^-]$, aspartate was used to replace Cl^- at equimolar concentrations. The standard isotonic bath solution was the same as the standard hypotonic solution except that the osmolarity was adjusted to 290-310 (302 ± 4) mOsm/kgH_2O by adding mannitol. Solution osmolarities were measured by freezing point depression (Osmomette A, Precision Systems Inc.).

Data Analysis

Single-channel current amplitudes were measured relative to the 0 current level. For the analysis of the open probability (P_o) and open- and closed-state kinetics, patches were held at the desired potential for at least 150 seconds (>100,000 transitions). P_o was obtained for patches with only one open peak and one closed peak in the amplitude histogram from the ratio of the area under the curve representing open events (fitted with a Gaussian equation by a curve-fitting program in Pstat) divided by the sum of the areas under the open- and closed-event histograms. The kinetics of open and closed events were analyzed for patches containing only one active channel (determined by all-points amplitude histogram) with a half-amplitude algorithm incorporated in Fetchan, and events were reviewed manually. Open and closed dwell-time analyses were performed using the unconditional distributions of these interval durations.[19] The interval durations were logarithmically binned and the number of events was transformed as a square-root of the ordinate in order to keep the errors approximately constant throughout the plot of the dwell-time histogram.[20] Log-binned open or closed dwell-time data were fitted using the maximum likelihood estimate (MLE) method or Marquardt least square method (program incorporated in Pstat) by 1, 2, 3 and 4 exponential terms (models 1-4). To test whether or not different models produce a statistically better fit, for each dwell-time distribution histogram we compared the sum of squared errors for each model (the F value) and the ratio of the natural logarithm of the MLE (log likelihood ratio, LLR) for different models. The "F" statistic was evaluated at α-levels of 90 and 95%. A LLR > 2 was taken to indicate statistical significance.

All results are expressed as mean ± S.E. Statistical comparisons were performed either by analysis of variance (ANOVA) with Scheffé contrasts for group data, or by Student's t test when only two groups were compared. The Chi square test was applied to compare the prevalence of active channels under isotonic versus hypotonic conditions. A two-tailed probability of <5% was taken to indicate statistical significance.

Results

Properties of unitary chloride channel current in cell-attached patches

Under isotonic conditions (290 to 310 mOsm/kg H_2O), most patches failed to show single-channel activity. However, in a minority of patches (21/367, 5.7%), single-channel activity of the type shown in Fig 1A was clearly visible. When present, channel activity was evident at either hyperpolarizing or depolarizing voltages immediately after the formation of cell-attached configuration and generally remained stable for >15 minutes. Single-channel currents showed strong outward rectification and reversed at 19 ± 1 mV (n=6) positive to RP at $[Cl^-]_p$ of 108 mmol/L. The average slope conductance of the channel was 49 ± 1 pS (n=6) over the range RP+20 to RP+140 mV (chord conductance = 28 ± 1 pS at reversal potential) when $[Cl^-]_p$ was 108 mmol/L (Figure 1B).

Three examples of single-channel currents elicited from a typical patch by 2-second hyperpolarizing (Fig 1C) and depolarizing (Fig 1D) pulses from the RP are shown at the bottom of Fig 1. The voltage steps shown are respectively about 60 mV negative (Fig 1C) and 60 mV positive (Fig 1D) to the current reversal potential at 108 mmol/L $[Cl^-]_p$, which averaged RP+19 mV. Ensemble-average currents from 60 pulses are shown at the bottom of each panel and indicate that the current carried by this channel is time-independent and outwardly rectifying.

To evaluate the ionic selectivity of the channel, we altered pipette [Cl^-] by equimolar substitution with aspartate, producing the type of recordings shown in Fig 2A-b, which had smaller outward currents and a more positive reversal potential than recordings at a physiologic [Cl^-]$_o$ of 108 mmol/L (Fig 2A-a). Increasing the concentration of NMDGCl (to increase [Cl^-]$_p$) had opposite effects, resulting in the type of recordings shown in Fig 2A-c. Mean (±SE, where error bars are not visible they fall within symbol for mean) I-V relations for single-channel current under each condition are shown in Fig 2B. A decrease in [Cl^-]$_p$ to 22 mmol/L decreased single-channel conductance in the outward direction (to 23±1 pS, over the range from RP+60 mV to RP+140 mV, chord conductance 20±2 pS, n=4) and shifted the reversal potential to more positive values (53±3 mV). Opposite effects were seen with an increase in [Cl^-]$_p$ to 208 mmol/L, which increased conductance in the outward direction (to 62±1 pS, over the range from RP+10 mV to RP+140 mV, chord conductance 33±1 pS, n=3) and shifted the reversal potential to more negative voltages (RP-6±1 mV). When mean reversal potentials (E_{rev}, expressed as voltages relative to RP) were plotted as a function of log ([Cl^-]$_p$), the points fell on a line (r=0.987) with a slope of -57.7 mV per decade (Fig 2C), indicating substantial Cl^- selectivity of the channel.

NMDG was the only cation in the pipette solution. Since cation channels are relatively impermeable to NMDG, inward currents across single channels studied with NMDGCl in the pipette are very unlikely to be due to cation entry into the cell. To address this possibility further. we eliminated NMDG from the pipette solution by substituting the even larger cation Tris for NMDG in the pipette. Fig 2D shows mean current-voltage relations obtained with either 108 mmol/L or 0 mmol/L NMDG in the pipette. The mean reversal potential of single-channel currents obtained with Tris substitution was RP+17±2 mV (n=4), not significantly different from the value obtained with 108 mmol/L NMDG in the pipette (RP+19±1 mV). Single-channel conductance over the range between RP+20 mV and RP+140 mV averaged 51±2 pS (n=4) with 0 mmol/L NMDG in the pipette, not significantly different from the value of 49±1 pS obtained with the use of 108 mmol/L NMDG.

Channel activity at all voltages showed long-duration openings with either brief or relatively longer-lasting closings, as shown in Figs 1-3. Amplitude histograms of unitary single-channel currents were consistent with the presence of only one channel with a single, dominant closed and open level for each of the seven patches studied to evaluate open-channel probability (Po). The open-channel probability averaged 0.68±0.02 at RP+120 mV (n=6), 0.66±0.04 at RP-40 mV (n=7), 0.63±0.03 at RP+60 mV (n=6), 0.62±0.03 at RP+80 mV (n=5), 0.65±0.03 at RP+100 mV (n=6), and 0.70±0.03 at RP+140 mV (n=5) (*P*=NS for voltage-dependence. ANOVA).

Channel kinetics were studied in seven patches in which single-channel activity was observed for at least 150 seconds. In each patch, single open and closed levels were determined from the all-points amplitude histogram. Results from a representative patch are shown in Fig 3. During hyperpolarization (to 40 mV negative to RP), channel opening elicited an inward current. The open and closed analysis using the unconditional interval distribution and maximum likelihood fitting indicated that the channel must have a minimum of three open kinetic states ($p < 0.01$ for model 3 vs model 2, $p > 0.05$ for model 4 vs model 3) with time constants of $\tau_1 = 2.1$ ms, $\tau_2 = 15.9$ ms, $\tau_3 = 120.8$ ms, and a minimum of four closed states ($p < 0.05$ for model 4 vs model 3, $p < 0.01$ for model 4 vs model 2, $p < 0.01$ for model 3 vs model 2) with time constants of $\tau_1 = 1.0$ ms, $\tau_2 = 6.1$ ms, $\tau_3 = 31.4$ ms, $\tau_4 = 246.7$ ms. Mean kinetic data from 7 patches under isotonic conditions are shown in Table 1.

Effects of Hypotonic Cell Swelling on Single-Channel Activity

In the first series of experiments, patches lacking single-channel activity in the presence of isotonic superfusate were monitored during the induction of cell swelling. Superfusion with hypotonic bath solution (210 to 220 mOsm/kg H_2O) for >15 minutes increased cell volume from 7895±524 μm^3 (length, 102±3 μm; width, 9.8±0.3 μm) to 14778±1080 μm^3 (length, 102±3 μm; width, 13.3±0.4 μm, n=54), representing an 88±6% increase in volume compared to control conditions ($P < .001$). Fig 4 shows an example of a patch without single-channel activity under isotonic conditions, that developed currents typical of ORCC in the presence of hypotonic swelling. Of 220 patches lacking channel activity under isotonic conditions with $[Cl^-]_p$ of 108 mmol/L that were followed for more than 15 minutes after the onset of hypotonic superfusion, 36 (16.4%) showed the type of response illustrated in Fig 4. The onset of channel opening was observed an average of 15±2 minutes after changing to hypotonic superfusate.

Another set of patches (n=14) that demonstrated channel activity under isotonic conditions was observed during the induction of hypotonic swelling. In some of these (n=3) cell swelling revealed the presence of a second channel in the patch, with unitary current properties resembling those of the channel under basal conditions. Fig 5 shows a representative recording of single-channel currents from these patches. Under isotonic conditions, the amplitude distribution histogram (right panel of Fig 5A) showed only a single, dominant open and closed level and was best fitted with a two-order Gaussian equation (r = 0.94, mean current amplitude = -0.43 pA, P_o = 0.65). Exposure of the same cell to hypotonic superfusate for 10 min caused the appearance of a second active channel in the same patch. The amplitude histogram (right panel of Fig 5B) showed two open levels and one closed level and was best fit with a 3-order Gaussian equation (r = 0.96). The mean current amplitude at each open level was the same (-0.43 pA) and the amplitude distributions were consistent with two channels with open probability about 0.6. These data suggest that the second channel activated by cell-swelling is identical to the first channel in the same patch recorded under isotonic conditions.

Finally, in one channel studied in the presence of 22 mmol/L $[Cl^-]_p$, the induction of hypotonic swelling caused the reappearance of the same channel activity that had disappeared spontaneously after a period of activity under isotonic conditions.

Comparison of Properties of ORCC Under Basal Conditions and in the Presence of Hypotonic Cell Swelling

Fig 6A shows mean (±SE, where error bars are not visible they fall within the symbol for mean) I-V relations of single-channel activity recorded in the presence of isotonic and hypotonic superfusate with $[Cl^-]_p$ of 108 mmol/L. The data superimpose, indicating identical conductance properties. The reversal potential of single-channel current in the presence of hypotonic superfusate was RP+18±1 mV. not significantly different from that of ORCC under basal isotonic conditions (RP+19±1 mV, *P*=NS). The chord conductance of single-channel outward current carried by channels recorded in the presence of cell swelling was 27±1 pS (n=14), similar to that of channels studied under basal conditions (28±1 pS, *P*=NS). Fig 6B shows the effects of reduced $[Cl^-]_p$ (22 mmol/L) on single-channel activity in the presence of hypotonic swelling, and compares unitary currents at this $[Cl^-]_p$ under hypotonic and isotonic conditions. At lower $[Cl^-]_p$, channels under hypotonic conditions showed a reduced conductance (chord conductance averaged 20±1 pS) and more positive reversal potential (RP+54±3 mV, n=5) compared to results at 108 mmol/L $[Cl^-]_p$. When values of the reversal potential of single-channel activity under hypotonic conditions (open squares in Fig 6C) at various $[Cl^-]_p$ are plotted along with those of channels observed under isotonic conditions (open circles in Fig 6C), they virtually superimpose on each other. The reversal potentials for single-channel currents recorded in the presence of hypotonic swelling fall close to the regression line obtained under isotonic conditions (dashed line), indicating high Cl^- selectivity (57.7 mV/decade, r = 0.99). Furthermore, a similar selectivity for Cl^- was observed for macroscopic $I_{Cl.b}$ (56.3 mV/decade, r = 0.99, n = 5) and $I_{Cl.swell}$ (56.9 mV/decade, r = 0.999, n = 5; data not shown).

The prevalence of channel activity was substantially greater in the presence of hypotonic swelling. Overall, single-channel activity was seen in 54/336 (16.1%) patches studied under hypotonic conditions with $[Cl^-]_p$ of 108 or 22 mmol/L. Of these, 41 patches had failed to show activity under isotonic conditions, and became active during exposure of the cell to hypotonic conditions. The remaining 13 patches showing channel activity were obtained by initially forming a patch under hypotonic conditions, and comprised 18.3% of the 71 patches studied in this fashion. The overall prevalence of channel activity under hypotonic conditions was thus much greater than under isotonic conditions (Fig 6D). On the other hand, the open probability of channels under hypotonic conditions was similar to that of channels recorded under isotonic conditions (Table 1).

Fig 7 illustrates the kinetic properties of channels recorded under hypotonic conditions. As was the case under isotonic conditions, the open-time distributions were best fit with a 3-exponential relation and the closed-time distributions were best fit with a 4-exponential relation. The mean time constants for both open and closed dwell times under hypotonic conditions (from 10 different patches) were of the same order as those observed under isotonic conditions ($P > 0.05$ for each time constant under hypotonic conditions compared to the corresponding time constant under isotonic conditions, Table 1). These data suggest that cell swelling activates the same set of Cl^- channels (ORCC) as recorded under isotonic conditions, and increases macroscopic current by recruiting additional channels without altering the properties of those already activated.

Inhibition of ORCC, $I_{Cl.b}$, and $I_{Cl.swell}$ by tamoxifen

Recent studies have shown that tamoxifen (an anti-estrogen) is a selective and potent inhibitor of $I_{Cl.swell}$ in both cardiac myocytes[7] and non-cardiac cells.[21] Vandenberg et al[7] reported that tamoxifen inhibits whole-cell $I_{Cl.swell}$ in guinea pig atrial and ventricular myocytes with a slow onset of action, suggesting that this agent may act from the intracellular surface of the channel.

Therefore, we studied the effects of tamoxifen on ORCC channels in cell-attached patches and on macroscopic $I_{Cl.b}$ and $I_{Cl.swell}$.

As shown in Fig 8, tamoxifen (10 μmol/L, 10 min) almost completely inhibited ORCC activated by cell swelling. The same effect was observed in all 4 cell-attached patches studied. Tamoxifen also inhibited $I_{Cl.b}$ and $I_{Cl.swell}$ (Fig. 9). Fig 9A shows the effect of tamoxifen on $I_{Cl.b}$. While the current showed no change over 20 minutes of recording, prior to drug infusion, tamoxifen (10 μmol/L) caused time-dependent inhibition (44, 71 and 88% reduction at +40 mV and 29%, 52%, and 82% at -100 mV after 2, 4, and 7 min respectively). The currents recorded after exposure to tamoxifen for 7 min are shown in panel c of Fig 9A. The tamoxifen-sensitive current (panel d of Fig 9A) reversed at -41.5 mV (estimated Cl^- equilibrium potential -39.3 mV). Fig 9B shows the effect of tamoxifen (10 μmol/L on swelling-induced currents. Tamoxifen strongly inhibited the current (panel c) within 10 min. Panel d shows average I-V curves from 4 cells: tamoxifen reduced total current by 90 ± 2% and 76 ± 4% at +40 mV and -100 mV respectively. The pharmacological data shown in Figs 8 and 9 support the role of ORCC in underlying both $I_{Cl.b}$ and $I_{Cl.swell}$.

Relation between single-channel and macroscopic currents

As mentioned above, the Cl^--dependence of ORCC was indistinguishable from those of $I_{Cl.b}$ and $I_{Cl.swell}$, as was the response to tamoxifen. To evaluate further the relation between macroscopic currents and ORCC, we compared the estimated macroscopic current expected ont the basis of the properties of ORCC with directly-measured whole-cell currents. The number of active channels per cell under isotonic conditions was estimated on the basis of the formula (CSA/PA)●(%prev), where CSA = cell surface area estimated from cell dimensions assuming right cylindrical geometry (πLW), PA = patch area estimated with an assumed circular electrode tip and a microscopically-measured diameter of 2 μm, and %prev is the proportion of patches showing channel activity. This provides an estimate of 67 active channels per cell. Mean unitary current at RP+120 mV, which corresponds to a transmembrane potential of +56 mV based on the mean measured resting potential, was 4.62 pA. Multiplying this value by the measured open probability of 0.68 and by the estimated number of channels per cell provides an expected macroscopic current of 210 pA at +56 mV. This compares with directly-measured mean values of macroscopic $I_{Cl.b}$ of 196 and 237 pA under isotonic conditions at +50 and +60 mV. The corresponding estimate under hypotonic conditions was obtained by multiplying the number of active channels per cell under isotonic conditions by ACT_{hypo}/ACT_{iso}, where ACT_{hypo} and ACT_{iso} are the mean prevalence of active channels/patch under hypotonic and isotonic conditions respectively. This provides an estimate of 189 channels/cell and a predicted macroscopic current at +56 mV (RP+120 mV) of 593 pA, similar to the measured mean values of total macroscopic Cl^- current of 568 and 678 pA at +50 and +60 mV respectively under hypotonic conditions. These results indicate that the ORCC recorded in cell-attached patches can account for all of the measured $I_{Cl.b}$ and $I_{Cl.swell}$ measured by whole-cell voltage clamp. In combination with the similar kinetics and conductance of ORCC under isotonic and hypotonic conditions, they suggest that cell swelling elicits $I_{Clswell}$ by increasing the number of active ORCC without altering the intrinsic behavior of active channels.

Discussion

In the present study, we have demonstrated that single outwardly-rectifying Cl^- channels (ORCC) can be recorded in the cell-attached mode in isolated rabbit atrial myocytes under isotonic conditions. These channels carry inward current in the absence of permeable cations in the pipette (extracellular) solution, and changes in pipette Cl^- concentration cause shifts in channel conductance and reversal potential consistent with a Cl^--selective channel. Several lines of evidence suggest that hypotonic cell swelling increases Cl^- conductance by activating the same channel. These include: (a) similar conductance, open probability, and kinetic properties of cell-swelling-induced single-channel currents to ORCC under hypotonic conditions; (b) a higher prevalence of active ORCC in the presence of hypotonic superfusate-induced swelling and the swelling-induced appearance of active channels in patches that lack such channels under basal conditions; and (c) a similar response to tamoxifen of ORCC, $I_{Cl.b}$, and $I_{Cl.swell}$. The correspondance between the pharmacologic response of ORCC, $I_{Cl.b}$ and $I_{Cl.swell}$, in their Cl^--dependence, and directly-measured $I_{Cl.b}$ and $I_{Cl.swell}$ suggest that the latter are carried by ORCC in rabbit atrial myocytes.

Comparison With Previous Studies of Unitary Cardiac Cl^- Channels

The first cardiac Cl^- current to have a unitary channel mechanism identified was the cyclic AMP-dependent Cl^- current ($I_{Cl.cAMP}$),[22] whose biophysical properties resemble those of the cystic fibrosis transmembrane conductance regulator (CFTR).[23-25] The single-channel mechanisms of other cardiac Cl^- currents remain largely unknown. We previously reported the presence of

ORCC, with properties similar to sarcolemmal Cl^- channels reported by Coronado and Latorre,[26] in excised patches from rabbit atrial myocytes.[15] In the present manuscript, we report the observation of ORCC during cell-attached patch recording on intact rabbit atrial myocytes, and, for the first time, provide strong direct evidence for a role of ORCC in underlying cell-swelling-induced cardiac Cl^- current $I_{Cl.swell}$.

Very recent studies from Collier et al investigated the possible single-channel mechanisms for $I_{Cl.PKC}$[27] and $I_{Cl.Ca}$[28]. In guinea pig ventricular cells, PKC-activated unitary Cl^- channels have properties similar to those of cardiac CFTR Cl^- channels.[27] In canine ventricular myocytes, Ca^{2+} applied to the cytosolic surface of inside-out membrane patches activated small conductance (1.0 - 1.3 pS) Cl^- channels.[28] The properties of cardiac ORCC, including their conductance, kinetics, rectification, and Ca^{2+}-sensitivity, are strikingly different from those of unitary cardiac Cl^- channels of $I_{Cl.cAMP}$,[22] $I_{Cl.PKC}$,[27] and $I_{Cl.Ca}$.[28]

Relation of Cardiac ORCC to Non-Cardiac ORCC

ORCC are found in a wide variety of mammalian tissues,[29-32] and may play a role in volume regulation, signal transduction, and transepithelial transport.[33-36] The properties of cardiac ORCC are in general quite similar to those of ORCC in non-cardiac cells in terms of conductance, outward rectification under symmetric Cl^- gradients, and pharmacologic properties. While ORCC have been observed often in cell-free patches from non-cardiac tissues, they have been more difficult to record in cell-attached mode. Moreover, the macroscopic equivalent of ORCC in these tissues is also still uncertain, leading to uncertainty about their physiologic function.[36,37]

In studies of Cl^- conductances in duct cells cultured from human fetal pancreas, Gray et al[37] observed spontaneous activity of ORCC in only one cell-attached patch. In this patch, they observed two active channels with conductances for inward and outward currents between 0 and ±60 mV of 19 and 59 pS, respectively. The open probability of these channels did not appear to be voltage dependent. These properties are strikingly similar to those of cardiac ORCC. Solc and Wine[35] recorded single-channel activity during cell swelling in epithelial cells, and observed an outwardly-rectifying channel with properties somewhat different from ORCC, including a slightly greater conductance, greater stability of the open state, voltage-dependent inactivation, and a strong tendency for time-dependent rundown. They concluded that the two types of channel may be distinct proteins or different functional states of the same channel. In the present study, the properties of ORCC recorded in the cell-attached mode under isotonic conditions and during cell swelling were identical and were similar to those of cardiac ORCC in excised, inside-out patches[15] in terms of conductance, rectification, and voltage-dependence.

Limitations

The true transpatch potential in cell-attached patches is the difference between the potential applied at the pipette tip and the transmembrane resting potential. Since the latter cannot be known unless the membrane is ruptured, current-voltage relationships have to be expressed relative to the resting potential. Inexact knowledge of transpatch potentials is not a limitation to the studies of reversal potential (E_{rev}) dependency on ionic gradients, since errors in the resting potential estimate will result in a constant change in E_{rev}, leaving the $E_{rev} - \log([Cl^-]_o$ slope unaffected.

Our estimate of macroscopic current carried by ORCC must be understood to be very approximate. We assumed a circular pipette cross-section, discoid patch shape and cylindrical cell shape, all of which may not precisely be the case. Furthermore, the effective cell surface area may be significantly greater than obtained from calculations based on right cylindrical geometry because of membrane infolding.[38]

We cannot exclude the possibility that a long-lived closed state was missed in our kinetic analysis, and underlies the smaller percentage of patches with active channels observed under isotonic conditions. Such a state could account for the presence of channels whose activity is not observed under isotonic conditions but is revealed upon exposure to hypotonic solutions, a possibility that is difficult to exclude experimentally.

Potential Significance of our Findings

Despite the broad distribution of cell-swelling-induced Cl^- currents that have been described in both cardiac[4-13] and non-cardiac tissues,[39-43] the underlying single-channel mechanisms for these currents are still unclear. The present study provides strong and direct evidence that ORCC underlie volume-regulated Cl^- currents in rabbit atrial cells. Further work is necessary in order to establish the role of ORCC in volume-sensitive Cl^- currents of other cardiac cell types and other species.

Our previous studies pointed towards a common ionic mechanism for $I_{Cl.swell}$ and $I_{Cl.b}$ in rabbit atrial myocytes.[6] Both currents are outwardly rectifying, volume-sensitive, inhibited by disulphonic stilbenes, and suppressed by α_1-adrenergic stimulation through a protein kinase C-mediated mechanism.[6] The present work further supports the notion of a common mechanism for these currents by providing direct evidence that they are mediated by the same unitary channel mechanism. Swelling-induced Cl^- currents are conventionally considered to be activated by cell swelling and to be inactive under normal physiologic conditions. It is possible, however, that such channels are active over a range of volume states that includes basal conditions, and therefore may play a role even in the absence of pathologic swelling. On the other hand, the cell isolation procedure and experimental manipulations may have allowed ORCC to be recorded under isotonic conditions, despite a lack of activity under physiologic conditions in vivo.

Stationary noise analysis studies of non-cardiac swelling-induced Cl^- currents have suggested a channel conductance in the range of 1 to 2 pS.[39-42] Recently, Jackson and Strange[43] showed that stationary noise analysis suggested a single-channel conductance of volume-sensitive currents of about 1 pS at 0 mV. They then applied non-stationary noise analysis, which does not assume a constant number of functional channels, and obtained a single-channel conductance of 50.6 ± 1 pS at +120 mV, in the range that we obtained for cardiac ORCC at positive voltages. They suggested that activation of volume-sensitive anion channels may involve an abrupt switching of channels from an OFF state, where channel open probability is zero, to an ON state, where open probability is substantial. Our results provide direct evidence supporting the theoretical basis of Jackson and Strange's analysis, in that hypotonic swelling appeared to increase current by increasing the number of channels in an active mode, without altering the open probability of active channels. It has been reported that there may be a cytoplasmic inhibitor of ORCC, which restricts activity in cell-attached mode.[44,45] Our results are consistent with these reports in that, under isotonic conditions, the prevalence of active channels and the open probability of ORCC in cell-attached patches are significantly lower than those of ORCC in inside-out patches.[15] Our findings are also compatible with preliminary observations reported by Zhang et al in 1992, who observed outwardly rectifying Cl^- channels with a chord conductance of 31 pS during hypotonic swelling in cultured chick heart cells.[12]

Cardiac ORCC share many similarities with ORCC in other tissues, including basic biophysical (e.g. the characteristic outward-rectifying I-V relation under symmetrical Cl^- concentrations) and pharmacological properties (e.g. inhibition by stilbene derivatives). Like cardiac ORCC,[6] ORCC from human airway epithelial cells are also inhibited by PKC,[46] and PTX-sensitive G-proteins ($G_{\alpha i\text{-}2}$).[47] A recently-cloned member of the voltage-gated Cl^- channel CLC family, CLC-3, is also inhibited by PKC.[48] CLC-3 is the most distantly related member of the CLC family (the 760 amino acid protein encoded by CLC-3 is only 24% homologous to previously reported CLC channels, but has a similar hydropathy profile) and may represent a new branch of this gene family. Unlike other members of the CLC family but similar to cardiac $I_{Cl.b}$ and $I_{Cl.swell}$, the current carried by CLC-3 shows strong outward rectification under symmetric Cl^- and is inhibited by PKC and stilbene derivatives.[6,15,48] The single-channel properties of CLC-3 are also similar to those of cardiac ORCC, including (a) strong outward rectification under symmetric Cl^- conditions, (b) 40 pS conductance (when intracellular Ca^{2+} is

200 nmol/L), (c) similar open- and closed-state kinetics, and (d) sensitivity to DIDS. Although CLC-3 appears not to be expressed in the heart,[48] two new members of the CLC family, CLCN4[50] and CLCN5,[51] which are strikingly similar to CLC-3, are expressed in the heart,[50,51] and a deficiency in CLCN4 has been associated with cardiac abnormalities.[50] Our finding that ORCC underlies cardiac volume-sensitive Cl^- currents may help in the delineation of the cellular mechanisms by which these genes contribute to cardiac function.

Conclusions

We have obtained for the first time direct evidence that ORCC underlie both basal and swelling-induced Cl^- currents in rabbit atrium, and may therefore play a potentially important physiological role in cardiac electrophysiology. These findings provide new insights into subcellular mechanisms controlling Cl^- movement across cardiac cell membranes, and open up new avenues for the exploration of their molecular control.

Acknowledgements

This study was supported by the Medical Research Council of Canada, the Quebec Heart Foundation and the Fonds de la recherche en santé du Québec, and NIH grant HL 52803 (J.R.H.). Dr. Duan was supported by a graduate studentship and subsequently by a fellowship from the Medical Research Council of Canada. We thank Dr. Lingyu Ye for excellent technical support, Dr. J.L. Kenyon for suggestions regarding single-channel analysis, and Luce Bégin for secretarial assistance.

lb\singvol.SN

References

1. Hoffmann EK, Simonsen LO. Membrane mechanisms in volume and pH regulation in vertebrate cells. *Physiol Rev.* 1989;69:315-382.
2. Franciolini F, Petris A. Chloride channels of biological membranes. *Biochim Biophys Acta.* 1990;1031:247-259.
3. Hume JR, Horowitz B. A plethora of cardiac chloride conductances: molecular diversity or a related gene family. *J Cardiovasc Electrophysiol.* 1995;6:325-331.
4. Sorota S. Swelling-induced chloride-sensitive current in canine atrial cells revealed by whole-cell patch-clamp method. *Circ Res.* 1992;70:679-687.
5. Tseng G-N. Cell swelling increases membrane conductance of canine cardiac cells: evidence for a volume-sensitive Cl channel. *Am J Physiol.* 1992;262:C1056-C1068.
6. Duan D, Fermini B, Nattel S. α-adrenergic control of volume-regulated Cl^- currents in rabbit atrial myocytes. *Circ Res.* 1995;77:379-393.
7. Vandenberg JI, Yoshida A, Kirk K, Powell T. Swelling-activated and isoprenaline-activated chloride currents in guinea pig cardiac myocytes have distinct electrophysiology and pharmacology. *J Gen Physiol.* 1994;104:997-1017.
8. Oz MC, Sorota S. Forskolin stimulates swelling-induced chloride current, not cardiac cystic fibrosis transmembrane-conductance regulator current, in human cardiac myocytes. *Circ Res.* 1995;76:1063-1070.
9. Sakai R, Hagiwara N, Kasanuki H, Hosoda S. Chloride conductance in human atrial cells. *J Mol Cell Cardiol.* 1995;27:2403-2408.

10. Li G-R, Feng J, Wang Z, Nattel S. Transmembrane chloride currents in human atrial myocytes. *Am J Physiol.* 1996;270:C500-C507.
11. Zhang J, Rasmusson RL, Hall SK, Lieberman M. A chloride current associated with swelling of cultured chick heart cells. *J Physiol (Lond).* 1993;472:801-820.
12. Zhang J-P, Rasmusson RL, Hall SK, Lieberman M. Hypo-osmotically activated Cl^- conductance in cultured chick heart cells. *J Gen Physiol.* 1992;100:31a. Abstract.
13. Coulombe A, Coraboeuf E. Large-conductance chloride channels of new-born rat cardiac myocytes are activated by hypotonic media. *Pflügers Arch.* 1992;422:143-150.
14. Duan D, Fermini B, Nattel S. Sustained outward current observed after I_{to1} inactivation in rabbit atrial myocytes is a novel Cl^- current. *Am J Physiol.* 1992;263:H1967-H1971.
15. Duan D, Nattel S. Properties of single outwardly rectifying Cl^- channels in heart. *Circ Res.* 1994;75:789-795.
16. Duan D, Nattel S. Single outwardly-rectifying chloride channels in cell-attached patches from rabbit atrial myocytes. *Biophys J.* 1995;68:A110. Abstract.
17. Duan D, Nattel S. A possible single-channel mechanism for volume-sensitive Cl^- currents in rabbit atrial myocytes. *Circulation.* 1995;92:I-638. Abstract.
18. Hamill OP, Marty AJ, Neher E, Sakmann B and Sigworth FT. Improved patch-clamp techniques for high resolution current recording from cells and cell-free membrane patches. *Pflügers Arch.* 1992;422:143-150.
19. Blatz AL, Magleby KL. Quantitative description of three models of activity of fast chloride channels from rat skeletal muscle. *J Physiol (Lond).* 1986;378:141-174

20. Sigworth FJ, Sine SM. Data transformations for improved display and fitting of single-channel dwell time histograms. *Biophys J.* 1987;52:1047-1054.

21. Valverde MA, Mintenig GM, Sepulveda FV. Different effects of tamoxifen and I$^-$ on three distinguishable chloride currents activated in T84 intestinal cells. *Pflügers Arch.* 1993;425:552-554.

22. Ehara T, Ishihara K. Anion channels activated by adrenaline in cardiac myocytes. *Nature.* 1990;347:284-286.

23. Nagel G, Hwang T-C, Nastiuk KL, Nairn AC, Gadsby DC. The protein kinase A-regulated cardiac Cl$^-$ channel resembles the cystic fibrosis transmembrane conductance regulator. *Nature.* 1992;360:81-84.

24. Gadsby DC, Nagel G, Hwang T-C. The CFTR chloride channel of mammalian heart. *Annu Rev Physiol.* 1995;57:387-416.

25. Hart P, Warth J, LEvesque PC, Collier ML, Geary Y, Horowitz B, Hume JR. Cystic fibrosis gene encodes a cAMP-dependent chloride channel in heart. *Proc Nat Acad Sci USA*. 1996; 93:6343-6348.

26. Coronado R, Latorre R. Detection of K$^+$ and Cl$^-$ channels from calf cardiac sarcolemma in planar lipid bilayer membranes. *Nature.* 1982;298:849-852.

27. Collier ML, Hume JR. Unitary Cl$^-$ channels activated by protein kinase C in guinea-pig ventricular myocytes. *Circ Res.* 1995;76:317-324.

28. Collier ML, Levesque PC, Kenyon JL, Hume JR. Unitary Cl$^-$ channels activated by cytoplasmic Ca^{2+} in canine ventricular myocytes. *Circ Res.* 1996; in press

29. Frizzell RA. Cystic fibrosis: a disease of ion channels? *Trends Neurosci.* 1987;10:190-193.

30. Barres BA, Chun LL, Corey DP. Ion channel expression by white matter. *Glia.* 1988;21:10-30.

31. Bear CE. Phosphorylation-activated chloride channels in human skin fibroblasts. *FEBS Lett.* 1988;237:145-149.

32. Garber SS. Outwardly rectifying chloride channels in lymphocytes. *J Membr Biol.* 1992;127:49-56.

33. Welsh MJ. Electrolyte transport by airway epithelia. *Physiol Rev.* 1987;67:1143-1184.

34. Lukacs GL, Moczydlowski E. A chloride channel from lobster walking leg nerves: characterization of single-channel properties in planar bilayers. *J Gen Physiol.* 1990;96:707-733.

35. Solc CK, Wine JJ. Swelling-induced and depolarization-induced Cl^- channels in normal and cystic fibrosis epithelial cells. *Am J Physiol.* 1991;261:C658-C674.

36. Guggino WB. Outwardly rectifying chloride channels and CF: a divorce and remarriage. *J Bioenerg Biomembr.* 1993;25:27-35.

37. Gray MA, Harris A, Coleman L, Greenwell JR and Argent BE. Two types of chloride channel on duct cells cultured from human fetal pancreas. *Am J Physiol.* 1989;257:C240-C251.

38. Masson-Pévet M, Gros D, Besselsen E. The caveolae in rabbit sinus node and atrium. *Cell Tissue Res.* 1980;208:183-196.

39. Doroshenko P, Neher E. Volume-sensitive chloride conductance in bovine chromaffin cell membrane. *J Physiol.* 1992;449:197-218.

40. Stoddard JS, Steinbach JH, Simchowitz L. Whole cell Cl^- currents in human neutrophils induced by cell swelling. *Am J Physiol.* 1993;265:C156-C165.

41. Lewis RS, Ross PE, Cahalan MD. Chloride channels activated by osmotic stress in T lymphocytes. *J Gen Physiol.* 1993;101:801-826.

42. Nilius B, Oike M, Zahradnik I, Droogmans G. Activation of a Cl^- current by hypotonic volume increase in human endothelial cells. *J Gen Physiol.* 1994;103:787-805.

43. Jackson PS, Strange K. Current activation occurs by abrupt switching of closed channels to an open state. *J Gen Physiol.* 1995;105:643-660.

44. Krick W, Disser J, Hazama A, Burckhardt G, Frömter E. Evidence for a cytosolic inhibitor of epithelial chloride channels. *Pflügers Arch.* 1991;418:491-499.

45. Kunzelmann K, Tilmann M, Hansen ChP, Greger R. Inhibition of epithelial chloride channels by cytosol. *Pflügers Arch.* 1991;418:479-490.

46. Li M, McCann JD, Anderson MP, Clancy JP, Liedtke CM, Nairn AC, Greengard P and Welsh MJ. Regulation of chloride channels by protein kinase C in normal and cystic fibrosis airway cells. *Science.* 1989;244:1353-1356.

47. Schwiebert EM, Gruenert DC, Guggino WB, Stanton BA. G-protein $G_{\alpha 1-2}$ inhibits outwardly rectifying chloride channels in human airway epithelial cells. *Am J Physiol* 1995; 269:C451-C456.

48. Kawasaki M, Uchida S, Monkawa T, Miyawaki A, Mikoshiba K, Marumo F, Sasaki S. Cloning and expression of a protein kinase C-regulated chloride channel abundantly expressed in rat brain neuronal cells. *Neuron*. 1994; 12:597-604.

49. Kawasaki M, Suzuki M, Uchida S, Sasaki S, Marumo F . Stable and functional expression of the CLC-3 chloride channel in somatic cell lines. *Neuron*. 1995; 14:1285-1291.

50. Slegtenhorst MA, Bassi MT, Borsani G, Wapenaar MC, Ferrero GB, Concillis L, Rugarli EI, Grillo A, Franco B, Zoghbi HY, Ballabio A. A gene from the Xp22.3 region shares homology with voltage-gated chloride channels. *Human Mol Genet* .1994; 3:547-552.

51. Lloyd SE, Pearce SHS, Fisher SE, Steinmeyer K, Schwappach B, Schienman SJ, Harding B, Bolino A, Devoto M, Goodyer P, Rigden SPA, Wrong O, Jentsch TJ, Cralg IW, Thakker RV. A common molecular basis for three inherited kidney stone diseases. *Nature*. 1996;379:445- 449.

Figure Legends

Figure 1: Cell-attached patch-clamp recordings of single-channel currents in rabbit atrial cells. **A.** Tracings of channel currents obtained at various patch potentials. Potentials are expressed as a change from resting potential (RP) as measured from the inside of the cell. The reversal potential was RP+20 mV and the pipette contained 108 mmol/L NMDGCl. **B.** Average current-voltage (I-V) relation (mean±SE) from six patches studied under the same conditions as in panel A. Standard error bars fall within symbols for means. **C.** Ensemble-average currents (lowest tracings) obtained by averaging 60 single-channel recordings (three examples shown at each voltage). The patch was pulsed to -40 mV (left panel) and +80 mV (right panel) relative to RP for 2 seconds at 0.1 Hz (values approximately 60 mV negative and 60 mV positive to the reversal potential respectively). The pipette (extracellular side) contained 108 mmol/L NMDGCl. Dashed line indicates closed-state (0 current) level.

Figure 2. Dependence of unitary channel current on pipette anion and cation concentrations. **A.** Recordings from cell-attached patches exposed to 108 mmol/L (**a**), 22 mmol/L (**b**), and 208 mmol/L (**c**) $[Cl^-]_p$. **B.** Average current-voltage (I-V) curves for patches studied at different values of $[Cl^-]_p$. Results are mean±SE, with error bars within means when not visible. **C.** Relation between mean reversal potentials (E_{rev}, expressed as voltage relative to resting potential) and $[Cl^-]_p$. Linear regression on the data provided the best-fit line shown (r=0.987; slope, -57.7 mV per decade). **D.** Average I-V curves recorded with 108 mmol/L or 0 mmol/L NMDG in the

pipette solution. Where standard error bars are not visible, they fall within symbols for means. The I-V curves superimpose, indicating no significant effect of substitution of Tris for NMDG on conductance.

Figure 3. Examples of single-channel currents and kinetic analysis of open and closed dwell times at RP-40 mV under isotonic conditions. **A.** Representitive 2.5-min recordings at different time resolutions. Low-pass filtered at 1 kHz. Dashed lines indicate the closed (0 current) level. **B.** Histograms of open (upper) and closed (lower) dwell time. The interval durations were log-binned and the number of events spent in each interval was transformed to square-root. Data fitting (see text for methods) indicated that the channel must have at least three open kinetic states (τ_1 = 2.1 ms, τ_2 = 15.9 ms, τ_3 = 120.8 ms), and a minimum of four closed kinetic states (τ_1 = 1.0 ms, τ_2 = 6.1 ms, τ_3 = 31.4 ms, τ_4 = 246.7 ms). Dashed lines indicate the fitting components and the solid line indicates the final fitting curve.

Figure 4. Recordings from a patch that failed to show single-channel activity under isotonic conditions (left), but showed typical outwardly-rectifying currents after the induction of hypotonic cell swelling (right).

Figure 5. Effect of hypotonic cell swelling on channel activity recorded at RP-40 mV in a cell-attached patch in the presence of 108 mmol/L $[Cl^-]_p$. Corresponding amplitude histograms are shown on the right of each panel. **A.** Recordings under isotonic conditions. **B.** Hypotonic swelling caused the appearance of a second active channel in this patch.

Figure 6. Comparison of properties of ORCC recorded under isotonic (Isot.) and hypotonic (Hypot.) conditions. **A.** I-V curves (mean±SE) recorded with $[Cl^-]_p$ of 108 mmol/L. The reversal potential averaged RP+18±1 mV (n=14) under hypotonic and RP+19±1 mV (n=6) under isotonic conditions. Slope conductances of outward current (from RP+20 mV to RP+140 mV) were 50±1 pS (n=14) and 49±1 pS (n=6) respectively. **B.** I-V curves recorded with lower (22 mmol/L) pipette chloride concentrations. The reversal potential was RP+54±3 mV (n=5) under hypotonic conditions and RP+53±3 mV (n=4) under isotonic conditions, while the slope conductance of outward current (from RP+60 mV to RP+140 mV) averaged 22±1 pS (n=5) and 23±1 pS (n=4) respectively. **C.** Reversal potentials of currents recorded from unitary channels under isotonic and hypotonic conditions at various $[Cl^-]_p$. Dashed line was obtained by linear regression of data from isotonic conditions. **D.** Prevalence of active channels in patches recorded under isotonic and hypotonic conditions.

Figure 7. Examples of single-channel currents and kinetic analysis of open and closed dwell times at RP-40 mV under hypotonic conditions. **A.** Representitive current tracings of 2.5-min recordings at different time resolutions. Low-pass filtered at 1 kHz. Dashed lines indicate the closed (0 current) level. **B.** Histograms of open (upper) and closed (lower) dwell time. The interval durations were log-binned and the number of events in each interval was transformed to square-root. Data fitting (see text for methods) indicated that the channel must have at least three open kinetic states (τ_1 = 2.1 ms,

τ_2 = 9.3 ms, τ_3 = 78.8 ms), and at least four closed kinetic states (τ_1 = 0.7 ms, τ_2 = 5.0 ms, τ_3 = 31.5 ms, τ_4 = 211.9 ms). Dashed lines indicate the fitting components and the solid line indicates the final fitting curve.

Figure 8. Effects of tamoxifen on ORCC activated by cell swelling. Examples of single-channel currents recorded at RP-40 mV for 2.5 min from the cell-attached patch when the cell was perfused with isotonic (**A**), hypotonic (**B**), and tamoxifen (10 μmol/L)-hypotonic (**C**) solutions are shown on the left and the corresponding amplitude histograms are shown on the right of each panel. P_o was 0, 0.72, and 0 under isotonic and hypotonic conditions and in the presence of tamoxifen, respectively.

Figure 9. Effects of tamoxifen on volume-regulated Cl^--currents. **A.** Basal currents recorded under isotonic conditions immediately after formation of the whole-cell configuration (**a**) and after 20 minutes of recording (**b**). Current amplitude and reversal potential (-40.5 mV) did not change over time. Subsequent exposure of the same cell to tamoxifen (10 μmol/L) for 7 min caused a substantial reduction in the current amplitude at all test potentials and shifted the reversal potential towards 0 mV (**c**). The tamoxifen-sensitive current (**d**) obtained by subtracting currents in (**c**) from those in (**b**) showed strong outward rectification and reversed at a potential (-41.5 mV) near the Cl^- equilibrium potential (-39.3mV). **B.** The cell-swelling-induced current (**b**) caused by hypotonic superfusion was also strongly inhibited by 10 μmol/L tamoxifen. The average I-V relations from 4 cells under isotonic (■) and hypotonic (●) conditions and in the presence of tamoxifen (▲) are shown in (**d**). The reversal

potential of current was -43.9 ± 1.2 mV under isotonic conditions and -44.1 ± 0.3 mV under hypotonic conditions.

TABLE 1. Kinetics of ORCC Under Different Conditions at RP-40 mV

	Isotonic (n=7)	Hypotonic (n=10)
P_o	0.66±0.04	0.66±0.03
Open τ_1	1.8±0.3	1.6 ± 0.2
Open τ_2	14.8±2.9	8.6±1.2
Open τ_3	97.6±17.5	90.6±21.2
Closed τ_1	0.8±0.1	0.6±0.1
Closed τ_2	4.6±0.9	4.3±0.9
Closed τ_3	29.2±4.5	28.9±6.3
Closed τ_4	217.8±63.8	196.3±43.1

All values for time constants (τ) are in ms, open probability (P_o) is dimensionless.

FIGURE 1

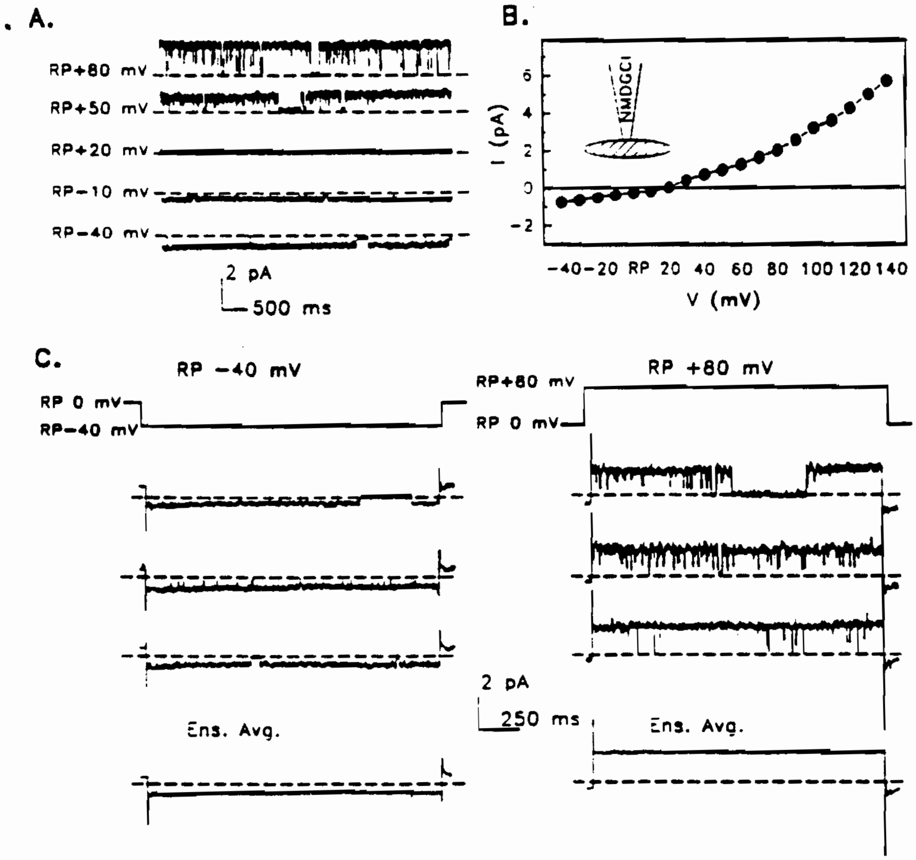
A.
RP+80 mV
RP+50 mV
RP+20 mV
RP−10 mV
RP−40 mV
2 pA
500 ms
B.
NMDGCl
I (pA)
6
4
2
0
−2
−40 −20 RP 20 40 60 80 100 120 140
V (mV)
C.
RP −40 mV
RP 0 mV
RP−40 mV
Ens. Avg.
RP +80 mV
RP+80 mV
RP 0 mV
2 pA
250 ms
Ens. Avg.

FIGURE 2

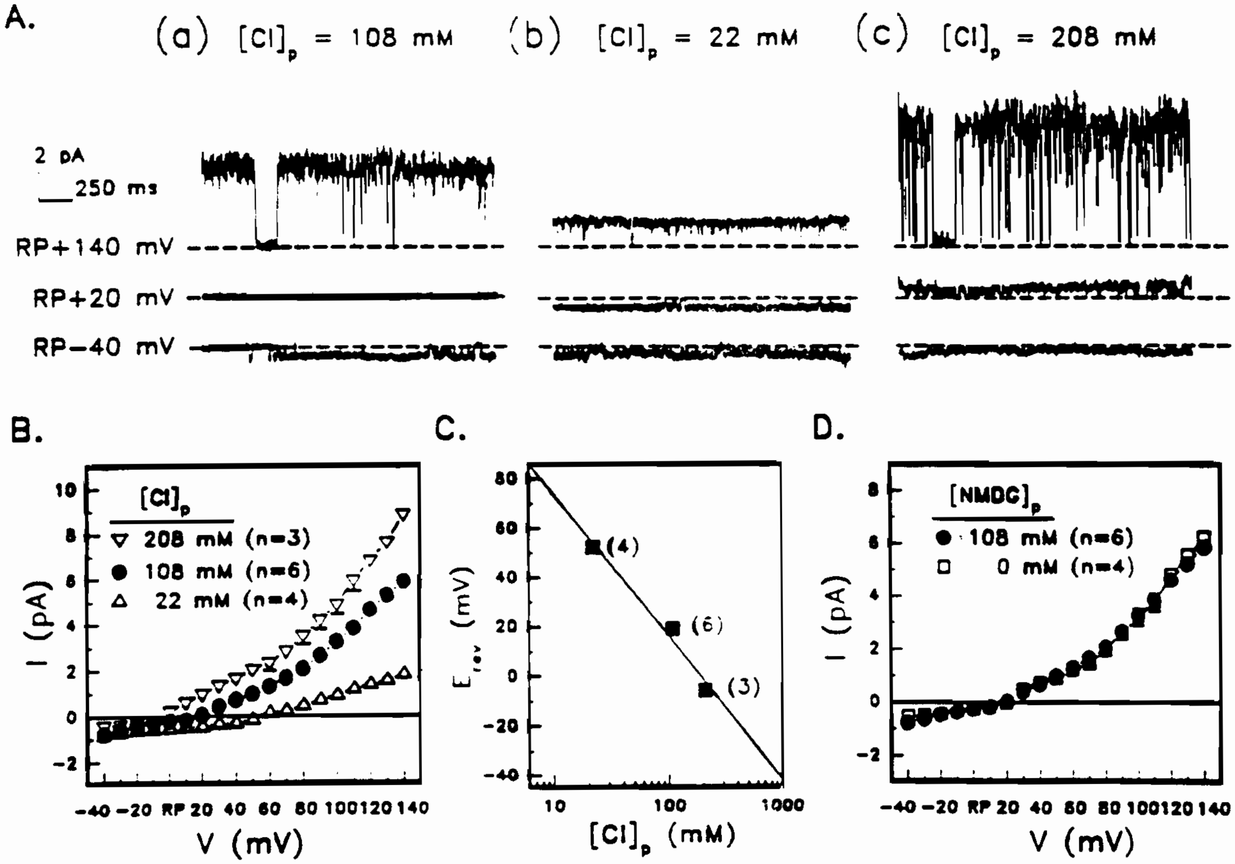
A.
(a) [Cl]$_p$ = 108 mM
(b) [Cl]$_p$ = 22 mM
(c) [Cl]$_p$ = 208 mM
2 pA
250 ms
RP+140 mV
RP+20 mV
RP−40 mV
B.
[Cl]$_p$
208 mM (n=3)
108 mM (n=6)
22 mM (n=4)
I (pA)
10
8
6
4
2
0
-2
-40 -20 RP 20 40 60 80 100 120 140
V (mV)
C.
E_{rev} (mV)
80
60
40
20
0
-20
-40
(4)
(6)
(3)
10
100
1000
[Cl]$_p$ (mM)
D.
[NMDG]$_p$
108 mM (n=6)
0 mM (n=4)
I (pA)
8
6
4
2
0
-2
-40 -20 RP 20 40 60 80 100 120 140
V (mV)

FIGURE 3

ISOTONIC

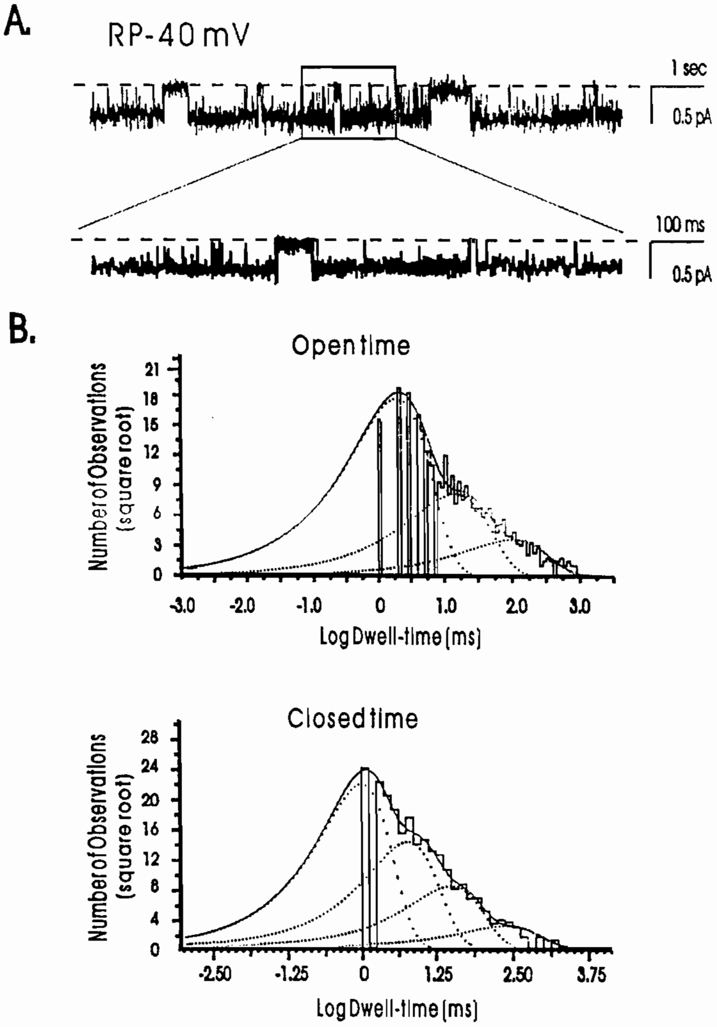

FIGURE 4

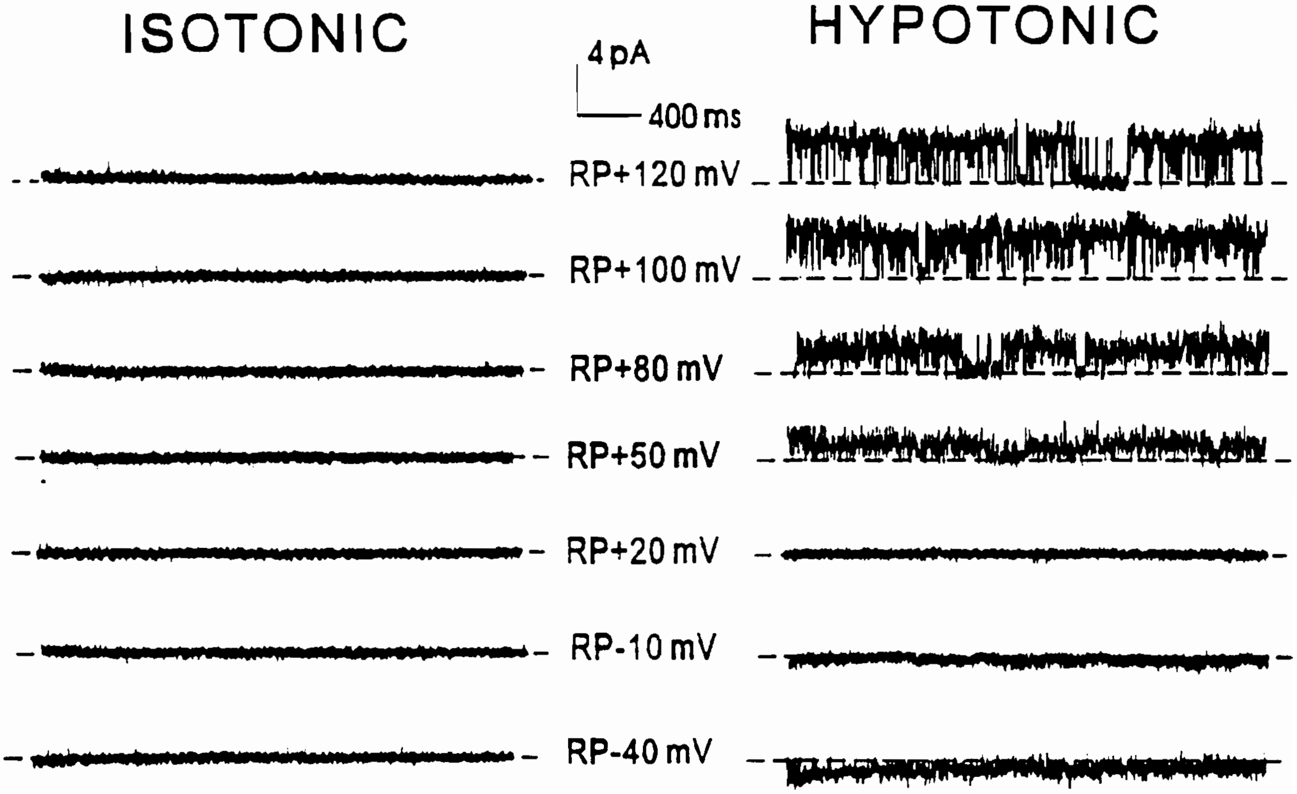
ISOTONIC
HYPOTONIC
4 pA
400 ms
RP+120 mV
RP+100 mV
RP+80 mV
RP+50 mV
RP+20 mV
RP-10 mV
RP-40 mV

FIGURE 5

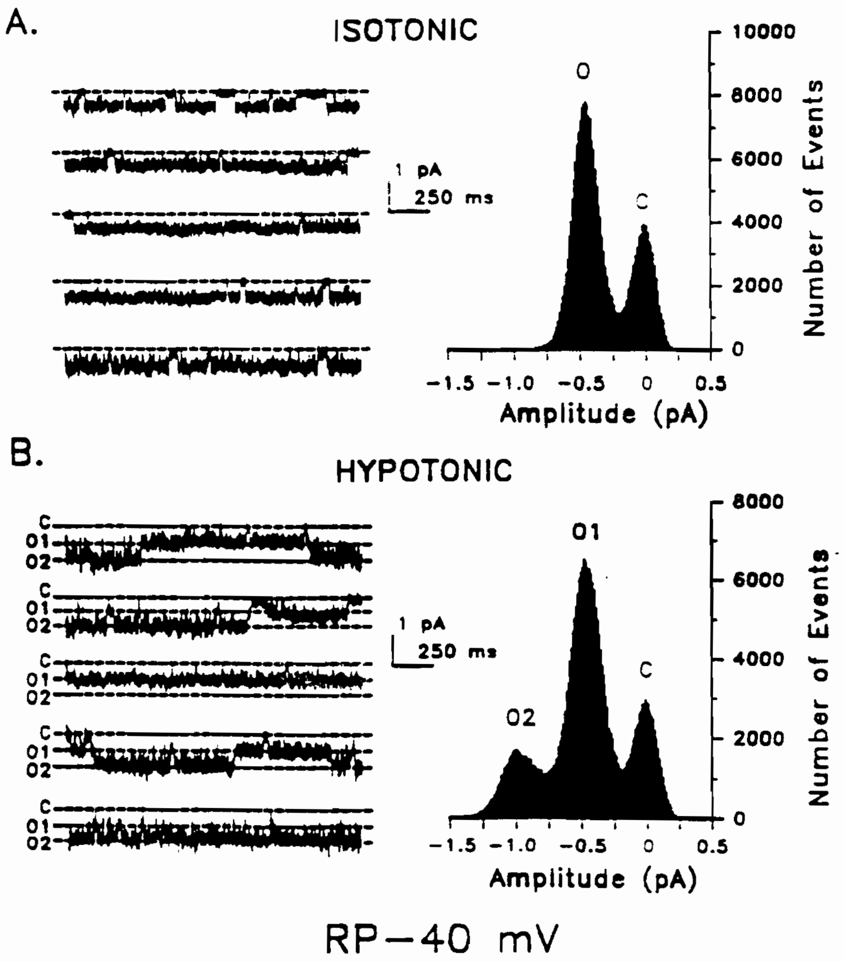
A.
ISOTONIC
1 pA
250 ms
O
C
10000
8000
6000
4000
2000
0
Number of Events
−1.5 −1.0 −0.5 0 0.5
Amplitude (pA)
B.
HYPOTONIC
C
O1
O2
1 pA
250 ms
O1
O2
C
8000
6000
4000
2000
0
Number of Events
−1.5 −1.0 −0.5 0 0.5
Amplitude (pA)
RP−40 mV

FIGURE 6

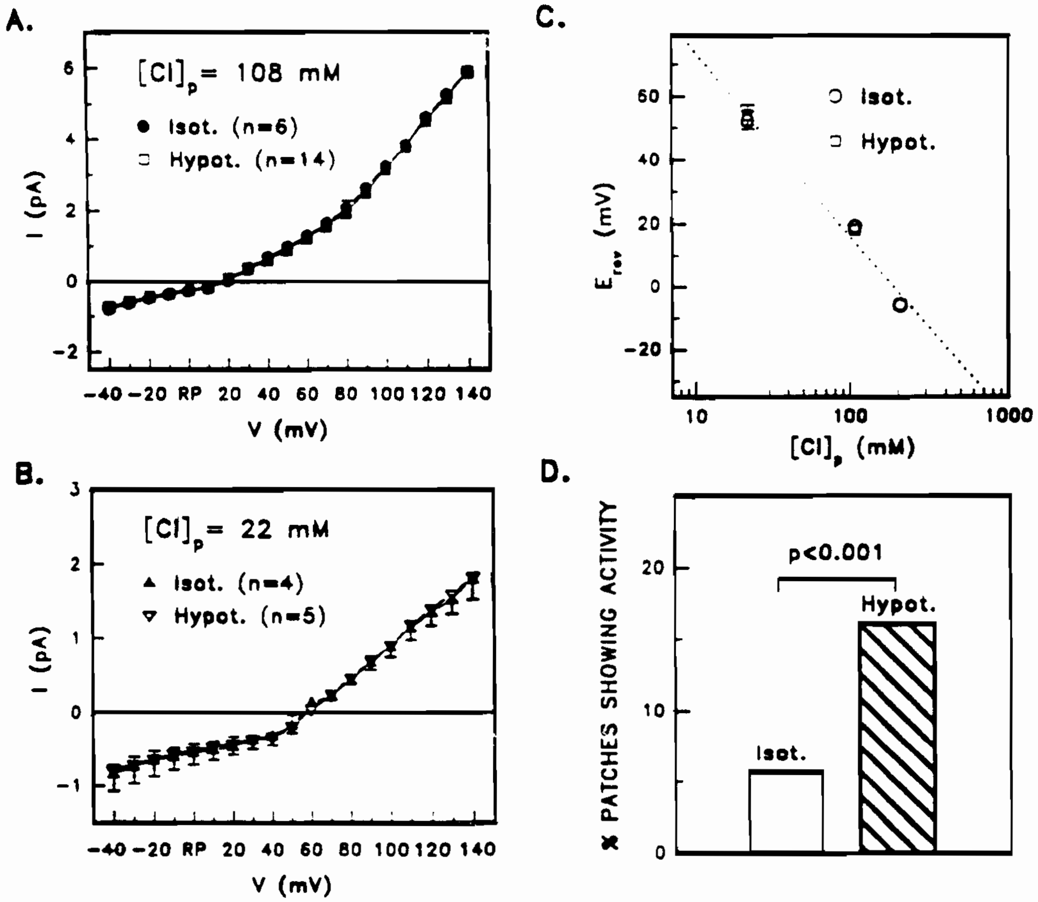
A.
[Cl]$_p$= 108 mM
● Isot. (n=6)
□ Hypot. (n=14)
I (pA)
6
4
2
0
-2
-40 -20 RP 20 40 60 80 100 120 140
V (mV)
B.
[Cl]$_p$= 22 mM
▲ Isot. (n=4)
▽ Hypot. (n=5)
I (pA)
3
2
1
0
-1
-40 -20 RP 20 40 60 80 100 120 140
V (mV)
C.
○ Isot.
□ Hypot.
E_{rev} (mV)
60
40
20
0
-20
10
100
1000
[Cl]$_p$ (mM)
D.
% PATCHES SHOWING ACTIVITY
p<0.001
Hypot.
Isot.
20
10
0

HYPOTONIC

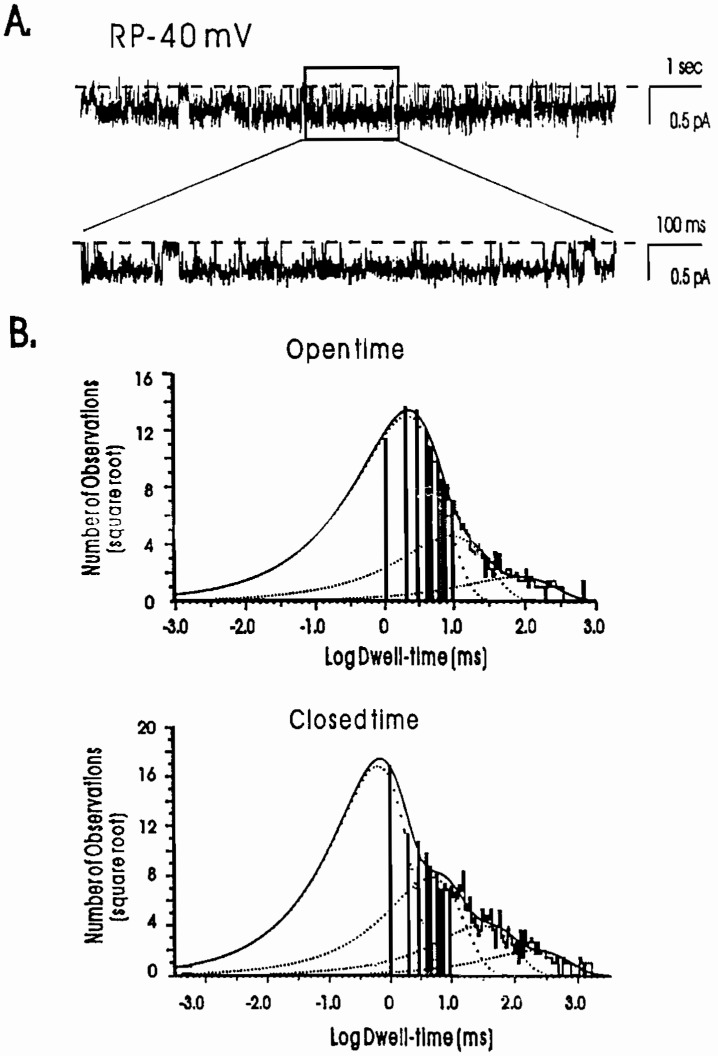
A.
RP-40 mV
1 sec
0.5 pA
100 ms
0.5 pA
B.
Open time
Number of Observations (square root)
16
12
8
4
0
-3.0
-2.0
-1.0
0
1.0
2.0
3.0
Log Dwell-time (ms)
Closed time
20
16
12
8
4
0
Number of Observations (square root)
-3.0
-2.0
-1.0
0
1.0
2.0
3.0
Log Dwell-time (ms)

FIGURE 8

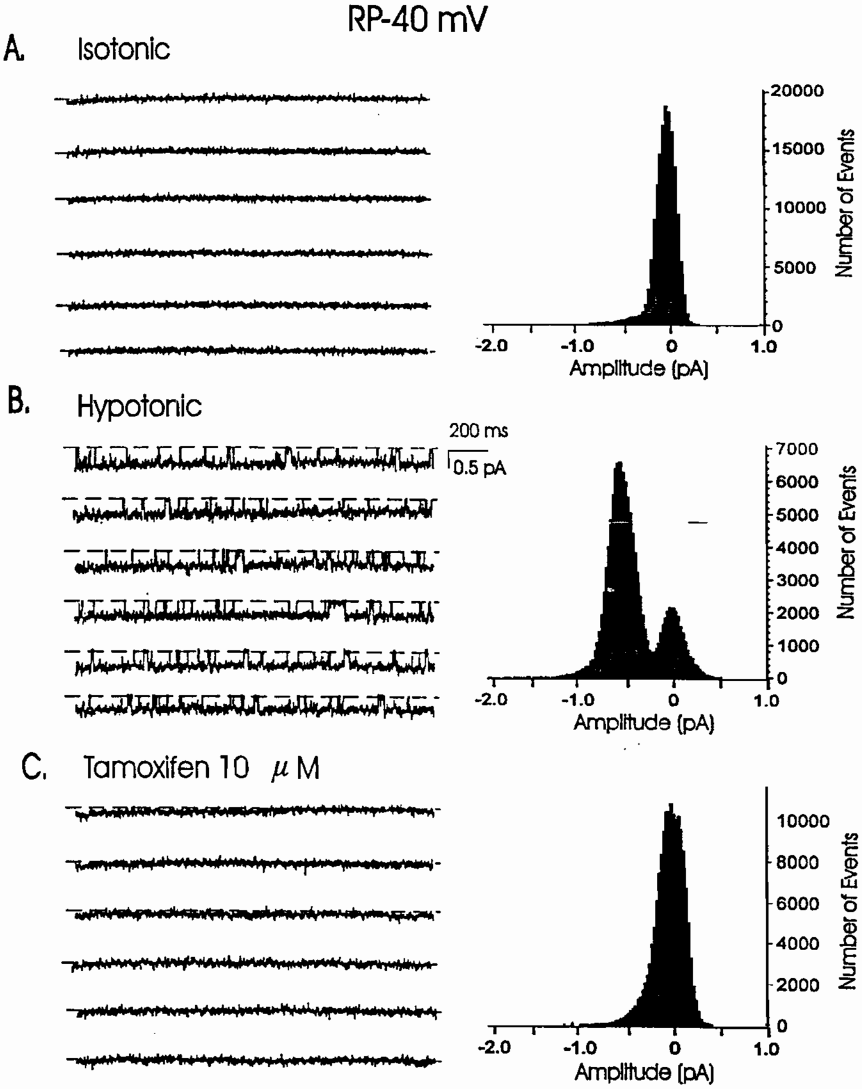
RP-40 mV
A. Isotonic
20000
15000
10000
5000
0
Number of Events
-2.0
-1.0
0
1.0
Amplitude (pA)
B. Hypotonic
200 ms
0.5 pA
7000
6000
5000
4000
3000
2000
1000
0
Number of Events
-2.0
-1.0
0
1.0
Amplitude (pA)
C. Tamoxifen 10 μM
10000
8000
6000
4000
2000
0
Number of Events
-2.0
-1.0
0
1.0
Amplitude (pA)

FIGURE 9

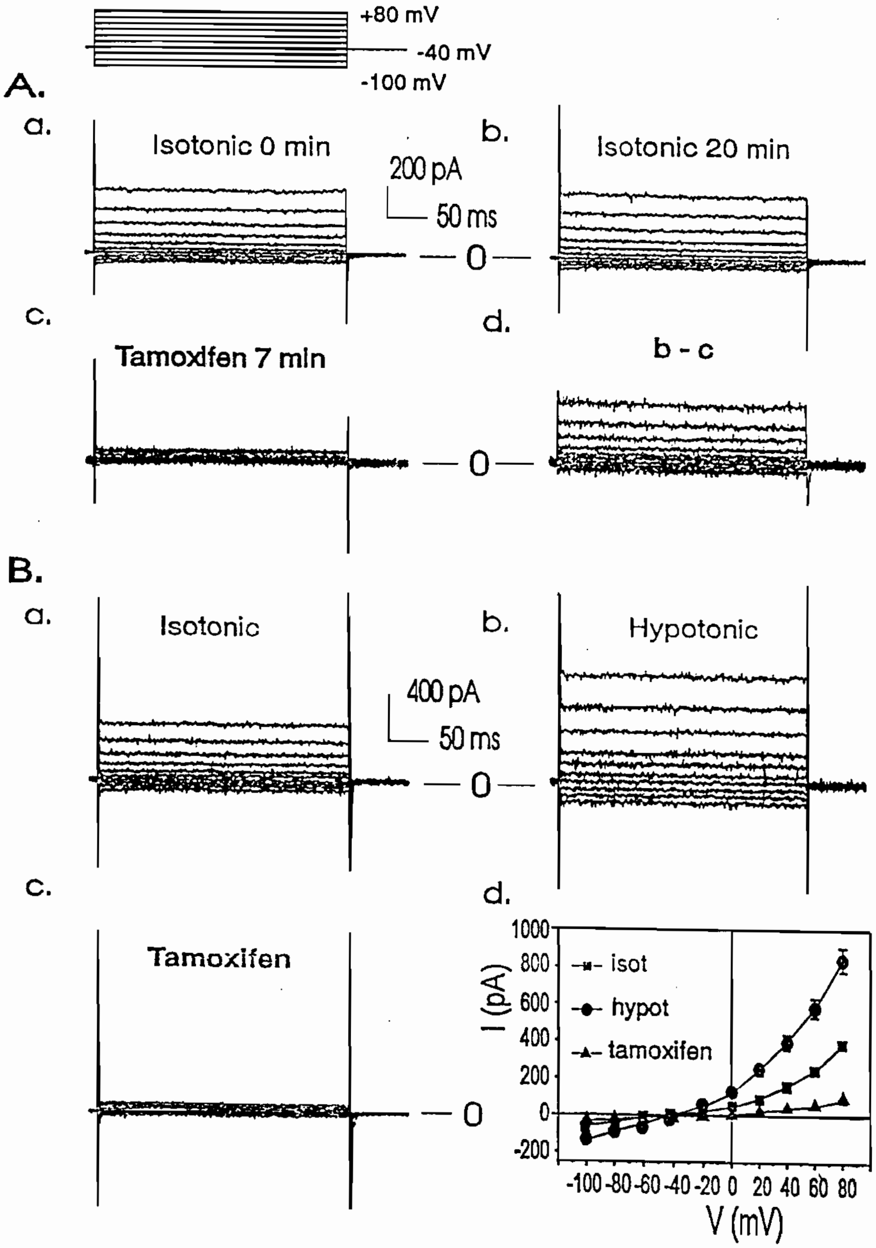
+80 mV
-40 mV
-100 mV
A.
a.
Isotonic 0 min
200 pA
50 ms
0
b.
Isotonic 20 min
c.
Tamoxifen 7 min
0
d.
b - c
B.
a.
Isotonic
400 pA
50 ms
0
b.
Hypotonic
c.
Tamoxifen
0
d.
1000
800
600
400
200
0
-200
I (pA)
isot
hypot
tamoxifen
-100 -80 -60 -40 -20 0 20 40 60 80
V (mV)

CHAPTER 5

REGULATION OF $I_{Cl.b}$ AND $I_{Cl.swell}$ BY α-ADRENERGIC RECEPTORS IN HEART - CHARACTERIZATION OF A NOVEL IONIC REGULATORY MECHANISM

In the heart, the function of Cl^- channels are still poorly understood. However, evidence is accumulating that cardiac Cl^- channel may participate in the regulation of cell volume and electrical activity. An outward Cl^- current activated during membrane depolarization should facilitate repolarization and cause a reduction in APD. It has long been known that α-adrenergic stimulation can prolong cardiac action potential duration. The mechanism for this effect is still not very clear. Although some studies suggest the inhibition of various K^+ currents as the possible mechanism, the ability of α-adrenergic stimulation to modulate Cl^- channels has not been studied. Therefore, our next experiments were designed to look at the modulation of $I_{Cl.b}$ and $I_{Cl.swell}$ by αAR in rabbit atrial myocytes. We first studied the concentration-dependence of αAR stimulation on both $I_{Cl.b}$ and $I_{Cl.swell}$. I then tried to determine the subtype-selectivity of these effects and finally characterized the possible second messenger pathways.

α-Adrenergic Control of Volume-Regulated Cl⁻ Currents in Rabbit Atrial Myocytes

Characterization of a Novel Ionic Regulatory Mechanism

Dayue Duan, Bernard Fermini, Stanley Nattel

Abstract α-Adrenergic stimulation is known to play a role in cardiac arrhythmogenesis and to modulate a variety of cardiac K^+ currents. The effects of α-adrenergic stimulation on Cl^- currents are largely unknown. Many cardiac cell types show a volume-sensitive Cl^- current induced by cell swelling ($I_{Cl.swell}$). The present experiments were designed to assess the potential α-adrenergic modulation of $I_{Cl.swell}$ in rabbit atrial myocytes. $I_{Cl.swell}$ was induced with the use of a hypotonic superfusate, under conditions designed to prevent currents carried by K^+, Na^+, and Ca^{2+} ions. A basal Cl^- current ($I_{Cl.b}$) was observed under isotonic conditions in 128 of 150 cells (85%), had the same dependency on $[Cl^-]_o$ as $I_{Cl.swell}$, and was reduced by cell shrinkage induced by hypertonic superfusion, suggesting that $I_{Cl.b}$ is carried by the same volume-sensitive Cl^- conductance as $I_{Cl.swell}$. Phenylephrine produced a concentration-dependent and near-complete inhibition of $I_{Cl.b}$ and $I_{Cl.swell}$, with EC_{50} values of 86±5 and 72±7 (mean±SEM) μmol/L, respectively, at +20 mV. Norepinephrine (administered in the presence of 1 μmol/L propranolol) also inhibited $I_{Cl.b}$ and $I_{Cl.swell}$, with EC_{50} values of 2.6±0.1 and 2.8±0.4 μmol/L, respectively. The concentration-response curve for phenylephrine was shifted significantly ($P<.001$) to the right by the α_1-adrenoceptor antagonist prazosin and by the α_{1A}-receptor antagonists (−)-niguldipine and 5-methylurapidil but was unaltered by the α_{1B}-receptor antagonist chloroethylclonidine (100 μmol/L). Inhibition of protein kinase C (PKC) with staurosporine, H-7, or 18-hour preincubation with the phorbol ester 4β-phorbol 12-myristate 13-acetate (PMA, 500 nmol/L) blocked the effects of phenylephrine on $I_{Cl.swell}$, and the highly selective PKC inhibitor bisindolylmaleimide blocked the effects of norepinephrine on $I_{Cl.swell}$ and $I_{Cl.b}$. Both PMA and 1-oleoyl-2-acetylglycerol inhibited $I_{Cl.swell}$ in a concentration-dependent fashion. In blinded studies, the phorbol ester phorbol 12,13-didecanoate (PDD) reduced $I_{Cl.swell}$ by 91±3%; its inactive analogue 4α-PDD had no effect (mean change, 3±1%). Preincubation with pertussis toxin (PTX) prevented the actions of phenylephrine on $I_{Cl.swell}$, indicating a role for a PTX-sensitive guanine nucleotide–binding (G) protein. We conclude that α-adrenergic agonists inhibit volume-sensitive Cl^- currents in rabbit atrial cells by interacting with an α_{1A}-adrenoceptor mechanism that is coupled to PKC via a PTX-sensitive G protein. These results suggest a potentially novel mechanism of α-adrenergic control of cardiac electrical activity, the inhibition of volume-sensitive Cl^- currents, and indicate that PKC, well known to elicit phosphorylation-dependent Cl^- currents in cat and guinea pig ventricular myocytes, is also capable of potently inhibiting other forms of cardiac Cl^- current. (***Circ Res*. 1995;77:379-393.**)

Key Words • action potential • Cl^- currents • ion channels • autonomic nervous system • phenylephrine

In most mammalian species, the stimulation of cardiac α-adrenoceptors increases action potential duration and the force of cardiac contraction.[1,2] A variety of arrhythmia mechanisms may be enhanced by α-adrenergic stimulation,[3] and α-adrenoceptor blockade can reduce the severity of arrhythmias induced by myocardial ischemia and reperfusion.[1] A number of actions of α-adrenergic receptor activation on ionic currents have been described. Consistent with its ability to prolong action potential duration, α_1-adrenoceptor activation inhibits a variety of K^+ currents, including I_{to}, in rat ventricular[4-6] and rabbit atrial[7-9] myocytes, I_{K1} in rabbit atrial and ventricular myocytes,[10,11] and I_{KACh} in rabbit atrial and ventricular cells.[10,11] In guinea pig myocytes, α-adrenergic stimulation shortens action potential duration,[12] apparently by enhancing I_K.[13]

Since the discovery in 1989 of $I_{Cl.cAMP}$ in guinea pig and rabbit ventricular myocytes,[14-16] the properties of several types of cardiac Cl^- currents have been described. These include $I_{Cl.cAMP}$,[14-18] $I_{Cl.Ca}$,[19-20] $I_{Cl.b}$,[21-22] $I_{Cl.swell}$,[23-26] $I_{Cl.purinergic}$,[27] and $I_{Cl.PKC}$.[28-31] At physiological Cl^- concentrations, the reversal potential for Cl^- currents has been estimated at values ranging from −65 to −30 mV.[26,32,33] Thus, Cl^- current can play a role both in the repolarization of the cell from plateau potentials and in phase 4 depolarization underlying spontaneous activity.

Although the actions of α-adrenoceptor stimulation on K^+ currents have been widely studied, α-adrenergic effects on Cl^- currents have not been extensively investigated. Preliminary data showing that α-adrenoceptor stimulation activates a Cl^- current by stimulating PKC in cat ventricular myocytes have been presented previously.[30] Cell swelling and cell stretch, both of which activate $I_{Cl.swell}$,[23-26] may occur during a variety of clinical conditions, including acute myocardial ischemia[34] and congestive heart failure. Increased catecholamine concentrations are a feature of both conditions,[35,36] so that the interactions of adrenergic agonists with $I_{Cl.swell}$ may be of physiological and clinical importance. Isoproterenol has been shown to enhance $I_{Cl.swell}$ in canine atrial myocytes, presumably by stimulating β-adrenoceptors.[23] The ability of α-adrenoceptor stimulation to modify $I_{Cl.swell}$ is presently unknown. The present experiments were designed to determine (1) the effects of α-adrenoceptor

---

Received July 13, 1994; accepted May 2, 1995.

From the Department of Pharmacology and Therapeutics, McGill University, Montreal, Quebec, Canada; the Department of Medicine, University of Montreal; and the Department of Medicine and the Research Center, Montreal Heart Institute.

Correspondence to Stanley Nattel, Research Center, Montreal Heart Institute, Montreal, Quebec, Canada H1T 1C8.

Selected Abbreviations and Acronyms

CEC = chloroethylclonidine
E_{max} = maximum effect of an agent
I_{Ca} = Ca^{2+} current
$I_{Cl.Ca}$ = Ca^{2+}-activated Cl^- current
$I_{Cl.cAMP}$ = cAMP-dependent Cl^- current
$I_{Cl.b}$ = basal Cl^- current
$I_{Cl.PKC}$ = PKC-activated Cl^- current
$I_{Cl.swell}$ = total Cl^- current in presence of swelling
I_K = delayed rectifier K^+ current
$I_{K.ACh}$ = acetylcholine-activated K^+ current
I_{K1} = inward rectifier K^+ current
I_{to} = transient outward current
I-V = current-voltage
NMDG = *N*-methyl-D-glucamine
OAG = 1-oleoyl 2-acetylglycerol
PDD = phorbol 12,13-didecanoate
PKC = protein kinase C
PMA = 4β-phorbol 12-myristate 13-acetate
PTX = pertussis toxin
4-AP = 4-aminopyridine
5MU = 5-methylurapidil

stimulation on $I_{Cl.swell}$ in rabbit atrial myocytes, (2) the ability of subtype-selective α-adrenoceptor antagonists to block any response seen, and (3) the signal transduction mechanisms linking α-adrenergic stimulation to changes in Cl^- current. The results to be presented show that in contrast to the effects of α-adrenergic and PKC-mediated enhancement of Cl^- currents in cat and guinea pig ventricular myocytes, α-adrenoceptor stimulation and the resulting activation of PKC cause concentration-dependent inhibition of $I_{Cl.swell}$.

Materials and Methods

Preparation of Single Cells

Single atrial cells were obtained from rabbit hearts by using a previously described dissociation technique.[21,37] Briefly, rabbits (1.5 to 2.0 kg) were killed by a blow on the neck, and the hearts were quickly removed and perfused in the Langendorff mode, first with a modified HEPES-buffered Tyrode's solution at 37°C, then with a nominally Ca^{2+}-free Tyrode's solution until the heart ceased to beat, and finally with the same solution containing 0.04% collagenase (CLS II, Worthington Biochemical) and 1.0% bovine serum albumin (Sigma Chemical Co) for 10 minutes. The left atrium was removed and further dissected into small pieces, and cell dissociation was achieved by gentle mechanical agitation. All cells studied were rod-shaped, had clear cross-striations, and lacked any visible blebs on their surfaces. Cell dimensions were determined with a calibrated graticule in the microscope, and cell volumes were estimated with assumed right cylindrical geometry according to the following equation:

$$V=\pi L(D/2)^2$$

where V, L, and D are cell volume, length, and diameter, respectively.

Electrophysiological Recording

The tight-seal whole-cell voltage-clamp configuration of the patch-clamp technique was used. Recordings were performed with an Axopatch 1D or 200 amplifier (Axon Instruments). Voltage-clamp pulses were generated by a 12-bit digital-to-analog (D/A) convertor. Membrane current data were acquired by an analog-to-digital (A/D) conversion board (Medical Systems) with a maximum sampling rate of 100 kHz and simultaneously digitized (model TM 125, Scientific Solutions) and stored on the hard disk of an IBM PC–compatible computer under the control of PCLAMP software (Axon Instruments). Recording pipettes were prepared from borosilicate glass electrodes (outer diameter, 1.5 mm) with tip resistances of 2 to 5 MΩ (3.4±0.2 MΩ, mean±SEM, n=118) when filled. Junction potentials were corrected before achieving the membrane seal. After a tight seal between the cell membrane and the pipette tip (seal resistance >10 GΩ) had been formed, the bath solution was changed from Tyrode's solution to the standard isotonic experimental solution. After seal formation, the membrane patch was ruptured with brief additional suction.

The capacitive transients elicited by symmetrical 5-mV steps from −40 mV were recorded at 100 kHz for subsequent calculation of capacitance and access resistance. The mean cellular capacitance was 75±2 pF, and the input resistance averaged 557±33 MΩ, a value of the same order as that obtained by Giles and van Ginneken[38] in rabbit atrial cells from the crista terminalis. Series resistance was then compensated to minimize the duration of the capacitive surge on the current record during 5-mV hyperpolarizations from −40 mV, and over 70% compensation was usually obtained. The time constant of the capacitive transient averaged 205±7 microseconds (n=118), and series resistance averaged 2.9±0.1 MΩ (n=118) after compensation. In most experiments, the maximum outward current was in the range of 1.5 nA, but in occasional experiments, the current at very positive voltages (eg, +80 mV) was larger, exceeding 2 nA. All analyses of drug action were therefore based on currents measured at +20 mV, a voltage in the physiologically-relevant range at which currents were always <1 nA.

To obtain whole-cell I-V relations, 300-millisecond hyperpolarizing and depolarizing pulses were imposed at 0.1 Hz in +10-mV increments between −100 and +80 mV from a holding potential of −40 mV. Current amplitudes were measured relative to the 0 current level. Leak-subtraction procedures were not used, but cells with evidence of a significant leak were rejected from study. All experiments were performed at 30±1°C. Na^+ current was inactivated before the voltage steps by holding the cell at −40 mV. $BaCl_2$ (500 μmol/L), $CdCl_2$ (100 μmol/L), ouabain (10 μmol/L), and propranolol (1 μmol/L) were added to all superfusion solutions to block I_{K1}, I_{Ca}, Na^+,K^+-ATPase, and β-adrenoceptors, respectively.

Solutions and Drugs

The modified Tyrode's solution for cell isolation contained (mmol/L) NaCl 126, KCl 5.4, $CaCl_2$ 2.0, $MgCl_2$ 1.0, NaH_2PO_4 0.33, glucose 10, and HEPES 10, with pH adjusted to 7.4 with NaOH. The high-K^+ storage solution contained (mmol/L) KCl 20, KH_2PO_4 10, glucose 10, potassium glutamate 70, β-hydroxybutyric acid 10, taurine 10, and EGTA 10, along with 1% bovine serum albumin, pH 7.4 (KOH). K^+-free pipette solutions were used to avoid contamination by outward K^+ currents. The pipette (internal) solution contained (mmol/L) NMDG chloride 100, HEPES 10, EGTA 5.0, and Mg^{2+}-ATP 5.0, with pH adjusted to 7.4 with NMDG hydroxide and osmolarity adjusted to 270 to 290 mOsm/kg H_2O by adding mannitol (mean final osmolarity, 284±2 mOsm/kg H_2O). Solution osmolarities were measured by freezing-point depression (Osmomette A, Precision Systems Inc). In experiments analyzing the response of currents to extracellular Cl^- replacement, the pipette solution contained (mmol/L) NMDG chloride 24, NMDG aspartate 100, HEPES 10, EGTA 5, and Mg^{2+}-ATP 5, with pH adjusted to 7.4 with NMDG hydroxide. $[Cl^-]_o$ was modified by equimolar replacement with aspartate. The standard isotonic bath solution contained (mmol/L) NaCl 126, CsCl 5.4, $MgCl_2$ 0.8, $CaCl_2$ 1.0, NaH_2PO_4 0.33, HEPES 10, and glucose 5.5, with pH adjusted to 7.4 with NaOH (mean osmolarity, 294±3 mOsm/kg H_2O). In some experiments, a hypertonic bath solution was used, which was prepared by adding 75 mmol/L mannitol to the standard isotonic solution to create a final osmolarity of 361±3 mOsm/kg H_2O. The standard hypotonic bath solution contained (mmol/L) NaCl 100,

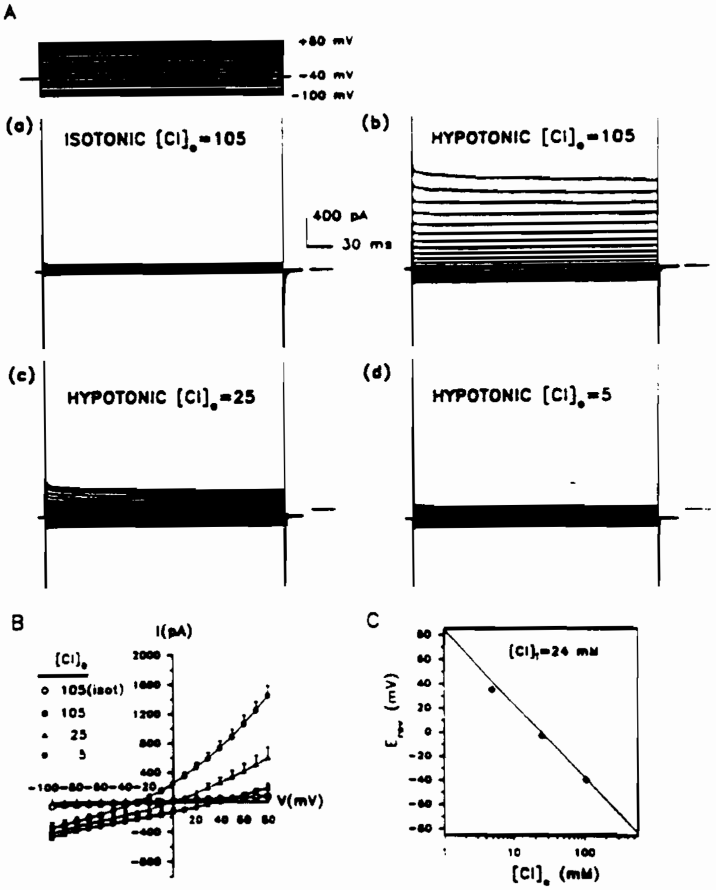

FIG 1. A, $I_{Cl.swell}$ in a cell lacking $I_{Cl.b}$. Results are shown from the same cell under control conditions (a) and then after hypotonic superfusate–induced cell swelling in the presence of $[Cl^-]_o$ of 105 (b), 25 (c), and 5 (d) mmol/L. In this and other figures showing original recordings, the horizontal line to the right of the recordings indicates the zero current level. Similar results were obtained in two other cells lacking $I_{Cl.b}$. B, Current-voltage relations from cells lacking $I_{Cl.b}$ under isotonic conditions (○) and in the presence of cell swelling at three values of $[Cl^-]_o$ (filled symbols). Results are mean±SEM in three cells. C, Relation between reversal potential (E_{rev}) of $I_{Cl.swell}$ and $[Cl^-]_o$ in cells lacking $I_{Cl.b}$. Results are mean±SEM, but error bar falls within symbol for mean. The square of the correlation coefficient for the relation between E_{rev} and $[Cl^-]_o$ is .999, and the slope is −57 mV per decade. The line shown is the relation predicted for a pure Cl^- conductance.

$MgCl_2$ 0.8, $CaCl_2$ 1.0, NaH_2PO_4 0.33, HEPES 10, and glucose 5.5, pH adjusted to 7.4 with NaOH (217±2 mOsm/kg H_2O). In some experiments, cell swelling was induced by using a hypertonic pipette solution that contained (mmol/L) CsCl 160, CsOH 40, $MgCl_2$ 1.0, HEPES 10, EGTA 5.0, and Mg^{2+}-ATP 5.0 (pH 7.4 with HCl, 400 to 420 mOsm/kg H_2O) while cells were perfused with standard bath solution (270 to 285 mOsm/kg H_2O) as described above. Similar results were obtained with either method of inducing cell swelling, and the experiments presented were performed with hypotonic superfusate-induced swelling.

Phenylephrine, norepinephrine, propranolol, prazosin, ouabain, and PTX were purchased from Sigma. H-7, staurosporine, PMA, and OAG were obtained from ICN Biochemicals. The highly selective PKC inhibitor bisindolylmaleimide, the phorbol ester PDD, and its inactive analogue 4α-PDD were purchased from Calbiochem/Novobiochem. CEC, 5MU, and *S*(+)-niguldipine were bought from Research Biochemicals Inc. The disulfonic stilbene Cl^- transport blockers DIDS and SITS were purchased from Sigma and made up as fresh solutions on the day of each experiment. Staurosporine, PMA, 4α-PDD, and PDD were prepared as 1 or 2 mmol/L stock solutions in dimethyl sulfoxide. OAG was first dissolved in chloroform, then dispersed in standard bath solution by sonication after evaporation of chloroform with N_2 gas, and finally diluted in the standard bath solution to obtain the desired concentration. Stock solutions of the other drugs were prepared in distilled water and added to known volumes of superfusion solution to produce the desired concentrations. In all experiments with staurosporine or H-7, staurosporine (0.1 μmol/L) or H-7 (20 μmol/L) was present in the pipette solution and was added to the superfusate at the times indicated in "Results."

Data Analysis

All analyses are based on comparisons of currents in the presence of a drug with those recorded before drug superfusion in the same cell. Dose-response experiments were performed by superfusing the same cell with control solutions and then with each concentration of the drug to be tested. All drug effects were assessed after a superfusion interval long enough to achieve steady state effects, which was 10 to 15 minutes unless otherwise indicated.

EC_{50} was calculated from the concentration-response relation with an E_{max} model,[39] in which the measured effect (E) of an agent at a known concentration C was fitted to the relation $E=E_{max}C/(C+EC_{50})$, where the variables determined by curve fitting are E_{max} (maximum effect) and EC_{50} (concentration for 50% of maximum effect). All results are expressed as mean±SEM. Statistical comparisons were performed either by ANOVA with Scheffé contrasts for group data or by Student's *t* test when only two groups were compared. A two-tailed probability of <5% was taken to indicate statistical significance.

Results

Properties of $I_{Cl.swell}$ and $I_{Cl.b}$

Fig 1A shows the properties of swelling-induced current in a myocyte lacking any significant conductance under basal conditions (Fig 1A, a). After exposure to hypotonic conditions, a substantial current is seen (Fig 1A, b). The current shows outward rectification and has a reversal potential (−36 mV) that is close to the calculated Cl^- equilibrium potential (−38.5 mV). Fig 1A, c and d, shows the effects of extracellular Cl^- replacement with aspartate on swelling-induced currents in the same cell. Reduction of $[Cl^-]_o$ shifted the reversal

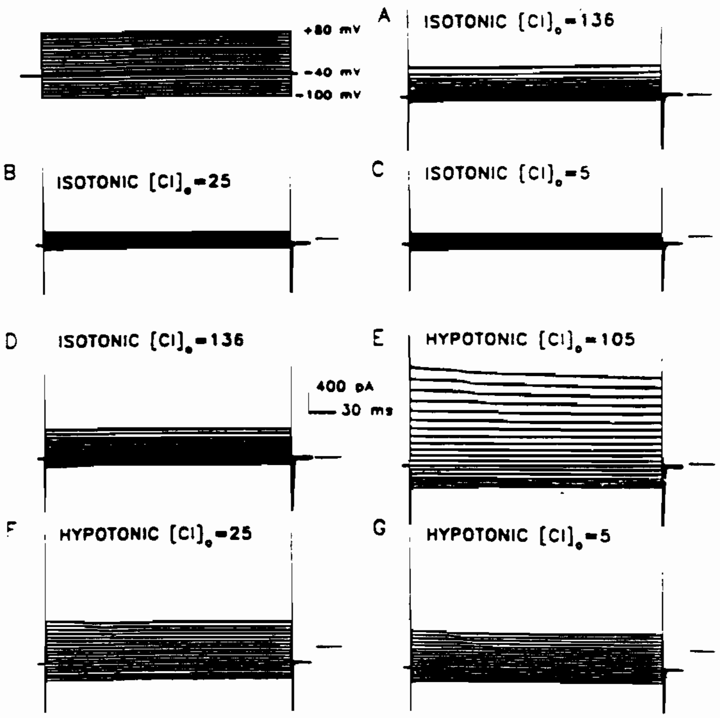

FIG 2. Currents under isotonic conditions (A through D) and in the presence of hypotonic superfusate–induced cell swelling (E through G) at the $[Cl]_o$ values shown.

potential to more positive values and strongly reduced the amplitude of outward currents. Fig 1B shows the I-V relations for swelling-induced currents in three cells that lacked any significant basal Cl^- conductance. Results (mean±SEM) before hypotonic cell swelling are shown by open symbols; the results after cell swelling are shown by filled symbols. Under basal conditions (open circles), the conductance is extremely small and reverses at 0 mV. Cell swelling induces a large outwardly rectifying conductance whose reversal potential shifts strongly with changes in $[Cl^-]_o$. Fig 1C shows the relation between mean reversal potential in these cells and the logarithm of $[Cl^-]_o$. The relation was highly linear (r^2=.999) and had a slope of −57 mV per decade. Experimentally determined values were close to the relation predicted for a pure Cl^--specific conductance, as calculated from the Nernst equation and shown by the line in the figure.

A minority of cells had the basal conductance characteristics shown in Fig 1. Of a total of 150 cells studied, 128 (85.3%) showed a significant basal conductance as illustrated in Fig 2A. $I_{Cl,b}$ was present immediately after membrane rupture and remained constant under isotonic conditions for observation periods of up to 40 minutes. $I_{Cl,b}$s were outwardly rectifying and reversed at a potential (−46 mV) very close to the calculated Cl^- equilibrium potential (−45.4 mV) in the presence of 136 mmol/L $[Cl^-]_o$ and 24 mmol/L $[Cl^-]_i$. Reductions in $[Cl^-]_o$ to 25 (Fig 2B) and 5 (Fig 2C) mmol/L reduced the outward current amplitude and shifted the reversal potential, changes that were reversible upon returning to a $[Cl^-]_o$ of 136 mmol/L (Fig 2D). Exposure to hypotonic conditions caused cell swelling and greatly increased the conductance (Fig 2E). Overall, cell size increased upon hypotonic swelling from 114±2×10.6±0.2 μm to 107±2×16.4±0.5 μm, corresponding to a calculated volume increase of 140±15%. Reducing $[Cl^-]_o$ reduced the magnitude of swelling-induced currents and shifted their reversal potential in the positive direction, as illustrated in Figs 2F and 2G.

Fig 3 shows a quantitative analysis of the effects of changes in $[Cl^-]_o$ on currents recorded under both hypotonic and isotonic conditions in six cells exposed to various $[Cl^-]$ values before and after cell swelling. For a given value of $[Cl^-]_o$, the I-V relation has the same form and a similar reversal potential under both isotonic and hypotonic superfusate conditions (Fig 3A). The relations between reversal potentials and $[Cl^-]_o$ under isotonic and hypotonic conditions are shown in Fig 3B. The relations were highly linear (r^2=.997 and .999 for isotonic and hypotonic conditions, respectively), with a slope of 56 mV per decade under each condition. Since currents were recorded with both hypotonic and isotonic superfusate at corresponding values of $[Cl^-]_o$ in each cell, we were able to determine the response of the swelling-induced component to changes in $[Cl^-]_o$ by subtracting $I_{Cl,b}$ (under isotonic conditions) from the current recorded in the presence of hypotonic cell swelling. The resulting values have the I-V relations shown by the open squares in Fig 3A. The reversal potential of the swelling-induced component follows the Cl^- equilibrium potential (Fig 3B) and has a linear relation to log ($[Cl^-]_o$), with an r^2 of .999 and a slope of 57 mV per decade. Values of the reversal potential of swelling-induced current in the absence of $I_{Cl,b}$, as illustrated in Fig 1C, are reproduced as open triangles in Fig 3B. Note that the reversal potentials of $I_{Cl,b}$ (open circles), the total current in the presence of swelling in cells with $I_{Cl,b}$ (open triangles), the swelling-induced component in cells with $I_{Cl,b}$ (open squares), and the swelling-induced current in cells without $I_{Cl,b}$ (open diamonds) virtually superimpose on each other at each $[Cl^-]_o$ (Fig 3B).

The results shown in Fig 3 suggest that $I_{Cl,b}$ may be carried by the same ionic current mechanism as the swelling-induced current. Therefore, we sought to deter-

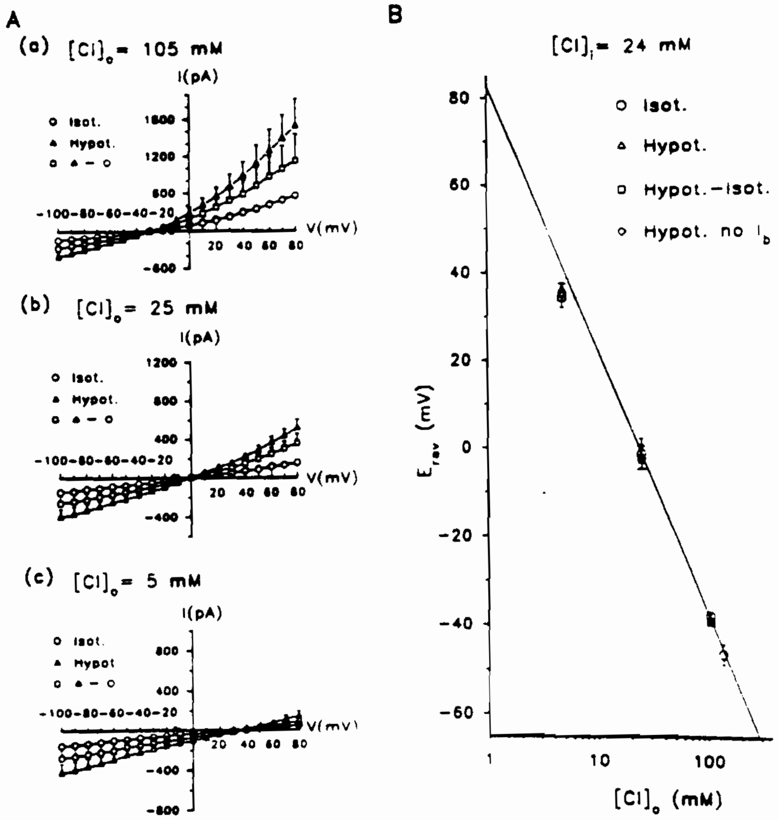

FIG 3. A. I-V relations before (○) and after (△) hypotonic-induced cell swelling at $[Cl^-]_o$ values of 105 (a), 25 (b), and 5 (c) mmol/L in six cells with $I_{Cl,b}$ exposed to various $[Cl^-]$ values under both control and swelling conditions. □ indicates the current induced by swelling, obtained by subtracting $I_{Cl,b}$ from total current in the presence of swelling. B. Relation between reversal potential (E_{rev}) and $[Cl]_o$ for currents shown in panel A (graphs a through c). Values are also shown for swelling-induced currents in cells lacking $I_{Cl,b}$ (◇, same data as in Fig 1C) and for $I_{Cl,b}$ at 136 mmol/L $[Cl]_o$. All results are mean±SEM. Isot. indicates isotonic; Hypot., hypotonic; and I_b, $I_{Cl,b}$.

mine whether $I_{Cl,b}$ is volume sensitive and can be suppressed by reducing cell volume with hypertonic superfusates. These experiments (and all others shown subsequently) were performed with pipettes containing 100 mmol/L $[Cl^-]$ in the pipette, bringing the Cl^- reversal potential toward 0 mV. Fig 4A, a, shows $I_{Cl,b}$ recorded immediately after rupturing the membrane and compensating for capacitance and series resistance. After 30 minutes of continued superfusion with isotonic solution, $I_{Cl,b}$ was unchanged (Fig 4A, b). Subsequent exposure to hypertonic superfusate caused a gradual reduction in current amplitude, with results after 30 minutes shown in Fig 4A, c. Similar results were obtained in a total of four cells studied in this fashion, for which the mean I-V relations before and after 30 minutes of exposure to hypertonic solution are shown in Fig 4B. Overall, exposure to hypertonic solution for 30 minutes reduced $I_{Cl,b}$ by 52±8% ($P<.001$) at +20 mV. Calculated mean volume of these cells averaged 9056±1514 μm^3 (length, 123±13 μm; width, 9.5±0.4 μm) under isotonic conditions and 4163±884 μm^3 (length, 121±12 μm; width, 6.5±0.4 μm) after hypertonic superfusion (a mean reduction in cell volume of 53±6%).

The data shown in Figs 1 through 3 indicate that $I_{Cl,b}$ and the current induced by swelling are anion currents that have a similar and substantial selectivity for Cl^- ions over aspartate and a similar I-V relation. Fig 4 shows that $I_{Cl,b}$ is volume sensitive and can be decreased by hypertonic superfusate-induced cell shrinkage. Therefore, it is quite likely that $I_{Cl,b}$ and the current induced by swelling are carried by the same underlying volume-

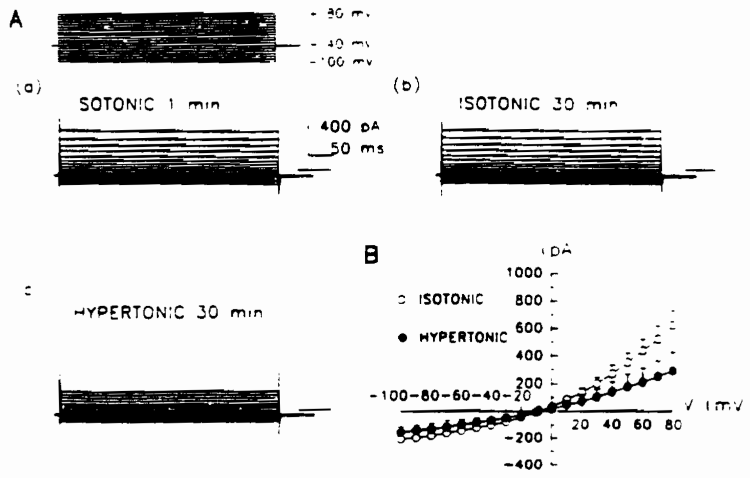

FIG 4. Response of $I_{Cl,b}$ to superfusion with hypertonic solution. A. Results from a typical cell. Results with isotonic superfusate are shown immediately after membrane rupture, capacitance, and series resistance compensation (a), after an additional 30 minutes of superfusion with isotonic solution (b), and after 30 minutes of superfusion with hypertonic superfusate (c). B. Effects of 30 minutes of exposure to hypertonic superfusate on the mean I-V relation of four cells. Calculated mean volume of these cells averaged 9056±1514 μm^3 under isotonic conditions and 4163±884 μm^3 after hypertonic superfusion.

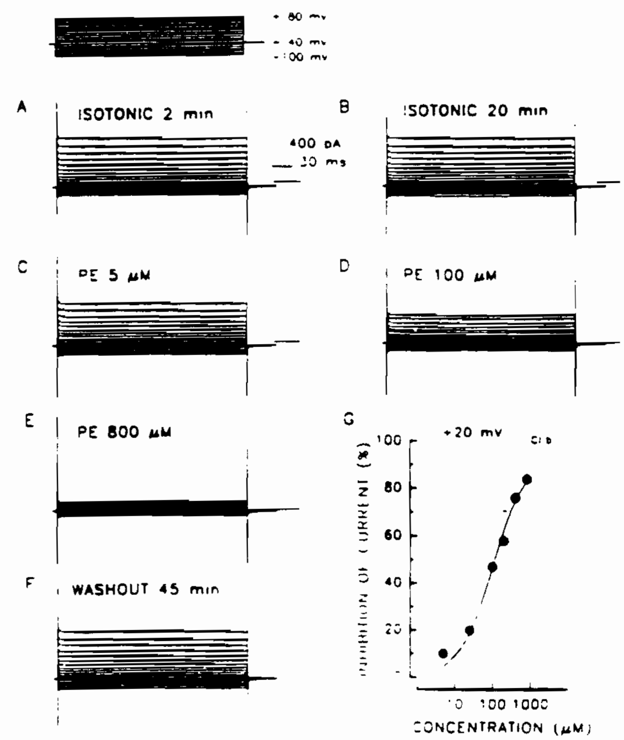

FIG 5. Effects of phenylephrine (PE) on $I_{Cl.b}$. Ionic currents shown in panels A through F were recorded from the same cell by imposing 10-mV 300-millisecond voltage steps from the holding potential of −40 mV to voltages between −100 and +80 mV (voltage protocol shown in inset). A, Currents recorded in the presence of isotonic superfusate, 2 minutes after membrane rupture. B, Currents recorded 20 minutes after membrane rupture. C through E, Currents recorded in the presence of incrementally increasing PE concentrations. F, Currents 45 minutes after washout of PE. G, Concentration-response curve for inhibition by PE of $I_{Cl.b}$ as measured upon steps to +20 mV in the cell shown in panels B through E. The best-fit curve (shown) to the E_{max} equation provided in the text had an EC_{50} of 101 μmol/L and an E_{max} of 94%. (In all current recordings, horizontal line indicates zero current level.)

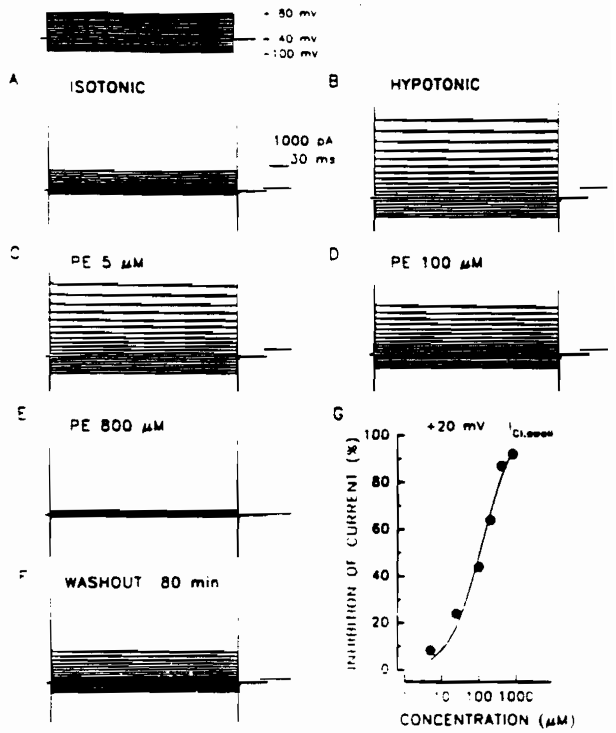

FIG 6. Response of $I_{Cl.swell}$ to phenylephrine (PE) in a representative cell. A, Recordings under isotonic conditions. B, Recordings obtained 16 minutes after changing to standard hypotonic superfusate. C through E, Response to increasing concentrations of PE. F, Partial reversal of the effect of PE after 80 minutes of washout. G, Concentration-response curve for PE-induced inhibition of $I_{Cl.swell}$ in the cell shown in panels B through E. The best-fit curve (shown) to the E_{max} equation provided in the text had an EC_{50} of 94 μmol/L and an E_{max} of 100%.

sensitive anion conductance. Since relatively few cells lack $I_{Cl.b}$, making it difficult to study swelling-induced current in isolation, we studied the α-adrenergic regulation of the total current in the presence of cell swelling, which we will call $I_{Cl.swell}$ in this article and which we believe to represent the total magnitude of volume-regulated Cl^- current in the presence of cell swelling in each cell. Several additional series of experiments were performed with both $I_{Cl.b}$ and $I_{Cl.swell}$ to determine whether they respond similarly to drug interventions, as would be expected if they are carried by the same underlying volume-sensitive current mechanism.

Effects of α-Adrenoceptor Stimulation on $I_{Cl.b}$ and $I_{Cl.swell}$

Fig 5 shows the effects of varying concentrations of phenylephrine on $I_{Cl.b}$. $I_{Cl.b}$ was present as soon as the first voltage-clamp steps could be made after membrane rupture, capacitance compensation, and measurement of series and input resistance (Fig 5A) and did not change during 20 minutes of observation (Fig 5B). Subsequent superfusion of the cells with the α-adrenoceptor agonist phenylephrine in the presence of the β-adrenoceptor antagonist propranolol (1 μmol/L) caused a concentration-dependent inhibition of $I_{Cl.b}$ (Fig 5C through 5E). At +20 mV in four experiments in which all drug concentrations could be tested in each cell, 5 μmol/L phenylephrine caused a 9.8±1.5% reduction ($P<.05$), and 100 μmol/L phenylephrine reduced the current by 48±1% ($P<.001$). At a greater concentration (800 μmol/L), phenylephrine suppressed $I_{Cl.b}$ by 82±4%, an effect that disappeared in the example shown after 45 minutes of washout (Fig 5F). The concentration-response curve for phenylephrine inhibition of outward current at +20 mV is shown in Fig 5G. The EC_{50} for phenylephrine inhibition of $I_{Cl.b}$ averaged 86±5 μmol/L in four cells in which all drug concentrations could be studied.

Fig 6 shows the response of $I_{Cl.swell}$ to phenylephrine. Under isotonic conditions, $I_{Cl.b}$ is present (Fig 6A). Membrane conductance started to increase 3 to 5 minutes after exposure to the hypotonic solution and approached steady state values within 20 minutes (Fig 6B). Subsequent exposure to phenylephrine caused a concentration-dependent inhibition of $I_{Cl.swell}$, which was partially reversible upon washout of the largest concentration (Fig 6F). At +20 mV, the EC_{50} for phenylephrine action on $I_{Cl.swell}$ averaged 72±7 μmol/L (n=9), not significantly different from the EC_{50} for phenylephrine inhibition of $I_{Cl.b}$. Although phenylephrine was somewhat more potent at inhibiting $I_{Cl.swell}$ at more positive potentials (EC_{50} of 90±13, 71±10, 72±7, 77±8, 64±4, and 64±5 μmol/L at test potentials of −100, −80, +20, +40,

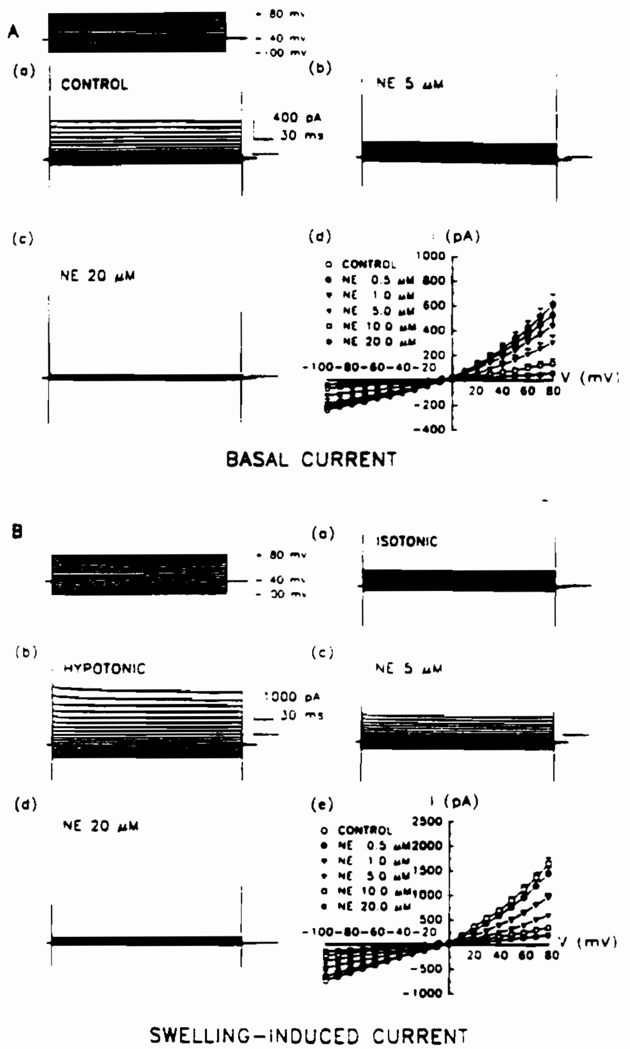

FIG 7. Inhibition of $I_{Cl.b}$ (A) and $I_{Cl.swell}$ (B) by norepinephrine (NE) in the presence of 1 μmol/L propranolol. A, Currents under isotonic control conditions (a) and in the presence of NE at 5 (b) and 20 (c) μmol/L. I-V relations for $I_{Cl.b}$ in the absence and presence of NE are shown (d). B, Currents under isotonic conditions (a), after superfusion with hypotonic superfusate (b), and in the presence of NE at 5 (c) and 20 (d) μmol/L. I-V relations for $I_{Cl.swell}$ in the absence and presence of NE are shown (e). Results shown for I-V relations of $I_{Cl.b}$ and $I_{Cl.swell}$ are for four cells, each studied under control conditions and in the presence of all [NE] values.

+60. and +80 mV. respectively; n=9 for each). these differences were not statistically significant (ANOVA).

To determine whether the changes observed with phenylephrine are also produced by the endogenous neurotransmitter norepinephrine, we studied the concentration-dependent effects of norepinephrine (in the presence of 1 μmol/L propranolol) on $I_{Cl.b}$ and $I_{Cl.swell}$, as shown in Fig 7. Norepinephrine produced a concentration-dependent and voltage-independent inhibition of $I_{Cl.b}$ (Fig 7A) and $I_{Cl.swell}$ (Fig 7B), with EC_{50} values of 2.6±0.1 μmol/L (n=4) and 2.8±0.4 μmol/L (n=4), respectively. The results shown in Figs 5 through 7 indicate that α-adrenergic stimulation is highly effective in inhibiting the volume-sensitive Cl^- currents ($I_{Cl.b}$ and $I_{Cl.swell}$) in rabbit atrial myocytes. The similar sensitivity of $I_{Cl.b}$ and $I_{Cl.swell}$ to both phenylephrine and norepinephrine supports the contention that both currents are carried by the same underlying mechanism.

Effects of Selective α-Receptor Antagonists on Phenylephrine Action

Fig 8 illustrates the antagonism of the effects of phenylephrine on $I_{Cl.swell}$ by the α_1-adrenoceptor antagonist prazosin. Fig 8A, a and b, shows currents before and after the induction of cell swelling in a representative myocyte. Exposure to prazosin (2 μmol/L) in the absence of phenylephrine did not alter $I_{Cl.swell}$ (Fig 8A, c). Exposure to 800 μmol/L phenylephrine in the continued presence of prazosin inhibited $I_{Cl.swell}$ (Fig 8A, d) but to a much smaller extent than the same concentration of phenylephrine in cells not exposed to prazosin (eg, compare with Figs 5E and 6E). Subsequent exposure to a superfusate containing the same concentration of phenylephrine in the absence of prazosin resulted in much stronger inhibition of $I_{Cl.swell}$ (Fig 8A, e), which was partially reversed by the reintroduction of prazosin (Fig 8A, f).

Fig 8B shows mean I-V relations for $I_{Cl.swell}$ under control conditions, in the presence of 2 μmol/L prazosin alone, in the presence of 800 μmol/L phenylephrine and 2 μmol/L prazosin, and in the presence of 800 μmol/L phenylephrine alone in four cells exposed to all conditions. Prazosin alone did not alter the I-V curve, and phenylephrine strongly inhibited the current at all voltages. The effect of phenylephrine was greatly attenuated by coadministration with prazosin. Prazosin (2 μmol/L) shifted the phenylephrine concentration-response curve in a parallel fashion to the right (Fig 8C), with the phenylephrine EC_{50} at +20 mV increased by prazosin from 72±7 to 737±99 μmol/L (n=6, $P<.001$).

To gain insights into the α_1-receptor subtype mediating the effect of phenylephrine on $I_{Cl.swell}$, we studied the effect of the α_{1A}-receptor antagonists (+)-niguldipine and 5MU and the α_{1B}-receptor antagonist CEC on the phenylephrine concentration-response curve. As shown in Fig 9, even large concentrations of CEC (100 μmol/L) did not perceptibly alter the response to phenylephrine. On the other hand, 0.1 μmol/L 5MU substantially inhibited the action of phenylephrine, with relatively little current inhibition occurring at a concentration of 800 μmol/L.

The actions of several antagonists were assessed quantitatively by studying their effects on the phenylephrine concentration-response curve (Fig 10). While CEC (100 μmol/L) did not significantly alter the phenylephrine EC_{50} (84±12 μmol/L in presence of CEC, n=8, P=NS vs phenylephrine alone), (+)-niguldipine, 5MU, and prazosin all significantly ($P<.001$ for each) increased the phenylephrine EC_{50} by shifting the concentration-response curve to the right in a parallel fashion (Fig 10). The action of (+)-niguldipine was concentration dependent [EC_{50} of 368±74 and 691±47 μmol/L for 0.1 and 1.0 μmol/L (+)-niguldipine, respectively; n=4 for each], and its potency was substantially less than that of 5MU. 5MU, at a concentration of 0.1 μmol/L, increased the phenylephrine EC_{50} in five cells to 2418±53 μmol/L, a greater increase than produced by a 10 times higher concentration of (+)-niguldipine. None of the antagonists significantly altered the E_{max} for phenylephrine, which averaged 93±4% under control conditions and 94±3%, 93±3%, 91±5%, 96±2%, and 99±1% in the presence of prazosin, CEC, niguldipine at 0.1 μmol/L, niguldipine at 1 μmol/L, and 5MU, respectively.

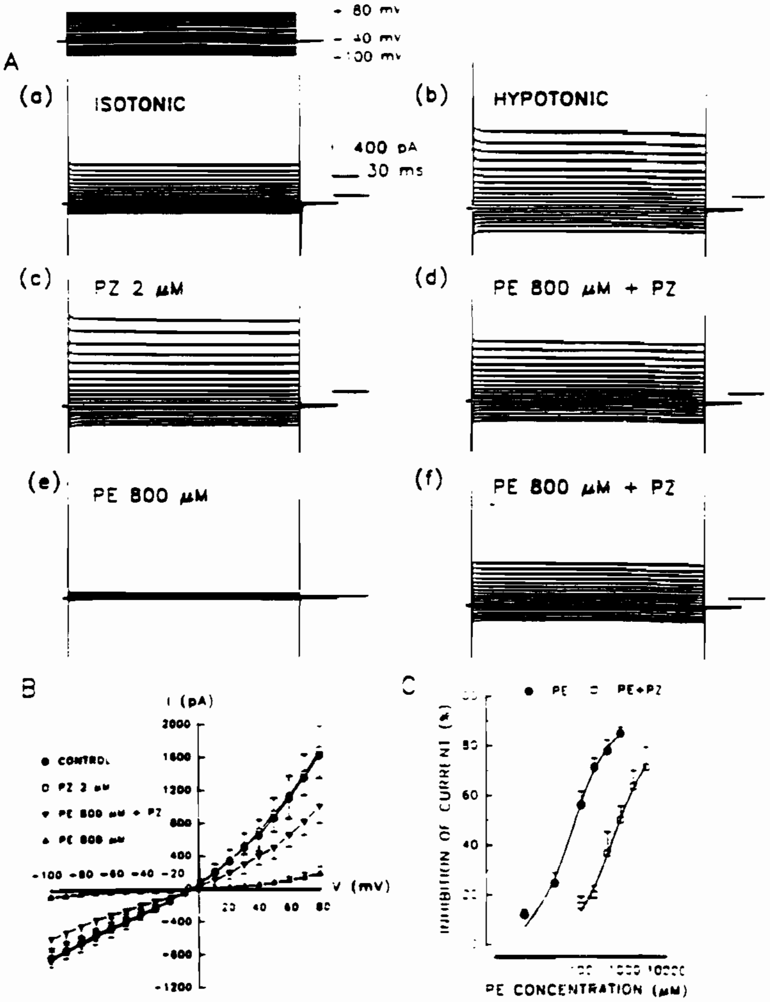

FIG 8. Inhibition of the effect of phenylephrine (PE) on $I_{Cl.swell}$ by 2 μmol/L prazosin (PZ). A, Sample recordings from a representative cell: a, recordings were obtained under isotonic conditions; b, currents were recorded after changing to standard hypotonic superfusate; c, recordings were obtained 5 minutes after changing to a hypotonic superfusate containing 2 μmol/L PZ (PZ did not alter the currents recorded); d, addition of 800 μmol/L PE in the presence of PZ caused a modest reduction in $I_{Cl.swell}$; e, currents were markedly reduced after a change to a hypotonic superfusate with PE in the absence of PZ; and f, currents increased when superfusion with a hypotonic solution containing both PE and PZ was resumed. B, I-V relations obtained under control conditions (●), in the presence of PZ (□), in the presence of both PE and PZ (▼), and in the presence of PE alone (▲) in four cells studied under all conditions. C, Concentration-response curve for PE inhibition of $I_{Cl.swell}$ at +20 mV in the absence (●, nine cells) and presence (□, six cells) of 2 μmol/L PZ. The best-fit curve (shown) to the E_{max} equation provided in the text had an EC_{50} of 635 μmol/L and an E_{max} of 85% in the presence of PZ and an EC_{50} of 61 μmol/L and an E_{max} of 91% in the absence of PZ.

Effects of PKC Inhibition on the Response of $I_{Cl.swell}$ and $I_{Cl.h}$ to α-Adrenoceptor Agonists

To determine whether the α-adrenoceptor–induced decrease in $I_{Cl.swell}$ is mediated by the activation of PKC, we applied phenylephrine in the presence of the PKC inhibitors staurosporine[40] and H-7.[41] Fig 11A shows the effect of staurosporine on the response of $I_{Cl.swell}$ to phenylephrine. In contrast to the reproducible inhibition caused by phenylephrine in the absence of PKC inhibitors (eg, Figs 5 and 6), 800 μmol/L phenylephrine had minimal effect on Cl^- current in their presence. Fig 11B shows overall data for the concentration-dependent inhibitory effects of phenylephrine on $I_{Cl.swell}$ under control conditions (n=9) and in the presence of 100 nmol/L staurosporine (n=6) and 20 μmol/L H-7 (n=5). In the presence of PKC inhibitors, no statistically significant effects of phenylephrine on $I_{Cl.swell}$ could be demonstrated at concentrations up to 1600 μmol/L.

Organic PKC inhibitors like H-7 and staurosporine are not completely specific in their actions. Therefore, additional experiments were performed to establish the effects of PKC inhibition on phenylephrine action. Prolonged stimulation (>6 hours) of PKC by phorbol esters such as PMA leads to a loss of PKC enzymatic activity and high-affinity phorbol ester binding.[9,11,42] This allows for the role of PKC to be tested in a fashion independent of the use of organic PMA inhibitors. Therefore, we incubated cells in the high-K^+ storage solution (for contents, see "Materials and Methods") overnight (>15 hours) at room temperature, with or without the addition of 500 nmol/L PMA. Experiments were done in a paired fashion, with the cells from each atrial isolate divided into two lots, one to be incubated with and the other without PMA. $I_{Cl.swell}$ and its response to phenylephrine were then assessed in cells from both groups in random order the next day. Fig 11C shows the mean concentration-response curve for phenylephrine inhibition of $I_{Cl.swell}$ at +20 mV in cells incubated with (n=5) or without (n=5) PMA, along with data from nine cells studied without prior overnight incubation. In cells incubated without PMA, phenylephrine caused a concentration-dependent inhibition of $I_{Cl.swell}$ with an EC_{50} of 66±8 μmol/L (n=5), a value not significantly different from that in cells studied without preincubation. In contrast, exposure to phenylephrine at concentrations up to 2 mmol/L did not significantly alter $I_{Cl.swell}$ in cells incubated overnight with PMA before study.

Finally, we used the recently developed and highly selective PKC inhibitor bisindolylmaleimide,[43] to determine whether PKC inhibition alters the response to norepinephrine (coadministered with 1 μmol/L propranolol). Fig 12 shows the effect of 30 nmol/L bisindolylmaleimide on the response of $I_{Cl.h}$ (panel A) and $I_{Cl.swell}$ (panel B) to norepinephrine at concentrations up to 20 μmol/L. In marked contrast to the strong inhibition of these currents caused by norepinephrine in the absence

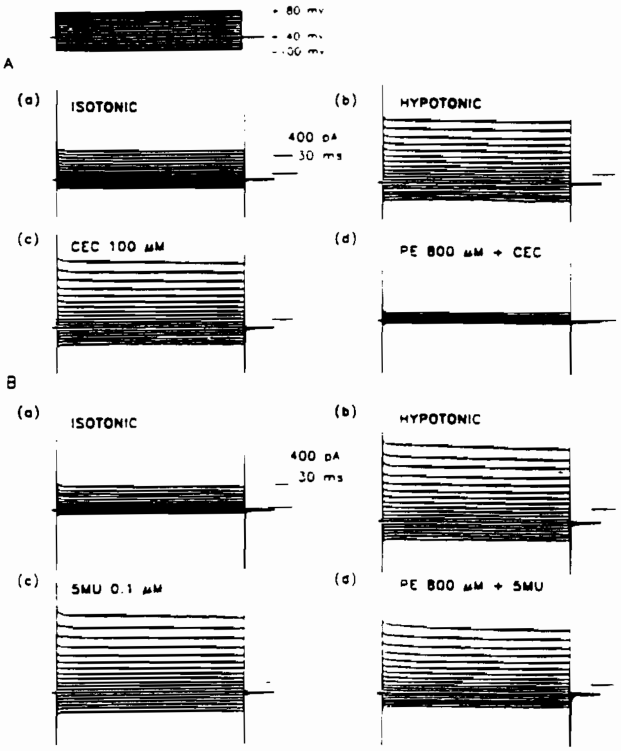

FIG 9. Changes in response to phenylephrine (PE) in the presence of CEC (A) and 5MU (B) in representative cells. A, Currents recorded in the absence of CEC are shown under isotonic (a) and hypotonic (b) conditions, followed by currents in the presence of CEC alone (c) and phenylephrine (800 μmol/L) in the presence of CEC (d). Similar results were obtained in a total of eight cells. B, Currents recorded in the absence of 5MU are similarly shown under isotonic (a) and hypotonic (b) conditions, followed by currents in the presence of 5MU alone (c) and phenylephrine (800 μmol/L) in the presence of 5MU (d). Similar results were obtained in a total of five cells.

of bisindolylmaleimide (Fig 7). PKC inhibition completely prevented α-adrenergic actions on these currents. Furthermore, the similar effects of PKC inhibition on the response to norepinephrine of $I_{Cl.b}$ and $I_{Cl.swell}$ suggest that these volume-sensitive currents are both inhibited by α-adrenergic agonists via the activation of PKC.

Effects of PKC Activators on $I_{Cl.swell}$

To further assess the ability of PKC activation to inhibit $I_{Cl.swell}$, we examined the effects of addition to the superfusate of PKC activators.[44] Fig 13 shows that PMA (50 to 800 nmol/L) induced a concentration-dependent decrease in $I_{Cl.swell}$. The EC_{50} for inhibition of $I_{Cl.swell}$ at +20 mV by PMA was 210±23 nmol/L (n=5) (Fig 13E). Similar results were obtained with OAG but at higher concentrations (5 to 200 μmol/L). The EC_{50} for inhibition of $I_{Cl.swell}$ by OAG was 47±14 μmol/L (n=5) at +20 mV (Fig 13F). To exclude a nonspecific action of phorbol esters unrelated to PKC activation, we performed blinded experiments in which coded stock solutions of either PDD or 4α-PDD (structurally very similar to PDD but ineffective in activating PKC) were used in a randomized fashion to study the changes in $I_{Cl.swell}$ caused by 1 μmol/L of each in the superfusate. Fig 14 shows results in one cell exposed to both compounds. 4α-PDD had no effect on $I_{Cl.swell}$, whereas PDD produced strong inhibition. Overall, PDD reduced $I_{Cl.swell}$ by 91±3% (n=4, $P<.001$), whereas the mean change in $I_{Cl.swell}$ occurring in the presence of 1 μmol/L 4α-PDD averaged 3±1% (n=6, P=NS). These results indicate that activators of PKC are capable of mimicking the effect of α-adrenoceptor stimulation on $I_{Cl.swell}$.

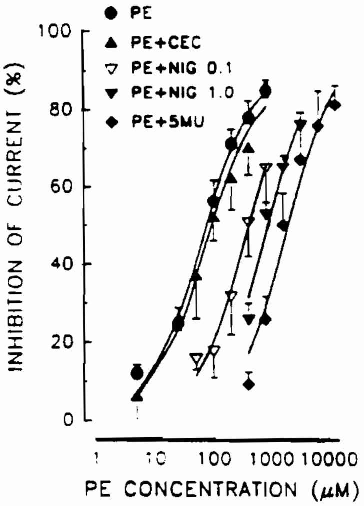

FIG 10. Concentration-dependent effects of phenylephrine (PE) alone and in the presence of CEC, (+)-niguldipine (NIG), and 5MU on $I_{Cl.swell}$. The PE concentration-response curve was not altered by 100 μmol/L CEC (▲). It was shifted to the right in a concentration-dependent way by 0.1 (▽) and 1.0 (▼) μmol/L NIG. A still greater shift was caused by 0.1 μmol/L 5MU (◆). The best-fit curves (shown) to the E_{max} equation provided in the text had EC_{50} values of 61 (PE alone), 69 (PE+CEC), 367 (PE+NIG, 0.1 μmol/L), 840 (PE+NIG, 1 μmol/L), and 1869 μmol/L (PE+5MU) and E_{max} values of 91%, 88%, 95%, 98%, and 97%, respectively.

Effects of PTX on Phenylephrine-Induced Inhibition of $I_{Cl.swell}$

Cardiac α_1-adrenoceptors are functionally linked to heterotrimeric GTP-binding regulatory proteins (G proteins),[45] which are thought to play an important role in mediating α_1-adrenoceptor–induced increases in phospholipase C activity[46,47] that result in PKC activation. PTX inactivates G proteins (G_o and G_i) that are potentially coupled with α_1-adrenoceptors.[1,48-50] by catalyzing the ADP ribosylation of the α subunit at a C-terminal cysteine residue and thus blocking the interaction between activated receptors and the holo-G protein.[51]

To determine whether the α_1-adrenergic inhibition of $I_{Cl.swell}$ is coupled via PTX-sensitive G proteins, we incubated myocytes for over 18 hours at room temperature in storage solution containing 0.5 μg/mL of PTX. This procedure has been reported to cause the ADP ribosylation of up to 90% of the available PTX-sensitive G proteins in rabbit atrial cells.[9,11] As shown in Fig 15, pretreatment of cells with PTX abolished the effect of phenylephrine (25 to 3200 μmol/L) on $I_{Cl.swell}$ (n=5). Preincubation of cells in the storage solution alone did not alter the response to phenylephrine (Fig 11C). These results indicate that PTX-sensitive G proteins are essential for the inhibition of $I_{Cl.swell}$ by α-adrenoceptor stimulation.

Discussion

We have shown that $I_{Cl.b}$ and $I_{Cl.swell}$ in rabbit atrial myocytes share properties of outward rectification, Cl⁻

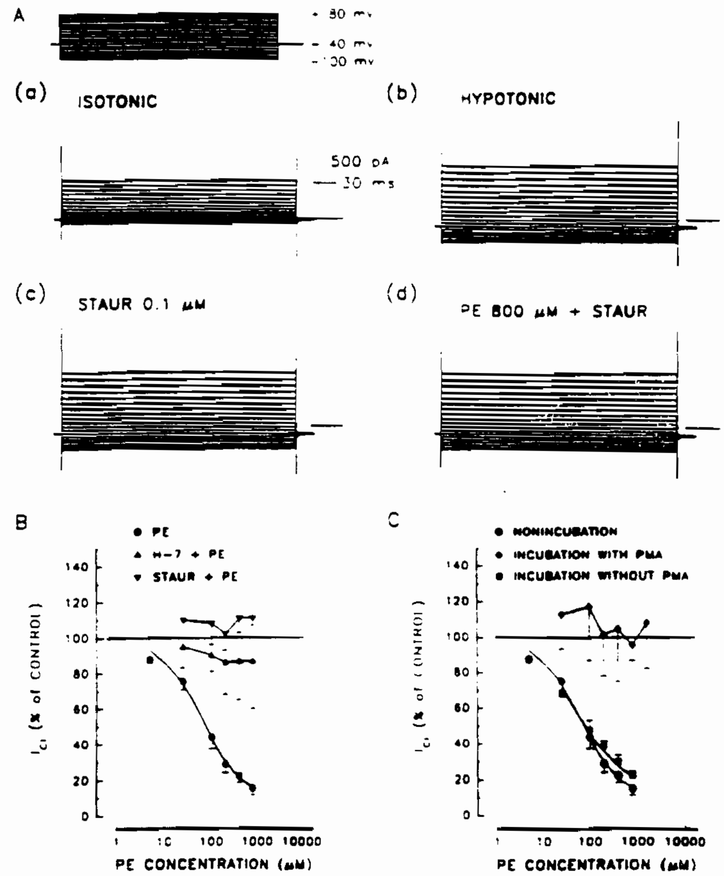

Fig 11. A, Effects of staurosporine (STAUR) on the response of $I_{Cl.swell}$ to phenylephrine (PE) in a representative cell. Currents were recorded in the presence of isotonic superfusate (a). $I_{Cl.swell}$ was recorded after superfusate was changed to hypotonic solution (b). The addition of STAUR (0.1 μmol/L) to the hypotonic superfusate did not alter $I_{Cl.swell}$ (c). When phenylephrine was added to the superfusate at 800 μmol/L in the presence of STAUR, $I_{Cl.swell}$ was not affected (d). STAUR (0.1 μmol/L) was in the pipette solution throughout the experiment. B, Concentration-response relation for PE alone (n=9 cells) and in the presence of 0.1 μmol/L STAUR (n=6) and 20 μmol/L H-7 (n=5). C, Effects of PKC downregulation with PMA on action of PE on $I_{Cl.swell}$ (I_{Cl}). Cells were incubated at room temperature in high-K^+ storage solution in the absence (n=5) or presence (n=5) of PMA. The PE concentration-response relation for cells incubated without PMA was not significantly different from that of fresh cells (nonincubation, n=9). In contrast, preincubation with PMA prevented any response to PE at concentrations up to 1600 μmol/L.

selectivity, volume regulation, and concentration-dependent inhibition by α-adrenergic agonists, suggesting that they are carried by the same underlying volume-sensitive anion conductance. The inhibitory actions of phenylephrine on $I_{Cl.swell}$ are antagonized by the α_1-receptor antagonist prazosin, not altered by the α_{1B}-receptor antagonist CEC, and prevented by the α_{1A}-selective receptor antagonists (+)-niguldipine and 5MU, indicating mediation by an α_{1A}-receptor subtype. The actions of α-adrenergic stimulation on volume-regulated Cl^- currents are mimicked by the PKC-stimulating phorbol esters PDD, PMA, and OAG and are prevented when PKC is inhibited by staurosporine, H-7, bisindolylmaleimide, or downregulation by prolonged exposure to PMA. Exposure to PTX also blocks α-adrenergic inhibition of $I_{Cl.swell}$, indicating the participation of a PTX-sensitive G protein in the signal transduction pathway leading to PKC activation by α_{1A}-receptor stimulation.

Properties of Cl^- Currents Studied

The properties of $I_{Cl.b}$ in the present experiments resemble those we have previously reported in the same preparation.[21,22] Although $I_{Cl.swell}$ has not previously been reported to exist in rabbit atrium, the properties of $I_{Cl.swell}$ described in the present article resemble those described in other cardiac preparations[23,24,26] and those of a stretch-induced Cl^- current in rabbit atrial cells.[25] The reversal potential of $I_{Cl.swell}$ responded to changes in $[Cl^-]$ gradient in a fashion consistent with a Cl^--selective current and with the same slope factor for $[Cl^-]_o$ dependence as $I_{Cl.b}$. Exposure to hyperosmotic superfusate substantially reduced $I_{Cl.b}$. $I_{Cl.b}$ and $I_{Cl.swell}$ were inhibited by α-adrenoceptor agonists in a quantitatively similar fashion, and α-adrenergic inhibition of either was PKC dependent. These findings suggest that both currents are carried by the same underlying volume-sensitive Cl^- channel.

Comparison With Previous Observations of α_1-Adrenoceptor Modulation of Ion Currents

Recent reports have indicated that α_1-adrenergic stimulation suppresses several K^+ currents, including I_{to},[6-9,52] I_{K1}, and I_{KACh}.[10,11] In their studies on rat ventricular myocytes, Ravens and colleagues[6,52] reported that α_1-adrenergic stimulation inhibited both the 4-AP–sensitive transient outward current and the 4-AP–insensitive sustained current.[6,52] In rabbit atrium, the sustained current activated by depolarization is resistant to 4-AP and has properties suggesting a potentially important contribution from $I_{Cl.b}$.[21] In the present study, we have found that α_1-adrenoceptor stimulation inhibits both $I_{Cl.b}$ and $I_{Cl.swell}$, at concentrations very similar to those found to inhibit K^+ current in other studies.[6-9,52] This is, to our knowledge, the first report of α-adrenergic inhibition of a cardiac Cl^- current.

Subtype Selectivity of α_1-Adrenoceptor Effects on $I_{Cl.swell}$

McGrath and Wilson[53] suggested the existence of two subtypes of α_1-adrenoceptors based on differences in agonist affinity. Han et al[54] and Minneman[55] classified α_1-adrenoceptors into α_{1A} and α_{1B} subtypes, based on tissue responses to various agonists and antagonists and on competitive ligand-binding studies with WB 4101 and CEC. The α_{1A} subtype has a high affinity for the competitive antagonist WB 4101 and is not inactivated by the

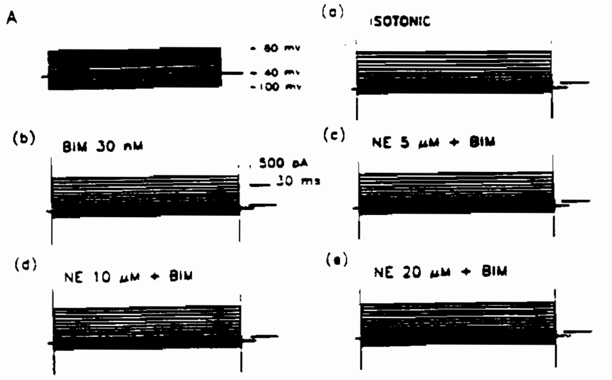

BASAL CURRENT

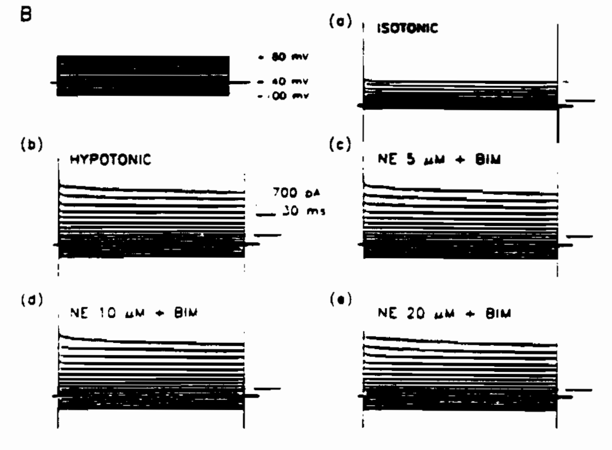

SWELLING-INDUCED CURRENT

FIG 12. Response of $I_{Cl.b}$ (A) and $I_{Cl.swell}$ (B) in typical cells to bisindolylmaleimide (BIM, 30 nmol/L) alone and to increasing concentrations of norepinephrine (NE) in the presence of 30 nmol/L BIM. Similar results were obtained in three cells for $I_{Cl.b}$ and in three cells for $I_{Cl.swell}$.

alkylating agent CEC. The α_{1B} subtype has a 20- to 1500-fold lower affinity for WB 4101 and is potently inhibited by CEC.[54-56] Additional α_{1A}-selective antagonists have been developed, including 5MU,[57,58] a serotonin antagonist, and (+)-niguldipine,[59,60] a dihydropyridine Ca^{2+} channel blocker. It has been suggested that 5MU is currently the best antagonist for identifying α_{1A}-receptor–mediated responses.[61] Recently, two additional subtypes of α-adrenoceptors, α_{1C} and α_{1D}, have been identified on the basis of molecular cloning.[62,63] The α_{1D}-receptor differs from the α_{1A}-receptor clone by two amino acids and, in contrast to the latter, is sensitive to inhibition by CEC.[62] The α_{1C}-receptor shows exquisite and equal sensitivity to inhibition by (+)-niguldipine and 5MU, whereas the α_{1A}-receptor is >10 times as sensitive to 5MU as it is to (+)-niguldipine.[63]

In the present study, phenylephrine-induced inhibition of $I_{Cl.swell}$ was unaffected by CEC at high concentrations but was inhibited by (+)-niguldipine and 5MU, showing particular sensitivity [>10-fold greater than that to (+)-niguldipine] to the latter agent. These observations suggest the involvement of an α_{1A} type of receptor. Both α_{1A}- and α_{1B}-receptors have been shown to exist in canine ventricle on the basis of radioligand and electrophysiological studies.[64] The α_{1A}-receptor–mediated system is involved in the induction of abnormal automaticity in canine cardiac Purkinje fibers exposed to ischemic conditions.[65-67] This system is PTX sensitive[66,67] and causes an increase in longitudinal resistance consistent with a decrease in membrane conductance.[67] It would be interesting to explore the possible activation of volume-sensitive Cl^- currents by ischemia in canine Purkinje fibers, which could be amenable to α-adrenergic inhibition by the system described in the present study.

Intracellular Signaling Mechanisms Underlying α-Adrenergic Modulation of $I_{Cl.swell}$

Stimulation of α_1-adrenoceptors leads to various biochemical responses, including enhanced Ca^{2+} influx, phospholipase C and A_2 activation, and changes in intracellular cyclic nucleotide levels.[2,55,68,69] In the heart, the most extensively documented signaling responses to α_1-adrenoceptor stimulation are mediated via phospholipase C–induced hydrolysis of phosphatidylinositol 4,5-diphosphate, giving rise to a variety of potential second messengers, including inositol 1,4,5-tris-phosphate and 1,2-diacylglycerol,[49,69-71] which is thought to be an endogenous activator of PKC.[68,69] PKC has been implicated in the modulation of ion channel function in numerous studies.[44] Many of the signaling mechanisms mediating α-adrenoceptor–induced responses are coupled by G proteins, at least two of which are sensitive to inhibition by PTX.[48]

PTX-sensitive G proteins, which may appear with development,[72] mediate the effects of α_1-adrenergic stimulation on abnormal automaticity in canine Purkinje fibers[66,67] and the positive chronotropic response to α agonists in rat hearts.[72] PKC produces action potential changes similar to those caused by methoxamine in guinea pig papillary muscles,[12] and phospholipase C produces positive chronotropic responses in canine Purkinje fibers similar to those resulting from α-adrenergic stimulation.[73] In contrast, α-adrenergic inhibition of a variety of K^+ currents in rabbit atrial myocytes is insensitive to PTX and agents that inhibit PKC activity.[9,11] In the present study, α_1-adrenergic inhibition of Cl^- current was found to be sensitive to inhibition by PTX and interventions that suppress PKC function, making this system a candidate to account for some of the electrophysiological effects of α-adrenergic activation. Our findings are consistent with studies in which PKC activation caused a reduction in Cl^- currents in a variety of noncardiac preparations.[74-76]

Limitations

Both $I_{Cl.b}$ and $I_{Cl.swell}$ are inhibited by α_1-agonists, which raises a potential problem. Since in many cells $I_{Cl.swell}$ is composed of both a basal ($I_{Cl.b}$) and swelling-induced component, the observed changes in total Cl^- current represent the sum of α-adrenergic effects on each. To have studied each selectively in each cell would have been prohibitively difficult, requiring exposure to control solutions, multiple drug concentrations, hypotonic solutions, and then the same drug concentrations again. We have presented extensive evidence (in Figs 1 through 7 and Fig 12), discussed above, suggesting that $I_{Cl.b}$ and $I_{Cl.swell}$ are due to the same volume-sensitive anion conductance and justifying the use of $I_{Cl.swell}$ as an index of mechanisms of α-adrenergic regulation of volume-sensitive Cl^- current.

The response of $I_{Cl.b}$ and $I_{Cl.swell}$ in rabbit atrial myocytes to α-adrenergic and PKC stimulation that we

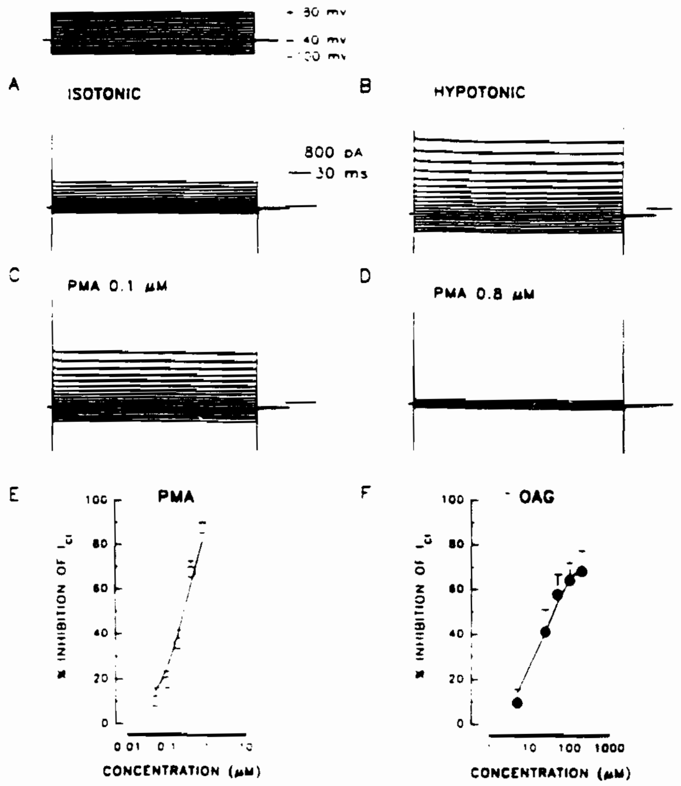

FIG 13. Concentration-dependent inhibition of $I_{Cl.swell}$ by PMA. Currents were recorded from one cell under isotonic (A) and hypotonic (B) superfusate conditions in the absence of PMA and then in the presence (C and D) of increasing PMA concentrations. E and F, Concentration-response curves for inhibition of $I_{Cl.swell}$ (I_{Cl}) by PMA (E) and OAG (F).

observed is opposite the response to the Cl^- current stimulation noted in feline and guinea pig ventricular myocytes by Zhang and colleagues[30,31] and Walsh and Long.[28,29] Recently published work by Zhang et al[31] suggests that PKC and protein kinase A may act on the same set of Cl^- channels to elicit Cl^- current in feline ventricular myocytes. Rabbit atrium lacks transcripts for the cystic fibrosis transmembrane conductance regulator[77] and $I_{Cl.cAMP}$,[78] which appears to be the target for PKC activation of Cl^- current.[31] This may explain the apparently simple inhibitory effect of α_1-adrenergic activation on $I_{Cl.b}$ and $I_{Cl.swell}$ that we observed. Under conditions that cause cell swelling in tissues that express both $I_{Cl.swell}$ and $I_{Cl.PKC}$, a more complex response to α_1-adrenergic activation, including both stimulation of $I_{Cl.PKC}$ and inhibition of $I_{Cl.swell}$, might occur. This question remains to be addressed in future studies. Walsh and Long[29] cite unpublished results suggesting that in guinea pig ventricular myocytes, which manifest $I_{Cl.PKC}$, $I_{Cl.swell}$ is absent.

The response of $I_{Cl.b}$ to hypertonic superfusate raises the question of whether cell swelling or cell stretch occurred during cell isolation, resulting in the activation of $I_{Cl.swell}$, which then appeared as a background current at the onset of whole-cell recording. An alternative explanation of these findings is that rabbit atrial cells have a background Cl^- current that is sensitive to cell volume (and possibly cell stretch), and can be enhanced by exposure to hypotonic media (which cause cell swelling) or suppressed by exposure to hypertonic media

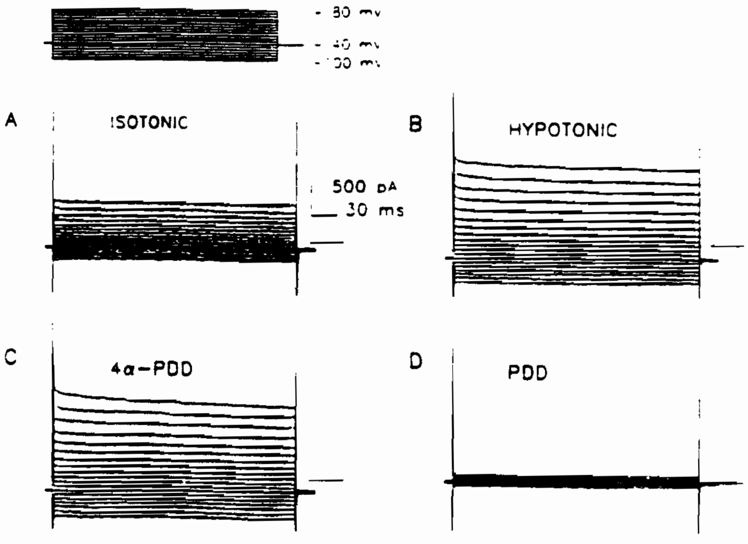

FIG 14. Effects of 1 μmol/L PDD and the same concentration of its inactive 4α analogue (4α-PDD) on $I_{Cl.swell}$ upon blinded administration to a typical cell. A, Currents were recorded under isotonic conditions. B, Currents were recorded after hypotonic superfusate–induced swelling. C, No changes in currents were observed 10 minutes after the addition of 1 μmol/L 4α-PDD. D, Ten minutes of subsequent superfusion with 1 μmol/L PDD produced profound depression of $I_{Cl.swell}$. Similar results were obtained in six cells with 4α-PDD and in four with PDD.

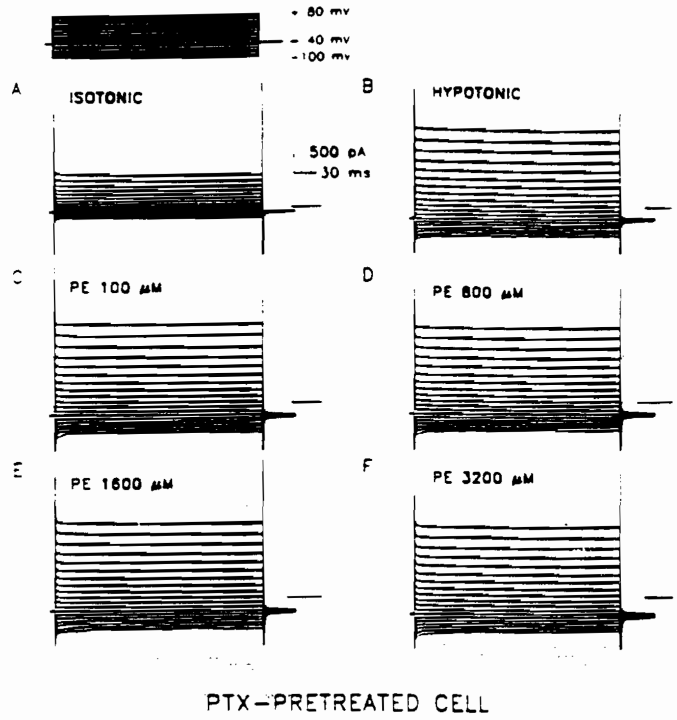

Fig 15. Effect of >18-hour incubation in high-K^+ storage solution containing 0.5 μg/mL PTX on the response to phenylephrine (PE). Currents in the absence of PE under isotonic (A) and hypotonic (B) conditions were similar to those recorded in fresh cells. The addition of increasing PE concentrations to the hypotonic superfusate (C through F) failed to alter $I_{Cl.swell}$ in cells pretreated with PTX. Similar results were obtained in a total of five cells incubated with PTX. Incubation in the storage solution alone did not alter the response of $I_{Cl.swell}$ to PE (squares in Fig 7).

(which cause cell shrinkage). If this were the case, the volume-sensitive Cl^- current could modulate cell function in response to either an increase or a decrease in cell volume.

We obtained concentration-response curves by exposing each cell to five or six drug concentrations over the steep portion of the concentration response curve. Since saturating concentrations were not studied in all cells, there is some uncertainty about the precise maximum inhibition caused by α-agonists, introducing some uncertainty in the calculation of EC_{50} values. These uncertainties are relatively small and do not alter the qualitative differences that were seen among various α-receptor antagonists.

Conclusions

We have found that α_1-adrenergic activation inhibits the volume-regulated Cl^- currents $I_{Cl,b}$ and $I_{Cl.swell}$ in rabbit atrial myocytes by a PTX-sensitive PKC-dependent mechanism. This is, to our knowledge, the first demonstration of the inhibition of Cl^- current by an α-adrenergic mechanism in the heart. It contrasts with the stimulatory effect of PKC on Cl^- current previously described in ventricular tissues from the cat and guinea pig and indicates the potential complexity of the α-adrenergic regulation of cardiac Cl^- currents. The inhibition of $I_{Cl,b}$ by α_1-adrenergic activation could contribute to some of the electrophysiological effects of the latter, and α-adrenergic inhibition of $I_{Cl.swell}$ may play a role in settings, such as acute myocardial ischemia and heart failure, in which catecholamine concentrations are increased and cell swelling and/or stretch can activate $I_{Cl.swell}$.

Acknowledgments

This study was supported by operating grants from the Medical Research Council of Canada, the Quebec Heart Foundation, and the Fonds de Recherche de l'Institut de Cardiologie de Montreal. D. Duan holds an MRC graduate studentship. The authors thank Guylaine Nicol and Ling Yu Ye for technical assistance and Martine Dufort and Luce Bégin for typing the manuscript.

References

1. Benfey BG. Function of myocardial α-adrenoceptors. *Life Sci*. 1990:46:743-757.
2. Fedida D. Modulation of cardiac contractility by α_1 adrenoceptors. *Cardiovasc Res*. 1993:27:1735-1742.
3. Rosen MR. Membrane effects of α adrenergic catecholamines. In: Rosen MR, Janse MJ, Wit AL, eds. *Cardiac Electrophysiology: A Textbook*. Mt Kisco, NY: Futura Publishing Co: 1990:847-856.
4. Apkon M, Nerbonne JM. α_1-Adrenergic agonists selectively depress voltage-dependent K^+ currents in rat ventricular myocytes. *Proc Natl Acad Sci U S A*. 1988:85:8756-8760.
5. Tohse N, Nakaya H, Hattori Y, Endou M, Kanno M. Inhibitory effect mediated by α_1-adrenoceptors on transient outward current in isolated rat ventricular cells. *Pflugers Arch*. 1990:415:575-581.
6. Wang X-L, Wettwer E, Gross G, Ravens U. Reduction of cardiac outward currents by alpha-1 adrenoceptor stimulation: a subtype-specific effect? *J Pharmacol Exp Ther*. 1991:259:783-788.
7. Fedida D, Shimoni Y, Giles WR. A novel effect of norepinephrine on cardiac cells is mediated by α_1-adrenoceptors. *Am J Physiol*. 1989:256:H1500-H1504.
8. Fedida D, Shimoni Y, Giles WR. α-Adrenergic modulation of the transient outward current in rabbit atrial myocytes. *J Physiol (Lond)*. 1990:423:257-277.
9. Braun AP, Fedida D, Clark RB, Giles WR. Intracellular mechanisms for α_1-adrenergic regulation of the transient outward current in rabbit atrial myocytes. *J Physiol (Lond)*. 1990:431:689-712.
10. Fedida D, Braun AP, Giles WR. α_1-Adrenoceptors reduce background K^+ current in rabbit ventricular myocytes. *J Physiol (Lond)*. 1991:441:673-684.
11. Braun AP, Fedida D, Giles WR. Activation of α_1-adrenoceptors modulates the inwardly rectifying potassium currents of mammalian atrial myocytes. *Pflugers Arch*. 1992:421:431-439.
12. Dirksen RT, Sheu SS. Modulation of ventricular action potential by α_1-adrenoceptors and protein kinase C. *Am J Physiol*. 1990:258:H907-H911.
13. Tohse N, Nakaya H, Kanno M. α_1-Adrenoceptor stimulation enhances the delayed rectifier K^+ current of guinea pig ventricular cells through the activation of protein kinase C. *Circ Res*. 1992:71:1441-1446.

14. Bahinski A, Nairn AC, Greengard P, Gadsby DC. Chloride conductance regulated by cyclic AMP-dependent protein kinase in cardiac myocytes. *Nature*. 1989;340:718-721.
15. Harvey RD, Hume JR. Autonomic regulation of a chloride current in heart. *Science*. 1989;244:983-985.
16. Harvey RD, Hume JR. Isoproterenol activates a chloride current, not the transient outward current, in rabbit ventricular myocytes. *Am J Physiol*. 1989;257:C1177-C1181.
17. Harvey RD, Clark CD, Hume JR. Chloride current in mammalian cardiac myocytes: novel mechanism for autonomic regulation of action potential duration and resting membrane potential. *J Gen Physiol*. 1990;95:1077-1102.
18. Matsuoka S, Ehara T, Noma A. Chloride-sensitive nature of the adrenaline-induced current in guinea-pig cardiac myocytes. *J Physiol (Lond)*. 1990;425:579-598.
19. Zygmunt AC, Gibbons WR. Calcium-activated chloride current in rabbit ventricular myocytes. *Circ Res*. 1991;68:424-437.
20. Zygmunt AC, Gibbons WR. Properties of the calcium-activated chloride current in heart. *J Gen Physiol*. 1992;99:391-414.
21. Duan D-Y, Fermini B, Nattel S. Sustained outward current observed after I_{to1} inactivation in rabbit atrial myocytes is a novel Cl^- current. *Am J Physiol*. 1992;263:H1967-H1971.
22. Duan D, Nattel S. Properties of single outwardly rectifying Cl^- channels in heart. *Circ Res*. 1994;75:789-795.
23. Sorota S. Swelling-induced chloride-sensitive current in canine atrial cells revealed by whole-cell patch-clamp method. *Circ Res*. 1992;70:679-687.
24. Tseng G-N. Cell swelling increases membrane conductance of canine cardiac cells: evidence for a volume-sensitive Cl channel. *Am J Physiol*. 1992;262:C1056-C1068.
25. Hagiwara N, Masuda H, Shoda M, Irisawa HJ. Stretch-activated anion currents of rabbit cardiac myocytes. *J Physiol (Lond)*. 1992;456:285-302.
26. Zhang J, Rasmusson RL, Hall SK, Lieberman M. A chloride current associated with swelling of cultured chick heart cells. *J Physiol (Lond)*. 1993;472:801-820.
27. Matsuura H, Ehara T. Activation of chloride current by purinergic stimulation in guinea pig heart cells. *Circ Res*. 1992;70:851-855.
28. Walsh KB. Activation of a heart chloride current during stimulation of protein kinase C. *Mol Pharmacol*. 1991;40:342-346.
29. Walsh KB, Long KJ. Properties of a protein kinase C–activated chloride current in guinea pig ventricular myocytes. *Circ Res*. 1994;74:121-129.
30. Zhang K, Barrington P, Ten Eick RE. A Cl^- dependent current induced by PHE and PMA mimics isoproterenol-induced DIDS-sensitive I_{Cl^-}. *Biophys J*. 1992;61:A146. Abstract.
31. Zhang K, Barrington PL, Martin RL, Ten Eick RE. Protein kinase–dependent Cl^- currents in feline ventricular myocytes. *Circ Res*. 1994;75:133-143.
32. Carmeliet EE. Chloride ions and the membrane potential of Purkinje fibers. *J Physiol (Lond)*. 1961;156:375-388.
33. Vaughan-Jones RD. Chloride activity and its control in skeletal and cardiac muscle. *Philos Trans R Soc Lond [Biol]*. 1982;299:537-548.
34. Tranum-Jensen J, Janse MJ, Fiolet JWT, Krieger WJG, D'Alnoncourt CN, Durrer D. Tissue osmolality, cell swelling, and reperfusion in acute regional myocardial ischemia in the isolated porcine heart. *Circ Res*. 1981;49:364-381.
35. Corr PB, Gillis RA. Autonomic neural influences on the dysrhythmias resulting from myocardial infarction. *Circ Res*. 1978;43:1-9.
36. Hasking GJ, Esler MD, Jennings GL, Burton D, Johns JA, Korner PI. Norepinephrine spillover to plasma in patients with congestive heart failure: evidence of increased overall and cardiorenal sympathetic nervous activity. *Circulation*. 1986;73:615-621.
37. Duan D, Fermini B, Nattel S. Potassium channel blocking properties of propafenone in rabbit atrial myocytes. *J Pharmacol Exp Ther*. 1993;264:1113-1123.
38. Giles WR, van Ginneken ACG. A transient outward current in isolated cells from the crista terminalis of rabbit heart. *J Physiol (Lond)*. 1985;368:243-264.
39. Tallarida RJ, Murray RB, eds. *Manual of Pharmacologic Calculation with Computer Programs*. New York, NY: Springer-Verlag; 1981.
40. Tamaoki T, Nomoto H, Takahashi I, Kato Y, Morimoto M, Tomita F. Staurosporine, a potent inhibitor of phospholipid/Ca^{2+} dependent protein kinase. *Biochem Biophys Res Commun*. 1986;135:397-402.
41. Hidaka H, Inagaki M, Kawamoto S, Sasaki Y. Isoquinolinesulfonamides, novel and potent inhibitors of cyclic nucleotide dependent protein kinase and protein kinase C. *Biochemistry*. 1984;23:5036-5041.
42. Henrich CJ, Simpson PC. Differential acute and chronic response of protein kinase C in cultured neonatal rat heart myocytes to α_1-adrenergic and phorbol ester stimulation. *J Mol Cell Cardiol*. 1988;20:1081-1085.
43. Toullec D, Pianetti P, Coste H, Bellevergue P, Grand-Perret T, Ajakane M, Baudet V, Boissin P, Boursier E, Loriolle F, Duhamel L, Charon D, Kirilovsky J. The bisindolylmaleimide GF 109203X is a potent and selective inhibitor of protein kinase C. *J Biol Chem*. 1991;266:15771-15781.
44. Shearman MS, Sekiguchi K, Nishizuka Y. Modulation of ion channel activity: a key function of the protein kinase C enzyme family. *Pharmacol Rev*. 1989;41:211-237.
45. Casey PJ, Gilman AG. G protein involvement in receptor-effector coupling. *J Biol Chem*. 1988;263:2577-2580.
46. Litosch I, Fain JN. Regulation of phosphoinositide breakdown by guanine nucleotides. *Life Sci*. 1986;39:187-194.
47. Boyer JL, Hepler JR, Harden TK. Hormones and growth factor receptor-mediated regulation of phospholipase C activity. *Trends Pharmacol Sci*. 1989;10:360-364.
48. Fleming JW, Wisler PL, Watanabe AM. Signal transduction by G proteins in cardiac tissues. *Circulation*. 1992;85:420-433.
49. Steinberg SF, Drugge ED, Bilezikian JP, Robinson RB. Acquisition by innervated cardiac myocytes of a pertussis toxin-specific regulatory protein linked to the α_1-receptor. *Science*. 1985;230:186-188.
50. Szabo G, Otero AS. G protein mediated regulation of K^+ channels in heart. *Annu Rev Physiol*. 1990;52:293-305.
51. Birnbaumer L, Abramowitz J, Brown AM. Receptor-effector coupling by G proteins. *Biochim Biophys Acta*. 1990;1031:163-224.
52. Ravens U, Wang X-L, Wettwer E. Alpha adrenoceptor stimulation reduces outward currents in rat ventricular myocytes. *J Pharmacol Exp Ther*. 1989;250:364-370.
53. McGrath J, Wilson V. Alpha$_1$-adrenoceptor classification by classical and response-related methods: same questions, different answers. *Trends Pharmacol Sci*. 1988;9:421-423.
54. Han C, Abel PW, Minneman KP. α_1-Adrenoceptor subtypes linked to different mechanisms for increasing intracellular Ca^{2+} in smooth muscle. *Nature*. 1987;329:333-335.
55. Minneman KP. α_1-Adrenergic receptor subtypes, inositol phosphates, and sources of cell Ca^{2+}. *Pharmacol Rev*. 1988;40:87-119.
56. Morrow AL, Creese I. Characterization of α_1-adrenergic receptor subtypes in rat brain: a reevaluation of [^{3}H]WB4104 and [^{3}H]prazosin binding. *Mol Pharmacol*. 1986;29:321-330.
57. Gross G, Hanft G, Rugevics C. 5-Methyl-urapidil discriminates between subtypes of the α_1-adrenoceptor. *Eur J Pharmacol*. 1988;151:333-335.
58. Hanft G, Gross G. Subclassification of α_1-adrenoceptor recognition sites by urapidil derivatives and other selective antagonists. *Br J Pharmacol*. 1989;97:691-700.
59. Boer R, Grassegger A, Schudt CH, Glossmann H. (+)-Niguldipine binds with very high affinity to Ca^{2+} channels and to subtype of α_1-adrenoceptors. *Eur J Pharmacol*. 1989;172:131-145.
60. Graziadei I, Zernig G, Boer R, Glossman H. Stereoselective binding of niguldipine enantiomers to α_{1A}-adrenoceptors labeled with ^{3}H-5-methyl-urapidil. *Eur J Pharmacol*. 1989;172:329-337.
61. Han C, Minneman KP. Interaction of subtype-selective antagonists with α_1-adrenergic receptor binding sites in rat tissues. *Mol Pharmacol*. 1991;40:531-538.
62. Perez D, Piascik MT, Graham RM. Solution-phase library screening for the identification of rare clones: isolation of an α_{1D}-adrenergic receptor cDNA. *Mol Pharmacol*. 1991;40:876-883.
63. Forray C, Bard JA, Wetzel JM, Chiu G, Shapiro E, Tang R, Lepor H, Hartig PR, Weinshank RL, Branchek TA, Gluchowski C. The α_1-adrenergic receptor that mediates smooth muscle contraction in human prostate has the pharmacological properties of the cloned human α_{1c} subtype. *Pharmacol Exp Ther*. 1994;45:703-708.
64. del Balzo U, Rosen MR, Malfatto G, Kaplan LM, Steinberg SF. Specific α_1-adrenergic receptor subtypes modulate catecholamine-induced increases and decreases in ventricular automaticity. *Circ Res*. 1990;67:1535-1551.
65. Molina-Viamonte V, Anyukhovsky EP, Rosen MR. An α_1-adrenergic receptor subtype is responsible for delayed afterdepolarizations and triggered activity during simulated ischemia and reperfusion of isolated canine Purkinje fibers. *Circulation*. 1991;84:1732-1740.
66. Anyukhovsky EP, Rybin VO, Nikashin AV, Budanova OP, Rosen MR. Positive chronotropic responses induced by α_1-adrenergic stimulation of normal and 'ischemic' Purkinje fibers have different receptor–effector coupling mechanisms. *Circ Res*. 1992;71:526-534.
67. Anyukhovsky EP, Steinberg SF, Cohen IS, Rosen MR. Receptor-effector coupling pathway for α_1-adrenergic modulation of

abnormal automaticity in 'ischemic' canine Purkinje fibers. *Circ Res*. 1994;74:937-944.

68. Exton JH. The roles of calcium and phosphoinositides in the mechanisms of α_1-adrenergic and other agonists. *Rev Physiol Biochem Pharmacol*. 1988;111:118-224.
69. Fedida D, Braun AP, Giles WR. α_1-Adrenoceptors in myocardium: functional aspects and transmembrane signaling mechanisms. *Physiol Rev*. 1993;73:469-487.
70. Brown JH, Buxton IL, Brunton LL. α_1-Adrenergic and muscarinic cholinergic stimulation of phosphoinositide hydrolysis in adult rat cardiomyocytes. *Circ Res*. 1985;57:532-537.
71. Otani H, Otani H, Das DK. α_1-Adrenoceptor-mediated phosphoinositide breakdown and inotropic response in rat left ventricular papillary muscles. *Circ Res*. 1988;62:8-17.
72. Han H-M, Robinson RB, Bilezikian JP, Steinberg SF. Developmental changes in guanine nucleotide regulatory proteins in the rat myocardial α_1-adrenergic receptor complex. *Circ Res*. 1989;65:1763-1773.
73. Molina Viamonte V, Steinberg SF, Chow Y-K, Legato MJ, Robinson RB, Rosen MR. Phospholipase C modulates automaticity of canine cardiac Purkinje fibers. *J Pharmacol Exp Ther*. 1990;252:886-893.
74. Madison DV, Malenka RC, Nicoll RC. Phorbol esters block a voltage-sensitive chloride current in hippocampal pyramidal cells. *Nature*. 1986;321:695-697.
75. Brinkmeier H, Jockusch H. Activators of protein kinase C induce myotonia by lowering chloride conductance in muscle. *Biochem Biophys Res Commun*. 1987;148:1383-1389.
76. Saigusa A, Kokubun S. Protein kinase C may regulate resting anion conductance in vascular smooth muscle cells. *Biochem Biophys Res Commun*. 1988;155:882-889.
77. Horowitz B, Tsung SS, Hart P, Levesque PC, Hume JR. Alternative splicing of CFTR Cl^- channels in heart. *Am J Physiol*. 1993;264:H2214-H2220.
78. Takano M, Noma A. Distribution of the isoprenaline-induced chloride current in rabbit heart. *Pflugers Arch*. 1992;420:223-226.

In summary, this work demonstrated that stimulation of α_{1A}-adrenergic receptors inhibits both $I_{Cl.b}$ and $I_{Cl.swell}$ in rabbit atrial myocytes by activation of protein kinase C which is coupled by a PTX-sensitive G-protein. These results suggest that α-adrenergic inhibition of cardiac Cl^- currents is a potentially novel mechanism of α-adrenergic control of cardiac electrical activity.

CHAPTER 6

GENERAL DISCUSSION AND DIRECTIONS FOR FUTURE RESEARCH

The research conducted for this thesis is presented as a compilation of published articles, and extensive discussion of the results, the potential implications and limitations of each specific project is presented in each paper. In order to avoid unnecessary repetition, this general discussion will focus mainly on the possible relations of cardiac ORCC to other cardiac and non-cardiac Cl^- channels, the significance of the present work, and suggestions for future studies on the molecular mechanism of cardiac ORCC and its potential functional roles in the heart.

6.1. Relations of cardiac $I_{Cl.b}$ and ORCC to other chloride channels

$I_{Cl.b}$ in rabbit atrial myocytes differs from the five Cl^- currents previously reported in heart in that it is active under basal unstimulated conditions. Since $I_{Cl.b}$ exhibits little, if any, intrinsic voltage- and time-dependence, like other cardiac Cl^- currents such as $I_{Cl.cAMP}$, $I_{Cl.PKC}$, $I_{Cl.ATP}$, and $I_{Cl.swell}$,[1] the possibility exists that some of these conductances may be due to a common channel molecule. Comparison of biophysical and pharmacological properties of $I_{Cl.b}$ with those of $I_{Cl.swell}$ in the same preparation[2] suggests these two macroscopic currents may be carried by the same underlying anion channels. At the single channel level, we have demonstrated that the ORCC recorded in inside-out patches of rabbit atrial myocytes is a candidate for macroscopic $I_{Cl.b}$.[3] ORCC is also present in cell-attached patches under basal physiological conditions, and the estimated magnitude of macroscopic current corresponding to ORCC matches the measured value of $I_{Cl.b}$, further strongly supporting the idea that ORCC underlies $I_{Cl.b}$.[4] Similar to the modulation of $I_{Cl.b}$ by cell volume, the cell-attached ORCC is also regulated by cell volume in that hyposmotic cell swelling increases the number of active channels without altering channel conductance or open probability.[4] These results suggest that ORCC is the single-channel mechanism underlying both macroscopic $I_{Cl.b}$ and $I_{Cl.swell}$ and may play a potentially important role in regulation of cardiac cell volume. It is unlikely that $I_{Cl.b}$ is the same as $I_{Cl.cAMP}$, $I_{Cl.PKC}$, and $I_{Cl.Ca}$ because the activation of $I_{Cl.b}$ does not require cAMP and intracellular Ca^{2+} and PKC inhibits $I_{Cl.b}$.[2-4] Recent single-channel studies of these Cl^- currents further support this notion. Properties of ORCC, including the conductance, rectification, and Ca^{2+}-sensitivity, are strikingly different from those of cardiac unitary currents of $I_{Cl.cAMP}$,[5-7] $I_{Cl.PKC}$,[8] and $I_{Cl.Ca}$,[9] strongly suggesting they may be due to separate channels. At present, there is not enough information to compare $I_{Cl.b}$ with $I_{Cl.ATP}$ in heart.

Cardiac ORCC is in general quite similar to ORCCs described in non-cardiac cells,[10-15] in terms of conductance (30-60 pS), the characteristic outwardly rectifying I-V relation, and sensitivity to disulfonic stilbenes. While currents through ORCCs have been observed often in cell-free patches from many non-cardiac tissues, it has been more difficult to record the ORCC in cell-attached mode in these tissues. Moreover, the macroscopic equivalent of ORCC in these tissues is also still uncertain. Solc and Wine reported a cell-swelling induced single Cl^- channel with properties somewhat different from ORCC, in that cell-attached ORCC were often closed at resting voltages, started to inactivate at more positive voltages, rectified more and had lower conductance, shorter mean open durations and more open-channel noise than the cell-swelling-induced channel.[14] They could not, however, differentiate whether two types of single Cl^- channel currents caused by cell-swelling are due to separate channel proteins or from the same channel molecule in different states per se. In my studies, comparison of properties of basal ORCC to those of cell-swelling-induced ORCC revealed no difference in conductance, Cl^- dependence, outward rectification, voltage-dependence, and open probability. Consequently, they may be carried by the same channel molecule, the ORCC. Our data provides strong and detailed evidence independently supporting the most recent results of non-stationary noise analysis and single-channel measurement of $I_{Cl.swell}$ in non-cardiac tissues reported by Strange et al.[16,17]

6.2. Physiological relevance of ORCC as a basally active Cl^- channel

The fact that the cell-attached ORCC and whole-cell $I_{Cl.b}$ are regulated by cell volume not only indicates the potential physiological role of ORCC or $I_{Cl.b}$ in cell volume regulation, but also raises the interesting question of whether $I_{Cl.swell}$ is due to a native endogenous background Cl^- channel that can be modulated in both directions by volume changes, in contrast to the conventional view of $I_{Cl.swell}$ which is that of a current seen only upon cell swelling. In fact, a very recent report have found that cardiac delayed rectifier K^+ current (I_k) could also be dually regulated by osmotic challenge[18]. Moreover, a native chloride current responsive to hypotonicity has been recently reported in *Xenopus* oocytes[19], a system being widely used to express cloned Cl^- channels, and pI_{Cln} may be a regulator of the endogenous Cl^- channel.[20] The conventional view of $I_{Cl.swell}$ is thus being challenged and needs to be reconsidered.

There has been a serious doubt and debate about whether ORCC plays any significant functional role in cell physiology and in cystic fibrosis.[12] While ORCC was suggested to mediate volume regulation, signal transduction, and transepithelial transport,[12,14,15] direct evidence for this is still missing. Using whole cell patch-clamp, Guggino's group have recently demonstrated that both CFTR and ORCC contribute to cAMP-stimulated whole-cell Cl^- current.[21] They have also identified the mechanism of interaction of CFTR and ORCC.[22] They first confirmed Cantiello's important observation that ATP can permeate through CFTR, i.e., CFTR itself can function as an ATP transporter[23] The secreted ATP activates a purinergic P_{2U} receptor, which in turn activates the ORCC, as had been previously observed.[24,25] Only nanomolar concentrations of extracellular ATP were needed to open ORCC, and enzymatic removal of extracellular ATP created the CF phenotype in CFTR-expressing cells.[22] These studies suggest that ATP may act as a mediator of the CFTR-ORCC regulatory relationship. The lack of CFTR in the membrane would represent a lack of cAMP-activated CFTR Cl^- channel activity as well as an inability to transport an activator of ORCC. A recent abstract from Guggino's group[26] reported that TMD-1 of CFTR was essential for its Cl^- conduction whereas NBF1 was required for ATP transport through CFTR and autocrine/paracrine stimulation of ORCC.

Although it is not known whether cardiac ORCC and non-cardiac ORCCs are the same molecule, as demonstrated for CFTR, studies of cardiac ORCC will certainly provide important insights not only into signalling pathways, regulatory mechanisms of ion channel function, and patterns of channel expression in heart, but also into the biophysical and molecular properties of non-cardiac, especially epithelial ORCC to which has been attributed a potentially important role in CF.

6.3. Possibility of ORCC as an endogenous Cl^- channel mediating cell volume regulation

While the single channel identity of macroscopic Cl^- currents elicited by pI_{Cln} and P-Gp, both have been implicated as a regulator of volume-regulated endogenous Cl^- channels,[19,20,27] are still missing, we now found that a basally active ORCC is regulated by cell volume in rabbit atrial myocytes and $I_{Cl.b}$ and $I_{Cl.swell}$ likely correspond to ORCC found in the same preparation.[2-4] This finding may explain the fact that activation of PKC through the coupling of a PTX-sensitive G-protein to α_{1A}-adrenoceptors can inhibit both $I_{Cl.b}$ and $I_{Cl.swell}$ in the heart. More interestingly, consistent with our finding in heart, a very recent study in epithelial cell lines has shown that ORCC is coupled with a PTX-sensitive G protein, $G_{\alpha i\text{-}2}$, and endogenous activity of this G protein inhibits the opening of ORCC.[28] These findings, furthermore, may be potentially important, not only because they suggest a novel and potentially important molecular mechanism of regulation of cardiac electrical activity and cell volume, but also because they may provide a possible link between ORCC and cloned Cl^- channels potentially involved in cell volume regulation (considering the similar inhibition by PKC of Cl^- currents elicited from ORCC, CLC-3, and P-Gp). A recent study in ciliary epithelial cells reported that PKC inhibitors upregulated whole cell Cl^- currents isosmotically. This Cl^- current has properties inconsistent with CLC-(0-2) and P-Gp channels but identical to volume-activated channels and the endogenous Cl^- channels regulated by pI_{Cln}[29]. Whether ORCC is the proposed native endogenous Cl^- channel regulated by pI_{Cln} or P-Gp through extracellular hypotonicity or not remains to be determined at a molecular level.

6.4. Directions for future research

We have found that ORCC is the single channel mechanism underlying both $I_{Cl.b}$ and $I_{Cl.swell}$ in rabbit atrial myocytes, suggesting a potentially important physiological role for ORCC in cardiac electrophysiology. ORCC can be a novel target for antiarrhythmic agents, particularly during states of myocardial swelling (for instance, ischemia).

To evaluate the physiological role of ORCC in heart in the control of the action potential plateau, it is necessary to better understand the distribution of these channels in different areas of the heart and in different species, including their role in human myocardial and conducting tissue. Is it possible that these channels may play a role in some types of pacemaker cells by contributing background inward current at pacemaker potentials? At this time, data from several laboratories suggest that $I_{Cl.swell}$ is expressed in human atrium.[30-32] Whether $I_{Cl.swell}$ is also present in the human ventricle and whether ORCC is the single-channel mechanism for $I_{Cl.swell}$ in the human heart remain to be investigated. Future electrophysiological studies should lead to a better understanding of the distribution and precise physiological role of ORCC in mammalian hearts.

Another aspect of further study of ORCC in heart is to understand this channel and its relation with other cardiac Cl^- channels at a molecular level, i.e., to clone the ORCC channel. While the molecular identity of ORCC is still unknown, many groups are actively trying to clone epithelial ORCC.[33] Cardiac ORCCs share many similarities with ORCC in other tissues, including the basic biophysical (e.g. outward rectification) and pharmacological properties (e.g. inhibition by DIDS and SITS). Most interestingly, like cardiac ORCC, epithelial ORCC from human airway is also inhibited by PKC[15] and PTX-sensitive G-protein ($G_{\alpha i\text{-}2}$,)[28]. A recently-cloned member of the CLC family, CLC-3, has been found to be inhibited by PKC[34]. CLC-3 is the most distantly related member of the CLC family (the 760 amino acid protein encoded by CLC-3 is only 24% identical to previously-cloned Cl^- channels but has a similar hydropathy profile). Different from other members of the family but similar to cardiac $I_{Cl.b}$ and $I_{Cl.swell}$, the whole-cell current of CLC-3 shows strong outward rectification under symmetric Cl^- condition and sensitivity to DIDS and SITS (but not to 9-AC and DPC?).[34] Most recently, the same group has reported stable expression of functional CLC-3 in somatic cell lines[35]. They found that CLC-3 was not only inhibited by PKC but also by intracellular Ca^{2+}. These two inhibitory mechanisms seem to be independent. The single channel currents of cloned CLC-3 also shows some similarities to ORCC: 1) Very strong outward rectification under symmetric Cl^- condition; 2) A conductance of 40 pS when intracellular Ca^{2+} was 200 nM; 3) 3 open and 4 closed kinetics states; 4) Anion permeability ratio sequence was $I^- > Br^- > Cl^- > F^-$; 5) Sensitivity to DIDS; 6) Regulation by PKC and intracellular Ca^{2+}; 7) Not recorded in cell-attached mode but became active in cell free mode and after depolarization. An intracellular inhibitory mechanism similar to that of ORCC in epithelial cells and cardiac cells was speculated. Although we don't know the nature of the inhibitory mechanism, our analysis of open probabilities of ORCC in cell-attached patches found that the open probabilities were significantly lower than those in cell-free patches. Recently, two new members of CLC family, CLCN4 and CLCN5, which are strikingly similar to CLC-3 and may belong to the same branch, were isolated from the human Xp22.3 and X11.22 region, respectively[36,37]. Both of them were found to be expressed in heart. A male patient (BA38) who possessed a partial deletion of CLCN4 suffered from cardiac abnormanities. Therefore, it would be interesting to know whether cardiac ORCC is a spliced form of ClC3/CLCN4/CLCN5 branch of CLC family in the heart and linked to X chromosome.

Although recent evidence suggests that pI_{Cln} might not be a transmembrane Cl^- channel but a regulator of an endogenous Cl^- channel,[19,20] it can not be strictly excluded that pI_{Cln} is a Cl^- channel. In support of the channel role, it has been reported that mutations in a putative nucleotide-binding region of pI_{Cln} affected the inhibition by extracellular nucleotides and conferred ion sensitivity to extracellular Ca^{2+}.[38] It seems difficult to reconcile these results with the cytoplasmic regulator mechanism. Antisense oligonucleotides directly against pI_{Cln} inhibit cell-volume-induced activation of Cl^- channels in 3T3 fibroblasts.[39] Injection of antibodies against

pI_{Cln} into *Xenopus* oocytes inhibits its swelling-induced current.[19] These results suggest that pI_{Cln} may be the Cl^- channel directly involved in cell volume regulation.

On the other hand, molecular homology may exist between pore regions of different cardiac Cl^- channels.[40] Hume et al found that all the tissues that exhibit expression of the TSI-VI region of CFTR but do not exhibit functional $I_{Cl.cAMP}$ express other types of Cl^- conductances, including $I_{Cl.b}$ and those activated by cell swelling, PKC, Ca^{2+} and ATP.[40] The TSI-VI region has previously been shown to contain the permeation pathway for the epithelial CFTR Cl^- channel.[41,42] Since the pore region is generally one of the most highly conserved regions in most K^+ and Na^+ channel families,[43,44] it seems reasonable to suggest that anomalous expression of the TSI-VI region of CFTR in tissues that do not exhibit functional $I_{Cl.cAMP}$ but exhibit other types of Cl^- currents may be due to sequence homology between pore regions of different Cl^- channels. While there presently exists little or no relevant data to support or refute this hypothesis, such a hypothesis points to several novel experimental approaches that might be useful in the future to identify the gene and corresponding proteins responsible for ORCC and other types of cardiac Cl^- conductances.

6.5. General conclusions

My work demonstrates that a novel cardiac Cl^- current ($I_{Cl.b}$) which is active under basal physiologic conditions, manifesting as a residual current after I_{to1} inactivation, exists in rabbit atrium. I also characterized a 60-pS outwardly-rectifying Cl^- channel (ORCC) which is the single-channel basis of this macroscopic current. The channel can be regulated by cell volume and controlled by neurotransmitter-mediated signal transduction. These findings are, to our knowledge, the first such reports in the literature, and provide new insights into the unique but poorly-understood modulatory role of Cl^- channels in the control of cardiac electric activity, volume status, and neural regulation. The potential physiological function of this Cl^- channel and its relationship to other types of cardiac Cl^- currents remain to be further studied at both electrophysiological and molecular biological levels.

6.6. References

1. Ackerman MJ and Clapham DE.: Cardiac chloride channels. *Trends Cardiovas Med* 1993; 3:23-28
2. Duan D, Fermini B and Nattel S: α-adrenergic control of volume-regulated Cl^- current in rabbit atrial myocytes - characterization of a novel ionic regulatory mechanism. *Circ Res* 1995; 77:379-393.
3. Duan D and Nattel S Properties of single outwardly rectifying Cl^- channels in heart. *Circ Res* 1994; 75:789-795.
4. Duan D and Nattel S: Evidence that outwardly-rectifying chloride channels underlie volume-regulated Cl^- currents in rabbit atrial myocytes. *Circ Res* 1996; in revision.
5. Ehara T and Ishihara K: Anion channels activated by adrenaline in cardiac myocytes. *Nature. (Lond)* 1990; 347:284-286.
6. Nagel GA, Hwang TC, Nastiuk KI, Nairn AC and Gadsby DC: The protein kinase A-regulated Cl^- channel resembles CFTR (Cystic Fibrosis Transmembrane Conductance Regulator). *Nature* 1992; 360:81-84
7. Ehara T and Matsuura H: Single channel study of the cyclic AMP-regulated chloride current in guinea-pig ventricular myocytes. *J Physiol* (Lond) 1993;464:307-320
8. Collier ML and Hume JR: Unitary chloride channels activated by protein kinase C in guinea pig ventricular myocytes. *Circ Res* 1995; 76:317-324
9. Collier ML, Levesque PC, Kenyon JL and Hume JR: Unitary Cl^- channels activated by cytoplasmic Ca^{2+} in canine ventricular myocytes. *Circ Res* 1996; in press
10. Welsh MJ: Electrolyte transport by airway epithelia. *Physiol Rev* 1987;67:1143-1184
11. Lukacs GL and Moczydlowski E: A chloride channel from lobster walking leg nerves: characterization of single-channel properties in planar bilayers. *J Gen Physiol* 1990;96:707-733
12. Guggino WB: Outwardly rectifying chloride channels and CF: A divorce and remarriage. *J Bioenerg Biomemb* 1991;25:27-35
13. Hwang T-C, Lu L, Zeitlin PL, Gruenert DC, Huganir R and Guggino WR: Chloride channels in CF: lack of activation by protein kinase C and cAMP-dependent protein kinase. *Science* 1989; 244:1351-1353

14. Solc CK and Wine JJ: Swelling-induced and depolarization-induced Cl- channels in normal and cystic fibrosis epithelial cells. *Am J physiol* 1991;261(cell physiol 30):C658-C674.

15. Li M, McCann JD, Anderson MP, Clancy JP, Liedtke CM, Nairn AC, Greengard P and Welsh MJ: Regulation of chloride channels by protein kinase C in normal and cystic fibrosis airway cells. *Science* 1989;244:1353-1356

16. Jackson PS and Strange K: Single channel properties of a swelling-activated anion conductance: current activation occurs by abrupt switching of closed channels to an open states. *J Gen Physiol* 1995;105:643-660

17. Boese S, Wehner F, Jackson PS, Strange K and Kinne RHK: Volume-sensitive anion channels in rat inner medullary collecting duct (IMCD) cells: single channel properties. *FASEB J* 1995;9:A4 Abstract

18. Sasaki N, Mitsuiye T, Wang Z and Noma A: Increase of the delayed rectifier K^+ and Na^+-K^+ pump currents by hypotonic solutions in guinea-pig cardiac myocytes. *Circ Res* 1994;75:887-895

19. Krapivinsky GB, Ackerman, MJ, Gordon EA, Krapivinsky LD and Clapham DE: Molecular characterization of a swelling-induced chloride conductance regulatory protein, pI_{Cln}. *Cell* 1994;76:439-448

20. Ackerman MJ, Krapivinsky GB, Gordon E, Krapivinsky L and Clapham DC: Characterization of a native swelling-induced chloride current, $I_{Cl.swel}l$, and its regulatory protein, pICln, in Xenopus Oocytes. *Jap J Physiol* 1994; 44:S17-S24

21. Schwiebert EM, Flotte T, Cutting GR and Guggino WB: Both CFTR and outwardly rectifying chloride channels contribute to cAMP-stimulated whole cell chloride currents. *Am J Physiol* 1994;266:C1464-C1477

22. Schwieberg EM, Egan ME, Hwang T-H, Fulmer SB, Allen SS, Cutting GR, and Guggino WB: CFTR regulates outwardly rectifying chloride channels theough an auticrine mechanism involving ATP. *Cell* 1995;81:1063

23. Reisin IL, Prat AG, Abraham EH, Amara JF, Gregory RJ, Ausiello DA and Cantiello HF: The cystic fibrosis transmembrane conductance regulator is a dual ATP and chloride channel. *J Biol Chem* 1994;269:20584-20591

24. Stutts MJ, Chinet TC, Mason SJ, Fullton JM, Clarke LL and Boucher RC: Regulation of Cl^- channels in normal and cystic fibrosis airway epithelial cells by extracellular ATP. *Proc Natl Acad Sci USA* 1992;89:1621-1625

25. Lusting KD,Shiau AK, Brake A, Julius D : Expression cloning of an ATP receptor from mouse neuroblastoma cells. *Proc Natl Acad Sci USA* 1993;90:5113-5117

26. Egan ME, Allen SS, Fulmer SB, Cutting GR and Guggino WB: Cellular mechanisms of CFTR-ORCC regulatory interaction. *Biophys J* 1996;70 (2):A10 Abstract

27. Hardy SP, Goodfellow HR, Valverde MA, Gill DR, Sepulveda FV and Higgins: Protein Kinase C -mediated phosphorylation of the human multidrug resistance P-glycoprotein regulates cell volume-activated chloride channels *EMBO J* 1995; 14:68-75

28. Schwiebert EM, Gruenert DC, Guggino WB and Stanton BA: G protein Gαi-2 inhibits outwardly rectifying chloride channels in human airway epithelial cells. *Am J Physiol* 1995;269:C451-C456

29. Coca-Prados M, Anguita J, Chalfant ML and Civan MM: PKC-sensitive Cl channels associated with ciliary epithelial homologue of pICln. *Am J Physiol* 1995;268:C572-C579

30. Oz MC and Sorota S: Forskolin stimulates swelling-induced chloride current, not cardiac cystic fibrosis transmembrane-conductance regulator current, in human cardiac myocytes. *Circ Res* 1995;76:1063-1079

31. Sakai R, Hagiwara N, Kasanuki H, Hosoda S. Chloride conductance in human atrial cells. *J Mol Cell Cardiol.* 1995;27:2403-2408.

32. Li G-R, Feng J, Wang Z and Nattel S: Transmembrane chloride currents in human atrial myocytes. *Am J Physiol* 1996;270:C500-C507

33. McDonough S and Lester HA: Overview of the relationship between structure and function in ion channels. *Drug Development Research* 1994; 33(3):190-202

34. Kawasaki M, Uchida S, Monkava T, Miyawaki A, Mikoshiba K, Marumo F and Sasaki S: Cloning and expression of a protein kinase C -regulated chloride channel abundantly expressed in rat brain neuronal cells. *Neuron* 1994;12:597-604

35. Kawasaki M, Suzuki M, Uchida S, Sasaki S, and Marumo F: Stable and functional expression of the CLC-3 chloride channel in somatic cell lines. *Neuron* 1995;14:1285-1291

36. Van Slegtenhorst MA, Bassi MT, Borsani G, Wapenaar MC, Ferrero GB, De Conciliis L, Rugarli E, Grillo A, Franco B, Zoghbi HY and Ballabio A: A gene from the human Xp22.3 region shares homology with voltage-gated chloride channels. *Hum Mol Genet* 1994;3:547-552

37. Lloyd SE, Pearce SHS, Fisher SE, Steinmeyer K, Schwappach B, Schienman SJ, Harding B, Bolino A, Devoto M, Goodyer P, Rigden SPA, Wrong O, Jentsch TJ, Cralg IW, Thakker RV. A common molecular basis for three inherited kidney stone diseases. *Nature*. 1996;379:445- 449.

38. Paulmichil M, Li Y, Wickmann K, Ackermann M, Peralta E and Clapham DE: New mammalian chloride channel identified by expression cloning. *Nature* 1992; 356:238-241

39. Gschwentner M, Nagl UO, Woll E, Schmarda A, Ritter M and Paulmichil M: Antisense oligonucleotides suppress cell-volume-induced activation of chloride channels. Pflugers Arch 1995;430:464-470

40. Hume JR and Horowitz B: A plethora of cardiac chloride conductances: Molecular diversity or a related gene family? *J Cardiovasc Electrophysiol* 1995;6:325-331

41. Anderson MP, Grergory RJ, Thompson S, Souza DW, Paul S, Mulligan RC, Smith AE and Welsh MJ: Demonstration that CFTR is a chloride channel by alternation of its anion selectivity. *Science* 1991;253:202-204

42. Sheppard DN, Ostedgaard LS, Rich DP et al: The amino-terminal portion of CFTR forms a regulated Cl^- channel. *Cell* 1994;76:1091-1098

43. Chandy KG and Gutman GA: Voltage-gated K^+ channels. In: *CRC Handbook of Receptors and Channels*. CRC Press, Boca Raton, 1995 (in press)

44. Catterall W: Cellular and molecular biology of voltage-gated sodium channels. *Physiol*